ISSN 0042-8469
e-ISSN 2217-4753
УДК 623 + 355/359

Вол. 68, бр. 3

2020

ВТГ

НАУЧНИ ЧАСОПИС МИНИСТАРСТВА ОДБРАНЕ И ВОЈСКЕ СРБИЈЕ

ВОЈНОТЕХНИЧКИ ГЛАСНИК

3 2020 ВОЈНОТЕХНИЧКИ ГЛАСНИК

ISSN 0042-8469
e-ISSN 2217-4753
УДК 623 + 355/359

Том 68, № 3
2020

НАУЧНЫЙ ЖУРНАЛ МИНИСТЕРСТВА ОБОРОНЫ
И ВООРУЖЁННЫХ СИЛ РЕСПУБЛИКИ СЕРБИЯ

ВОЕННО-ТЕХНИЧЕСКИЙ ВЕСТНИК

3 2020 ВОЕННО-ТЕХНИЧЕСКИЙ ВЕСТНИК

втг.мо.упр.срб
www.vtg.mod.gov.rs

MILITARY TECHNICAL COURIER 2020 3

ISSN 0042-8469
e-ISSN 2217-4753
UDC 623 + 355/359

Vol. 68, Issue 3
2020

MTC

SCIENTIFIC JOURNAL OF THE MINISTRY OF DEFENCE AND SERBIAN ARMED FORCES

MILITARY TECHNICAL COURIER

втг.мо.упр.срб

www.vtg.mod.gov.rs

ISSN 0042-8469
e-ISSN 2217-4753
UDC 623 + 355/359

НАУЧНИ ЧАСОПИС МИНИСТАРСТВА ОДБРАНЕ И ВОЈСКЕ СРБИЈЕ

ВОЈНОТЕХНИЧКИ ГЛАСНИК

ВОЛУМЕН 68 • БРОЈ 3 • ЈУЛ – СЕПТЕМБАР 2020.

NAUČNI ČASOPIS MINISTARSTVA ODBRANE I VOJSKE SRBIJE

VOJNOTEHNIČKI GLASNIK

VOLUMEN 68 • BROJ 3 • JUL – SEPTEMBAR 2020.

втг.мо.упр.срб
www.vtg.mod.gov.rs
COBISS.SR-ID 4423938
DOI: 10.5937/VojnotehnickiGlasnik

ISSN 0042-8469
e-ISSN 2217-4753
UDC 623 + 355/359

НАУЧНЫЙ ЖУРНАЛ МИНИСТЕРСТВА ОБОРОНЫ И ВООРУЖЁННЫХ СИЛ РЕСПУБЛИКИ СЕРБИЯ

ВОЕННО-ТЕХНИЧЕСКИЙ ВЕСТНИК

ТОМ 68 • НОМЕР ВЫПУСКА 3 • ИЮЛЬ- СЕНТЯБРЬ 2020.

SCIENTIFIC JOURNAL OF THE MINISTRY OF DEFENCE AND SERBIAN ARMED FORCES

MILITARY TECHNICAL COURIER

VOLUME 68 • ISSUE 3 • JULY- SEPTEMBER 2020

втг.мо.упр.срб
www.vtg.mod.gov.rs
COBISS.SR-ID 4423938
DOI: 10.5937/VojnotehnickiGlasnik

Власници:
МИНИСТАРСТВО ОДБРАНЕ и ВОЈСКА СРБИЈЕ

Издавач:
УНИВЕРЗИТЕТ ОДБРАНЕ У БЕОГРАДУ

Ректор
Доц. др Горан Радовановић, генерал-потпуковник

ГЛАВНИ И ОДГОВОРНИ УРЕДНИК ВОЈНОТЕХНИЧКОГ ГЛАСНИКА
мр Небојша Гаћеша, потпуковник
e-mail: nebojsa.gacesa@mod.gov.rs, tel.: 011/3603-260, 066/87-00-123, http://orcid.org/0000-0003-3217-6513

Адреса редакције: ВОЈНОТЕХНИЧКИ ГЛАСНИК, Вељка Лукића Курјака 33, 11042 Београд
http://www.vtg.mod.gov.rs
http://aseestant.ceon.rs/index.php/vtg/issue/current
http://scindeks.nb.rs/journaldetails.aspx?issn=0042-8469
http://elibrary.ru/title_about.asp?id=53280
https://doaj.org/toc/2217-4753

e-mail: vojnotehnicki.glasnik@mod.gov.rs

Претплата на штампано издање: e-mail: vojnotehnicki.glasnik@mod.gov.rs; тел. 066/87-00-123

Рукописи се не враћају

Часопис излази тромесечно

Први штампани број *Војнотехничког гласника* објављен је 1. 1. 1953. године

Прво електронско издање *Војнотехничког гласника* на Интернету објављено је 1. 1. 2011. године

Војнотехнички гласник је лиценциран код EBSCO Publishing-а, највећег светског агрегатора часописа, периодике и осталих извора у пуном тексту. Комплетан текст *Војнотехничког гласника* доступан је у базама података EBSCO Publishing-а.

Штампа: Војна штампарија – Београд, Ресавска 40б, e-mail: vojna.stamparija@mod.gov.rs

Собственники:
МИНИСТЕРСТВО ОБОРОНЫ и ВООРУЖЁННЫЕ СИЛЫ РЕСПУБЛИКИ СЕРБИЯ
Издательство:
УНИВЕРСИТЕТ ОБОРОНЫ В Г. БЕЛГРАД
РЕКТОР
Генерал-лейтенант доц. д-р Горан Радованович
ГЛАВНЫЙ И ОТВЕТСТВЕННЫЙ РЕДАКТОР ЖУРНАЛА «ВОЕННО-ТЕХНИЧЕСКИЙ ВЕСТНИК»
Кандидат технических наук Небойша Гачеша, подполковник
e-mail: nebojsa.gacesa@mod.gov.rs, тел.: +381 11 3603 260, +381 66 87 00 123, http://orcid.org/0000-0003-3217-6513

Адрес редакции: ВОЈНОТЕХНИЧКИ ГЛАСНИК, Ул. Велька Лукича Куряка 33, 11042 Белград, Республика Сербия
http://www.vtg.mod.gov.rs
http://aseestant.ceon.rs/index.php/vtg/issue/current
http://scindeks.nb.rs/journaldetails.aspx?issn=0042-8469
http://elibrary.ru/title_about.asp?id=53280
https://doaj.org/toc/2217-4753
e-mail: vojnotehnicki.glasnik@mod.gov.rs
Подписка на печатную версию журнала: e-mail: vojnotehnicki.glasnik@mod.gov.rs; тел. +381 66 87 00 123
Присланные в редакцию журнала статьи не возвращаются.
Журнал выпускается ежеквартально.
Первый номер журнала «Военно-технический вестник» выпущен 1.1.1953 года.
Первая электронная версия журнала размещена на интернет странице 1.1.2011 года.
«Военно-технический вестник» включен в систему EBSCO – всемирная академическая база данных и сервисов.
Типография: Војна штампарија – Белград, Ресавска 40б, e-mail: vojna.stamparija@mod.gov.rs

Owners:
MINISTRY OF DEFENCE and SERBIAN ARMED FORCES

Publisher:
UNIVERSITY OF DEFENCE IN BELGRADE

Rector
Lieutenant General Goran Radovanović, PhD, Assistant Professor

EDITOR IN CHIEF OF THE MILITARY TECHNICAL COURIER
Lt Col Nebojša Gaćeša MSc
e-mail: nebojsa.gacesa@mod.gov.rs, tel: +381 11 3603 260, +381 66 87 00 123, http://orcid.org/0000-0003-3217-6513

Address: VOJNOTEHNIČKI GLASNIK/MILITARY TECHNICAL COURIER, Veljka Lukića Kurjaka 33, 11042 Belgrade, Republic of Serbia
http://www.vtg.mod.gov.rs/index-e.html
http://aseestant.ceon.rs/index.php/vtg/issue/current
http://scindeks.nb.rs/journaldetails.aspx?issn=0042-8469
http://elibrary.ru/title_about.asp?id=53280
https://doaj.org/toc/2217-4753

e-mail: vojnotehnicki.glasnik@mod.gov.rs

Subscription to print edition: e-mail: vojnotehnicki.glasnik@mod.gov.rs; Tel. +381 66 87 00 123

Manuscripts are not returned

The journal is published quarterly

The first printed issue of the *Military Technical Courier* appeared on 1st January 1953.

The first electronic edition of the *Military Technical Courier* on the Internet appeared on 1st January 2011.

Military Technical Courier has entered into an electronic licensing relationship with EBSCO Publishing, the world's most prolific aggregator of full text journals, magazines and other sources. The full text of Military Technical Courier can be found on EBSCO Publishing's databases.

Printed by Vojna štamparija – Belgrade, Resavska 40b, e-mail: vojna.stamparija@mod.gov.rs

С А Д Р Ж А Ј

С О Д Е Р Ж А Н И Е

C O N T E N T S

WHAT COULD HAPPEN AFTER THE FIRST WAVE OF COVID-19 DIFFUSION IN ITALY: LEARNING FROM THE 1918 INFLUENZA PANDEMIC

Nicola Fabiano[a], *Stojan* N. Radenović[b]
[a] Ton Duc Thang University, Faculty of Mathematics and Statistics, Ho Chi Minh City, Vietnam;
Ton Duc Thang University, Nonlinear Analysis Research Group, Ho Chi Minh City, Vietnam,
e-mail: nicola.fabiano@tdtu.edu.vn, **corresponding author**,
ORCID iD: https://orcid.org/0000-0003-1645-2071
[b] University of Belgrade, Faculty of Mechanical Engineering, Belgrade, Republic of Serbia,
e-mail: radens@beotel.net,
ORCID iD: https://orcid.org/0000-0001-8254-6688

DOI: 10.5937/vojtehg68-26500; https://doi.org/10.5937/vojtehg68-26500

FIELD: Mathematics
ARTICLE TYPE: Original scientific paper

Summary:

Introduction/purpose: A comparison of the 1918 "Spanish" influenza to the 2020 COVID–19 pandemic could shed some light on the evolution of the latter.
Method: A mathematical method previously applied to the description of the behavior of the spread of COVID–19 in time is used this time to the 1918 influenza.
Results: The obtained results were compared and some conclusions made about some possible forecasts for the next waves of COVID-19.
Conclusions: Some further waves of the 2020 pandemic should be expected in the future.

Keywords: 1918 Influenza, Coronavirus, COVID-19, differential equation, data fit.

1918 Spanish Influenza and a mathematical model

In 1918, the influenza pandemic known as "Spanish" caused, according to some estimates, about 50 million deaths worldwide, with about 500 million infected, about one third of world population

(Taubenberger & Morens, 2006, pp.15-22). The disease, considered the deadliest pandemic that ever happened, was spread in more waves across the years 1918 and 1919. In Figure 1, we show the death counts per thousands for the population of the United Kingdom in the period 1918–1919.

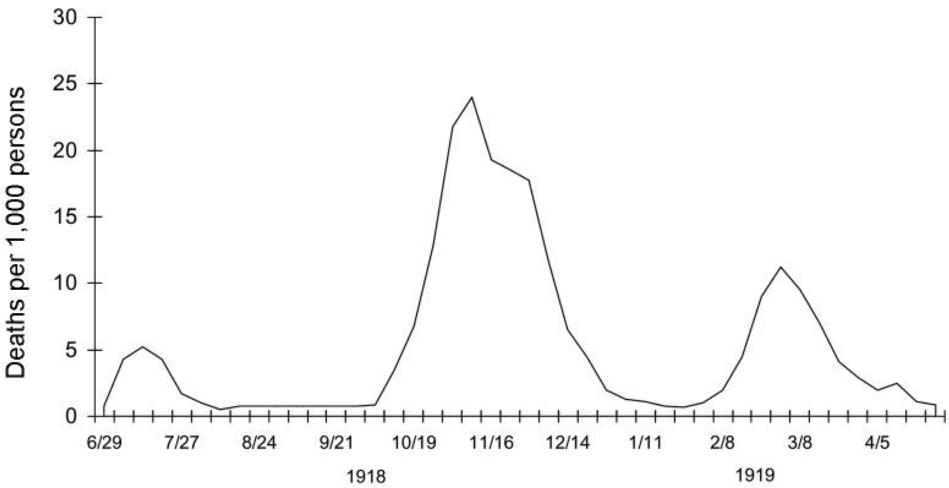

Figure 1 – Keywords: Spanish influenza deaths per thousands in the United Kingdom for the period 1918–1919
Рис. 1 – Ключевые слова: Число смертных случаев (в тысячах) от испанского гриппа в Соединенном Королевстве в период с 1918 по 1919 год
Слика 1 – Кључне речи: број смртних случајева у хиљадама од шпанског грипа у Уједињеном Краљевству у периоду 1918–1919.

In (Fabiano & Radenović, 2020, pp.216-224) a mathematical model of population growth due to (Verhulst, 1838, pp.113-121) was used to describe the spread in time of COVID-19 for the Italian population. Even though the model used only three parameters, it showed an excellent agreement with the available data.

In summary, the number of cases of COVID-19 in the population as a function of time, $x(t)$, is given by the differential equation

$$\frac{dx(t)}{dt} = \frac{x(t)}{a}\left(1 - \frac{x(t)}{c}\right), \quad (1)$$

with a solution given by

$$x(t) = \frac{c}{1 + \exp((b-t)/c)} \quad (2)$$

where in particular the variation of cases in time is explicitly written as

$$\frac{dx(t)}{dt} = \frac{c}{a} \frac{\exp[(b-t)/a]}{(1+\exp[(b-t)/a])^2} . \tag{3}$$

The parameters *a, b,* and *c* are to be determined with a fit to the data, in particular *a* and *c* are linked to the height and width of the bell–shaped function (3), while *b* translates in time its maximum value, which is *c/(4a).* We will use the same model in order to describe the peaks of the 1918 influenza shown in (1). As there is no numerical data available for this figure, we had to resort to software extraction of the above data from (1). Subsequently, we isolated every visible peak and fitted it with (3), determining for each case the parameters *a, b,* and *c*. The results are shown ordered in time starting from the earliest occurrence of a peak. The abscissa shows the number of days from the start of the peak.

The zeroth peak:

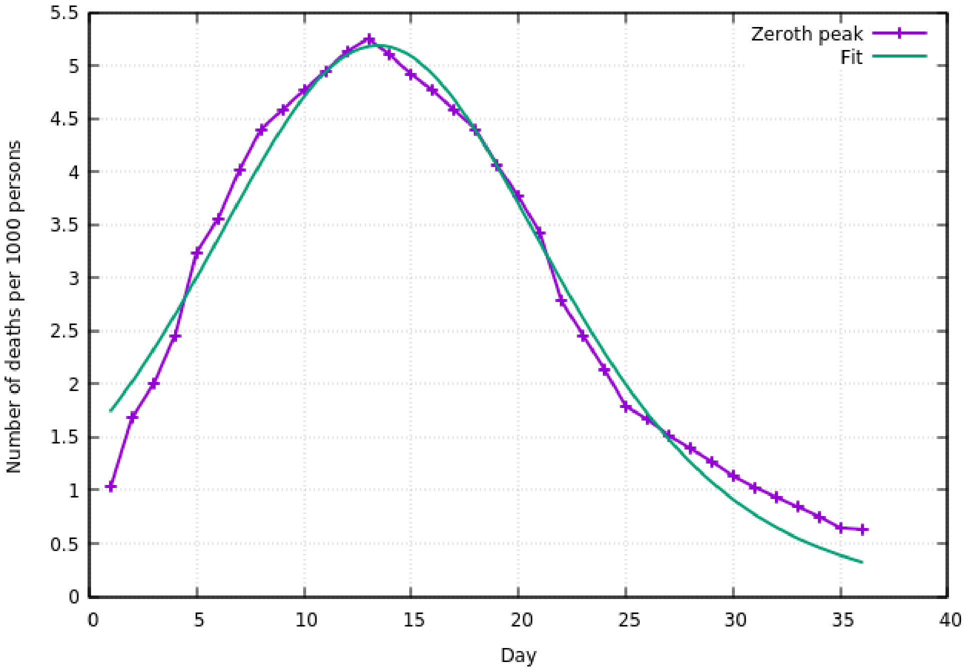

Figure 2 – Zeroth peak
Рис. 2 – Нулевой пик
Слика 2 – Нулти пик

Table 1 – Fit parameters for the peak in Figure 2
Таблица 1 – Согласованные параметры пика на рис. 2
Табела 1 – Параметри уклапања за пик на слици 2

Parameter	Value	Error	Error %
a	5.46429	0.1222	2.236
b	13.452	0.1553	1.154
c	113.44	1.96	1.728

The first peak:

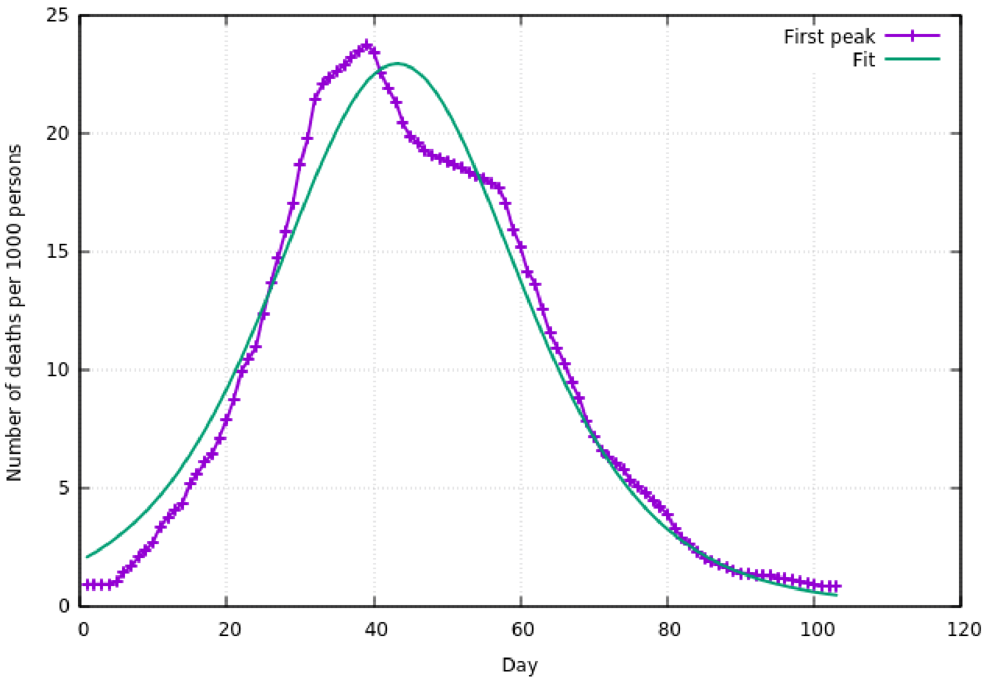

Figure 3 – First peak
Рис. 3 – Первый пик
Слика 3 – Први пик

Table 2 – Fit parameters for the peak in Figure 3
Таблица 2 – Согласованные параметры пика на рис. 3
Табела 2 – Параметри уклапања за пик на слици 3

Parameter	Value	Error	Error %
a	11.2462	0.2014	1.791
b	43.2221	0.2806	0.6491
c	1031.4	14.79	1.434

The second peak:

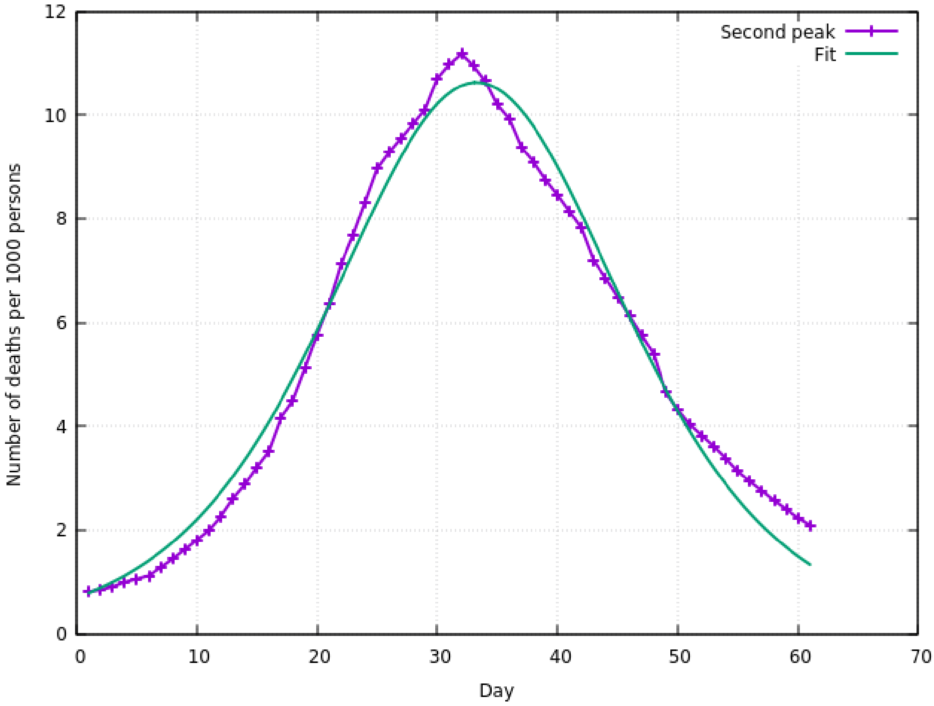

Figure 4 – Second peak
Рис. 4 – Второй пик
Слика 4 – Други пик

Table 3 – Fit parameters for the peak in Figure 4
Таблица 3 – Согласованные параметры пика на рис. 4
Табела 3 – Параметри уклапања за пик на слици 4

Parameter	Value	Error	Error %
a	8.1634	0.1196	1.465
b	33.2618	0.1621	0.4875
c	347.021	4.02	1.158

The (possible) third peak:

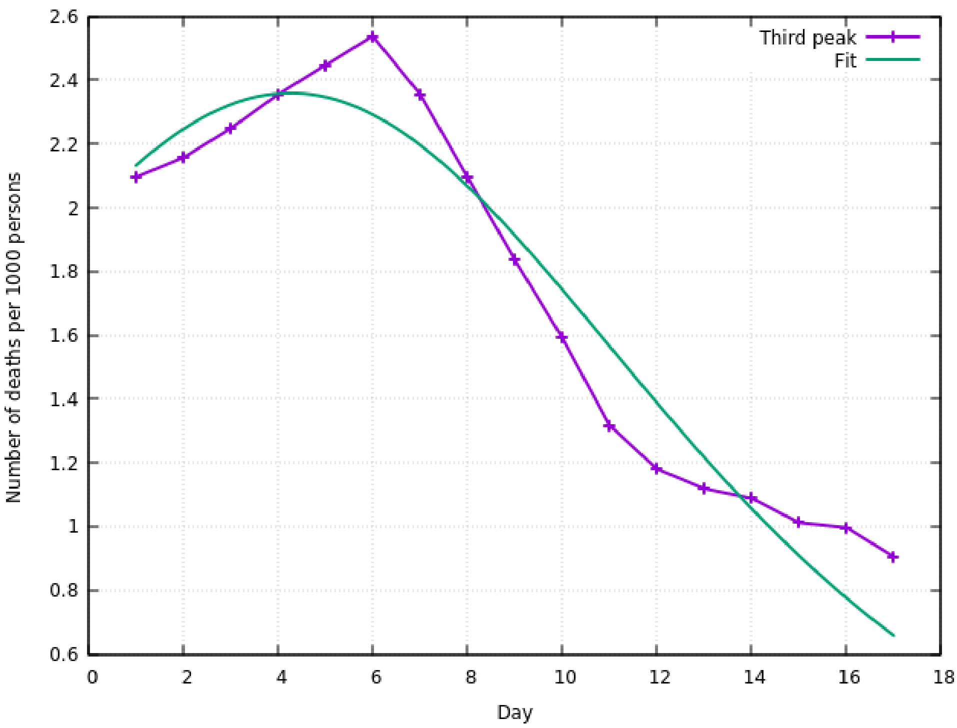

Figure 5 – Third peak
Рис. 5 – Третий пик
Слика 5 –Трећи пик

Table 4 – Fit parameters for the peak in Figure 5
Таблица 4 – Согласованные параметры пика на рис. 5
Табела 4 – Параметри уклапања за пик на слици 5

Parameter	Value	Error	Error %
a	5.08329	0.4081	8.029
b	4.26393	0.5602	13.14
c	47.9721	3.584	7.471

As we can see, the agreement of eqs. (1) and (3) with the peaks found in Fig. (1) is excellent. The relative error of the parameters is almost always less than 2% for the first three peaks, as per Tables (1), (2), and (3). Even with the unclear last peak shown in Fig. (5), the relative error of the parameters is of the order of 10%, in Table (4).

These results show that the mathematical description of a pandemic given by equation (1) is once again very accurate.

Relation to COVID-19

Our aim now is to apply what we have learned from the 1918 pandemic to the evolution of the 2020 pandemic. The relaxation of quarantine rules could lead to other peaks of cases as seen in the 1918 case, when the second peak was much higher than the first.

In Table 5, we report the height of the four peaks found for the 1918 influenza and their relative heights normalized to the largest one. We also show the *c* parameter values and again their relative values normalized to the largest one, obtained again the second peak encountered. The *c* parameter is of particular interest because it is related to the duration of the infection (Fabiano & Radenović, 2020, pp.216-224): the larger the *c* value, the longer the length of infection.

We had normalized here the peaks to the largest one, which actually belongs to the second wave of infection and not to the first one. Even in this more favorable case, one could expect that the next infection wave would have an intensity of almost half of the first one (about 46%), for a total number of cases of a third (about 33%). The third and the last wave would have an intensity of about 10% of the original one, and a relative total number of cases of about 5%.

Table 5 – Heights and relative heights together with the c parameter and its relative values of peaks in Figure 1
Таблица 5 – Высоты и относительные высоты вместе с параметром с и его относительными значениями пиков на рис. 1
Табела 5 – Висине и релативне висине заједно са параметром с и његовим релативним вредностима пикова на слици 1

Peak n.	Height	Rel. to max height %	c	Rel. to max c %
1	22.928	100.0	1031.4	100.0
2	10.627	46.352	347.021	33.646
0	5.190	22.637	113.44	10.999
3	2.359	10.290	47.9721	4.651

All this of course in the case that the first wave was the strongest one. If this is not the case, from Table 5 we see that the relative height of the first two waves is almost 4-fold, while the *c* value is 9 times larger.

Notice that even in the so-called Hong Kong pandemic flu of 1968 the second wave was much deadlier than the first one (Rogers, 2020).

A few remarks are in order here. First of all, we have compared, because other data were unavailable, the deaths of the United Kingdom for influenza in 1918 to the number of COVID-19 cases in Italy in 2020. This should be acceptable as the population number of the two countries is similar; we assume that the number of deaths in a pandemic is proportional to the number of total cases of the disease, and that the proportionality constant is actually such, i.e. it does not change in time during the pandemic.

It should be also clear that the obtained results will provide the relative intensities and duration of the disease, mainly for the lack of data. In 1918, there were no tests available for the positivity of a virus infection, and a virus image was yet to be seen, as the necessary electron microscope was first built in 1931.

Another question of great interest for the current COVID-19 pandemic is when the subsequent peaks would happen. Actually, the speculations on those timings have been a subject of discussion for decades without a definitive answer. One could infer that due to the shorter persistency of this virus to higher temperatures (Fathizadeh et al, 2020) the next wave could occur in the next autumn, thus overlapping with the flu season.

Conclusion

Using a model of population growth with only 3 parameters, we have verified that it is able to describe the 1918 influenza pandemic extremely well. The same model already described the 2020 COVID–19 pandemic in excellent agreement with data. We have used the results obtained for the various waves of the 1918 disease to try to describe the possible waves for the 2020 disease. According to the data, there are serious possibilities to expect subsequent waves of the COVID–19 infection of the same order of magnitude as the present one. The severity of the possible future situation should suggest constant monitoring of the population for a further outbreak of infection and a plan for an immediate lockdown in this case.

References

Fabiano, N. & Radenović, S. 2020. On COVID-19 diffusion in Italy: data analysis and possible outcome. *Vojnotehnički glasnik/ Military Technical Courier*, 68(1), pp.216-224. Available at: https://doi.org/10.5937/vojtehg68-25948.

Fathizadeh, H., Maroufi, P., Momen-Heravi, M., Dao, S., Köse, S., Ganbarov, K., Pagliano, P., Espsoito, S., & Kafil, H.S. 2020. Protection and disinfection policies against SARS-CoV-2 (COVID-19). *Le infezioni in medicina*, 2020, 28(2), pp.185-191 [online]. Available at: https://www.infezmed.it/media/journal/Vol_28_2_2020_8.pdf [Accessed: 8 May 2020].

Rogers, K. 2020. 1968 flu pandemic. In: *Encyclopædia Britannica*. London: Encyclopædia Britannica, Inc. [online]. Available at: https://www.britannica.com/event/Hong-Kong-flu-of-1968 [Accessed: 8 May 2020].

Taubenberger, J.K. & Morens, D.M. 2006. 1918 Influenza: the Mother of All Pandemics. *Emerging Infectious Diseases*, 12(1), pp.15-22. Available at: https://doi.org/10.3201/eid1201.050979.

Verhulst, PF. 1838. Notice sur la loi que la population suit dans son accroissement. *Correspondance mathématique et physique*, 10, pp.113–121 (in French).

ЧТО МОГЛО ПРОИЗОЙТИ ПОСЛЕ ПЕРВОЙ ВОЛНЫ ЭПИДЕМИИ COVID-19 В ИТАЛИИ: ОПЫТ ПАНДЕМИИ ГРИППА В 1918 ГОДУ

Никола Фабиано[а], *Стоян* Н. Раденович[б]

[а] Университет Тон Дук Тханг,Факультет математической статистики, Хо Ши Мин, Вьетнам;
Университет Тон Дук Тханг, Исследовательский отдел нелинейного анализа, Хо Ши Мин, Вьетнам, **корреспондент**

[б] Белградский университет, Машиностроительный факультет, г. Белград, Республика Сербия

РУБРИКА ГРНТИ: 27.00.00 МАТЕМАТИКА;
27.29.00 Обыкновенные дифференциальные уравнения
ВИД СТАТЬИ: оригинальная научная статья

Резюме:

Введение/цель: Сравнение пандемии испанского гриппа 1918 года с пандемией COVID-19 в 2020 году может пролить некоторый свет на развитие современной пандемии.
Методы: В статье использован математический метод, примененный ранее для описания характера распространения COVID-19, в данном случае на материале испанского гриппа 1918 года.
Результаты: На основании сравнения полученных результатов были сделаны выводы и прогнозы касательно возможности последующих волн вируса COVID-19.
Выводы: В будущем следует ожидать новых волн пандемии 2020 года.

Ключевые слова: грипп 1918 года, Коронавирус, COVID-19, дифференциальное уравнение, совпадение данных.

ШТА ЈЕ МОГЛО ДА СЕ ДОГОДИ НАКОН ПРВОГ ТАЛАСА ШИРЕЊА COVID-19 У ИТАЛИЈИ: ИСКУСТВА ИЗ ПАНДЕМИЈЕ ГРИПА 1918. ГОДИНЕ

Никола Фабиано[а], *Стојан* Н. Раденовић[б]

[а] Универзитет Тон Дук Танг, Факултет математике и статистике, Хо Ши Мин, Вијетнам;
Универзитет Тон Дук Танг, Истраживачка група за нелинеарну анализу, Хо Ши Мин, Вијетнам, **аутор за преписку**

[б] Универзитет у Београду, Машински факултет, Београд, Република Србија

ОБЛАСТ: математика
ВРСТА ЧЛАНКА: оригинални научни рад

Сажетак:

Увод/циљ: Поређење шпанског грипа 1918. године са пандемијом COVID-19 могло би донекле разјаснити развој данашње пандемије.
Методе: У раду је коришћена математичка метода која је примењена за опис ширења COVID-19, а овог пута према грипу који је владао 1918. године.
Резултати: Упоређени су добијени резултати на основу којих су изведени закључци о могућим прогнозама за следеће таласе COVID-19.
Закључци: У будућности би требало очекивати нове таласе пандемије COVID-19.

Кључне речи: грип 1918. године, корона вирус, COVID-19, диференцијална једначина, уклапање података.

Paper received on / Дата получения работы / Датум пријема чланка: 08.05.2020.
Manuscript corrections submitted on / Дата получения исправленной версии работы / Датум достављања исправки рукописа: 31.05.2020.
Paper accepted for publishing on / Дата окончательного согласования работы / Датум коначног прихватања чланка за објављивање: 01.06.2020.

VOJNOTEHNIČKI GLASNIK / MILITARY TECHNICAL COURIER, 2020, Vol. 68, Issue 3

MONITORING COVID-19 IS LIKE INSTRUMENT FLYING

Petar V. Kočović[a], *Zoran* V. Kočović[b], *Vladimir* P. Kočović[c]
[a] University Union "Nikola Tesla", School for Information Technology and Engineering, Belgrade, Republic of Serbia,
e-mail: petar.kocovic@fpsp.edu.rs, **corresponding author**,
ORCID iD: https://orcid.org/0000-0001-8289-1385
[b] Omni Logika, Belgrade, Republic of Serbia,
e-mail: impulslxi@gmail.com,
ORCID iD: https://orcid.org/0000-0003-4815-0350
[c] IGT, Belgrade, Republic of Serbia,
e-mail: kocovic.vladimir@gmail.com,
ORCID iD: https://orcid.org/0000-0002-3943-6341

DOI: 10.5937/vojtehg68-26557; https://doi.org/10.5937/vojtehg68-26557

FIELD: Mathematics
ARTICLE TYPE: Original Scientific Paper

Summary:

Introduction/purpose: To monitor the COVID-19 epidemic in every single country in the world, this team has developed a specific system that consists of the following diagrams and mathematical models: a) epidemiological curve, b) histogram of infected people, c) histogram of infected people in last five days, d) double logarithmic curve for monitoring the speed of the epidemic, e) epidemic pipeline and f) Gaussian and Boltzmann S curves. As it is shown in this paper, monitoring an epidemic is like flying a plane using instruments.

Methods: The most complex model is the calculation of the truncated Gaussian curve, and this model will be discussed in more detail in this paper. Also, there is time coincidence between the Gaussian curve and the S-curve. The input data were found in the World Health Organization's daily reports. The full set of data consists of the Gaussian curve, the double logarithmic curve, and the epidemic curve. In some cases, using only one of the three specified parameters is not enough.

Results: To prove a specified methodology, the paper has dozens of results in the form of diagrams.

Conclusion: The Gaussian curve was formed, and the end of the epidemic was calculated. But, in some cases, the epidemic curve was not well-formed (the end of the epidemic is not clear since many countries did not declare the number of recovered people in a proper way). This is the reason why we must include a flow of the double logarithmic curve into consideration. Only a combination of these three diagrams can give the right insight into the right decision.

Keywords: COVID-19, Gaussian curve, S-curve.

Introduction

This paper aims to describe a set of mathematical models for decision making about critical decisions in the epidemic. Besides medical decisions, the economic impact on each country, state, and territory is also very important. How long to close some industries, what will be the impact on jobs, and dismissal of workers are the key ones. This team has developed software for monitoring all specified data daily for the top 50 countries. (Kočović et al, 2020)

The main curve is epidemiological (EpiCurve). The epidemiological curve can be shown with the following formula:

$$\textit{Still infected} = \textit{totally infected} - \textit{death} - \textit{recovered} \qquad (1)$$

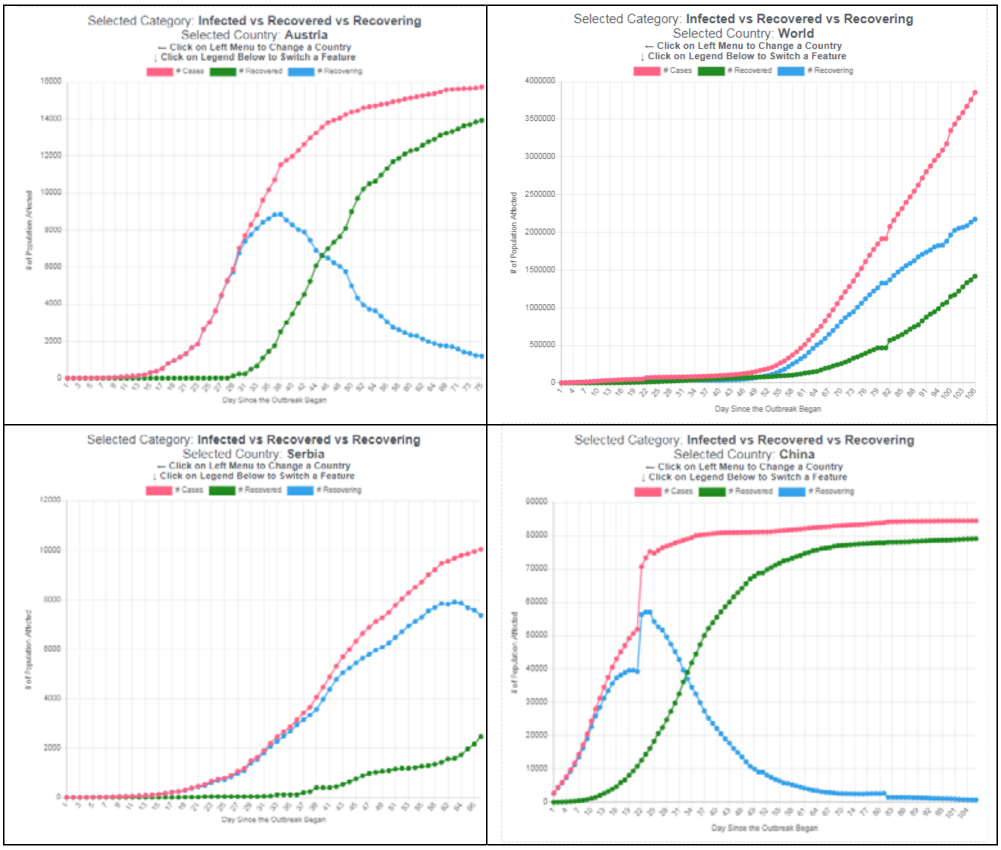

Figure 1 – EpiCurves a) Austria, b) World, c) Serbia, and d) China
Рис. 1 – Эпидемиологическая кривая а) Австрия, б) мир, в) Сербия и г) Китай
Слика 1 – Епидемиолошка крива: а) Аустрија, б) свет, в) Србија и г) Кина

Figure 1 is showing the EpiCurves for three territories and the whole world. The epidemiological curves are related to single countries.

The meanings of the symbols in the figures are:

- #Cases – the total number of the infected from the beginning of the epidemic in a particular country
- #Recovered – the number of people recovered from the beginning of the epidemic in a particular country
- #Recovering – the number of people calculated from formula (1)

As we can see in Figure 1, the curve(s) of the #Recovering is(are) the EpiCurve. In the cases of 1a) Austria and 1d) China, the curves are closed. In two other examples, the curves are in the phase of the initial (1b) World) or the middle phase (1c). All four examples show that #Cases follow the shape of the letter "S" and have the name of the S (or Sigmoid) curve.

These curves are real, so we cannot make any forecasts from these curves. Instead, mathematical modeling and forecasting techniques are used in these calculations.

Histograms and 5-day histograms

The curves denoted as #Recovering look like Gaussian curves. But there is one exception between the uses of a Gaussian distribution when a full curve is formed. In epidemic modeling, there are new data on the infected every day. For these purposes, histograms and 5-day histograms have been developed (Mann, 1994).

Histograms represent the number of infected per day[1]. Even if they do not look like a Gaussian distribution, in many cases we can fit them within the Gaussian curve. Figure 2 shows two examples of the histograms for COVID-19 cases.

In Figure 2a), the case of Brazil shows that a Gaussian distribution is not visible. The same situation is in Figure 2b).

Also, a short 5-day histogram can represent good or bad trends. Good trends are when the number of the infected decreases in five consecutive days and bad trends are the opposite – when in five consecutive days the number of the infected grows. Figure 3 shows two examples – Germany and Japan.

Most of the 5-day trends show intermediate results. Notice that if there is just one day with a very high number of the infected– this will prolong the recovery period.

[1] Data about COVID-19 can be found in the separate reports on the web site of the World Health Oranization (World Health Organzation, 2020).

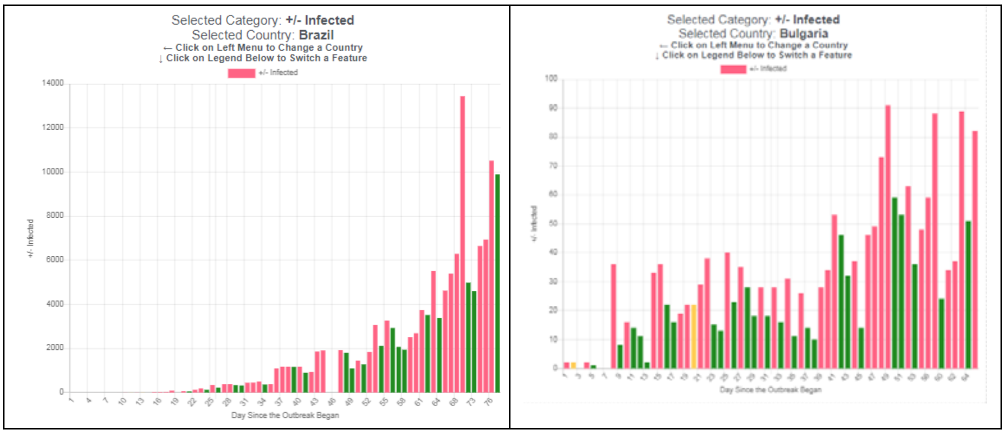

Figure 2 – Histograms a) Brazil, b) Bulgaria
Рис. 2 – Гистограмма а) Бразилия, б) Болгария
Слика 2 – Хистограм: а) Бразил, б) Бугарска

This 5-day trend represents a very good visual form for simplifying the monitoring of the epidemic. In the period of the epidemic growth, there are more red bars.

The histograms are basic tools for Gaussian and Sigmoid/S-curves. However, significant assumptions were made for both of them.

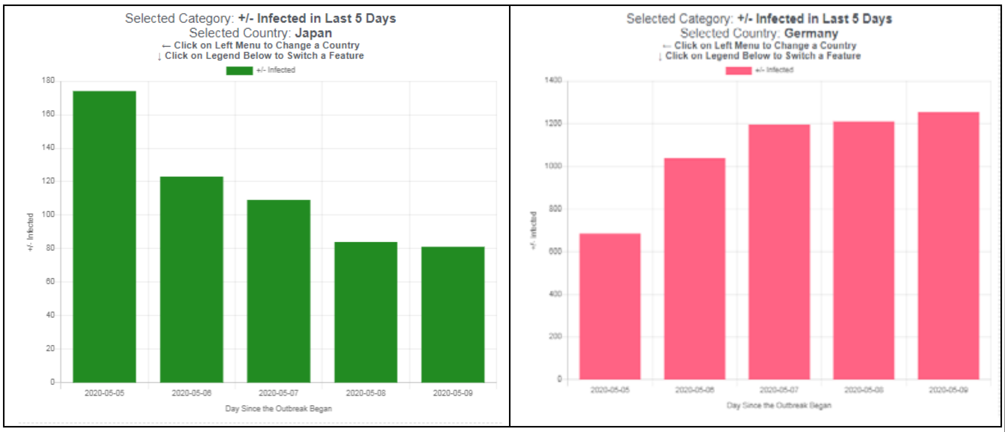

Figure 3 – Five-day trends- a) good – Japan, and b) bad – Germany. Both of them are in the period May 5 – May 9, 2020
Рис. 3 – Пятидневный тренд – а) положительный – Япония и б) отрицательный – Германия. Оба тренда за период с 5 по 9 мая 2020 года.
Слика 3 – Петодневни тренд: а) добар – Јапан и б) лош – Немачка. Оба тренда односе се на период 5–9. мај 2020. године

Gaussian distribution

For defining Gaussian curves (Gauss, 1809), (Stahl, 2006), the standard Laplace-Gauss formula is used (2) with a few modifications (Laplace, 1774):

$$f(x) = \frac{1}{\sigma\sqrt{2\pi}} e^{-\frac{1}{2}\left(\frac{x-\mu}{\sigma}\right)^2} \qquad (2)$$

For calculating this curve, the standard error was used. The maximum number of iterations is 1,000 for these calculations.

The infections start outgrowing exponentially at first, then whatever response the host country enacts, after some time, new infections go back to near zero. At least this is the back-of-the-envelope theory, developed by Enrico Fermi[2]. There are undoubtedly better models, but the Gaussian model was used as the first shot in this mathematical model.

The Gaussian model is defined by only three parameters: N, μ, and σ, and looks like this:

- N is the infection rate at its peak, the midpoint of the epidemic.
- μ is the date of the peak infection rate, and
- σ controls the width, the period of time the pandemic is experienced by the country.

Figure 4 shows the statements given above:

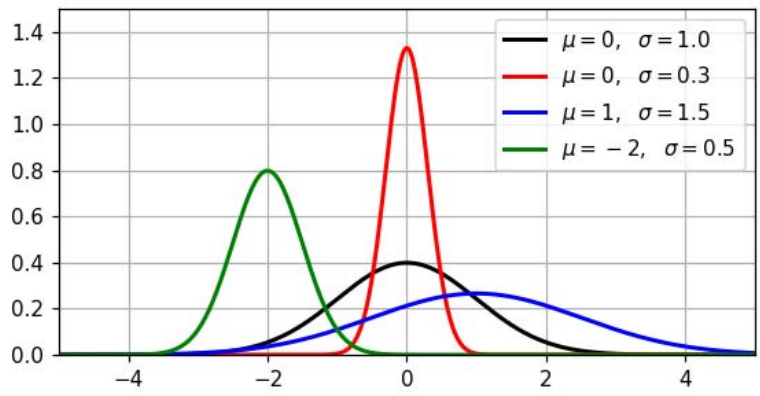

Figure 4 – The Normal, or the Gaussian curve
Рис. 4 – Кривая нормального распределения Гаусса
Слика 4 – Нормална или Гаусова крива

[2] The term Back of the envelope calculation is a rough calculation. It is more than a guess, but less than a mathematical proof.

Using the model

The alternative names for the Gaussian distribution are 6 SIGMA or LEAN 6 SIGMA. However, the model was extended adding two extra periods. Instead of 6SIGMA, 8 SIGMA model was used, Figure 5.

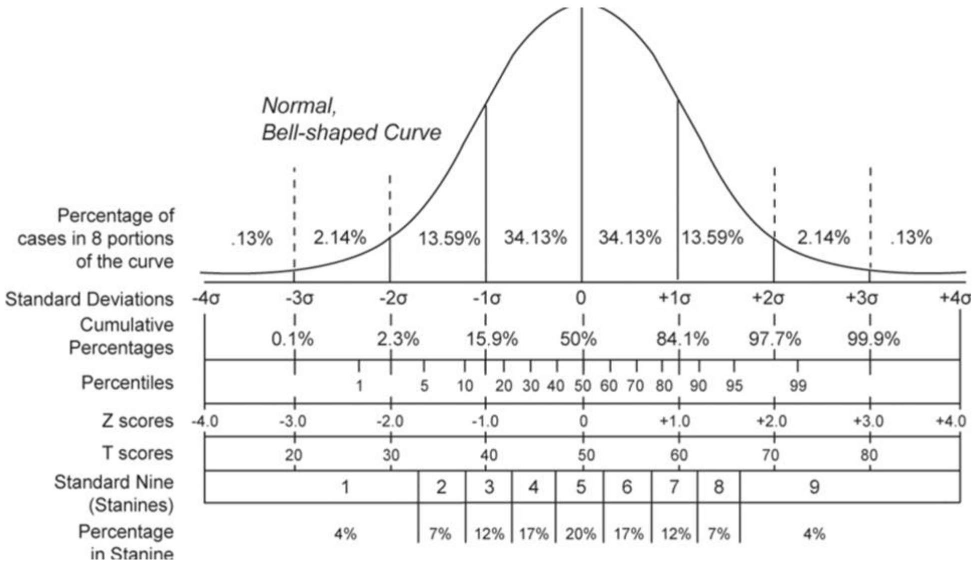

Figure 5 – Gaussian distribution extended to 8 SIGMA
Рис. 5 – Кривая распределения Гаусса расширена за 8 СИГМ
Слика 5 – Гаусова расподела проширена на 8 СИГМА

Why is an extension to eight periods important? Because the intersections between the Gaussian curve and the vertical lines that present SIGMAs are the places for decision making. Figure 6 represents this scenario (Kočović, 2020).

For calculating the Gaussian curve and the Sigmoid (S) curve, programming language Python was used. Figure 7 shows the examples for the following countries: Austria, Peru, Hungary, and Serbia.

A mathematical model can calculate the whole distribution if histograms are covered with more than 50% of the data. The algorithm calculates distribution if the minimum 3 SIGMA conditions are fulfilled, and there are no extreme peaks in one day. Otherwise, the Gaussian curve cannot be formed.

Figure 6 – Truncated Gaussian curve for Serbia, on April 23, 2020. At that time, the forecasted end of the epidemic was May 24, 2020. The dots represent the dates when critical decisions should be made.
Рис. 6 – Усеченная кривая Гаусса, относящаяся к Сербии, на 23 апреля 2020 года. По прогнозу, произведенному в тот день, эпидемия должна была остановится 24 мая 2020 года. Точками обозначены даты, когда должны были быть приняты критические решения.
Слика 6 – Делимична Гаусова крива за Србију на дан 23. априла 2020, када је предвиђено да ће знавични крај епидемије у Србији бити 24. маја 2020. године. Тачке представљају дане када је требало донети критичне одлуке.

Figure 7 represents four different countries with four different histograms and Gaussian curves. Given N and σ, the total area under the model curve is:

$$Total\ \ Area = N\sigma\sqrt{2\pi} \quad (3)$$

Here are the results for Serbia for May 10, 2020.
Total cases until that day, 10114.0
Model Cases (model total area), 10374
Accuracy of the Gaussian model, 103%
Area fraction - Serbia is about 97% into COVID-19
The forecasted day of the 7σ is May 26, 2020.

As it is shown, the model can predict, mathematically, the end of the epidemic. But, one thing is mathematics, another is real life.

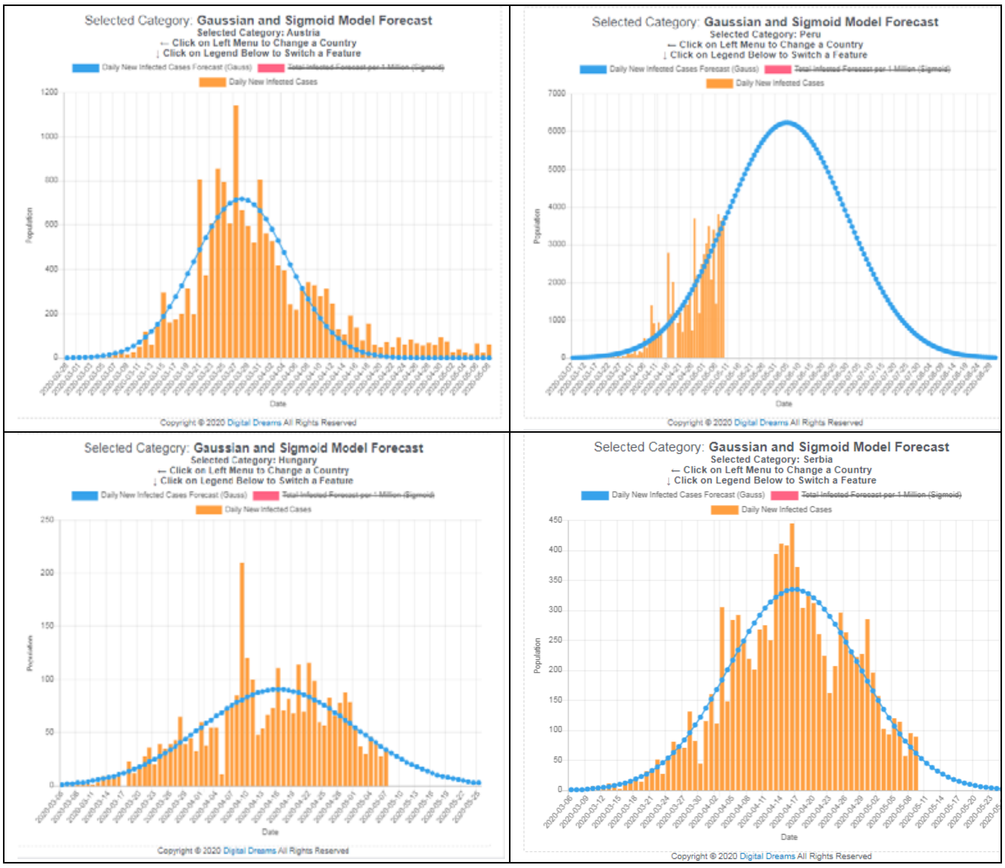

Figure 7 – Gaussian curve used for predicting the end of the epidemic per country: a) Austria, b) Peru, c) Hungary, and d) Serbia
Рис. 7 – Кривая Гаусса, относящаяся к концу эпидемии по государствам: а) Австрия, б) Перу, в) Венгрия и г) Сербия
Слика 7 – Гаусова крива коришћена за крај епидемије по државама: а) Аустрија, б) Перу, в) Мађарска и д) Србија

Link between the Gaussian curve and the Sigmoid Curve

As it was shown in Figure 1, the EpiCurve is real, but we always need forecasts. To link mathematics with real life, the Sigmoid or S-curve was used. On the other hand, the authors found a link between Gaussian and Boltzmann or Sigmoid (S) curves (Reséndiz-Muñoz et al, 2017, pp.1043-1047). In Figure 8, the link between the Gaussian curve and the S-curve was shown.

The reader can see that the starting points, the endpoints, and the slope points are shown on the curves. The vertical line is the day of the epidemic. Once again – compare #Cases in Figure 1, and the S-curve in Figure 8.

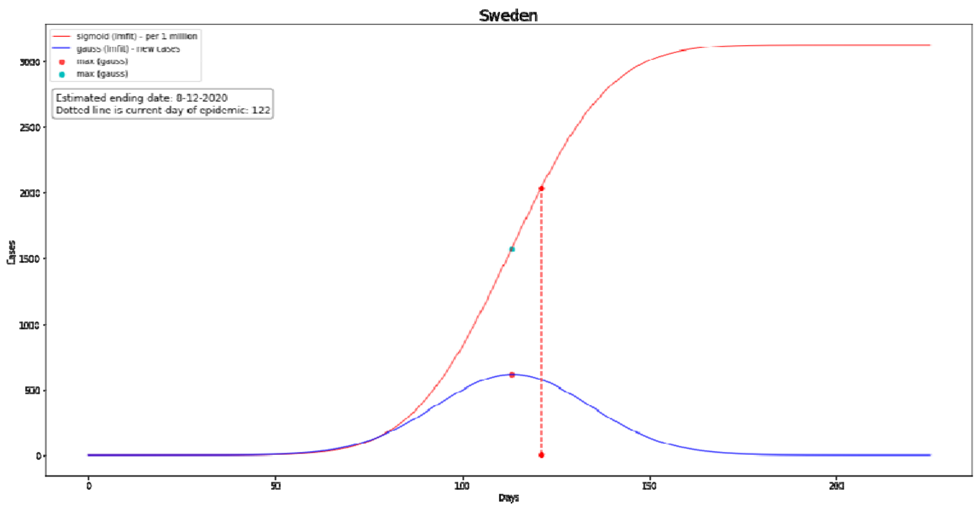

Figure 8 – COVID-19 Gaussian curve and S-curve for Sweden, on May 1st, 2020
Рис. 8 – Кривая COVID-19 по модели кривой Гаусса и С-кривой, относящаяся к Швеции на 1 мая 2020 года.
Слика 8 – Криве за COVID-19 по моделу Гаусове криве и С-криве за Шведску, 1. маја 2020. године

Final Step – fine-tuning

The Gaussian curve can calculate the date of the end of the epidemic with a probability of 99.9996%. This means that the chances are ONE in a MILLION for citizens to become ill with COVID-19 after the Gaussian distribution has ended. For Serbia – this number is 7 (sometimes this number will be 20, sometimes 0). For example, for Mexico, this number is 129.

However, for better decision making, a double logarithmic curve model was developed. Four examples are shown in Figure 9.

The x-axis contains the total number of the infected. On the y-axis, there are the numbers of the infected in the last 7 days, for every day in the epidemic. Both axes are in the logarithmic scale. The days are shown in the trajectory, so this is the third dimension presented on the curve (Kočović, 1998).

Why is this curve important?

Even in the case that the condition of 7SIGMA is fulfilled on the Gaussian curve, on the double log curve it is not. Let us compare the data for Serbia: Figure 7d for the Gaussian curve and Figure 9a for the double logarithmic curve. In Figure 7d, it seems that the epidemic was almost finished. In Figure 9a, we can see that this is not the case. Therefore, the double logarithmic curve is used for fine-tuning.

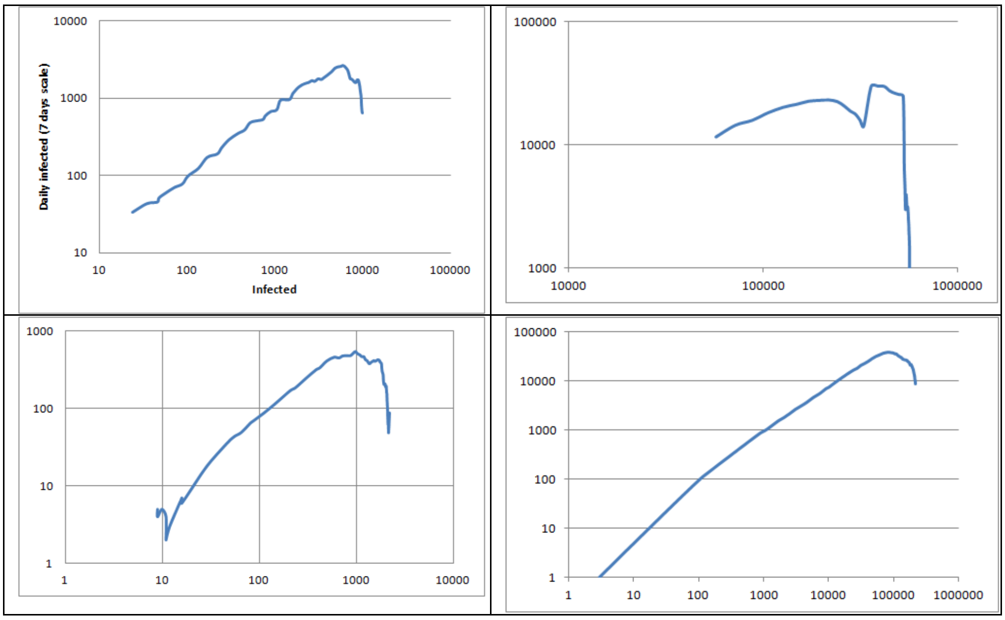

Figure 9 – Double logarithmic curve for a) Serbia, b) China, c) Croatia, and d) Italy, on May 10, 2020

Рис. 9 – Кривая в двойном логарифмическом масштабе, относящаяся к: а) Сербии, б) Китаю, в) Хорватии и г) Италии, на 10 мая 2020 г.

Слика 9 – Двострука логаритамска крива за: а) Србију, б) Кину, в) Хрватску и д) Италију, 10. маја 2020. године

Conclusion

For this research, a model presented in (Kočović et al, 2020) was developed. Further development of the epidemic/pandemic is going to link the Gaussian curve with the economic development of the countries. A smaller 8SIGMA means a shorter period of the epidemic, and eventually a higher peak. This means that more medical staff will be needed. If the curve is flattened – the duration will be longer and a possible number of the infected and the dead will be smaller. Some countries, such are United Kingdom (Flaxman et al, 2020), (Ferguson et al, 2020), USA (McKinsey & Company, 2020), and Sweden used this model of free infection. But finally, they had to change their initial decision.

References

Ferguson, N.M., & et al. 2020. *Impact of non-pharmaceutical interventions (NPIs) to reduce COVID19 mortality and healthcare demand*. Report 9, Imperial College London, pp.1-20. Available at: https://doi.org/10.25561/77482.

Flaxman, S., & et al. 2020. *Estimating the number of infections and the impact of non-pharmaceutical interventions on COVID-19 in 11 European countries*. Report 13, Imperial College London, pp.1-35. Available at: https://doi.org/10.25561/77731.

Gauss, C.F. 1809. *Theoria motus corporum coelestium in sectionibus conicis solem ambientium*. Hamburgi: sumtibus Frid. Perthes et I. H. Besser (in Latin). Available at: https://doi.org/10.3931/e-rara-522.

Kočović, P. 1998. *Geometrijsko modeliranje*, vol 1. Belgrade: Petar Kočović (in Serbian).

Kočović, P. 2020. *Petar Kočović - Gausova kriva i prognoza COVID-19 epidemije* [online] Available at: https://www.youtube.com/watch?v=4kguYa7Po2U [Accessed: 29 April 2020].

Kočović, P., Kočović, Z., & Kočović, V. 2020. *Petar Kočović's COVID-19 statistics and trends* [online]. Available at: http://digital-dreams.biz/COVID-19/index.php [Accessed: 29 April 2020].

Laplace, P.S. 1774. Mémoire sur la probabilité des causes par les évènements. *Mémoires de Mathematique et de Physique,* 6, pp.621-656 (in French) [online]. Available at: https://www.biodiversitylibrary.org/item/86068#page/7/mode/1up [Accessed: 1 May 2020].

Mann, P.S. 1994. *Statistics for Business and Economics.* Hoboken, New Jersey: Willey.

-McKinsey & Company. 2020. *COVID-19: briefing Materials* [online]. Available at: https://www.mckinsey.com/~/media/mckinsey/business%20functions/risk/our%20insights/covid%2019%20implications%20for%20business/covid%2019%20april%2013/COVID-19-facts-and-insights-april-24.ashx [Accessed: 12 April 2020].

Reséndiz-Muñoz, J., Corona-Rivera, M.A., Fernández-Muñoz, J.L., Zapata-Torres, M., Márquez-Herrera, A., & Ovando-Medina, V.M. 2017. Mathematical model of Boltzmann's sigmoidal equation applicable to the set-up of the RF-magnetron co-sputtering in thin films deposition of $Ba_xSr_{1-x}TiO_3$. *Bulletin of Materials Science*, 40, pp.1043-1047. Available at: https://doi.org/10.1007/s12034-017-1441-x.

Stahl, S. 2006. The Evolution of the Normal Distribution. *Mathematic Magazine,* 79(2), pp.96-113. Available at: https://doi.org/10.1080/0025570X.2006.11953386.

-World Health Organization. 2020. *Coronavirus disease (COVID-2019) situation reports* [online]. Available at: https://www.who.int/emergencies/diseases/novel-coronavirus-2019/situation-reports/ [Accessed: 18 May 2020].

МОНИТОРИНГ КОРОНАВИРУСА COVID-19 ПОДОБНО ПОЛЕТУ САМОЛЕТА ПО ПРИБОРАМ

Петар В. Кочович[а], *Зоран* В. Кочович[б], *Владимир* П. Кочович[в]

[а] Университет Унион «Никола Тесла», Факультет информационных технологий и инжиниринга, г. Белград, Республика Сербия, **корреспондент**

[б] Омни Логика, г. Белград, Республика Сербия

[в] IGT, г. Белград, Республика Сербия

РУБРИКА ГРНТИ: 27.00.00 МАТЕМАТИКА;
27.43.17 Математическая статистика,
27.43.51 Применение теоретико-вероятностных и статистических методов
ВИД СТАТЬИ: оригинальная научная статья

Резюме:

Введение/цель: Данная команда, в целях эпидемиологического мониторинга за COVID-19 в каждой отдельной стране мира, разработала специальную систему, которая состоит из следующих диаграмм и математических моделей: а) эпидемиологическая кривая, б) гистограмма зараженных людей, в) гистограмма зараженных людей за последних пять дней, г) кривая в двойном логарифмическом масштабе для мониторинга скорости распространения эпидемии, д) эпидемиологическое многопараметровое наблюдение и е) кривые Гаусса и Больцмана (С-кривые). В данной статье эпидемиологический мониторинг за развитием эпидемии представлен подобно полету самолета по приборам.

Методы: Наиболее сложной моделью является вычисление усеченной кривой Гаусса. В данной связи модель подробно представлена в этой статье. Кроме того, существует совпадение во времени между кривой Гаусса и С-кривой. Данные были взяты с официального сайта Всемирной организации здравоохранения. Полный набор данных состоит из кривой Гаусса, двойной кривой в логарифмическом масштабе и эпидемиологической кривой, которые рассматриваются *параллельно. В большинстве случаев использование только одного из трех указанных параметров недостаточно.*

Результаты: С целью доказательства достоверности, выбранной методологии в статье приведены десять результатов в виде диаграмм.

Выводы: При точном вычислении кривой Гаусса можно будет рассчитать и конец эпидемии. Но в некоторых случаях кривую Гаусса вычислить невозможно и в таком случае продолжительность эпидемии остается неизвестной (конец эпидемии невозможно с точностью вычислить, так как многие страны не опубликовали должным образом количество выздоровевших). В этом и заключается причина необходимости учета двойной кривой в логарифмическом масштабе. Только при сочетании этих трех диаграмм появляется правильное понимание о выборе соответствующего решения.

Ключевые слова: COVID-19, Кривая Гаусса, С-кривая.

ПРАЋЕЊЕ КОРОНА ВИРУСА COVID-19 СЛИЧНО ЈЕ ИНСТРУМЕНТАЛНОМ ЛЕТЕЊУ

Петар В. Кочовић[а], *Зоран* В. Кочовић[б], *Владимир* П. Кочовић[в]

[а] Универзитет Унион „Никола Тесла”, Факултет за информационе технологије и инжењерство, Београд, Република Србија, **аутор за преписку**

[б] Омни Логика, Београд, Република Србија

[в] IGT, Београд, Република Србија

ОБЛАСТ: математика
ВРСТА ЧЛАНКА: оригинални научни рад

Сажетак:

Увод/циљ: Ради посматрања епидемије COVID-19 у свакој појединачној држави на свету развили смо специфичан систем који се састоји од следећих дијаграма и математичких модела: а) епидемиолошке криве, б) хистограма заражених особа, в) хисторама заражених особа у претходних пет дана, г) двоструке логаритамске криве за посматрање брзине ширења епидемије, х) епидемиолошког вишепараметарског праћења и) Гаусове и Болцманове С-криве. Као што је показано у овом раду посматрање тока епидемије налик је инструменталном летењу.

Методе: Најкомплекснији модел представља израчунавање непотпуне Гаусове криве, што је детаљније анализирано у раду. Такође, показано је да постоји временска зависност између Гаусове и С-криве. Подаци су преузети са сајта Светске здравствене организације. Потпуни скуп података састоји се од

Гаусове криве, двоструке логаритамске криве и епидемиолошке криве, које се посматрају упоредо. Посматрање само једне од назначене три криве у великом броју случајева није довољно.

Резултати: Како би се доказале изабране методологије, рад садржи десетак резултата у облику дијаграма.

Закључак: Када се израчуна Гаусова крива може се доћи до податка о крају епидемије. Међутим, у неким случајевима Гаусова крива се не може израчунати, па крај епидемије није јасан, најчешће зато што многе државе нису декларисале број опорављених пацијената на адекватан начин. Зато се мора узети у обзир двострука логаритамска крива. Само комбинацијама три дијаграма добија се прави увид у доошење исправних одлука.

Кључне речи: COVID-19, Гаусова крива, С-крива.

Paper received on / Дата получения работы / Датум пријема чланка: 30.04.2020.
Manuscript corrections submitted on / Дата получения исправленной версии работы / Датум достављања исправки рукописа: 18.05.2020.
Paper accepted for publishing on / Дата окончательного согласования работы / Датум коначног прихватања чланка за објављивање: 20.05.2020.

SOLUTIONS AND ULAM-HYERS STABILITY OF DIFFERENTIAL INCLUSIONS INVOLVING SUZUKI TYPE MULTIVALUED MAPPINGS ON *b*-METRIC SPACES

Mujahid Abbas[a], *Basit* Ali[b], *Talat* Nazir[c], *Nebojša* M. Dedović[d], *Bandar* Bin-Mohsin[e], *Stojan* N. Radenović[f]

[a] Government College University, Department of Mathematics, Lahore, Islamic Republic of Pakistan;
University of Pretoria, Department of Mathematics and Applied Mathematics, Pretoria, Republic of South Africa,
e-mail: abbas.mujahid@gmail.com,
ORCID ID: https://orcid.org/0000-0001-5528-1207

[b] University of Management and Technology, Department of Mathematics, Lahore, Islamic Republic of Pakistan,
e-mail: basit.aa@gmail.com,
ORCID ID: https://orcid.org/0000-0003-4111-5974

[c] COMSATS University Islamabad, Department of Mathematics, Abbottabad Campus, Islamic Republic of Pakistan;
University of South Africa, Department of Mathematical Science, Science Campus, Johannesburg, Republic of South Africa,
e-mail: talat@ciit.net.pk,
ORCID ID: https://orcid.org/0000-0001-6516-3212

[d] University of Novi Sad, Faculty of Agriculture, Department of Agricultural Engineering, Novi Sad, Republic of Serbia,
e-mail: nebojsa.dedovic@polj.uns.ac.rs, **corresponding author**,
ORCID ID: https://orcid.org/0000-0002-4628-1405

[e] King Saud University, College of Science, Department of Mathematics, Riyadh, Kingdom of Saudi Arabia,
e-mail: balmohsen@ksu.edu.sa,
ORCID ID: https://orcid.org/0000-0002-2160-4159

[f] University of Belgrade, Faculty of Mechanical Engineering, Belgrade, Republic of Serbia,
e-mail: radens@beotel.rs,
ORCID ID: https://orcid.org/0000-0001-8254-6688

DOI: 10.5937/vojtehg68-26718; https://doi.org/10.5937/vojtehg68-26718

FIELD: Mathematics
ARTICLE TYPE: Original Scientific Paper

ACKNOWLEDGMENT: The work of the fourth author Nebojša M. Dedović is supported by the Ministry of Education, Science and Technological Development of the Republic of Serbia, project TR-37017.

Abstract:

Introduction/purpose: This paper presents coincidence and common fixed points of Suzuki type $(\alpha_* - \psi)-$ multivalued operators on b-metric spaces.

Methods: The limit shadowing property was discussed as well as the well-posedness and the Ulam-Hyers stability of the solution for the fixed point problem of such operators.

Results: The upper bound of the Hausdorff distance between the fixed point sets is obtained. Some examples are presented to support the obtained results.

Conclusion: The application of the obtained results establishes the existence of differential inclusion.

Keywords: b-metric space, multi-valued mapping, fixed point problems, Ulam-Hyers stability, initial value problem.

Introduction and preliminaries

Euclidean distance is an important measure of "nearness" between two real or complex numbers. Fréchet (1905) introduced the concept of a metric to obtain the distance between two arbitrary objects. Since then, this notion has been generalized further in one to many directions, see (An et al, 2015a), among which one of the most important generalizations is the concept of a b-metric initiated by (Czerwik, 1993). For more details of b-metric spaces see (Aleksić et al, 2018), (Hussain et al, 2012), (Kirk & Shahzad, 2014) and the references therein.

Definition 1.1 Let X be a nonempty set. A mapping $d: X \times X \to [0, +\infty)$ is said to be a b-metric on X if there exists some real constant $b \geqslant 1$ such that for any $x, y, z \in X$, the following condition holds:

a$_1$): $d(x, y) = 0$ if and only if $x = y$;

a$_2$): $d(x, y) = d(y, x)$;

a$_3$): $d(x, y) \leqslant bd(x, z) + bd(z, y)$

The pair (X, d) is termed a b-metric space with b-metric constant b. Every metric is b-metric for $b = 1$ but the converse does not hold in general (Ćirić et al, 2012), (Czerwik, 1993), (Singh & Prasad, 2008).

In the sequel, the letters, $\mathbb{R}^+$, $\mathbb{R}$, $\mathbb{N}$ and $\mathbb{Z}^+$ will denote the set of all nonnegative real numbers, the set of all real numbers, the set of all natural numbers and the set of all nonnegative integer numbers, respectively.

Let (X,d) be a b-metric space and $P(X)$ a collection of all subsets of X. Denote $Cl(X), CB(X)$, and $K(X)$ by the collection of closed, closed and bounded and compact subsets of X, respectively.

Let $U,V \in P(X)$. The gap functional D, the excess generalized function ρ, the Pompeiu-Hausdorff generalized functional H, and the functional δ induced by a b-metric d on X are defined as:

$$(1)\quad D(U,V)=\begin{cases}\inf_{u\in U,v\in V} d(u,v), \text{if } U\neq V\neq \emptyset\neq U,\\ 0, \text{if } U=V=\emptyset,\\ \infty, \text{otherwise.}\end{cases}$$

$$(2)\quad \rho(U,V)=\begin{cases}\sup_{u\in U} D(u,V), \text{if } U\neq V\neq \emptyset\neq U,\\ 0, \text{if } U=\emptyset,\\ \infty, \text{if } V=\emptyset, U\neq\emptyset.\end{cases}$$

$$(3)\quad H(U,V)=\begin{cases}\max\{\rho(U,V),\rho(V,U)\}, \text{if } U\neq V\neq \emptyset\neq U,\\ 0, \text{if } U=V=\emptyset,\\ \infty, \text{otherwise.}\end{cases}$$

$$\delta(U,V)=\begin{cases}\sup_{u\in U,v\in V} d(u,v), \text{if } U\neq V\neq \emptyset\neq U,\\ 0, \text{if } U=V=\emptyset,\\ \infty, \text{otherwise.}\end{cases}$$

An et al (2015b) studied the topological properties of b-metric spaces and stated that a b-metric is not necessarily continuous in each variable. If a b-metric is continuous in one variable, then it is continuous in other variable. A ball $B(u_0,\epsilon)=\{v\in X: d(u_0,v)<\epsilon\}$ in a b-metric space (X,d) is not necessarily an open set. A ball is an open set if d is continuous in one variable.

Let (X,d) be a b-metric space. We call (f,T) a hybrid pair of mappings if $f: X\to X$ and $T: X\to CB(X)$.

A mapping f is called a contraction if there is some real constant $r\in[0,1)$ such that for any $u,v\in X$, we have $d(fu,fv)\leqslant rd(u,v)$.

A point u in X is a fixed point of f, if $u=fu$, a fixed point of T, if $u\in Tu$, a coincidence point of (f,T) if $fu\in T$, and a common fixed point of (f,T) if $u=fu\in Tu$. Denote $F(f), F(T)$ by the fixed points of f and T, respectively, and $C(f,T)$ and $F(f,T)$ by coincidence and common fixed point of (f,T), respectively.

Definition 1.2, *compare with (Abbas et al, 2012). A pair (f,T) is w-compatible if $f(Tu) \subseteq T(fu)$ for all $u \in C(f,T)$. The mapping f is T-weakly commuting at some point $u \in X$ if $f^2(u) \in T(fu)$.*

Using an axiom of choice, Haghi et al (2011) proved the following lemma.

Lemma 1.3 *(Haghi et al, 2011) Let $f: X \to X$ be a self-mapping of a nonempty set X, then there exists a subset $E \subseteq X$ such that $f(E) = f(X)$ and f is one-to-one on E.*

Lemma 1.4, *compare (Rus et al, 2003). Let (X,d) be a b-metric space, $U,V \in P(X)$. If there exists a $\lambda > 0$ such that for each $u \in U$, there exists a $v \in V$ such that $d(u,v) \leqslant \lambda$, and for each $v \in V$, there exists a $u \in U$ such that $d(u,v) \leqslant \lambda$, then $H(U,V) \leqslant \lambda$.*

We need following lemmas given in (Czerwik, 1993), (Singh & Prasad, 2008).

Lemma 1.5 *Let (X,d) be a b-metric space, $u,v \in X$, $\{u_n\}$ a sequence in X and $U,V \in CB(X)$. The following statements hold:*

b_1-: *$(CB(X),H)$ is a b-metric space and $(CB(X),H)$ is complete whenever (X,d) is complete;*

b_2-: *$D(u,V) \leqslant H(U,V)$ for all $u \in U$;*

b_3-: *$D(u,U) \leqslant bd(u,v) + bD(v,U)$;*

b_4-: *for $h > 1$ and $u \in U$, there is a $v \in V$ such that $d(u,v) \leqslant hH(U,V)$;*

b_5-: *for every $h > 0$ and $u \in U$, there is a $v \in V$ such that $d(u,v) \leqslant H(U,V) + h$;*

b_6-: *$D(u,U) = 0$ if and only if $u \in \overline{U} = U$;*

b_7-: *$d(u_0,u_n) \leqslant bd(u_0,u_1) + \ldots + b^{n-1}d(u_{n-2},u_{n-1}) + b^{n-1}d(u_{n-1},u_n)$;*

b_8-: *$\{u_n\}$ is a Cauchy sequence if and only if for $\epsilon > 0$, there exists $n(\epsilon) \in N$ such that for each $n,m \geqslant n(\epsilon)$ we have $d(u_n,u_m) < \epsilon$;*

b_9-: *$\{u_n\}$ is a convergent sequence if and only if there exists $u \in X$ such that for all $\epsilon > 0$ there exists $n(\epsilon) \in N$ such that for all $n \geqslant n(\epsilon)$, $d(u_n,u) < \epsilon$.*

A sequence $\{u_n\}$ is convergent to $u \in X$ if and only if $\lim_{n\to+\infty} d(u_n,u) = 0$.

A subset $Y \subset X$ is closed if and only if for each sequence $\{u_n\}$ in Y that converges to an element u, $u \in Y$. A subset $Y \subset X$ is bounded if diam(Y) is finite, where diam$(Y) = \sup\{d(u,v): u,v \in Y\}$. A b-metric space (X,d) is said to be complete if every Cauchy sequence in X is convergent in X.

Following are some known classes of mappings given in (Berinde, 1993), (Berinde, 1996), (Berinde, 1997), (Bota et al, 2015), (Rus, 2001).

Let $\psi, \varphi: \mathbb{R}^+ \to \mathbb{R}^+$, then

c$_1$-: $\Psi_1 = \left\{\psi: \psi \text{ is increasing}, \lim_{n\to+\infty} \psi^n(t) = 0, \text{for any } t \geqslant 0\right\}$.

The elements in this class are called comparison functions. If $\psi \in \Psi_1$, then the nth iterate of ψ is a comparison function, ψ is continuous at $t = 0$, and $\psi(t) < t$, for any $t > 0$.

c$_2$-: $\Psi_2 = \{\psi: \sum_{n=1}^{\infty} \psi^n(t) < +\infty \text{ for all } t > 0 \text{ and} \psi \text{ is nondecreasing}\}$.

c$_3$-: $\Psi_3 = \begin{Bmatrix} \psi: \psi \text{ is increasing, there exists a } n_0 \in \mathbb{N}, a \in (0,1), \\ \text{a sequence } u_n \geqslant 0 \text{ such that } \sum_{n=1}^{\infty} u_n < +\infty \text{and} \\ \psi^{n+1}(t) \leqslant a\psi^n(t) + u_n \text{ for all } n \geqslant n_0,\ t \geqslant 0 \end{Bmatrix}$

is called the class of (c) −comparison functions.

c$_4$-: $\Psi_4 = \begin{Bmatrix} \psi: \psi \text{ is increasing, there exists a } n_0 \in \mathbb{N}, a \in (0,1), \\ b \geqslant 1, \text{a sequence } u_n \geqslant 0 \text{ such that } \sum_{n=1}^{\infty} u_n < +\infty \text{and} \\ b^{n+1}\psi^{n+1}(t) \leqslant ab^n\psi^n(t) + u_n \text{ for all } n \geqslant n_0,\ t \geqslant 0 \end{Bmatrix}$

is known as the class of (b) −comparison functions.

Note that $\Psi_2 \subseteq \Psi_1$. If $b = 1$, then $\Psi_3 = \Psi_4$.

Lemma 1.6 *(Berinde, 1993) If $\psi \in \Psi_4$ with $b \geqslant 1$, then the series $\sum_{n=0}^{\infty} b^n\psi^n(t)$ converges for all $t \in \mathbb{R}^+$, and $r_b(t) = \sum_{n=0}^{\infty} b^n\psi^n(t)$ is increasing and continuous at $t = 0$.*

In the light of the above lemma, $\Psi_4 \subseteq \Psi_1$.

Lemma 1.7 *(Păcurar, 2010) If $\psi \in \Psi_4$ with $b \geqslant 1$, and $\{a_n\} \subseteq \mathbb{R}^+$ is such that $\lim_{n\to+\infty} a_n = 0$, then*

$$\lim_{k\to+\infty} \sum_{n=0}^{\infty} b^{k-n}\psi^{k-n}(a_n) = 0.$$

Example 1.8 Let $\psi(t) = qt$, where $q \in [0,1)$ and $t \in \mathbb{R}^+$. Consider $\sum_{k=0}^{\infty} u_k(t)$, where $u_k(t) = b^k\psi^k(t)$ and $b \geqslant 1$. If $t = 0$, then $\sum_{k=0}^{\infty} u_k(t)$

converges trivially. If $t > 0$, then by the generalized ratio test (Berinde, 1993), $\sum_{k=0}^{\infty} u_k(t)$ is convergent for any $t > 0$. Hence for some $n_0 \in \mathbb{N}, b^{n+1}\psi^{n+1}(t) \leqslant ab^n\psi^n(t) + u_n$ for all $n \geqslant n_0$ and $t \geqslant 0$. Consequently, we have $\psi \in \Psi_4$.

The Banach contraction principle (BCP) (Banach, 1922) states that a contraction mapping on a complete metric space has a unique fixed point.

Let $\alpha: X \times X \to \mathbb{R}^+$. A mapping $f: X \to X$ is called an α −admissible if for all $u, v \in X, \alpha(u, v) \geqslant 1$ implies that $\alpha(fu, fv) \geqslant 1$. Samet et al (2012), Theorem 1, obtained the following generalization of BCP.

Theorem 1.9 *Let (X, d) be a complete metric space and $f: X \to X$ an α −admissible mapping. Suppose that there is an element u_0 in X with $\alpha(u_0, fu_0) \geqslant 1$. If for any $u, v \in X$, there exists $\psi \in \Psi_2$ such that $\alpha(u, v)d(fu, fv) \leqslant \psi(d(u, v))$,then $F(f)$ is nonempty provided that f is continuous.*

Suzuki (2008) provided an interesting generalization of BCP that characterizes metric completeness.

For some other important generalizations of BCP, see (Berinde, 1993), (Berinde, 1996), (Berinde, 1997), (Bhaskar & Lakshmikantham, 2006), (Nieto & Rodríguez-López, 2005), (Nieto & Rodríguez-López, 2007), (Ran & Reurings, 2004) and references therein. A number of fixed point theorems have been obtained in b-metric spaces (Aleksić et al, 2019a), (Aleksić et al, 2019b), (Ali & Abbas, 2017), (An et al, 2015a), (An et al, 2015a), (Ćirić et al, 2012), (Chifu & Petruşel, 2014), (Czerwik, 1993), (Karapinar et al, 2020), (Latif, 2015), (Mitrović, 2019), (Păcurar, 2010).

The development of the metric fixed point theory of multivalued mappings was initiated by (Nadler, 1969). He introduced the concept of set-valued contraction mappings and extended the Banach contraction principle to set-valued mappings by using the Hausdorff metric as follows.

Theorem 1.10 *Let (X, d) be a complete metric space. If a multivalued mapping $T: X \longrightarrow CB(X)$ satisfies $H(Tu, Tv) \leqslant rd(u, v)$ for all $u, v \in X$ and for some $r \in [0,1)$, then $F(T)$ is nonempty.*

The fixed point theory of multivalued mappings provides a useful machinery to analyze the problems of pure, applied and computational mathematics which can be reformulated in the form of an inclusion for an appropriate multivalued mapping.

For more results in this direction, we refer to (Abbas et al, 2012), (Abbas et al, 2013), (Asl et al, 2012), (Rus et al, 2003), (Mitrović et al, 2020).

Khojasteh et al (2014) proved a new type of the fixed point theorem for multivalued mappings in metric spaces as follows.

Theorem 1.11 *Let (X,d) be a complete metric space. If a multivalued mapping $T: X \longrightarrow CB(X)$ satisfies*

$$H(Tu,Tv) \leqslant \left(\frac{D(u,Tv)+D(v,Tu)}{1+\delta(u,Tu)+\delta(v,Tv)}\right) d(u,v) \tag{1.1}$$

for all $u,v \in X$, then $F(T)$ is nonempty.

Recently, Rhoades (2015) improved the result of Khojasteh for two multivalued mappings as follows.

Theorem 1.12 *(Rhoads, 2015) Let (X,d) be a complete metric space. If multivalued mappings $S,T: X \longrightarrow CB(X)$ satisfy $H(Su,Tv) \leqslant n_{S,T}(u,v) m_{S,T}(u,v)$ for all $u,v \in X$, then $F(T) \cap F(S)$ is nonempty, where*

$$\begin{aligned} n_{S,T}(u,v) &= \left(\frac{\max\{d(u,v), D(u,Su)+D(v,Tv), D(u,Tv)+D(v,Su)\}}{1+\delta(u,Su)+\delta(v,Tv)}\right) \\ m_{S,T}(u,v) &= \max\left\{d(u,v), D(u,Su), D(v,Tv), \frac{D(u,Tv)+D(v,Su)}{2}\right\}. \end{aligned} \tag{1.2}$$

If $S = T$ in above theorem then we get the following result.

Theorem 1.13, *(Rhoads, 2015). Let (X,d) be a complete metric space. If a multivalued mapping $T: X \longrightarrow CB(X)$ satisfiesfor all $u,v \in X, H(Tu,Tv) \leqslant n_{T,T}(u,v) m_{T,T}(u,v)$, then $F(T)$ is nonempty.*

Let $\alpha: X \times X \to \mathbb{R}^+$ and $U,V \in P(X)$. Define $\alpha_*(U,V) = \inf_{u \in U, v \in V} \alpha(u,v)$.

A multivalued mapping $T: X \to Cl(X)$ is called α_*-admissible mapping if for any $u,v \in X, \alpha(u,v) \geqslant 1$ implies that $\alpha_*(Tu,Tv) \geqslant 1$. The concepts of α_*-admissible mapping coincides with $\alpha-$admissible mapping in case of a single valued mapping.

Asl et al (2012), Theorem 1, defined $(\alpha_* - \psi) -$contractive multifunctions and proved the following result.

Theorem 1.14 Let (X, d) be a complete metric space and $T: X \to Cl(X)$ an $\alpha_* -$admissible mapping that satisfies $\alpha_*(Tu, Tv)H(Tu, Tv) \leqslant \psi(d(u, v))$ for all $u, v \in X$ and $\psi \in \Psi_2$. Moreover, if there exists a $u_0 \in X$ and $u_1 \in Tu_0$ such that $\alpha(u_0, u_1) \geqslant 1$, then $F(T)$ is nonempty provided that if $\{u_n\}$ is a sequence in X such that $\alpha(u_n, u_{n+1}) \geqslant 1$ for all n and $\lim_{n \to +\infty} u_n = u$, then $\alpha(u_n, u) \geqslant 1$ for all n.

In what follows, we assume that a b-metric d is continuous in one variable.

Definition 1.15, compare with (Rus et al, 2003). Let (X, d) be a b-metric space. A mapping $T: X \to Cl(X)$ is called a multivalued weakly Picard operator (MWP operator), if for all $u \in X$ and for some $v \in Tu$, there exists a sequence $\{u_n\}$ satisfying (a$_1$) $u_0 = u, u_1 = v$, (a$_2$) $u_{n+1} \in Tu_n$ for all $n \geqslant 0$, (a$_3$) $\{u_n\}$ converges to some $z \in F(T)$. The sequence $\{u_n\}$ satisfying (a$_1$) and (a$_2$) is called a sequence of successive approximations (ssa) of T starting from (u, v). If T is a single-valued mapping, then we call it a Picard operator if it satisfies (a$_1$) to (a$_3$).

Recently Bota et al (2015) proved the fixed point theorem for $(\alpha_* - \psi) -$contractive multivalued mappings as follows.

Theorem 1.16 Let (X, d) be a complete b-metric space, $\alpha: X \times X \to \mathbb{R}^+$ and $T: X \to Cl(X)$ an $\alpha_* -$admissible multivalued operator that satisfies

$$\alpha_*(Tu, Tv)H(Tu, Tv) \leqslant \psi(d(u, v))$$

for all $u, v \in X$ and $\psi \in \Psi_4$. Assume that there exists a $u_0 \in X$ and $u_1 \in Tu_0$ such that $\alpha(u_0, u_1) \geqslant 1$. Then T is a MWP operator provided that if there is a sequence $\{u_n\}$ in X such that $u_n \to u$, then $\alpha(u_n, u) \geqslant 1$ for all $n \in \mathbb{N}_1$.

A mapping $T: X \to Cl(X)$ is called $(\alpha_* - f)$ –admissible mapping if $u, v \in X, \alpha(fu, fv) \geqslant 1$ implies that $\alpha_*(Tu, Tv) \geqslant 1$.

Let (X, d) be a b-metric space, $g: X \to X$ and $T: X \to Cl(X)$. Set

$$N_T(u,v)=\frac{\max\{d(u,v),D(u,Tu)+D(v,Tv),D(u,Tv)+D(v,Tu)\}}{b(\delta(u,Tu)+\delta(v,Tv)+1)},$$
$$M_T(u,v)=\max\left\{d(u,v),D(u,Tu),D(v,Tv),\frac{D(u,Tv)+D(v,Tu)}{2b}\right\},$$

and

$$N_{g,T}(u,v)=\frac{\max\{d(gu,gv),D(gu,Tu)+D(gv,Tv),D(gu,Tv)+D(gv,Tu)\}}{b(\delta(gu,Tu)+\delta(gv,Tv)+1)}$$
$$M_{g,T}(u,v)=\max\left\{d(gu,gv),D(gu,Tu),D(gv,Tv),\frac{D(gu,Tv)+D(gv,Tu)}{2b}\right\}.$$

We now give the following definitions.

Definition 1.17 *Let (X,d) be a b-metric space. A mapping $T:X\to Cl(X)$ is called Suzuki type $(\alpha_*-\psi)$ – multivalued operator if there exists a $\psi\in\Psi_4$ such that*

$$\frac{1}{2}D(u,Tu)\leqslant bd(u,v) \qquad (1.3)$$

implies

$$\alpha_*(Tu,Tv)H(Tu,Tv)\leqslant max\{1,N_T(u,v)\}\psi(M_T(u,v)) \qquad (1.4)$$

for all $u,v\in X$.

If in the above definition we replace a mapping T by a single valued mapping $f:X\to X$, then we call it a Suzuki type $(\alpha_*-\psi)$ – operator.

Definition 1.18 *Let (X,d) be a b-metric space. A hybrid pair (g,T) is called a Suzuki type $(\alpha_*-\psi)$ – hybrid pair of operators if there exists a $\psi\in\Psi_4$ such that*

$$\frac{1}{2}D(gu,Tu)\leqslant bd(gu,gv) \qquad (1.5)$$

implies

$$\alpha_*(Tu,Tv)H(Tu,Tv)\leqslant \max\{1,N_{g,T}(u,v)\}\psi\big(M_{g,T}(u,v)\big) \qquad (1.6)$$

for all $u,v\in X$.

In case T is replaced by a single valued mapping $f: X \to X$, we call it a Suzuki type $(\alpha_* - \psi)$ – pair of operators.

Fixed point of Suzuki type $(\boldsymbol{\alpha_*} - \boldsymbol{\psi})$ – multivalued operators on b-metric spaces

In this section, we prove that Suzuki type $(\alpha_* - \psi)$ – multivalued operators are MWP operators.

Theorem 2.1 *Let (X, d) be a complete b-metric space, $\alpha: X \times X \to \mathbb{R}^+$ and $T: X \to Cl(X)$ a Suzuki type $(\alpha_* - \psi)$ –multivalued operator. Further, assume that T is α_* –admissible mapping and there exists $x_0 \in X$ and $x_1 \in Tx_0$ such that $\alpha(x_0, x_1) \geqslant 1$. If for any sequence $\{x_n\}$ converging to x in X, we have $\alpha(x_n, x) \geqslant 1$ for all $n \in \mathbb{Z}^+$, then*

d₁-: *T is an MWP operator.*

d₂-: *If there is some $u \in F(T)$ such that $u \neq z$ and $\alpha(z, u) \geqslant 1$, then $d(z, u) > \frac{1}{2}$ provided that $1 \leqslant N_T(x, y)$ for all $x, y \in X$.*

Proof. (d_1) By the given assumption, there exists $x_0 \in X$ and $x_1 \in Tx_0$ such that $\alpha(x_0, x_1) \geqslant 1$. If $x_0 = x_1$, then $x_0 \in Tx_0$. Define a sequence $\{x_n\}$ in X by $x_n = x_1 = x_0$ for all $n \in \mathbb{Z}^+$. Thus $x_n \in Tx_n$ for all $n \geqslant 0$ and $\{x_n\}$ converges to $x = x_0 \in F(T)$ and hence T is an MWP operator. Let $x_0 \neq x_1$. Since T is $\alpha_* -$ admissible mapping, $\alpha_*(x_0, x_1) \geqslant 1$ implies that $\alpha_*(Tx_0, Tx_1) \geqslant 1$. As T is a Suzuki type $(\alpha_* - \psi) -$ multivalued operator and

$$\frac{1}{2} D(x_0, Tx_0) \leqslant d(x_0, x_1) \leqslant bd(x_0, x_1), \qquad (2.1)$$

so from (1.4), we obtain

$$\begin{aligned} &< D(x_1, Tx_1) \leqslant H(Tx_0, Tx_1) < \alpha_*(Tx_0, Tx_1) H(Tx_0, Tx_1) \\ &\leqslant \max\{1, N_T(x_0, x_1)\} \psi(M_T(x_0, x_1)) \\ &= \max\left\{1, \left(\frac{\max\{d(x_0, x_1), D(x_0, Tx_0) + D(x_1, Tx_1), D(x_0, Tx_1) + D(x_1, Tx_0)\}}{b(1 + \delta(x_0, Tx_0) + \delta(x_1, Tx_1))}\right)\right\} \\ &\quad \psi\left(\max\left\{d(x_0, x_1), D(x_0, Tx_0), D(x_1, Tx_1), \frac{D(x_0, Tx_1) + D(x_1, Tx_0)}{2b}\right\}\right) \end{aligned}$$

$$\leqslant \frac{\psi\left(\max\left\{d(x_0,x_1),D(x_1,Tx_1),\frac{d(x_0,x_1)+D(x_1,Tx_1)}{2}\right\}\right)}{\max\left\{1,\left(\frac{\max\{d(x_0,x_1),d(x_0,x_1)+D(x_1,Tx_1),bd(x_0,x_1)+bD(x_1,Tx_1)\}}{b(1+d(x_0,x_1)+D(x_1,Tx_1))}\right)\right\}}$$

$$\leqslant \frac{\psi\left(\max\left\{d(x_0,x_1),D(x_1,Tx_1),\frac{d(x_0,x_1)+D(x_1,Tx_1)}{2}\right\}\right)}{\max\left\{1,\left(\frac{d(x_0,x_1)+D(x_1,Tx_1)}{1+d(x_0,x_1)+D(x_1,Tx_1)}\right)\right\}}$$

$$\leqslant \psi(\max\{d(x_0,x_1),D(x_1,Tx_1)\}).$$

That is

$$0 < D(x_1,Tx_1) \leqslant \psi(\max\{d(x_0,x_1),D(x_1,Tx_1)\}). \tag{2.2}$$

If $\max\{d(x_0,x_1),D(x_1,Tx_1)\} = D(x_1,Tx_1)$, then (2.2) implies that

$$0 < D(x_1,Tx_1) \leqslant \psi(D(x_1,Tx_1)). \tag{2.3}$$

As $D(x_1,Tx_1) > 0$ and $\psi \in \Psi_4$, (2.3) give

$$0 < D(x_1,Tx_1) \leqslant \psi(D(x_1,Tx_1)) < D(x_1,Tx_1),$$

a contradiction. Hence $\max\{d(x_0,x_1),D(x_1,Tx_1)\} = d(x_0,x_1)$. From (2.3), it follows that

$$0 < D(x_1,Tx_1) \leqslant \psi(d(x_0,x_1)). \tag{2.4}$$

Let $q > 1$. We may choose $x_2 \in Tx_1$ such that

$$0 < D(x_1,Tx_1) \leqslant d(x_1,x_2) < qD(x_1,Tx_1) \leqslant q\psi(d(x_0,x_1)).$$

That is

$$0 < d(x_1,x_2) < qD(x_1,Tx_1) \leqslant q\psi(d(x_0,x_1)). \tag{2.5}$$

Since $\alpha(x_1,x_2) \geqslant \alpha(Tx_0,Tx_1) \geqslant 1$, we get $\alpha(Tx_1,Tx_2) \geqslant 1$. Set $c_0 = d(x_0,x_1) > 0$, then from (2.5) we get $x_1 \neq x_2$ and $d(x_1,x_2) < q\psi(c_0)$. As $\psi \in \Psi_4$, so

$$\psi(d(x_1,x_2)) < \psi\big(q\psi(c_0)\big). \tag{2.6}$$

If $q_1 = \frac{\psi(q\psi(c_0))}{\psi(d(x_1,x_2))}$, then by (2.6) $q_1 > 1$. Now, if $x_2 \in Tx_2$ then the proof is finished. Let $x_2 \notin Tx_2$. Note that

$$\frac{1}{2}D(x_1, Tx_1) \leqslant d(x_1, x_2) \leqslant bd(x_1, x_2).$$

By (1.4)

$$\begin{aligned}
&< D(x_2, Tx_2) \leqslant H(Tx_1, Tx_2) < \alpha_*(Tx_1, Tx_2)H(Tx_1, Tx_2) \\
&\leqslant \max\{1, N_T(x_1, x_2)\}\psi(M_T(x_1, x_2)) \\
&= \max\left\{1, \left(\frac{\max\{d(x_1,x_2), D(x_1,Tx_1) + D(x_2,Tx_2), D(x_1,Tx_2) + D(x_2,Tx_1)\}}{b\big(1 + \delta(x_1,Tx_1) + \delta(x_2,Tx_2)\big)}\right)\right\} \\
&\quad \psi\left(\max\left\{d(x_1,x_2), D(x_1,Tx_1), D(x_2,Tx_2), \frac{D(x_1,Tx_2) + D(x_2,Tx_1)}{2b}\right\}\right) \\
&\leqslant \max\left\{1, \left(\frac{\max\{d(x_1,x_2), d(x_1,x_2) + D(x_2,Tx_2), b(d(x_1,x_2) + D(x_2,Tx_2))\}}{b(1 + d(x_1,x_2) + D(x_2,Tx_2))}\right)\right\} \\
&\quad \psi\left(\max\left\{d(x_1,x_2), d(x_1,x_2), D(x_2,Tx_2), \frac{d(x_1,x_2) + D(x_2,Tx_2)}{2}\right\}\right) \\
&\leqslant \max\left\{1, \left(\frac{d(x_1,x_2) + D(x_2,Tx_2)}{1 + d(x_1,x_2) + D(x_2,Tx_2)}\right)\right\} \\
&\quad \psi\left(\max\left\{d(x_1,x_2), d(x_1,x_2), D(x_2,Tx_2), \frac{d(x_1,x_2) + D(x_2,Tx_2)}{2}\right\}\right) \\
&\leqslant \psi(\max\{d(x_1,x_2), D(x_2,Tx_2)\}).
\end{aligned}$$

That is

$$0 < D(x_2, Tx_2) \leqslant \psi(\max\{d(x_1,x_2), D(x_2,Tx_2)\}). \tag{2.7}$$

If $\max\{d(x_1,x_2), D(x_2,Tx_2)\} = D(x_2,Tx_2)$, then

$$0 < D(x_2, Tx_2) \leqslant \psi(D(x_2,Tx_2)). \tag{2.8}$$

Now $D(x_2,Tx_2) > 0$, $\psi \in \Psi_4$ and (2.8) give

$$0 < D(x_2,Tx_2) \leqslant \psi(D(x_2,Tx_2)) < D(x_2,Tx_2),$$

a contradiction. Hence

$$0 < D(x_2,Tx_2) \leqslant \psi(d(x_1,x_2)). \tag{2.9}$$

We may choose $x_3 \in Tx_2$ such that

$$0 < D(x_2, Tx_2) \leqslant d(x_2, x_3) < q_1 D(x_2, Tx_2) \leqslant q_1 \psi(d(x_1, x_2)) = \psi\big(q\psi(c_0)\big).$$

That is

$$0 < d(x_2, x_3) < q_1 D(x_2, Tx_2) \leqslant q_1 \psi(d(x_1, x_2)) = \psi\big(q\psi(c_0)\big). \qquad (2.10)$$

As $\alpha(x_2, x_3) \geqslant \alpha(Tx_1, Tx_2) \geqslant 1$, so $\alpha(Tx_2, Tx_3) \geqslant 1$. From (2.10), we get $x_2 \neq x_3$ and

$$\psi(d(x_2, x_3)) < \psi^2\big(q\psi(c_0)\big). \qquad (2.11)$$

Set $q_2 = \frac{\psi^2(q\psi(c_0))}{\psi(d(x_2,x_3))} > 1$. If $x_3 \in Tx_3$ then we are done. Suppose that $x_3 \notin Tx_3$. Similarly, we obtain $x_4 \in Tx_3$ such that

$$0 < d(x_3, x_4) < q_1 D(x_3, Tx_3) \leqslant q_2 \psi(d(x_2, x_3)) = \psi^2\big(q\psi(c_0)\big). \qquad (2.12)$$

Continuing this way, we can obtain a sequence $\{x_n\}$ in X such that $x_{n+1} \in Tx_n, x_{n+1} \neq x_n, \alpha(x_{n+1}, x_{n+2}) \geqslant 1$, and it satisfies:

$$0 < D(x_{n+1}, Tx_{n+1}) \leqslant \psi(d(x_n, x_{n+1})) \qquad (2.13)$$

and

$$0 < d(x_{n+1}, x_{n+2}) < \psi^n\big(q\psi(c_0)\big) \qquad (2.14)$$

for all $n \in \mathbb{Z}^+$. From (2.14), for $n, m \in \mathbb{N}$ with $m > n$, we have

$$\begin{aligned} d(x_n, x_m) &\leqslant bd(x_n, x_{n+1}) + b^2 d(x_{n+1}, x_{n+2}) + \ldots \\ &\quad + b^{m-n} d(x_{m-2}, x_{m-1}) + b^{m-n} d(x_{m-1}, x_m) \\ &\leqslant b\psi^{n-1}\big(q\psi(c_0)\big) + b^2\psi^n\big(q\psi(c_0)\big) + \ldots \\ &\quad + b^{m-n}\psi^{m-3}\big(q\psi(c_0)\big) + b^{m-n}\psi^{m-2}\big(q\psi(c_0)\big) \\ &= \frac{1}{b^{n-2}}\Big(b^{n-1}\psi^{n-1}\big(q\psi(c_0)\big) + b^n\psi^n\big(q\psi(c_0)\big) + \ldots \\ &\quad + b^{m-2}\psi^{m-2}\big(q\psi(c_0)\big)\Big) \end{aligned}$$

$$= \frac{1}{b^{n-2}} \sum_{i=n-1}^{m-2} b^i \psi^i\big(q\psi(c_0)\big)$$

$$= \frac{1}{b^{n-2}} \left(\sum_{i=0}^{m-2} b^i \psi^i\big(q\psi(c_0)\big) - \sum_{i=0}^{n-2} b^i \psi^i\big(q\psi(c_0)\big) \right).$$

That is

$$d(x_n, x_m) \leqslant \frac{1}{b^{n-2}} \left(\sum_{i=0}^{m-2} b^i \psi^i\big(q\psi(c_0)\big) - \sum_{i=0}^{n-2} b^i \psi^i\big(q\psi(c_0)\big) \right). \tag{2.15}$$

Set $S_n = \sum_{i=0}^{n} b^i \psi^i\big(q\psi(c_0)\big)$. Then from (2.15) we obtain that

$$d(x_n, x_m) \leqslant \frac{1}{b^{n-2}} (S_{m-2} - S_{n-2}). \tag{2.16}$$

By Lemma 1.6, $\sum_{i=0}^{\infty} b^i \psi^i(t)$ converges for any $t \geqslant 0$. Hence $\lim_{n\to+\infty} S_{n-2} = S$ for some $S \in \mathbb{R}^+$. If $b = 1$, then from (2.16) we get $\lim_{n\to+\infty} d(x_n, x_m) \leqslant \lim_{n\to+\infty} S_{m-1} - \lim_{n\to+\infty} S_{n-1} = 0$. If $b > 1$, then from (2.16) we have

$$\lim_{n\to+\infty} d(x_n, x_m) \leqslant \lim_{n\to+\infty} \frac{1}{b^{n-1}} (S_{m-1} - S_{n-1}) \leqslant \lim_{n\to+\infty} \frac{S_{m-1}}{b^{n-1}} = 0$$

for all $m, n \in \mathbb{N}$. Hence $\{x_n\}$ is a Cauchy sequence in X. There exists $z \in X$ such that

$$\lim_{n\to+\infty} d(x_n, z) = 0. \tag{2.17}$$

Now we show that $z \in F(T)$. If $D(z, Tz) > 0$, then we claim that one of the following two inequalities

$$\frac{1}{2} D(x_n, Tx_n) \leqslant b d(x_n, z) \tag{2.18}$$

$$\frac{1}{2}D(x_{n+1},Tx_{n+1}) \leqslant bd(x_{n+1},z) \tag{2.19}$$

holds for all $n \in \mathbb{Z}^+$. Assume on the contrary that there exists an $n_0 \in \mathbb{Z}^+$ such that

$$\frac{1}{2}D(x_{n_0},Tx_{n_0}) > bd(x_{n_0},z) \tag{2.20}$$

and

$$\frac{1}{2}D(x_{n_0+1},Tx_{n_0+1}) > bd(x_{n_0+1},z). \tag{2.21}$$

Now from (2.13), (2.20) and (2.21), we have

$$\begin{aligned}
&d(x_{n_0},x_{n_0+1}) \leqslant bd(x_{n_0},z) + bd(z,x_{n_0+1})\\
&< \tfrac{1}{2}D(x_{n_0},Tx_{n_0}) + \tfrac{1}{2}D(x_{n_0+1},Tx_{n_0+1})\\
&\leqslant \tfrac{1}{2}d(x_{n_0},x_{n_0+1}) + \tfrac{1}{2}\psi\big(d(x_{n_0},x_{n_0+1})\big)\\
&< \tfrac{1}{2}d(x_{n_0},x_{n_0+1}) + \tfrac{1}{2}d(x_{n_0},x_{n_0+1})\\
&= d\big(x_{n_0},x_{n_0+1}\big)
\end{aligned}$$

a contradiction. Hence either (2.18) or (2.19) holds for an infinite subset N_1 of $\mathbb{Z}^+$. By the given assumption, it follows that $\alpha(x_n,z) \geqslant 1$. As T is α_* −admissible, $\alpha(Tx_n,Tz) \geqslant 1$. Now if (2.18) holds for all $n \in \mathbb{Z}^+$, then from (1.4) we get

$$\begin{aligned}
D(x_{n+1},Tz) &\leqslant H(Tx_n,Tz) < \alpha_*(Tx_n,Tz)H(Tx_n,Tz)\\
&\leqslant \max\{1,N_T(x_n,z)\}\psi(M_T(x_n,z))\\
&= \max\left\{1,\left(\frac{\max\{d(x_n,z),D(x_n,Tx_n)+D(z,Tz),D(x_n,Tz)+D(z,Tx_n)\}}{b(1+\delta(x_n,Tx_n)+\delta(z,Tz))}\right)\right\}\\
&\quad \psi\left(\max\left\{d(x_n,z),D(x_n,Tx_n),D(z,Tz),\frac{D(x_n,Tz)+D(z,Tx_n)}{2b}\right\}\right)\\
&\leqslant \max\left\{1,\left(\frac{\max\{d(x_n,z),d(x_n,x_{n+1})+D(z,Tz),D(x_n,Tz)+d(z,x_{n+1})\}}{b(1+d(x_n,x_{n+1})+D(z,Tz))}\right)\right\}\\
&\quad \psi\left(\max\left\{d(x_n,z),d(x_n,x_{n+1}),D(z,Tz),\frac{D(x_n,Tz)+d(z,x_{n+1})}{2b}\right\}\right).
\end{aligned}$$

On taking limit as $n \to +\infty$, we have

$$\lim_{n\to+\infty} D(x_{n+1}, Tz) \leqslant \lim_{n\to+\infty} \max\left\{1, \left(\frac{\max\{d(x_n,z), d(x_n,x_{n+1}) + D(z,Tz), D(x_n,Tz) + d(z,x_{n+1})\}}{b(1 + d(x_n,x_{n+1}) + D(z,Tz))}\right)\right\} \psi\left(\max\left\{d(x_n,z), d(x_n,x_{n+1}), D(z,Tz), \frac{D(x_n,Tz) + d(z,x_{n+1})}{2b}\right\}\right).$$

As ψ is continuous at $0, \psi \in \Psi_4$ and $D(z,Tz) > 0$, we have

$$D(z,Tz) \leqslant \max\left\{1, \frac{D(z,Tz)}{b(1 + D(z,Tz))}\right\} \psi(D(z,Tz)) = \psi(D(z,Tz)) < D(z,Tz).$$

a contradiction. Consequently, $z \in Tz$. Similarly, we obtain $z \in Tz$ when (2.19) holds for an infinite subset N_1 of $\mathbb{Z}^+$.

To prove part (d $_2$), let $u \in F(T)$ such that $u \neq z$ and $\alpha(z,u) \geqslant 1$. Since T is α_* −admissible, $\alpha_*(Tz,Tu) \geqslant 1$. Now $\frac{1}{2} D(z,Tz) = 0 \leqslant d(z,u)$ implies that

$$\begin{aligned}
d(z,u) &\leqslant bD(z,Tz) + bD(Tz,u) \leqslant bH(Tz,Tu) \\
&\leqslant b\alpha_*(Tz,Tu)H(H(Tz,Tu)) \\
&\leqslant b\max\left\{1, \left(\frac{\max\{d(z,u), D(z,Tz) + D(u,Tu), D(z,Tu) + D(u,Tz)\}}{b(1 + \delta(z,Tz) + \delta(u,Tu))}\right)\right\} \psi\left(\max\left\{d(z,u), D(z,Tz), D(u,Tu), \frac{D(z,Tu) + D(u,Tz)}{2b}\right\}\right) \\
&\leqslant b\max\left\{1, \left(\frac{\max\{d(z,u), d(z,z) + d(u,u), d(z,u) + d(u,z)\}}{b(1 + d(z,z) + d(u,u))}\right)\right\} \psi\left(\max\left\{d(z,u), d(z,z), d(u,u), \frac{d(z,u) + d(u,z)}{2b}\right\}\right) \\
&\leqslant b\max\left\{1, \left(\frac{2d(z,u)}{b}\right)\right\} \psi(d(z,u)).
\end{aligned}$$

Now, $\max\{1, N_T(x,y)\} = N_T(x,y)$ gives

$$d(z,u) \leqslant 2d(z,u)\psi(d(z,u)) < 2d^2(z,u)$$

and hence $d(z,u) > \frac{1}{2}$.

Corollary 2.2 *Let (X,d) be a complete b-metric space, $\alpha: X\times X\to \mathbb{R}^+$ and $T: X\to Cl(X)$ an α_*- admissible mapping such that*

$$\frac{1}{2}D(x,Tx)\leqslant bd(x,y)$$

implies that

$$\alpha_*(Tx,Ty)H(Tx,Ty)\leqslant max\{1,N_T(x,y)\}\psi(d(x,y))$$

for all $x,y\in X,\psi\in\Psi_4$. Further, assume that there exists $x_0\in X$ and $x_1\in Tx_0$ such that $\alpha(x_0,x_1)\geqslant 1$. If for any sequence $\{x_n\}$ converging to x in X, we have $\alpha(x_n,x)\geqslant 1$ for all $n\in\mathbb{Z}^+$ then

e_1-: *T is an MWP operator*

e_2-: *If there is some $u\in F(T)$ such that $u\neq z$ and $\alpha(z,u)\geqslant 1$, then $d(z,u)>\frac{1}{2}$ provided that*

$$max\{1,N_T(x,y)\}=N_T(x,y) \text{ for all } x,y\in X.$$

Corollary 2.3 *Let (X,d) be a complete b-metric space, $\alpha: X\times X\to \mathbb{R}^+$ and $T: X\to Cl(X)$ an α_*- admissible mapping such that*

$$\frac{1}{2}D(x,Tx)\leqslant bd(x,y)$$

implies that

$$\alpha_*(Tx,Ty)H(Tx,Ty)\leqslant max\left\{1,\frac{d(x,y)}{b(1+\delta(x,Tx)+\delta(y,Ty))}\right\}\psi(d(x,y))$$

for all $x,y\in X,\psi\in\Psi_4$. Further, assume that there exists $x_0\in X$ and $x_1\in Tx_0$ such that $\alpha(x_0,x_1)\geqslant 1$. If for any sequence $\{x_n\}$ converging to x in X, we have $\alpha(x_n,x)\geqslant 1$ for all $n\in\mathbb{Z}^+$ then

e_3-: T is an MWP operator.

e_4-: If there is some $u\in F(T)$ such that $u\neq z$ and $\alpha(z,u)\geqslant 1$, then $d(z,u)>1$ provided that

$$max\left\{1,\frac{d(x,y)}{b(1+\delta(x,Tx)+\delta(y,Ty))}\right\}=\frac{d(x,y)}{b(1+\delta(x,Tx)+\delta(y,Ty))}$$

for all $x,y\in X$.

Proof. Follows from Corollary 2.3.

Corollary 2.4 Let (X,d) be a complete b-metric space, $\alpha: X\times X\to\mathbb{R}^+$ and $T: X\to Cl(X)$ an α_*-admissible mapping such that

$$\frac{1}{2}D(x,Tx)\leqslant bd(x,y)$$

implies that

$$\alpha_*(Tx,Ty)H(Tx,Ty)\leqslant N_T(x,y)\psi(M_T(x,y))$$

for all $x,y\in X,\psi\in\Psi_4$. Further, assume that there exists $x_0\in X$ and $x_1\in Tx_0$ such that $\alpha(x_0,x_1)\geqslant 1$. If for any sequence $\{x_n\}$ converging to x in X, we have $\alpha(x_n,x)\geqslant 1$ for all $n\in\mathbb{Z}^+$ then

e$_5$-: T is an MWP operator.

e$_6$-: If there is some $u\in F(T)$ such that $u\neq z$ and $\alpha(z,u)\geqslant 1$, then $d(z,u)>\frac{1}{2}$.

Proof. Take $\max\{1,N_T(x,y)\}=N_T(x,y)$ in Theorem 2.1.

Corollary 2.5 Let (X,d) be a complete b-metric space, $\alpha: X\times X\to\mathbb{R}^+$ and $T: X\to Cl(X)$ an α_*-admissible mapping such that

$$\frac{1}{2}D(x,Tx)\leqslant bd(x,y)\text{impliesthat}\alpha_*(Tx,Ty)H(Tx,Ty)\leqslant N_T(x,y)\psi(d(x,y)) \quad (2.22)$$

for all $x,y\in X,\psi\in\Psi_4$. Further, assume that there exists $x_0\in X$ and $x_1\in Tx_0$ such that $\alpha(x_0,x_1)\geqslant 1$. If for any sequence $\{x_n\}$ converging to x in X, we have $\alpha(x_n,x)\geqslant 1$ for all $n\in\mathbb{Z}^+$ then

e$_7$-: T is an MWP operator.

e_8-: If there is some $u \in F(T)$ such that $u \neq z$ and $\alpha(z,u) \geqslant 1$, then $d(z,u) > \frac{1}{2}$.

Proof. Take $M_T(x,y) = d(x,y)$ in Corollary 2.4.

The following Corollary is a Suzuki type generalization of (Asl et al, 2012), Theorem 2.1 (Bota et al, 2015), Theorem 1 (Mohammadi, 2013), Theorem 3.1 (Samet et al, 2012), Theorem 2.2 and references therein in the context of b-metric spaces.

Corollary 2.6 Let (X,d) be a complete b-metric space, $\alpha: X \times X \to \mathbb{R}^+$ and $T: X \to Cl(X)$ an α_* – admissible mapping such that

$$\frac{1}{2}D(x,Tx) \leqslant bd(x,y) \text{ implies that } \alpha_*(Tx,Ty)H(Tx,Ty) \leqslant \psi(M_T(x,y)) \tag{2.23}$$

for all $x,y \in X, \psi \in \Psi_4$. Further, assume that there exists $x_0 \in X$ and $x_1 \in Tx_0$ such that $\alpha(x_0,x_1) \geqslant 1$. Then T is an MWP operator provided that for any sequence $\{x_n\}$ converging to x in X, we have $\alpha(x_n,x) \geqslant 1$ for all $n \in \mathbb{Z}^+$.

Proof. Take $\max\{1, N_T(x,y)\} = 1$ in Theorem 2.1.

Corollary 2.7 Let (X,d) be a complete b-metric space, $\alpha: X \times X \to \mathbb{R}^+$ and $T: X \to Cl(X)$ an α_* – admissible mapping such that

$$\alpha_*(Tx,Ty)H(Tx,Ty) \leqslant \psi(M_T(x,y)) \tag{2.24}$$

for all $x,y \in X, \psi \in \Psi_4$. Further, assume that there exists $x_0 \in X$ and $x_1 \in Tx_0$ such that $\alpha(x_0,x_1) \geqslant 1$. Then T is an MWP operator provided that for any sequence $\{x_n\}$ converging to x in X, we have $\alpha(x_n,x) \geqslant 1$ for all $n \in \mathbb{Z}^+$.

Corollary 2.8 Let (X,d) be a complete b-metric space, $\alpha: X \times X \to \mathbb{R}^+$ and $T: X \to Cl(X)$ an α_* – admissible mapping such that

$\frac{1}{2}D(x,Tx) \leqslant bd(x,y)$

implies that

$$\alpha_*(Tx,Ty)H(Tx,Ty) \leqslant \psi(d(x,y)) \tag{2.25}$$

for all $x, y \in X, \psi \in \Psi_4$. Further, assume that there exists $x_0 \in X$ and $x_1 \in Tx_0$ such that $\alpha(x_0, x_1) \geqslant 1$. Then T is an MWP operator provided that for any sequence $\{x_n\}$ converging to x in X, we have $\alpha(x_n, x) \geqslant 1$ for all $n \in \mathbb{Z}^+$.

Proof. Take $M_T(x, y) = d(x, y)$ in Corollary 2.6.

Now we state Theorem 2.1 in the context of single valued mapping $f: X \to X$, where X is a b-metric space. The existence of a fixed point follows immediately from Theorem 2.1. To prove the uniqueness of the fixed point, we need the condition H, given as follows:

(H): for all $x, y \in X$, there exists a $z \in X$ such that $\alpha(x, z) \geqslant 1$ and $\alpha(y, z) \geqslant 1$.

Corollary 2.9 Let (X, d) be a complete b-metric space and $\alpha: X \times X \to \mathbb{R}^+$ and $f: X \to X$ an $\alpha -$ admissible mapping such that

$$\frac{1}{2} d(x, fx) \leqslant bd(x, y)$$

implies that

$$\alpha(fx, fy) d(fx, fy) \leqslant max\{1, N_f(x, y)\} \psi(M_f(x, y)) \tag{2.26}$$

for all $x, y \in X, \psi \in \Psi_4$. Further, assume that there exists $x_0 \in X$ and $x_1 = fx_0$ such that $\alpha(x_0, x_1) \geqslant 1$ and for any sequence $\{x_n\}$ converging to x in X, we have $\alpha(x_n, x) \geqslant 1$ for all $n \in \mathbb{Z}^+$. If the condition (H) is satisfied, then f is a Picard operator and for an arbitrary $z \in X$, the sequence $\{f^n z\}$ converges to some $w \in F(f)$ and

e$_9$-: $F(f) = \{w\}$ if $max\{1, N_f(x, y)\} = 1$,

e$_{10}$-: $d(u, w) > \frac{b}{2}$ for any $u \in F(f)$ such that $u \neq w$ provided that $max\{1, N_f(x, y)\} = N_f(x, y)$.

Proof. Theorem 2.1, f is a Picard operator and $F(f)$ is nonempty. Let $u, v \in F(f)$ such that $u \neq v$. By the condition (H), there exists a $z \in X$ such that $\alpha(u, z) \geqslant 1$ and $\alpha(v, z) \geqslant 1$. Note that $\{f^n z\}$ is a Picard sequence which converges to some $w \in F(f)$. As f is an $\alpha -$ admissible mapping, so for all $n \geqslant 1$ we have $\alpha(u, f^n z) \geqslant 1$ and $\alpha(v, f^n z) \geqslant 1$. Since

$$\frac{1}{2}d(u,fu)=0\leqslant bd(u,f^{n-1}z),$$

by (2.26) we have

$$\begin{aligned}
&d(u,f^nz)=d(fu,f^nz)\\
&\leqslant \alpha(fu,ff^{n-1}z)d(fu,ff^{n-1}z)\\
&\leqslant \max\{1,N_f(u,f^{n-1}z)\}\psi(M_f(u,ff^{n-1}z))\\
&\leqslant \max\left\{1,\left(\frac{\max\{d(u,f^{n-1}z),d(u,fu)+d(f^{n-1}z,ff^{n-1}z),d(u,ff^{n-1}z)+d(f^{n-1}z,fu)\}}{b(1+d(u,fu)+d(f^{n-1}z,ff^{n-1}z))}\right)\right\}\\
&\psi\left(\max\left\{d(u,f^{n-1}z),d(u,fu),d(f^{n-1}z,ff^{n-1}z),\frac{d(u,ff^{n-1}z)+d(f^{n-1}z,fu)}{2b}\right\}\right)\\
&\leqslant \max\left\{1,\left(\frac{\max\{d(u,f^{n-1}z),d(u,u)+d(f^{n-1}z,f^nz),d(u,f^nz)+d(f^{n-1}z,u)\}}{b(1+d(u,u)+d(f^{n-1}z,f^nz))}\right)\right\}\\
&\psi\left(\max\left\{d(u,f^{n-1}z),d(u,u),d(f^{n-1}z,f^nz),\frac{d(u,f^nz)+d(f^{n-1}z,u)}{2b}\right\}\right).
\end{aligned}$$

On taking limit as $n\to+\infty$, we obtain that

$$\begin{aligned}
d(u,w)\leqslant\ &\max\left\{1,\left(\frac{\max\{d(u,w),d(u,u)+d(w,w),d(u,w)+d(w,u)\}}{b(1+d(u,u)+d(w,w))}\right)\right\}\\
&\psi\left(\max\left\{d(u,w),d(u,u),d(w,w),\frac{d(u,w)+d(w,u)}{2b}\right\}\right)\\
&=\max\left\{1,\left(\frac{2d(u,w)}{b}\right)\right\}\psi(d(u,w)).
\end{aligned}$$

That is

$$d(u,w)\leqslant \max\left\{1,\left(\frac{2d(u,w)}{b}\right)\right\}\psi(d(u,w)). \tag{2.27}$$

Now, If $\max\{1,N_f(x,y)\}=1$, and $w\neq u$, then we have

$$d(u,w)\leqslant\psi(d(u,w))<d(u,w). \tag{2.28}$$

Also, if $\max\{1,N_f(x,y)\}=1$, and $v\neq w$, then we have

$$d(v,w)\leqslant\psi(d(v,w)). \tag{2.29}$$

A contradiction in both cases. Thus $w = u = v$, and hence $F(f)$ is singleton. If $\max\{1, N_f(x,y)\} = N_f(x,y)$ and $u \neq w$ then from (2.27) we get

$$d(u,w) \leqslant \frac{2d(u,w)}{b}\psi(d(u,w)) < \frac{2}{b}d^2(u,w)$$

and $d(u,w) > \frac{b}{2}$.

Corollary 2.10 Let (X,d) be a complete b-metric space and $\alpha: X \times X \to \mathbb{R}^+$ and $f: X \to X$ an $\alpha-$admissible mapping such that

$$\frac{1}{2}d(x,fx) \leqslant bd(x,y) \text{ implies that } \alpha(fx,fy)d(fx,fy) \leqslant \psi(M_f(x,y))$$

for all $x, y \in X, \psi \in \Psi_4$. Further, assume that there exists $x_0 \in X$ and $x_1 = fx_0$ such that $\alpha(x_0,x_1) \geqslant 1$ and for any sequence $\{x_n\}$ converging to x in X, we have $\alpha(x_n,x) \geqslant 1$ for all $n \in \mathbb{Z}^+$. If the condition (H) is satisfied, then f is a Picard operator and for an arbitrary $z \in X$, the sequence $\{f^n z\}$ converges to $w \in F(f)$ and $F(f) = \{w\}$.

Corollary 2.11 Let (X,d) be a complete b-metric space and $\alpha: X \times X \to \mathbb{R}^+$. Let $f: X \to X$ be an $\alpha-$admissible mapping that satisfies

$$\frac{1}{2}d(x,fx) \leqslant bd(x,y)$$

implies that

$$\alpha(fx,fy)d(fx,fy) \leqslant \max\{1, N_f(x,y)\}\psi(d(x,y))$$

for all $x, y \in X, \psi \in \Psi_4$. Moreover, suppose that there exists $x_0 \in X$ and $x_1 = fx_0$ such that $\alpha(x_0,x_1) \geqslant 1$ and if there is a sequence $\{x_n\}$ in X such that $x_n \to x$, then $\alpha(x_n,x) \geqslant 1$ for all $n \in \mathbb{Z}^+$. Further, assume that there exists $x_0 \in X$ and $x_1 = fx_0$ such that $\alpha(x_0,x_1) \geqslant 1$ and for any sequence $\{x_n\}$ converging to x in X, we have $\alpha(x_n,x) \geqslant 1$ for all $n \in \mathbb{Z}^+$. If the condition (H) is satisfied, then f is a Picard operator and for an arbitrary $z \in X$, the sequence $\{f^n z\}$ converges to $w \in F(f)$ and $F(f) = \{w\}$. Also, $d(u,w) > \frac{b}{2}$ for any $u \in F(f)$ such that $u \neq w$ provided that $\max\{1, N_f(x,y)\} = N_f(x,y)$.

Example 2.12 Let $X=\{x_1,x_2,x_3,x_4,x_5\}$ and $d: X\times X\to\mathbb{R}^+$ be defined as

$$d(x_2,x_5)=d(x_3,x_4)=d(x_3,x_5)=d(x_2,x_4)=6,$$
$$d(x_2,x_3)=9, d(x_1,x_4)=d(x_1,x_5)=10,$$
$$d(x_1,x_2)=d(x_1,x_3)=4, d(x_4,x_5)=1,$$
$$d(x,x)=0 \text{ and } d(x,y)=d(y,x) \text{ for all } x,y\in X.$$

As $9=d(x_2,x_3)\nleq d(x_2,x_1)+d(x_1,x_3)=8$, so d is not a metric on X. Indeed,(X,d) is a b-metric space with $b=\frac{9}{8}>1$. Consider a mapping $T: X\longrightarrow Cl(X)$ defined by $Tx_1=Tx_2=Tx_3=\{x_1\}, Tx_4=\{x_2\}$ and $Tx_5=\{x_3\}$. If we take $\psi(t)=\frac{9}{10}t$ for $t\in\mathbb{R}^+$, then $\psi\in\Psi_4$ (see 1.8). If mapping $\alpha: X\times X\to\mathbb{R}^+$ is defined as $\alpha(x_i,x_j)=1$ for all $i,j\in\{1,2,3,4,5\}$, then T is an α_* −admissible mapping. For $x,y\in\{x_1,x_2,x_3\}$, we have $H(Tx,Ty)=0\leqslant \max\{1,N_T(x,y)\}\psi(M_T(x,y))$. For (x,y) when $x\in\{x_1,x_2,x_3\}$ and $y\in\{x_4,x_5\}$, we obtain that

$$\alpha(Tx_1,Tx_4)H(Tx_1,Tx_4)=d(x_1,x_2)=4\leqslant 9=\psi(d(x_1,x_4))$$
$$\leqslant \max\{1,N_T(x_1,x_4)\psi(M_T(x_1,x_4)),$$
$$\alpha(Tx_2,Tx_4)H(Tx_2,Tx_4)=d(x_1,x_2)=4\leqslant \frac{54}{10}=\psi(d(x_2,x_4))$$
$$\leqslant \max\{1,N_T(x_2,x_4)\psi(M_T(x_2,x_4)),$$
$$\alpha(Tx_3,Tx_4)H(Tx_3,Tx_4)=d(x_1,x_2)=4\leqslant \frac{54}{10}=\psi(d(x_3,x_4))$$
$$\leqslant \max\{1,N_T(x_3,x_4)\psi(M_T(x_3,x_4)),$$
$$\alpha(Tx_1,Tx_5)H(Tx_1,Tx_5)=d(x_1,x_3)=4\leqslant 9=\psi(d(x_1,x_5))$$
$$\leqslant \max\{1,N_T(x_1,x_5)\psi(M_T(x_1,x_5)),$$
$$\alpha(Tx_2,Tx_5)H(Tx_2,Tx_5)=d(x_1,x_3)=4\leqslant \frac{54}{10}=\psi(d(x_2,x_5))$$
$$\leqslant \max\{1,N_T(x_2,x_5)\psi(M_T(x_2,x_5)),$$
$$\alpha(Tx_3,Tx_5)H(Tx_3,Tx_5)=d(x_1,x_3)=4\leqslant \frac{54}{10}=\psi(d(x_3,x_5))$$
$$\leqslant \max\{1,N_T(x_3,x_5)\psi(M_T(x_3,x_5)).$$

Note that

$$\frac{1}{2}D(x_4,Tx_4)=\frac{1}{2}d(x_4,x_2)=3>\frac{9}{8}=bd(x_4,x_5),$$

and

$$\frac{1}{2}D(x_5,Tx_5)=\frac{1}{2}d(x_5,x_3)=3>\frac{5}{4}=bd(x_5,x_4).$$

Hence

$$\frac{1}{2}(D(x,Tx) \leqslant bd(x,y)) \leqslant 0$$

implies

$$\alpha(Tx,Ty)H(Tx,Ty) \leqslant \max\{1, N_T(x,y)\}\psi(M_T(x,y))$$

holds for all $x, y \in X$. Thus all the conditions of Theorem 2.1 are satisfied. On the other hand, if we take $x = x_4, y = x_5$, then $\alpha(Tx_4, Tx_5)H(Tx_4, Tx_5) = d(x_2, x_3) = 9 > \psi(d(x_4, x_5)) = \psi(1) = \frac{9}{10}$ and $\alpha(Tx_4, Tx_5)H(Tx_4, Tx_5) \nleq \psi(d(x_4, x_5))$. Consequently, Theorem 1.16 in (Bota et al, 2015) does not hold in this case.

The following example illustrates an assumption $\max\{1, N_T(x,y)\} > 1$.

Example 2.13 Let $X = \{x_1, x_2, x_3\}$ and $d: X \times X \to \mathbb{R}^+$ be defined as

$d(x_1, x_2) = 4, d(x_1, x_3) = 1, d(x_2, x_3) = 2,$
$d(x,x) = 0$ and $d(x,y) = d(y,x)$ for all $x, y \in X$.

As $4 = d(x_1, x_2) \nleq d(x_1, x_3) + d(x_3, x_2) = 3$, so d is not a metric on X. Indeed, (X, d) is a b-metric space with $b = \frac{4}{3} > 1$. Consider a mapping $T: X \longrightarrow Cl(X)$ defined by

$$Tx = \begin{cases} \{x_2\} \text{ if } x = x_1, \\ \{x_1\} \text{ if } x = x_2, \\ \{x_2\} \text{ if } x = x_3. \end{cases}$$

If we take $\psi(t) = \frac{8}{9}t$ for $t \in \mathbb{R}^+$, then $\psi \in \Psi_4$ (see Example 1.8). If $\alpha: X \times X \to \mathbb{R}^+$ is defined as $\alpha(x_i, x_j) = 1$ for all $i, j \in \{1,2,3\}$, then T is α_* − admissible. Note that

$$N_T(x_1, x_2) = \frac{3\max\{d(x_1,x_2), D(x_1,Tx_1) + D(x_2,Tx_2), D(x_1,Tx_2) + D(x_2,Tx_1)\}}{4(1 + \delta(x_1,Tx_2) + \delta(x_2,Tx_1))}$$
$$= \frac{3\max\{d(x_1,x_2), d(x_1,x_2) + d(x_2,x_1), d(x_1,x_1) + d(x_2,x_2)\}}{4(1 + d(x_1,x_1) + d(x_2,x_2))}$$
$$= \frac{3\max\{4,8,0\}}{4(1+0)} = 6 > 1.$$

Hence $\max\{1, N_T(x,y)\} = 6 > 1$. Note that

$$
\begin{aligned}
N_T(x_1,x_3) &= \frac{3\max\{d(x_1,x_3), D(x_1,Tx_1)+D(x_3,Tx_3), D(x_1,Tx_3)+D(x_3,Tx_1)\}}{4(1+\delta(x_1,Tx_3)+\delta(x_3,Tx_1))} \\
&= \frac{3\max\{d(x_1,x_3), d(x_1,x_2)+d(x_3,x_3), d(x_1,x_3)+d(x_3,x_2)\}}{4(1+d(x_1,x_3)+d(x_3,x_2))} \\
&= \frac{3\max\{1,4,3\}}{4(1+1+2)} = \frac{3}{4},
\end{aligned}
$$

and

$$
\begin{aligned}
N_T(x_2,x_3) &= \frac{3\max\{d(x_2,x_3), D(x_2,Tx_2)+D(x_3,Tx_3), D(x_2,Tx_3)+D(x_3,Tx_2)\}}{4(1+\delta(x_2,Tx_3)+\delta(x_3,Tx_2))} \\
&= \frac{3\max\{d(x_2,x_3), d(x_2,x_1)+d(x_3,x_3), d(x_2,x_3)+d(x_3,x_1)\}}{4(1+d(x_2,x_3)+d(x_3,x_1))} \\
&= \frac{3\max\{2,4,3\}}{4(1+2+1)} = \frac{3}{4}.
\end{aligned}
$$

Also,

$$
\begin{aligned}
\alpha(Tx_1,Tx_2)H(Tx_1,Tx_2) = d(x_2,x_1) = 4 < \frac{64}{3} = N_T(x_1,x_2)\psi(d(x_1,x_2)) \\
\leqslant \max\{1, N_T(x_1,x_2)\psi(M_T(x_1,x_2)), \\
\alpha(Tx_1,Tx_3)H(Tx_1,Tx_3) = d(x_2,x_3) = 2 < \frac{8}{3} = N_T(x_1,x_3)\psi(d(x_1,Tx_1)) \\
\leqslant \max\{1, N_T(x_1,x_3)\psi(M_T(x_1,x_3)), \\
\alpha(Tx_2,Tx_3)H(Tx_2,Tx_3) = d(x_1,x_3) = 1 < \frac{4}{3} = N_T(x_2,x_3)\psi(d(x_2,x_3)) \\
\leqslant \max\{1, N_T(x_2,x_3)\psi(M_T(x_2,x_3)).
\end{aligned}
$$

Thus all the conditions of Theorem 2.1 are satisfied. On the other hand, if we take $x = x_1, y = x_2$, then $\alpha(Tx_1,Tx_2)H(Tx_1,Tx_2) = d(x_2,x_3) = 4 > \psi(d(x_1,x_2)) = \psi(4) = \frac{32}{9}$. Hence $\alpha(Tx_1,Tx_2)H(Tx_1,Tx_2) \nleq \psi(d(x_1,x_2))$. Consequently Theorem 1.16 in (Bota et al, 2015) is not applicable in this case which is a generalization of Theorems 1.14 and 1.9.

For $b = 1$, Theorem 2.1 reduces to the following important Corollary.

Corollary 2.14 Let (X,d) be a complete metric space, $\alpha: X \times X \to \mathbb{R}^+$ and $T: X \to Cl(X)$ satisfies the following implication

$$\frac{1}{2}D(x,Tx) \leqslant d(x,y) \text{implies} \max\{1, n_{T,T}(x,y)\}\psi(m_{T,T}(x,y))$$

for all $x, y \in X$ and $\psi \in \Psi_4$ where $n_{T,T}(x,y)$ and $m_{T,T}(x,y)$ are the same as given in (1.2), Further, assume that there exists $x_0 \in X$ and $x_1 \in Tx_0$ such that $\alpha(x_0, x_1) \geqslant 1$ and for any sequence $\{x_n\}$ converging to x in X, we have $\alpha(x_n, x) \geqslant 1$ for all $n \in \mathbb{Z}^+$. Then

e_{11}-: T is an MWP operator.

e_{12}-: If there is some $u \in F(T)$ such that $u \neq z$ and $\alpha(z,u) \geqslant 1$, then $d(z,u) > \frac{1}{2}$ provided that

$$\max\{1, n_{T,T}(x,y)\} = n_{T,T}(x,y).$$

Next we present an example which shows that Corollary 2.14 is a potential generalization of Theorems 1.14, 1.9, 1.11, 1.13.

Example 2.15 Let$X = \{x_1, x_2, x_3, x_4, x_5\}andd: X \times X \to \mathbb{R}^+$bedefined by

$$d(x_2,x_5) = d(x_3,x_4) = d(x_3,x_5) = d(x_2,x_4) = 5,$$
$$d(x_1,x_4) = d(x_1,x_5) = 9, d(x_1,x_2) = d(x_1,x_3) = 4,$$
$$d(x_4,x_5) = 2, d(x_2,x_3) = 8,$$
$$d(x,x) = 0 \text{ and } d(x,y) = d(y,x) \text{ for all } x, y \in X.$$

Note that d is a metric on X. Consider a mapping $T: X \longrightarrow Cl(X)$ defined by $Tx_1 = Tx_2 = Tx_3 = \{x_1\}, Tx_4 = \{x_2\}$ and $Tx_5 = \{x_3\}$. If we take $\psi(t) = \frac{8}{9}t$ for $t \in \mathbb{R}^+$, then $\psi \in \Psi_i$ for each $i = 1,2,3,4$ (see Example 1.8). If $\alpha: X \times X \to \mathbb{R}^+$ is defined as $\alpha(x_i, x_j) = 1$ for all $i, j \in \{1,2,3,4,5\}$, then T is α_* – admissible mapping. For $x, y \in \{x_1, x_2, x_3\}$, we have $H(Tx, Ty) = 0 \leqslant \max\{1, N_T(x,y)\}\psi(M_T(x,y))$. For (x,y), when $x \in \{x_1, x_2, x_3\}$ and $y \in \{x_4, x_5\}$, we obtain that

$$\alpha(Tx_1, Tx_4)H(\alpha(Tx_1, Tx_4)) = d(x_1, x_2) = 4 \leqslant 8 = \psi(d(x_1, x_4))$$
$$\leqslant \max\{1, n_{T,T}(x_1, x_4)\psi(m_{T,T}(x_1, x_4)),$$
$$\alpha(Tx_2, Tx_4)H(Tx_2, Tx_4) = d(x_1, x_2) = 4 \leqslant \frac{40}{9} = \psi(d(x_2, x_4))$$
$$\leqslant \max\{1, n_{T,T}(x_2, x_4)\psi(m_{T,T}(x_2, x_4)),$$
$$\alpha(Tx_3, Tx_4)H(Tx_3, Tx_4) = d(x_1, x_2) = 4 \leqslant \frac{40}{9} = \psi(d(x_3, x_4))$$

$$\leqslant \max\{1, n_{T,T}(x_3,x_4)\psi(m_{T,T}(x_3,x_4)),$$
$$\alpha(Tx_1,Tx_5)H(Tx_1,Tx_5) = d(x_1,x_3) = 4 \leqslant 8 = \psi(d(x_1,x_5))$$
$$\leqslant \max\{1, n_{T,T}(x_1,x_5)\psi(m_{T,T}(x_1,x_5)),$$
$$\alpha(Tx_2,Tx_5)H(Tx_2,Tx_5) = d(x_1,x_3) = 4 \leqslant \frac{40}{9} = \psi(d(x_2,x_5))$$
$$\leqslant \max\{1, n_{T,T}(x_2,x_5)\psi(m_{T,T}(x_2,x_5)),$$
$$\alpha(Tx_3,Tx_5)H(Tx_3,Tx_5) = d(x_1,x_3) = 4 \leqslant \frac{40}{9} = \psi(d(x_3,x_5))$$
$$\leqslant \max\{1, n_{T,T}(x_3,x_5)\psi(m_{T,T}(x_3,x_5)).$$

Note that $\frac{1}{2}D(x_4,Tx_4) = \frac{1}{2}d(x_4,x_2) = \frac{5}{2} > 1 = d(x_4,x_5)$, and $\frac{1}{2}D(x_5,Tx_5) = \frac{1}{2}d(x_5,x_3) = \frac{5}{2} > 1 = d(x_5,x_4)$.

Hence

$$\frac{1}{2}(D(x,Tx) \leqslant d(x,y))$$

implies

$$\alpha(Tx,Ty)H(Tx,Ty) \leqslant \max\{1, N_T(x,y)\psi(M_{TT}(x,y))$$

holds for all $x, y \in X$. Thus all the conditions of Corollary 2.14 are satisfied. On the other hand, if we take $x = x_4, y = x_5$,
then

$$\alpha(Tx_4,Tx_5)H(Tx_4,Tx_5) = d(x_2,x_3) = 8 > \psi(d(x_4,x_5)) = \psi(1) = \frac{8}{9}.$$

Hence,

$$\alpha(Tx_4,Tx_5)H(Tx_4,Tx_5) = 8 \nleq \frac{8}{9} = \psi(d(x_4,x_5)).$$

Consequently, Theorem 1.14 is not applicable in this case. Note that Theorem 1.14 is a generalization of Theorem 1.9. Now

VOJNOTEHNIČKI GLASNIK / MILITARY TECHNICAL COURIER, 2020, Vol. 68, Issue 3

$$n_{T,T}(x_4,x_5)=\frac{\max\{d(x_4,x_5),D(x_4,Tx_4)+D(x_5,Tx_5),D(x_4,Tx_5)+D(x_5,Tx_4)\}}{1+\delta(x_4,Tx_4)+\delta(x_5,Tx_5)}$$
$$=\frac{\max\{d(x_4,x_5),d(x_4,x_2)+d(x_5,x_3),d(x_4,x_3)+d(x_5,x_2)\}}{1+d(x_4,x_2)+d(x_5,x_3)}$$
$$=\frac{\max\{1,10,10\}}{11}=\frac{10}{11}\neq 1$$

$$m_{T,T}(x_4,x_5)=\max\left\{d(x_4,x_5),D(x_4,Tx_4),D(x_5,Tx_5),\frac{D(x_4,Tx_5)+D(x_5,Tx_4)}{2}\right\}$$
$$=\max\{1,5,5,5\}=5$$

implies that $\alpha(Tx_4,Tx_5)H(Tx_4,Tx_5)=8\nleq\frac{50}{11}=n_{T,T}(x_4,x_5)m_{T,T}(x_4,x_5)$. Hence, Theorem 1.13 which is a generalization of Theorem 1.11 does not hold in this case.

Coincidence and common fixed point results in b-metric spaces

As an application of Theorem 2.1, we obtain the existence of coincidence and common fixed point of Suzuki type $(\alpha_*-\psi)-$hybrid pair of operators in b-metric spaces.

Theorem 3.1 Let (X,d) be a b-metric space and (g,T) a Suzuki type $(\alpha_*-\psi)-$hybrid pair of operators such that T an $(\alpha_*-g)-$admissible mapping. Suppose that there exists $x_0\in X$ and $gx_1\in Tx_0$ such that $\alpha(gx_0,gx_1)\geqslant 1$ and for any sequence $\{x_n\}$ in X with $gx_n\to gx$, we have $\alpha(gx_n,gx)\geqslant 1$ for all $n\in\mathbb{Z}^+$. Then there exists x in X such that $gx\in Tx$ provided that $T(X)\subseteq g(X)$ and $g(X)$ is complete. Moreover, if there is some $gy\in Ty$ such that $gx\neq gy$ and $\alpha(gx,gy)\geqslant 1$ then $d(gx,gy)\geqslant\frac{1}{2}$. Further, $F(g,T)$ is nonempty if any of the following conditions hold:

f$_1$-: The hybrid pair (g,T) is $w-$compatible, $\lim_{n\to+\infty}g^n(x)=w$ for some $w\in X$ and $x\in C(g,T)$ and g is continuous at w.

f$_2$-: The mapping g is $T-$weakly commuting at some $x\in C(g,T)$ and $g^2x=gx$.

f₃-: The mapping g is continuous at at some $x \in C(g,T)$ and $\lim_{n\to+\infty} g^n(w) = x$ for some $w \in X$.

Proof. Lemma 1.3, there is a set $E \subseteq X$ such that $g: E \to X$ is one-to-one and $g(E) = g(X)$. Define a mapping $\mathcal{T}: g(E) \to CB(X)$ by $\mathcal{T}gx = Tx$ for all $g(x) \in g(E)$. The mapping $\mathcal{T}$ is well defined because g is one–to-one. Since (g,T) is a Suzuki type $(\alpha_* - \psi)$ – hybrid pair of operators, therefore

$$\begin{cases} \frac{1}{2}D(gx,Tx) \leqslant bd(gx,gy)) \\ \text{implies} \\ \alpha_*(Tx,Ty)H(Tx,Ty) \leqslant \max\{1, N_{g,T}(x,y)\}\psi(M_{g,T}(x,y)) \\ = \begin{array}{l} \max\left\{1, \frac{\max\{d(gx,gy), D(gx,Tx)+D(gy,Ty), D(gx,Ty)+D(gy,Tx)\}}{b(1+\delta(gx,Tx)+\delta(gy,Ty))}\right\} \\ \psi\left(\max\left\{d(gx,gy), D(gx,Tx), D(gy,Ty), \frac{D(gx,Ty)+D(gy,Tx)}{2b}\right\}\right) \end{array} \end{cases}$$

for all $x, y \in X$ for some $\psi \in \Psi_4$ and $\varphi \in \Phi$. Thus

$$\begin{cases} \frac{1}{2}D(gx,\mathcal{T}gx) \leqslant bd(gx,gy)) \\ \text{implies} \\ \alpha_*(\mathcal{T}gx,\mathcal{T}gy)H(\mathcal{T}gx,\mathcal{T}gy) \leqslant \max\{1, N_{\mathcal{T}}(x,y)\}\psi(M_{\mathcal{T}}(x,y)) \\ = \begin{array}{l} \max\left\{1, \frac{\max\{d(gx,gy), D(gx,\mathcal{T}gx)+D(gy,\mathcal{T}gy), D(gx,\mathcal{T}gy)+D(gy,\mathcal{T}gx)\}}{b(1+\delta(gx,\mathcal{T}gx)+\delta(gy,\mathcal{T}gy))}\right\} \\ \psi\left(\max\left\{d(gx,gy), D(gx,\mathcal{T}gx), D(gy,\mathcal{T}gy), \frac{D(gx,\mathcal{T}gy)+D(gy,\mathcal{T}gx)}{2b}\right\}\right) \end{array} \end{cases}$$

for all $gx, gy \in g(E)$. Since $g(E) = g(X)$ is complete. By the given assumption, there exists $x_0 \in X$ and $gx_1 \in Tx_0$ such that $\alpha(gx_0, gx_1) \geqslant 1$. As T is $(\alpha_* - g)$ – admissible, we have $\alpha(Tx,Ty) \geqslant 1$ which implies that $\alpha(\mathcal{T}gx,\mathcal{T}gy) \geqslant 1$. Thus $\mathcal{T}$ is α_* –admissible. Hence $\mathcal{T}$ satisfies all the conditions of Theorem 2.1. Consequently, $\mathcal{T}$ is an MWP operator on $g(E)$, and we obtain a point $u \in g(E)$ such that $u \in \mathcal{T}u$. Since $u \in g(E)$, there is a point x in X such that $gx = u$. This implies that $gx \in \mathcal{T}gx = Tx$. By Theorem 2.1 if there is some $w \in \mathcal{T}w$ such that $u \neq w$ and $\alpha(u,w) \geqslant 1$, then we have $d(u,w) \geqslant \frac{1}{2}$ if $\max\{1, N_{g,T}(x,y)\} = N_{g,T}(x,y)$. For $w \in \mathcal{T}w$ there is a y in X such that such $gy = w$ and $gy \in \mathcal{T}gy =$

Ty. Consequently, $d(gx, gy) \geqslant \frac{1}{2}$. Now we prove that $F(g,T) \neq \emptyset$. First consider the case when (C_1) holds. Since the pair (g,T) is $w-$compatible and $\lim_{n\to+\infty} g^n(x) = u$ for some $u \in X$, the continuity of g at u implies that $gu = u$ and $\lim_{n\to+\infty} g^n(x) = gu$. Now $\alpha(g^n(x), gu) \geqslant 1$ and$(\alpha_* - g)-$admissibility of T imply that $\alpha(Tg^{n-1}(x), Tu) \geqslant 1$. By $w-$compatibility of the pair (g,T), we have $g^n(x) \in T(g^{n-1}(x))$, that is $g^n(x) \in C(g,T)$ for all $n \in \mathbb{N}$. Note that

$$\frac{1}{2}D(g^n(x), T(g^{n-1}(x))) \leqslant d(g^n(x), g^n(x)) = 0 \leqslant bd(gg^{n-1}(x), gu).$$

Since (g,T) is a generalized Suzuki type $(\alpha_* - \psi)-$hybrid pair of operators, therefore

$$\begin{aligned}
&D(g^n x, Tu)\\
&\leqslant H(Tg^{n-1}x, Tu) \leqslant \alpha(Tg^{n-1}(x), Tu)H(Tg^{n-1}x, Tu)\\
&\leqslant \max\left\{1, \frac{\max\{d(g^n x, gu), D(g^n x, Tg^{n-1}x) + D(gy, Tu), D(g^n x, Tu) + D(gu, Tg^{n-1}x)\}}{b(1+\delta(g^n x, Tg^{n-1}x) + \delta(gu, Tu))}\right\}\\
&\quad \psi \max\left\{d(g^n x, gu), D(g^n x, Tg^{n-1}x), D(gu, Tu), \frac{D(g^n x, Tu) + D(gu, Tg^{n-1}x)}{2b}\right\}\\
&\leqslant \max\left\{1, \frac{\max\{d(g^n x, gu), d(g^n x, g^n x) + D(gu, Tu), D(g^n x, Tu) + d(gu, g^n x)\}}{b(1+d(g^n x, g^n x) + D(gu, Tu))}\right\}\\
&\quad \psi \max\left\{d(g^n x, gu), d(g^n x, g^n x), D(gu, Tu), \frac{D(g^n x, Tu) + d(gu, g^n x)}{2b}\right\}.
\end{aligned}$$

On taking limit as $n \to +\infty$, we obtain that

$$D(gu, Tu) \leqslant \max\left\{1, \frac{D(gu, Tu)}{b(1 + D(gu, Tu))}\right\}\psi(D(gu, Tu)) = \psi(D(gu, Tu)).$$

If $D(gu, Tu) > 0$, then we have $D(gu, Tu) < D(gu, Tu)$, a contradiction. Consequently, $u = gu \in Tu$. That is $F(g,T) \neq \emptyset$. Now let (C_2) hold, then $g^2 x = gx$ for some $x \in C(g,T)$. By $T-$weakly commuting of g, we have $gx = g^2 x \in Tgx$. Hence $gx \in F(g,T)$. In case (C_3) holds, $\lim_{n\to+\infty} g^n(u) = x$ for some $u \in X$ and $x \in C(g,T)$. By continuity of g, we obtain that $x = gx \in Tx$.

Hence $F(g,T) \neq \emptyset$.

Corollary 3.2 Let (X,d) be a b-metric space and (g,T) a hybrid pair such that T is an $(\alpha_* - g)$ – admissible. If there exists a $\psi \in \Psi_4$ such that

$$\frac{1}{2}D(gx,Tx) \leqslant bd(gx,gy)$$

implies that

$$\alpha_*(Tx,Ty)H(Tx,Ty) \leqslant \max\{1, N_{g,T}(x,y)\}\psi(d(x,y))$$

for all $x,y \in X$. Suppose that there exists $x_0 \in X$ and $gx_1 \in Tx_0$ such that $\alpha(gx_0,gx_1) \geqslant 1$ and for any sequence $\{x_n\}$ in X such that $gx_n \to gx$, we have $\alpha(gx_n,gx) \geqslant 1$ for all $n \in \mathbb{Z}^+$. Then there exists x in X such that $gx \in Tx$ provided that $T(X) \subseteq g(X)$ and $g(X)$ is complete. Moreover, if there is some $gy \in Ty$ such that $gx \neq gy$ and $\alpha(gx,gy) \geqslant 1$, then $d(gx,gy) \geqslant \frac{1}{2}$. Further, $F(g,T)$ is nonempty if the conditions (j_1)-(j_3) Theorem 3.1 hold.

Corollary 3.3 Let (X,d) be a b-metric space and (g,T) a hybrid pair such that T is an $(\alpha_* - g)$ – admissible. If there exists a $\psi \in \Psi_4$ such that

$$\frac{1}{2}D(gx,Tx) \leqslant bd(gx,gy)$$

implies

$$\alpha_*(Tx,Ty)H(Tx,Ty) \leqslant \psi(d(x,y))$$

for all $x,y \in X$. Suppose that there exists $x_0 \in X$ and $gx_1 \in Tx_0$ such that $\alpha(gx_0,gx_1) \geqslant 1$ and for any sequence $\{x_n\}$ in X such that $gx_n \to gx$, we have $\alpha(gx_n,gx) \geqslant 1$ for all $n \in \mathbb{Z}^+$. Then there exists x in X such that $gx \in Tx$ provided that $T(X) \subseteq g(X)$ and $g(X)$ is complete. Moreover, if there is some $gy \in Ty$ such that $gx \neq gy$ and $\alpha(gx,gy) \geqslant 1$, then $d(gx,gy) \geqslant \frac{1}{2}$. Further, $F(g,T)$ is nonempty if the conditions (j_1)-(j_3) in Theorem 3.1 hold.

Data dependence of fixed point sets and Ulam-Hyers stability results

Consider the following class of functions

$$\Theta = \{\xi : \mathbb{R}^+ \to \mathbb{R}^+ \text{such that } \xi \text{ is increasing and continuous at } 0\}.$$

Let (X,d) be a b-metric space and $T: X \to P(X)$. The fixed point problem of T is to find an $x \in X$ such that

$$x \in Tx. \tag{4.1}$$

Inequality (4.1) is also known as fixed point inclusion. The fixed point inclusion is said to be generalized Ulam-Hyers stable if there exists a function $\xi \in \Theta$ such that for each $\varepsilon > 0$ and for each solution u_* of the inequality

$$D(u, Tu) \leqslant \varepsilon \tag{4.2}$$

there exists a solution z_* of the fixed point problem (4.1) such that $d(u_*, z_*) \leqslant \xi(\varepsilon)$.

Further, if there exists a $c > 0$ such that $\xi(t) = ct$ for each $t \in \mathbb{R}^+$, then the fixed point problem (4.1) is said to be Ulam-Hyers stable. Let $F(T)$ and U be the sets of solutions of (4.1) and (4.2), respectively. For more on Ulam-Hyers stability of fixed point problems, we refer the interested reader to (Ulam, 1964), (Lazar, 2012), (Petru et al, 2011), (Rus, 2009), (Hyers, 1941). Let (X, d) be a b-metric space and $T: X \to Cl(X)$ be a multivalued mapping then $E(T) = \{x \in X: \{x\} = Tx\}$.

Define a multivalued operator $T^\infty: G(T) \to P(F(T))$ by

$$T^\infty(x, y) = \{z \in F(T): \text{there is an ssa of } T \text{at } (x, y) \text{converging to } z\}$$

where $G(T) = \{(x, y): x \in X, y \in Tx\}$ is a graph of T.

A selection of $T: X \longrightarrow P(X)$ is a single valued mapping $t: X \to X$ such that $tx \in Tx$ for all $x \in X$.

Definition 4.1 *(Rus et al, 2003). Let (X, d) be a metric space and $c > 0$. An MWP operator $T: X \longrightarrow P(X)$ is called a$c-$multivalued weakly Picard (briefly c −MWP) operator if there exists a selection t^∞ of T^∞ such that $d(x, t^\infty(x, y)) \leqslant cd(x, y)$ for all $(x, y) \in G(T)$.*

One of the main results concerning $c-$MWP operators is the following:

Theorem 4.2 *(Rus, 2001). Let (X, d) be a metric space and $T_1, T_2: X \to P(X)$. If T_i is a c_i −MWP operator for each $i \in \{1,2\}$ and there exists $\lambda > 0$ such that $H(T_1x, T_2x) \leqslant \lambda$, for all $x \in X$. Then $H(F(T_1), F(T_2)) \leqslant \lambda max\{c_1, c_2\}$.*

Now we prove the following result.

Theorem 4.3 *Let* (X, d) *be a complete b-metric space and* $\alpha: X \times X \to \mathbb{R}^+$. *Suppose that*

g₁-: *for each* $i \in \{1,2\}, T_i: X \to Cl(X)$ *are multivalued operators such that*

$$\frac{1}{2} D(x, T_i x) \leqslant bd(x, y)$$

implies that

$$\alpha_*(T_i x, T_i y) H(T_i x, T_i y) \leqslant max\{1, N_{T_i}(x, y)\} \psi_i(d(x, y)) \quad (4.3)$$

for all $x, y \in X, \psi_i \in \Psi_4$.

g₂-: *for each* $i \in \{1,2\}, T_i$ *is* $\alpha_* -$ *admissible mapping,*

g₃-: *there exists* $x_0 \in X$ *and* $x_1 \in T_i x_0$ *such that* $\alpha(x_0, x_1) \geqslant 1$ *for each* $i \in \{1,2\}$,

g₄-: *if there is a sequence* $\{x_n\}$ *in* X *such that* $x_n \to x$, *then* $\alpha(x_n, x) \geqslant 1$ *for all* $n \in \mathbb{Z}^+$,

g₅-: *there exists* $\lambda > 0$ *such that* $H(T_1 x, T_2 x) \leqslant \lambda$, *for all* $x \in X$.

Then $Fix(T_i) \in Cl(X), i \in \{1,2\}$ *and each* T_i *is an MWP operator such that*

$$H(Fix(T_1), Fix(T_2)) \leqslant bmax\{\lambda_1, \lambda_2\}$$

where $\lambda_i = \sum_{k=0}^{\infty} b^k \psi_i^k(\lambda)$ *for each* $i \in \{1,2\}$.

Proof. From Theorem 2.1, it follows that $Fix(T_i) \neq \emptyset$ for each $i \in \{1,2\}$. Let $\{x_n\}$ be a sequence in $Fix(T_1)$ such that $x_n \to z$ as $n \to +\infty$. This implies that $\alpha(x_n, z) \geqslant 1$. Since T_1 is $\alpha_* -$admissible mapping, $\alpha(T_1 x_n, T_1 z) \geqslant 1$. As

$$\frac{1}{2} D(x_n, T_1 x_n) = 0 \leqslant bd(z, x_n),$$

so we get

$$
\begin{aligned}
&D(z,T_1z)\\
&\leqslant bd(z,x_n)+bD(x_n,T_1z)\\
&\leqslant bd(z,x_n)+bH(T_1z,T_1x_n)\leqslant bd(z,x_n)+b\alpha(T_1x_n,T_1z)H(T_1z,T_1x_n)\\
&\leqslant bd(z,x_n)+\max\{1,N_{T_1}(x,y)\}\psi_1(d(x,y))\\
&\leqslant\left(b\max\left\{1,\frac{\max\left\{\begin{matrix}d(z,x_n),D(z,T_1z)+D(x_n,T_1x_n),\\ D(z,T_1x_n)+D(x_n,T_1z)\end{matrix}\right\}}{b(1+\delta(z,T_1z)+\delta(x_n,T_1x_n))}\right\}\psi_1(d(z,x_n))\right.\\
&\quad\left.+bd(z,x_n)\right)\\
&\leqslant\left(b\max\left\{1,\frac{\max\left\{\begin{matrix}d(z,x_n),D(z,T_1z)+d(x_n,x_n),\\ d(z,x_n)+D(x_n,T_1z)\end{matrix}\right\}}{b(1+D(z,T_1z)+d(x_n,x_n))}\right\}\psi_1(d(z,x_n))\right.\\
&\quad\left.+bd(z,x_n)\right)
\end{aligned}
$$

On taking limit as $n\to+\infty$, we obtain that $D(z,T_1z)\leqslant 0$, that is, $z\in T_1z$ and hence $F(T_1)$ is closed.

Similarly, $F(T_2)$ is a closed subset of X.

From Corollary 2.2, we conclude that T_i for each $i\in\{1,2\}$ is an MWP operator.

By a similar process as followed in Theorem 2.1 starting from $x_1\in F(T_1)$ and $x_2\in T_2x_1$, we obtain a sequence $\{x_n\}$ such that $x_{n+1}\in T_2x_n$ for all $n\geqslant 1$, $x_{n+1}\neq x_n, \alpha(x_{n+1},x_{n+2})\geqslant 1, 0<D(x_{n+1},Tx_{n+1})\leqslant \psi_2(d(x_n,x_{n+1}))$ and

$$
0<d(x_{n+1},x_{n+2})<\psi_2^n\big(q\psi(c_0)\big) \qquad (4.4)
$$

for all $n\geqslant 1$, where $c_0=d(x_1,x_2)$.

Following the arguments similar to those in the proof of Theorem 2.1, we conclude that $\{x_n\}$ is a Cauchy sequence and there is an element u in X such that $x_n\to u$ as $n\to+\infty$ and $u\in T_2u$.

Note that

$$
\begin{aligned}
&d(x_n, x_{n+p})\\
&\leqslant bd(x_n, x_{n+1}) + b^2 d(x_{n+1}, x_{n+2}) + \ldots + b^{p-1} d(x_{n+p-2}, x_{n+p-1})\\
&\qquad + b^p d(x_{n+p-1}, x_{n+p})\\
&\leqslant b\psi_2^{n-1}\big(q\psi_2(c_0)\big) + b^2\psi_2^{n}\big(q\psi_2(c_0)\big) + \ldots + b^{p-1}\psi_2^{n+p-3}\big(q\psi_2(c_0)\big)\\
&\qquad + b^p\psi_2^{n+p-2}\big(q\psi_2(c_0)\big)\\
&\leqslant \frac{1}{b^{n-2}}\Big(b^{n-1}\psi_2^{n-1}\big(q\psi_2(c_0)\big) + b^n\psi_2^{n}\big(q\psi_2(c_0)\big) + \ldots + b^{n+p-2}\psi_2^{n+p-2}\big(q\psi_2(c_0)\big)\Big)\\
&= \frac{1}{b^{n-2}}\sum_{k=n-1}^{n+p-2} b^k\psi_2^k\big(q\psi_2(c_0)\big) \leqslant \frac{1}{b^{n-2}}\sum_{k=n-1}^{n+p-2} b^k\psi_2^k\big(q\psi_2(\lambda)\big)\\
&= \frac{1}{b^{n-2}}\left(\sum_{k=0}^{n+p-2} b^k\psi_2^k\big(q\psi_2(\lambda)\big) - \sum_{k=0}^{n-1} b^k\psi_2^k\big(q\psi_2(\lambda)\big) + b^{n-1}\psi_2^{n-1}\big(q\psi_2(\lambda)\big)\right).
\end{aligned}
$$

That is,

$$
\begin{aligned}
d(x_n, x_{n+p}) \leqslant \frac{1}{b^{n-2}}\Bigg(&\sum_{k=0}^{n+p-2} b^k\psi_2^k\big(q\psi_2(\lambda)\big) - \sum_{k=0}^{n-1} b^k\psi_2^k\big(q\psi_2(\lambda)\big)\\
&+ b^{n-1}\psi_2^{n-1}\big(q\psi_2(\lambda)\big)\Bigg).
\end{aligned}
\tag{4.5}
$$

On taking limit as $p \to +\infty$, we get

$$
\begin{aligned}
d(x_n, u) \leqslant \frac{1}{b^{n-2}}\Bigg(&\sum_{k=0}^{\infty} b^k\psi_2^k\big(q\psi_2(\lambda)\big) - \sum_{k=0}^{n-1} b^k\psi_2^k\big(q\psi_2(\lambda)\big)\\
&+ b^{n-1}\psi_2^{n-1}\big(q\psi_2(\lambda)\big)\Bigg).
\end{aligned}
\tag{4.6}
$$

By Lemma 1.6, $\sum_{k=0}^{\infty} b^k\psi_2^k(t)$ converges for any $t \geqslant 0$, there exists $\lambda_2 \geqslant 0$ such that $\sum_{k=0}^{\infty} b^k\psi_2^k(\lambda) = \lambda_2$ and hence

$$d(x_n,u) \leqslant \frac{1}{b^{n-2}}\left(\lambda_2 - \sum_{k=0}^{n-1} b^k\psi_2^k\big(q\psi(\lambda)\big) + b^{n-1}\psi_2^{n-1}\big(q\psi_2(\lambda)\big)\right). \quad (4.7)$$

For $n = 1$, we get $d(x_1,u) \leqslant b\lambda_2$. Thus for $x_0 \in F(T_1)$, there exists $u \in F(T_2)$ such that $d(x_0,u) \leqslant b\lambda_2$. Similarly for each $z_0 \in F(T_2)$, we get $v \in F(T_1)$ and $\lambda_1 \geqslant 0$ such that $d(z_0,v) \leqslant b\lambda_1$. It follows from Lemma 1.4 that

$$H(F(T_1),F(T_2)) \leqslant b\max\{\lambda_1,\lambda_2\}.$$

Now we discuss the Ulam-Hyers stability results.

Theorem 4.4 *Let (X,d) be a b-metric space and $T: X \to Cl(X)$. Assume that all the hypotheses of Corollary 2.3 hold. Then we have*

h$_1$-: *The fixed point inclusion (4.1) is ζ_i^{-1} – generalized Ulam-Hyers stable for $i = 1,2$, provided that for each $x \in F(T)$ there exists $z \in U$ such that $\alpha(x,z) \geqslant 1$, where $\zeta_1,\zeta_2: \mathbb{R}^+ \to \mathbb{R}^+$ defined by $\zeta_1(t) = t - b^2\psi(t), \zeta_2(t) = t - bt\psi(t)$ are strictly increasing, onto and continuous at $t = 0$.*

h$_2$-: *If $E(T) \neq \emptyset$, then the fixed point inclusion (4.1) is ζ_i^{-1} – generalized Ulam-Hyers stable for $i = 3,4$, provided that for $x \in E(T)$ there exists $z \in U$ such that $\alpha(x,z) \geqslant 1, \zeta_3,\zeta_4: \mathbb{R}^+ \to \mathbb{R}^+$ defined by $\zeta_3(t) = t - b\psi(t), \zeta_4(t) = t - t\psi(t)$ are strictly increasing, onto and continuous at $t = 0$.*

h$_3$-: *(Estimate between the fixed point sets of two multivalued mappings) If $S: X \to Cl(X)$ is such that for $x \in F(S)$ there exists $z \in F(T)$ with $\alpha(x,z) \geqslant 1$ and for $x \in F(T)$ there exists $z \in F(S)$ with $\alpha(x,z) \geqslant 1$, and $H(S(x),T(x)) \leqslant \lambda$ for all $x \in X$, then $H(F(S),F(T)) \leqslant \max_{i=1,2}\zeta_i^{-1}(b^2\lambda)$ where ζ_i is same as in (h$_1$) for each $i = 1,2$.*

h$_4$-: *(Estimate between the fixed point sets of two multivalued mappings) If $S: X \to Cl(X)$ is such that for $x \in F(S)$, there exists $z \in E(T)$ with $\alpha(x,z) \geqslant 1$ and for $x \in E(T)$ there exists $z \in F(S)$ with $\alpha(x,z) \geqslant 1$, and $H(S(x),T(x)) \leqslant \lambda$ for all $x \in X$, then $H(F(S),F(T)) \leqslant \max_{i=3,4}\zeta_i^{-1}(b\lambda)$ where ζ_i is same as in (h$_2$) for each $i = 3,4$.*

h$_5$-: *(Well-posedness of the fixed point problem with respect to b-metric d) If for any sequence $\{x_n\}$ in X, there exists a unique point $x^* \in E(T)$ such that $\alpha(x_n,x^*) \geqslant 1$ and $lim_{n\to+\infty}D(x_n,Tx_n) = 0$, then $lim_{n\to+\infty}d(x_n,x^*) = 0$.*

h$_6$-: *(Well-posedness of the fixed point problem with respect to b-metric H) If for any sequence $\{x_n\}$ in X, there exists a unique point $x^* \in E(T)$ such that $\alpha(x_n, x^*) \geqslant 1$ and $lim_{n\to+\infty} H(\{x_n\}, Tx_n) = 0$, then $lim_{n\to+\infty} d(x_n, x^*) = 0$.*

h$_7$-: *(Limit shadowing property of the multivalued operators) If for any sequence $\{x_n\}$ in X, there exists a unique point $x^* \in E(T)$ with $\alpha(x_n, x^*) \geqslant 1$ and $lim_{n\to+\infty} D(x_n, Tx_n) = 0$, then there exists a sequence of successive approximations $\{y_n\}$ such that $lim_{n\to+\infty} d(x_n, y_n) = 0$.*

Proof. (h$_1$) From Corollary 2.3, T is an MWP operator and hence $F(T)$ is nonempty. If $x^* \in F(T)$, then by given condition there exists a $y^* \in U$ such that $\alpha(x^*, y^*) \geqslant 1$. The α_*-admissibility of T gives that $\alpha(Tx^*, Ty^*) \geqslant 1$. Since $y^* \in U$, for any given $\varepsilon > 0$, we have $D(y^*, Ty^*) \leqslant \varepsilon$. Note that

$$\frac{1}{2} D(x^*, Tx^*) = 0 \leqslant bd(x^*, y^*).$$

Then

$$\begin{aligned} d(x^*, y^*) &\leqslant bD(x^*, Tx^*) + bD(Tx^*, y^*) = bD(Tx^*, y^*) \\ &\leqslant b^2(H(Tx^*, Ty^*) + D(Ty^*, y^*)) \\ &\leqslant b^2(\alpha(Tx^*, Ty^*)H(Tx^*, Ty^*) + \varepsilon) \\ \text{(u-3)} \quad &\leqslant b^2\left(\max\left\{1, \frac{d(x^*, y^*)}{b(1 + \delta(x^*, Tx^*) + \delta(y^*, Ty^*))}\right\}\psi(d(x^*, y^*)) + \varepsilon\right) \\ &\leqslant b^2\left(\max\left\{1, \frac{d(x^*, y^*)}{b(1 + d(x^*, x^*) + D(y^*, Ty^*))}\right\}\psi(d(x^*, y^*)) + \varepsilon\right) \\ &\leqslant b^2\left(\max\left\{1, \frac{d(x^*, y^*)}{b}\right\}\psi(d(x^*, y^*)) + \varepsilon\right). \end{aligned}$$

If $\max\left\{1, \frac{d(x^*, y^*)}{b}\right\} = 1$, then we have $d(x^*, y^*) \leqslant b^2(\psi(d(x^*, y^*)) + \varepsilon)$. If $\zeta_1(d(x^*, y^*)) = d(x^*, y^*) - b^2\psi(d(x^*, y^*))$, then from the above inequality we get $\zeta_1(d(x^*, y^*)) \leqslant b^2\varepsilon$ and hence $d(x^*, y^*) \leqslant \zeta_1^{-1}(b^2\varepsilon)$. Consequently, the fixed point inclusion (4.1) is $\xi-$generalized Ulam-Hyers stable, where $\xi = \zeta_1^{-1}$.

If $\max\left\{1, \frac{d(x^*, y^*)}{b}\right\} = \frac{d(x^*, y^*)}{b}$, then $d(x^*, y^*) \geqslant b$. From (4.1) we obtain

that

$$
\begin{aligned}
d(x^*,y^*) &\leqslant b^2\left(\frac{d(x^*,y^*)}{b}\psi(d(x^*,y^*))+\varepsilon\right)\\
&\leqslant bd(x^*,y^*)\psi(d(x^*,y^*))+b^2\varepsilon\\
&\leqslant bd(x^*,y^*)\psi(d(x^*,y^*))+b^2\varepsilon.
\end{aligned}
$$

Now if $\zeta_2(d(x^*,y^*))=d(x^*,y^*)-bd(x^*,y^*)\psi(d(x^*,y^*))$, then from the above inequality we get $\zeta_2(d(x^*,y^*))\leqslant b^2\varepsilon$ and hence $d(x^*,y^*)\leqslant \zeta_2^{-1}(b^2\varepsilon)$. Consequently, the fixed point inclusion (4.1) is $\xi-$generalized Ulam-Hyers stable, where $\xi=\zeta_2^{-1}$.

(h_2) Let $E(T)\neq\emptyset$, and $x^*\in E(T)$ then

$$d(x^*,y^*)=D(Tx^*,y^*)\leqslant b(H(Tx^*,Ty^*)+D(Ty^*,y^*)).$$

Following the arguments similar to those in the proof of (h_1), the result follows.

(h_3) Let $x^*\in F(S)$, then there exists a $y^*\in F(T)$ such that $\alpha(x^*,y^*)\geqslant 1$. By α_*-admissibility of T we get $\alpha(Tx^*,Ty^*)\geqslant 1$. Note that

$$\frac{1}{2}D(y^*,Ty^*)=0\leqslant bd(x^*,y^*).$$

Then by the given assumption on T, we obtain that

$$
\begin{aligned}
d(x^*,y^*) &\leqslant bD(x^*,Sx^*)+bD(Sx^*,y^*)\\
&= bD(Sx^*,y^*)\leqslant b^2(H(Sx^*,Tx^*)+D(Tx^*,y^*))\\
&\leqslant b^2(H(Sx^*,Tx^*)+H(Tx^*,Ty^*))\leqslant b^2(\lambda+H(Tx^*,Ty^*))\\
&\leqslant b^2(\lambda+\alpha(Tx^*,Ty^*)H(Tx^*,Ty^*))\\
&\leqslant b^2\left(\lambda+\max\left\{1,\frac{d(x^*,y^*)}{b(1+\delta(x^*,Tx^*)+\delta(y^*,Ty^*))}\right\}\psi(d(x^*,y^*))\right)\\
&\leqslant b^2\left(\lambda+\max\left\{1,\frac{d(x^*,y^*)}{b(1+d(x^*,x^*)+D(y^*,Ty^*))}\right\}\psi(d(x^*,y^*))\right)\\
&\leqslant b^2\left(\lambda+\max\left\{1,\frac{d(x^*,y^*)}{b(1+d(x^*,x^*)+D(y^*,Ty^*))}\right\}\psi(d(x^*,y^*))\right)\\
&\leqslant b^2(\lambda+\psi(d(x^*,y^*))).
\end{aligned}
$$

If $\max\left\{1,\frac{d(x^*,y^*)}{b}\right\}=1$, and

$$\zeta_1(d(x^*,y^*))=d(x^*,y^*)-b^2(\psi(d(x^*,y^*))),$$

then from the above inequality we get $\zeta_1(d(x^*,y^*))\leqslant b^2\lambda$. Consequently, for every $x^*\in F(S)$, there exists a $y^*\in F(T)$ such that $d(x^*,y^*)\leqslant \zeta_1^{-1}(b^2\lambda)$. Similarly, it can be proved that for every $y^*\in F(T)$, there exists a $x^* \in F(T)$ such that $d(x^*, y^*) \leqslant \zeta_1^{-1}(b^2\lambda)$. Hence by Lemma 1.4, we obtain that

$$H(F(S), F(T)) \leqslant \zeta_1^{-1}(b^2\lambda).$$

If $\max\left\{1, \frac{d(x^*,y^*)}{b}\right\} = \frac{d(x^*,y^*)}{b}$, then for $\zeta_1(d(x^*, y^*)) = d(x^*, y^*) - bd(x^*, y^*)\psi(d(x^*, y^*))$ we get

$$H(F(S), F(T)) \leqslant \zeta_2^{-1}(b^2\lambda).$$

Consequently,

$$H(F(S), F(T)) \leqslant \max_{i=1,2} \zeta_i^{-1}(b^2\lambda).$$

(h_4) This can be proved on the similar lines as in (h_3) using the definition of $E(T)$.

(h_5) If $\{x_n\}$ is a sequence in X, there exists a unique $x^* \in E(T)$ such that $\alpha(x_n, x^*) \geqslant 1$ and $\lim_{n\to+\infty} D(x_n, Tx_n) = 0$. Then there exists $u_n \in Tx_n$ such that $\lim_{n\to+\infty} D(x_n, Tx_n) = \lim_{n\to+\infty} d(x_n, u_n) = 0$. Since T is α_* – admissible, $\alpha(Tx_n, Tx^*) \geqslant 1$. As $\frac{1}{2}D(x^*, Tx^*) = 0 \leqslant bd(x_n, x^*)$, by given assumption we have

$$\begin{aligned}
d(x_n, x^*) &\leqslant b(D(x_n, Tx_n) + D(Tx_n, x^*)) \\
&\leqslant b(D(x_n, Tx_n) + H(Tx_n, Tx^*)) \\
&\leqslant b(D(x_n, Tx_n) + \alpha(Tx_n, Tx^*)H(Tx_n, Tx^*)) \\
&\leqslant b\Big(D(x_n, Tx_n) \\
&\quad + \max\left\{1, \frac{d(x_n, x^*)}{b(1 + D(x_n, Tx_n) + D(x^*, Tx^*))}\right\}\psi(d(x_n, x^*))\Big) \\
&\leqslant b\Big(D(x_n, Tx_n) \\
&\quad + \max\left\{1, \frac{d(x_n, x^*)}{b(1 + D(x_n, Tx_n))}\right\}\psi(d(x_n, x^*))\Big) \\
&\leqslant b\left(D(x_n, Tx_n) + \max\left\{1, \frac{d(x_n, x^*)}{b}\right\}\psi(d(x_n, x^*))\right).
\end{aligned}$$

If $\max\left\{1, \frac{d(x_n,x^*)}{b}\right\} = 1$, then we have

$$d(x_n, x^*) - b\psi(d(x_n, x^*))) \leqslant bD(x_n, Tx_n).$$

That is, $\zeta_3(d(x_n, x^*)) \leqslant bD(x_n, Tx_n)$. Similarly, if $\max\left\{1, \frac{d(x_n,x^*)}{b}\right\} = \frac{d(x_n,x^*)}{b}$, we get $\zeta_4(d(x_n, x^*)) \leqslant bD(x_n, Tx_n)$. This implies for each $i \in \{3,4\}$ we get $d(x_n, x^*) \leqslant \zeta_i^{-1}(bD(x_n, Tx_n))$. On taking limit as $n \to +\infty$ and using the continuity of ζ_i at 0, for each $i \in \{3,4\}$ we get the desired result.

VOJNOTEHNIČKI GLASNIK / MILITARY TECHNICAL COURIER, 2020, Vol. 68, Issue 3

(h$_6$) follows from (h$_5$) as $D(x_n, Tx_n) \leqslant H(\{x_n\}, Tx_n)$.

(h$_7$) From (h$_5$) it is clear that $\lim_{n\to+\infty} d(x_n, x^*) = 0$. Since $x^* \in E(T)$, so there exists a sequence of successive approximations defined by $y_n = x^*$ for all n such that $\lim_{n\to+\infty} d(x_n, y_n) = \lim_{n\to+\infty} d(x_n, x^*) = 0$.

Existence and stability of solutions of differential inclusions

Let $Cl_c(\mathbb{R})$ be collection of nonempty closed and convex subsets of $\mathbb{R}$ and $F: \mathbb{R} \to Cl_c(\mathbb{R})$ a lower semicontinuous multivalued mapping. Consider the initial value problem

$$\begin{aligned} &x'(t) \in F\big(x(t)\big), \text{for} t \in J, \\ &x(t) = x_0 \text{for} t = a_1, \\ &x \in C(J), \end{aligned} \tag{4.8}$$

where $J = [a_1, a_2]$ and $C(J)$ is a Banach space of absolutely continuous real valued functions defined on J. Since $\mathbb{R}$ with usual metric is paracompact, F is a lower semicontinuous multivalued mapping with $F(u)$ closed and convex for each $u \in \mathbb{R}$, by Michael's Theorem (Michael, 1956), there exists a continuous function $f: \mathbb{R} \to \mathbb{R}$ such that $f(u) \in F(u)$ for all $u \in \mathbb{R}$.

Now consider the following initial value problem

$$\begin{aligned} &x'(t) = f\big(x(t)\big), \text{for} t \in J, \\ &x(t) = x_0 \text{for} t = a_1, \\ &x \in C(J). \end{aligned} \tag{4.9}$$

Note that the solution of problem (4.9) is a solution of problem (4.8). Integrating from a_1 to t, we obtain

$$\int_{a_1}^{t} x'(s)ds = \int_{a_1}^{t} f\big(x(s)\big)ds,$$

that is,

$$x(t) = x_0 + \int_{a_1}^{t} f(x(s))ds, \text{for} t \in J. \tag{4.10}$$

On the other hand, if (4.10) holds then (4.9) holds. Thus (4.9) and (4.10) are equivalent.

Suppose that $f:\mathbb{R}\to\mathbb{R}$satisfies the following hypotheses:

$\int_{a_1}^{t} f(x(s))ds = 0$, for $t \in J$ if and only if $x(t) = x_0(t)$ for all $t \in J$.

There exists a nonnegative real number L_f such that $L_f(a_2 - a_1) < \frac{1}{b^2}$, where b is b-metric constant and for all $u, v \in \mathbb{R}$, the relation $\|f(u) - f(v)\| \leqslant L_f\|u(t) - v(t)\|$ holds.

Define $T: X \to X$, where $X := C(J)$ by

$$T(x(t)) = x_0 + \int_{a_1}^{t} f(x(s))ds, \text{for} t \in J. \tag{4.11}$$

Let $d: C(J) \times C(J) \to \mathbb{R}^+$ be defined as

$$d(x, y) := \max_{t\in J}\|x(t) - y(t)\|^2.$$

Then $(C(J), d)$ is complete b-metric space. Define $\alpha: C(J) \times C(J) \to \mathbb{R}^+$ by

$$\alpha(x,y) = \begin{cases} k & \text{for} x \neq x_0, y \neq y_0, \text{where} k \geqslant 1, \\ 0 & \text{otherwise.} \end{cases}$$

Let $\psi: \mathbb{R}^+ \to \mathbb{R}^+$ be defined as $\psi(t) := L_f^2(a_2 - a_1)t$. Clearly, $\psi \in \Psi_4$.

First we show that mapping T is $\alpha_* -$admissible. As $\alpha(x, y) \geqslant 1$ implies that $\alpha(x, y) = k$. For $x \neq x_0$ and $y \neq x_0$, from (i$_1$-) we have $Tx \neq x_0$ and $Ty \neq x_0$ on J. It follows that $\alpha_*(Tx, Ty) = k \geqslant 1$ and hence T is $\alpha_* -$admissible. Now, by (i$_2$-) for all $x, y \in X$,

$$d(Tx, Ty) = \max_{t\in J}\left\|\int_{a_1}^{t} f(x(s))ds - \int_{a_1}^{t} f(y(s))ds\right\|^2$$

$$\leqslant \max_{t\in J}\int_{a_1}^{t} \| f(x(s))ds - f(y(s))ds \|^2$$

$$\leqslant \max_{t\in J}\int_{a_1}^{t} L_f^2 \parallel x(s)-y(s) \parallel^2 ds$$

$$\leqslant L_f^2\max_{t\in J}\int_{a_1}^{t} \max_{s\in J} \parallel x(s)-y(s) \parallel^2 ds$$

$$= L_f^2 d(x,y)\max_{t\in J}\int_{a_1}^{t} ds = L_f^2(a_2-a_1)d(x,y) = \psi(d(x,y)).$$

By Corollary 2.3, we obtain the solution of problem (4.9) which provides the solution of problem (4.8) as well. Define the mappings $\zeta_1, \zeta_2: \mathbb{R}^+ \to \mathbb{R}^+$ by

$$\zeta_1(t) = t - b^2L_f^2(a_2-a_1)t = t - b^2\psi(t),$$
$$\zeta_2(t) = t - bL_f^2(a_2-a_1)t^2 = t - bt\psi(t),$$

where $\psi(t) = L_f^2(a_2-a_1)t$. Clearly the mapping ζ_1 is strictly increasing and onto. Consequently, all the axioms of Theorem 4.4 hold with mapping ζ_1. Hence the fixed point inclusion (4.8) is $\zeta_1^{-1}-$generalized Ulam-Hyers stable. Now $\frac{d}{dt}\zeta_2(t) > 0$ if $1-2bL_f^2(a_2-a_1)t > 0$. As $bL_f^2(a_2-a_1) < 1$, hence the fixed point inclusion (4.8) is $\zeta_2^{-1}-$generalized Ulam-Hyers stable if $t < \frac{1}{2}$.

Let $F: J\times\mathbb{R}\times\mathbb{R} \to Cl_c(\mathbb{R})$ be a lower semicontinuous multivalued mapping. Consider the initial value problem

$$\begin{aligned} &x'(t) \in F(t, x(t), x(t-h)), \text{for} t \in J,\\ &x(t) = x_0 \text{for} t \in [a_1-h, a_1],\\ &x \in C(J), \end{aligned} \tag{4.12}$$

where h is a positive real number. Then there exists a selection f such that $f(s,u,v) \in F(s,u,v)$ for all $u,v\in\mathbb{R}$ and $s \in [a_1-h, a_1]$, see (Michael, 1956). Note that any solution of the problem

$$\begin{aligned} &x'(t) = f\big(t, x(t), x(t-h)\big), \text{for} t \in J,\\ &x(t) = x_0 \text{for} t \in a_1-h, a_1],\\ &x \in C(J) \end{aligned} \tag{4.13}$$

is a solution for problem (4.12). Further, (4.13) is equivalent to

$x(t) = x_0 + \int_{a_1}^{t} f(s, x(s), x(s-h)ds, \text{for} t \in J,$
$x(t) = x_0 \text{for} t \in a_1 - h, a_1].$

We suppose that f satisfies the following hypotheses:

$\int_{a_1}^{t} f(s, x(s), x(s-h))ds = 0$, for $t \in J$ if and only if $x = x_0$ on J.

$\|f(t, u_1, v_1) - f(t, u_2, v_2)\| \leqslant L_f(\|u_1 - u_2\| + \|v_1 - v_2\|),$

for all $u_1, u_2, v_1, v_2 \in \mathbb{R}$, where $L_f(a_2 - a_1) < \frac{1}{4b^2}$ and b is a metricconstant.

Define the operator $T: Y \to Y$, where $Y := C[a_1 - h, a_2] \times \mathbb{R} \times \mathbb{R}$ by

$$T(x(t)) = \begin{cases} x_0 + \int_{a_1}^{t} f(s, x(s), x(s-h))ds, \text{for} t \in J, \\ x(t) = x_0 \text{for} t \in a_1 - h, a_1]. \end{cases} \quad (4.14)$$

From the definition of α, the admissibility of T follows. Now by (i_4-) for all $x, y \in Y$, we have

$$\begin{aligned} d(Tx, Ty) &= \max_{t \in J} \| \int_{a_1}^{t} f(s, x(s), x(s-h))ds - \int_{a_1}^{t} f(s, x(s), y(s-h))ds \|^2 \\ &\leqslant \max_{t \in J} \int_{a_1}^{t} \| f(s, x(s), x(s-h))ds - f(s, x(s), y(s-h))ds \|^2 \\ &\leqslant \max_{t \in J} \int_{a_1}^{t} L_f^2 \| x(s) - y(s) \|^2 (2^2)ds \\ &= 4L_f^2 \max_{t \in J} \int_{a_1}^{t} \| x(s) - y(s) \|^2 ds \\ &\leqslant 4L_f^2(a_2 - a_1)\psi(d(x, y)), \end{aligned}$$

where $\psi(t) = 4L_f^2(a_2 - a_1)t$. By Corollary 2.3, we obtain the solution of problem (4.13) which is also being the selection is the solution for (4.12). If $\zeta_1(t) = t - 4b^2 L_f^2(a_2 - a_1)t$ and $\zeta_2(t) = t - 4bL_f^2(a_2 - a_1)t^2$, then the fixed point inclusion (4.12) is ζ_1^{-1} – generalized Ulam-Hyers stable. Now $\frac{d}{dt}\zeta_2(t) > 0$ if $1 - 8bL_f^2(a_2 - a_1)t > 0$. As $4bL_f^2(a_2 - a_1) < 1$, hence the fixed point inclusion (4.12) is ζ_2^{-1} – generalized Ulam-Hyers stable if $t < \frac{1}{2}$.

References

Abbas, M., Ali, B., & Vetro, C. 2013. A Suzuki type fixed point theorem for a generalized multivalued mapping on partial Hausdorff metric spaces. *Topology and its Applications,* 160(3), pp.553-563. Available at: https://doi.org/10.1016/j.topol.2013.01.006.

Abbas, M., Ćirić, Lj., Damjanović, B., & Khan, M.A. 2012. Coupled coincidence and common fixed point theorems for hybrid pair of mappings on a test. *Fixed Point Theory and Applications,* art.number:4. Available at: https://doi.org/10.1186/1687-1812-2012-4.

Aleksić, S., Došenović, T., Mitrović, D.Z., & Radenović, S. 2019a. Remarks on common fixed point results for generalized $\alpha_* - \psi$- contraction multivalued mappings in *b*-metric spaces. *Advances in Fixed Point Theory,* 9(1), pp.1-16. Available at: https://doi.org/10.28919/afpt/3731.

Aleksić, S., Huang, H, Mitrović, D.Z., & Radenović, S. 2018. Remarks on some fixed point results in *b*-metric spaces. *Journal of Fixed Point Theory and Applications,* 20(art.number:147). Available at: https://doi.org/10.1007/s11784-018-0626-2.

Aleksić, S., Mitrović, Z.D., & Radenović, S. 2019b. Picard sequences in b-metric spaces. *Fixed Point Theory*, 21(1), pp.35-46. Available at: https://doi.org/10.24193/fpt-ro.2020.1.03.

Ali, B., & Abbas, M. 2017. Existence Ulam–Hyers stability of fixed point problem of generalized Suzuki type (α_*, ψ_φ)-contractive multivalued operators. *Revista de la Real Academia de Ciencias Exactas, Físicas y Naturales. Serie A. Matemáticas (RACSAM),* 111(4), pp.1129-1146. Available at: https://doi.org/10.1007/s13398-016-0351-x.

An, T.V., Dung, N.V., Kadelburg, Z., & Radenović, S. 2015a. Various generalizations of metric spaces and fixed point theorems. *Revista de la Real Academia de Ciencias Exactas, Físicas y Naturales. Serie A. Matemáticas (RACSAM),* 109, pp.175-198. Available at: https://doi.org/10.1007/s13398-014-0173-7.

An, T.V., Tuyen, L.Q., & Dung, N.V. 2015b. Stone-type theorem on b-metric spaces and applications. *Topology and its Applications,*185-186, pp.50-64. Available at: https://doi.org/10.1016/j.topol.2015.02.005.

Asl, J.H., Rezapour, Sh., & Shahzad, N. 2012. On fixed points of $\alpha - \psi$-contractive multifunctions. *Fixed Point Theory and Applications,* art.number:212. Available at: https://doi.org/10.1186/1687-1812-2012-212.

Banach, S. 1922. Sur les opérations dans les ensembles abstraits et leur applications aux équations intégrales. *Fundamenta Mathematicae,* 3, pp.133-181 (in French). Available at: https://doi.org/10.4064/fm-3-1-133-181.

Berinde, V. 1993. Generalized contractions in quasimetric spaces. In: *Seminar on Fixed Point Theory,* Babeş-Bolyai University, Cluj-Napoca, pp.3-9.

Berinde, V. 1996. Sequences of operators and fixed points in quasimetric spaces. *Studia Universitatis Babeş-Bolyai Mathematica,* 41(4), pp.23-27.

Berinde, V. 1997. *Contracţii generalizate şi aplicaţii*. Baia Mare: Editura Club Press (in Romanian).

Bhaskar, T.G., & Lakshmikantham, V. 2006. Fixed point theorems in partially ordered metric spaces and applications. *Nonlinear Analysis: Theory, Methods &Applications,* 65(7), pp.1379-1393. Available at: https://doi.org/10.1016/j.na.2005.10.017.

Bota, M.F., Ilea, V., Karapınar, E., & Mleşniţ, O. 2015. On $\alpha_* - \psi$-contractive multivaalued operators in *b*-metric spaces and applications. *Applied Mathematics & Information Sciences,* 9(5), pp.2611-2620 [online]. Available at: http://www.naturalspublishing.com/Article. Asp?ArtcID=9576 [Accessed: 21 May 2020].

Chifu, C., & Petruşel, G. 2014. Fixed points for multivalued contractions in b-metric spaces with applications to fractals. *Taiwanese Journal of Mathematics,* 18(5), pp.1365-1375. Available at: https://doi.org/10.11650/tjm.18.2014.4137.

Czerwik, S. 1993. Contraction mappings in *b*-metric spaces. *Acta Mathematica et Informatica Universitatis Ostraviensis,* 1(1), pp.5-11 [online]. Available at: https://dml.cz/dmlcz/120469[Accessed: 21 May 2020].

Ćirić, Lj., Abbas, M., Rajović, M., & Ali, B. 2012. Suzuki type fixed point theorems for generalized multi-valued mappings on a set endowed with two *b*-metric. *Applied Mathematics and Computation,* 219(4), pp.1712-1723. Available at: https://doi.org/10.1016/j. Amc.2012.08.011.

Fréchet, M. 1905. La notion d'écart et le calcul fonctionnel. *Comptes Rendus Hebdomadaires des Scéances de l'Académie des Sciences,* 140(1), pp.772-774 [online]. Available at: https://www.biodiversitylibrary.org/item/31541#page/778/mode/1up (in French) [Accessed: 21 May 2020].

Haghi, R.H., Rezapour, Sh., & Shahzad, N. 2011. Some fixed point generalisations are not real generalizations. *Nonlinear Analysis: Theory, Methods & Applications,* 74(5), pp.1799-1803. Available at: https://doi.org/10.1016/j.na.2010.10.052.

Hussain, N., Đorić, D., Kadelburg, Z., & Radenović, S. 2012. Suzuki-type fixed point results in metric type spaces. *Fixed Point Theory and Applications,* art.number:126. Available at: https://doi.org/10.1186/1687-1812-2012-126.

Hyers,D.H. 1941. On the stability of the linear functional equation. In: *Proceedings of the National Academy of Sciences of the USA,* 27(4), pp.222-224, April 15. Available at: https://doi.org/10.1073/pnas.27.4.222.

Karapinar, E., Mitrović, Z.D., Ozturk, A., & Radenović, S. 2020. On a theorem of Cirić in *b*-metric spaces. *Rendiconti del Circolo Matematico di palermo Series 2*. Available at: https://doi.org/10.1007/s12215-020-00491-9.

Khojasteh, F., Abbas, M., & Costache, S. 2014. Two new types of fixed point theorems in complete metric spaces. *Variational Analysis, Optimization, and Fixed Point Theory,* art.ID325840. Available at: https://doi.org/10.1155/2014/325840.

Kirk, W., & Shahzad, N. 2014. *Fixed Point Theory in Distance Spaces*. Cham, Switzerland: Springer International Publishing.

Latif, A., Parvaneh, V., Salimi, P., & Al-Mazrooei, A.E. 2015. Various Suzuki type theorems in *b*-metric spaces. *Journal of Nonlinear Sciences and Applications (JNSA),* 8(4), pp.363-377. Availableat: https://doi.org/10.22436/jnsa.008.04.09.

Lazar, V.L. 2012. Ulam-Hyers stability for partial differential inclusions. *Electronic Journal of Qualitative Theory of Differential Equations,* 21, pp.1-19. Available at: https://doi.org/10.14232/ejqtde.2012.1.21.

Michael, E. 1956. Continuous selections. I. A*nnals of Mathematics,* 63(2), pp.361-382. Available at: https://doi.org/10.2307/1969615.

Mitrović, Z.D. 2019. A note on the results of Suzuki, Miculescu and Mihail. *Journal of Fixed Point Theory and Applications*, 21(art.number:24). Available at: https://doi.org/10.1007/s11784-019-0663-5.

Mitrović, Z.D., Parvaneh, V., Mlaiki, N., Hussain, N., & Radenović, S. 2020. On some new generalizations of Nadler contraction in b-metric spaces. *Cogent Mathematics and Statistics*, 7(1), art.number:1760189. Available at: https://doi.org/10.1080/25742558.2020.1760189.

Mohammadi, B., Dinu, S., & Rezapour, Sh. 2013. Fixed points of Suzuki type quasi-contractions. *U.P.B. Scientific Bulletin, Series A,*75(3), pp.3-12 [online]. Available at: https://www.scientificbulletin.upb.ro/rev_docs_arhiva/fulld89_199620.pdf. [Accessed: 21 May 2020].

Nadler, Jr. S.B. 1969. Multi-valued contraction mappings. *Pacific Journal of Mathematics,* 30(2), pp.475-488. Available at: https://doi.org/10.2140/pjm.1969.30.475.

Nieto, J.J., & Rodríguez-López, R. 2005. Contractive mapping theorems in partially ordered sets and applications to ordinary differential equation. *Order,* 22, pp.223-239. Available at: https://doi.org/10.1007/s11083-005-9018-5.

Nieto, J.J., & Rodríguez-López, R. 2007. Existence and uniqueness of fixed point in partially ordered sets and applications to ordinary differential equations. *Acta Mathematica Sinica, English Series,* 23, pp.2205-2212. Available at: https://doi.org/10.1007/s10114-005-0769-0.

Păcurar, M. 2010. A fixed point result for φ-contractions on *b*-metric spaces without the boundedness assumption. *Fasciculi Mathematici,* 43, pp.127-137 [online]. Available at: http://www.math.put.poznan.pl/artykuly/FM43(2010)-PacurarM.pdf [Accessed: 21 May 2020].

Petru, T.P., Petrusel, A., & Yao, J.-C. 2011. Ulam-Hyers stability for operatorial equations inclusions via nonself operators. *Taiwanese Journal of Mathematics,* 15(5), pp.2195-2212. Available at: https://doi.org/10.11650/twjm/1500406430.

Ran, A.C.M., & Reurings, M.C.B. 2004. A fixed point theorem in partially ordered sets and some applications to matrix equations. *Proceedings of the American Mathematical Society,* 132(5), pp.1435-1443. Available at: https://doi.org/10.1090/S0002-9939-03-07220-4.

Rhoads, B.E. 2015. Two new fixed point theorem. *Gen. Math. Notes,* 27(2), pp.123-132 [online]. Available at: https://www.emis.de/journals/GMN/yahoo_site_admin/assets/docs/12_GMN-7082-V27N2.154194604.pdf[Accessed: 21 May 2020].

Rus, I. A. 2001. *Generalized contractions and applications.* Cluj: University Press.

Rus, I. A. 2009. Remarks on Ulam stability of the operatorial equations. *Fixed Point Theory,*10(2), pp.305-320 [online]. Available at: http://www.math.ubbcluj.ro/~nodeacj/vol__10(2009)_no_2.php[Accessed: 21 May 2020].

Rus, I. A., Petruşel, A., & Sîntămărian, A. 2003. Data dependence of the fixed point set of some multivalued weakly Picard operators. *Nonlinear Analysis: Theory, Methods & Applications,* 52(8), pp.1947-1959. Available at: https://doi.org/10.1016/S0362-546X(02)00288-2.

Samet, B., Vetro, C., & Vetro, P. 2012. Fixed point theorems for $\alpha - \psi$-contractive type mappings. *Nonlinear Analysis: Theory, Methods & Applications,* 75(4), pp.2154-2165. Available at: https://doi.org/10.1016/j.na.2011.10.014.

Singh, S.L., & Prasad, B. 2008. Some coincidence theorems and stability of iterative procedures. *Computers & Mathematics with Applications,* 55(11), pp.2512-2520. Available at: https://doi.org/10.1016/j.camwa.2007.10.026.

Suzuki, T. 2008. A generalized Banach contraction principle that characterizes metric completeness. *Proceedings of the American Mathematical Society,* 136(5), pp.1861-1869. Available at: https://doi.org/10.1090/S0002-9939-07-09055-7.

Ulam, S.M. 1964. *Problems in Modern Mathematics.* New York, NY: John Wiley and Sons.

РЕШЕНИЯ И УСТОЙЧИВОСТЬ ДИФФИРЕНЦИАЛЬНЫХ ВКЛЮЧЕНИЙ ПО УЛАМУ-ХАЙЕРСУ, ВКЛЮЧАЯ РАЗНОВИДНОСТИ МНОГОЗНАЧНЫХ ОТОБРАЖЕНИЙ ПО СУДЗУКИ В *b*-МЕТРИЧЕСКИХ ПРОСТРАНСТВАХ

Муджахид Абас[а], *Басит* Али[б], *Талат* Назир[в], *Небойша* М. Дедович[г], *Бандар* Бин-Мохсин[д], *Стоян* Н. Раденович[е]

[а] Правительственный колледж в Лахоре - Университет, кафедра математики, г. Лахор, Исламская Республика Пакистан; Преторийский университет, кафедра математики и прикладной математики, г. Претория, Южно-Африканская Республика

[б] Университет менеджмента и технологий, кафедра математики, г. Лахор, Исламская Республика Пакистан

[в] Университет COMSATS в Исламабаде, кафедра математики, Кампус в г. Абботтабад, Исламская Республика Пакистан; Университет Южной Африки, кафедра математических наук, Научный кампус, г. Йоханнесбург, Южно-Африканская Республика

[г] Нови-Садский университет, Сельскохозяйственный факультет, Департамент сельскохозяйственного машиностроения, г. Нови-Сад, Республика Сербия, **корреспондент**

[д] Университет им. Короля Сауда, Колледж физико-математических наук, кафедра математики, Эр-Рияд, Королевство Саудовская Аравия

[е] Белградский университет, Машиностроительный факультет, г. Белград, Республика Сербия

РУБРИКА ГРНТИ: 27.00.00 МАТЕМАТИКА;
27.25.17 Метрическая теория функций,
27.39.27 Нелинейный функциональный анализ
ВИД СТАТЬИ: оригинальная научная статья

Резюме:

Введение/цель: В данной статье представлены совпадения и общие неподвижные точки многозначного отображения типа Судзуки в b-метрических пространствах.

Методы: Обсуждаются предельные свойства, корректность и устойчивость решенийзадачс неподвижной точкой таких отображений по методу Улама-Хайерса.

Результаты: Получена верхняя граница расстояния Хаусдорфа между неподвижными точками множеств. В качестве доказательства полученных результатов, в статье приведено несколько примеров.

Выводы: Применение полученных результатов доказывает существование дифференциальных включений.

Ключевые слова: b-метрические пространства, многозначные отображения, неподвижная точка и задачи, Улам-Хайерс стабильность, начальная задача.

РЕШЕЊА И УЛАМ-ХИЕРОВА СТАБИЛНОСТ ДИФЕРЕНЦИЈАЛНИХ ИНКЛУЗИЈА, УКЉУЧУЈУЋИ СУЗУКИЈЕВЕ ВРСТЕ ВИШЕЗНАЧНОГ ПРЕСЛИКАВАЊА НА *b*-МЕТРИЧКИМ ПРОСТОРИМА

Муџахид Абас[а], *Басит* Али[б], *Талат* Назир[в], *Небојша* М. Дедовић[г], *Бандар* Бин-Мохсин[д], *Стојан* Н. Раденовић[ђ]

[а] Владин колеџ – Универзитет, Одсек математике, Лахоре, Исламска Република Пакистан; Универзитет у Преторији, Одсек за математику и примењену математику, Преторија, Јужноафричка Република

[б] Универзитет за менаџмент и технологију, Одсек за математику, Лахоре, Исламска Република Пакистан

[в] Универзитет COMSATS у Исламабаду, Одсек за математику, Кампус Аботабад, Исламска Република Пакистан; Универзитет Јужне Африке, Одсек за математичке науке, Научни кампус, Јоханесбург, Јужноафричка Република

[г] Универзитет у Новом Саду, Пољопривредни факултет, Департман за пољопривреду технику, Нови Сад, Република Србија, **аутор за преписку**

[д] Универзитет краља Сауда, Колеџ природно-математичких наука, Одсек за математику, Ријад, Краљевина Саудијска Арабија,

[ђ] Универзитет у Београду, Машински факултет, Београд, Република Србија

ОБЛАСТ: математика
ВРСТА ЧЛАНКА: оригинални научни рад

Сажетак:

Увод/циљ: У раду су представљене коинцидентне и заједничке фиксне тачке Сузукијеве врсте вишезначног пресликавања на b-метричким просторима.

Методе: Анализирана су гранична својства, добра постављеност и Улам-Хиерова стабилност решења за фиксни проблем вишезначних пресликавања.

Резултати: Добијена је горња граница Хауздорфовог растојања између фиксних тачака скупова. Наведени су примери који подржавају добијене резултате.

Закључак: Применом представљених резултата установљена је егзистенција диференцијалне инклузије.

Кључне речи: b-метрички простори, вишезначно пресликавање, фиксна тачка и проблеми, Улам-Хиерова стабилност, почетни проблем.

Paper received on / Дата получения работы / Датум пријема чланка: 25.05.2020.
Manuscript corrections submittedon / Дата получения исправленной версии работы / Датум достављања исправки рукописа: 03.06.2020.
Paper accepted for publishingon / Дата окончательного согласования работы / Датум коначног прихватања чланка за објављивање: 05.06.2020.

PARTIAL STABILITY OF MULTI ATTRIBUTE DECISION-MAKING SOLUTIONS FOR INTERVAL DETERMINED CRITERIA WEIGHTS - THE PROBLEM OF NONLINEAR PROGRAMMING

Radomir R. Đukić
independent researcher, Kruševac, Republic of Serbia,
e-mail: raddjukic@gmail.com,
ORCID iD: https://orcid.org/0000-0002-3799-8009

DOI: 10.5937/vojtehg68-27014; https://doi.org/10.5937/vojtehg68-27014

FIELD: Mathematics, Nonlinear programming
ARTICLE TYPE: Original scientific paper

Abstract:

Introduction/purpose: The paper presents a designed procedure for solving a class of nonlinear programming (NLP) tasks with the nonlinear and differentiable objective function, linear natural constraints (intervals of possible arguments values - variables) and the normalization condition for arguments. The procedure was applied to determine the partial stability of the solution of the problem of multi attibute decision-making (MADM).

Methods: The basis of the procedure is to define the nodes of argument pairs and their parameters for the allowable multidimensional points. The parameters are implemented in the gradient method, the favorable directions method and the line search method. In the development of the procedure, the basics of the TOPSIS method for MADM with interval-given criteria weights were used, primarily due to the nonlinearity of the reference function.

Results: The paper elaborates the procedure of determining extreme and other admissible solutions of the reference function (boundary and basic solutions) and all vertices of the convex set of the function definition. This forms a complete graph of the function, i.e. the required solutions from the allowable set can be determined. A procedure for determining a set of solutions for defining a separating hyperplane of a set of function values has been developed; in this way, as a specific case, a set of solutions of partial stability of the variant is defined as MADM solutions. Adequate procedures have been proposed to eliminate the degeneration of the procedure (wedging and oscillation of the solution).

Conclusions: The most significant contribution of the paper is the definition of the nodes of argument pairs and their parameters which ensure the *normalization condition in each node and for each allowable point, non-negativity of variables and independence of argument changes in nodes, within active constraints. An original procedure for determining function graphs has been developed. An appropriate real numerical example is given.*

Keywords: criteria weights, nodes of argument pairs, gradient method, favorable direction method, system of basic solutions, multi attribute decision-making, partial stability of solutions.

Introduction

Problems of nonlinear programming (NLP) with the nonlinear objective function, linear natural constraints of arguments (intervals of possible values of arguments) and the normalization condition for arguments cannot be solved by applying classical NLP methods. The normalization condition implies a constant sum and positive values of arguments in each multidimensional point from the admissible convex set of the function definitions. Relying on the knowledge and procedures from the classical NLP methods (Petrić, 1979), (Hadley, 1964), (Zangville, 1969), (Bazaraa et al, 2006), (Luenberger & Ye, 2016), developed for problems with or without limitations, the procedure developed in this paper can be applied for the development of the procedure for solving this class of NLP tasks. At the same time, the necessary procedures based on the introduced concept of *nodes of arguments* (or *nodes of criterion*) for the problem of multi attribute decision-making (MADM) have been developed, thus transforming the criterion function and constraints and creating a new NLP model based on node parameters. The new model does not contain a singled out normalization condition, because it is built into each feasible point through the node parameters.

As the aim of the paper is conceived on two bases - to show a possible procedure for solving this class of NLP tasks while including consideration of partial stability of MADM solutions - a complex method TOPSIS (Technique for Order Preference by Similarity to Ideal Solution) was chosen as an example (Hwang & Yoon, 1981), (Yoon, 1987). The chosen method is based on multiple distances of quantitative indicators of quality of variants (values according to the established criteria - criteria values from the best and most unfavorable existing ("perceived") criteria values. The method was chosen solely because of the nonlinearity of the reference function, since in most other methods this function is linear (VIKOR, MABAC, COPRAS, AHP), and not because of preference over some other methods. The above procedure can also be applied to these, as well as other methods with a continuous reference function. The function of partial stability of one variant in relation to the another one represents a set of weight points for which the difference of the reference TOPSIS values of these variants is positive. Feasible weight points are given to components whose values are within a certain interval, which can be the result of determining the value of weights using group methods, combining multiple methods, incomplete or unreliable information, uncertainty of decision makers and the like.

By applying the TOPSIS method, a reference nonlinear objective function is obtained, the constraints of the variables are linear, and their values must meet the normalization condition, which limits the application of standard NLP methods for conditional optimization. Based on the constraints and possible changes in the values of the weight components (variables), *the nodes of the pairs of criteria (arguments)* are formed. They ensure the normalization condition, non-negativity of variables and independence of weight changes in one node from changes in other nodes, under active constraints. The Cauchy gradient method of the fastest fall (growth) (Vujičić et al, 1980, pp.89-92) and the line search method, adapted to the conditional optimization and characteristics of the nodes of the pairs of criteria, were applied as a basis for the proposed procedure for solving the NLP problem. The first part of the paper defines the function of similarity of a variant to an ideal solution, the nodes of criteria pairs and their characteristics for one variant, and also presents the procedure for determining the extremum of a function (exact and approximate solutions). The way of solving a possible occurrence of degeneration of the procedure (*wedging or oscillation of the solution* in the "vicinity" of the boundary of the set of feasible solutions) is also shown. In the second part of the paper, the partial stability of one variant in relation to the other ones is defined and the already performed parameter relations for one variant are applied to the partial stability function. Based on the introduced system of basic solutions for the required value of the reference TOPSIS function (separating the hyperplane of the values set of the function), a set of solutions was determined for which one variant is better in relation to the other selected variant. The paper does not explicitly deal with the analysis of the influence of criteria weights on the values of quantitative indicators of variant quality, but with the procedure of determining weight points from the set of admissible points, for which the stability of one variant in relation to the other one from the set of available variants can be determined. As an illustration of the procedure, a corresponding real numerical example is given.

The objective function (the similarity function of the variant to the ideal solution)

An MADM problem: There are *m* variants $V_i; i=\overline{1,m} \in I$ available and each of them is described with *n* attributes that are used as criteria $K_j; j=\overline{1,n} \in J$ in the decision-making process: the MADM problem is defined as a requirement to determine the variant $V_p; p \in I$ that is best according to all criteria K_j, as well as a ranking list of all variants. In the decision matrix $C=\{c_{ij}; i=\overline{1,m}; j=\overline{1,n}\}$ ($c_{ij} \in R$ are criteria values), the criteria are associated with numerical values of weights $w_j \in (0,1)$ with the normalization condition $\sum_{j=1}^{j=n} w_j = 1$ and the operators - min/max criteria: $L_j = -1$ (min) or $L_j = +1$ (max).

The TOPSIS method: It is based on compromise decision making and Lp metrics (Hwang & Yoon, 1981), (Zeleny, 1982), (Yoon, 1987) and can be displayed in several steps, when determining:

- Normalized criteria values:

a) $a_{ij} = c_{ij} \Big/ \sqrt{\sum_{i=1}^{i=m} c_{ij}^2}$, for *za* $L_j = +1$ (maximum),

b) $a_{ij} = c_{ij}^{\prime} \Big/ \sqrt{\sum_{i=1}^{i=m} c_{ij}^{\prime\,2}}$, $c_{ij}^{\prime} = c_j^* + c_j^- - c_{ij}$,), for $L_j = -1$ (minimum), (1)

where c_j^* are the best and c_j^- are the most unfavorable criteria ("perceived" ideal and anti-ideal)[1], when all criteria become maximizing $(L_j = +1)$.

- Distances of *Lp* metrics for $p = 1,2,\infty$ according to the normalized values of the "perceived" ideal $V^* = (a_j^* = max_j\{a_{ij}\})$ and the anti-ideal $V^- = (a_j^- = min_j\{a_{ij}\})$:

a) $t_{p,i}^* = L_p(V^*; V_i) = [\sum_{j=1}^{j=n} w_j^p (a_j^* - a_{ij})^p]^{1/p}$,

b) $t_{p,i}^- = L_p(V^-; V_i) = [\sum_{j=1}^{j=n} w_j^p (a_{ij} - a_j^-)^p]^{1/p}$, $p = 1,2,\infty$. (2)

- Unified distances of variants from ideals and anti-ideals:

[1] It is possible to apply linear normalization $a_{ij} = (c_{ij} - c_j^-) \big/ (c_j^* - c_j^-)$ which increases the range of normalized criteria values $0 \le a_{ij} \le 1$. The decision maker can determine both the absolute best (desirable) and the worst (undesirable or critical) values of the criteria functions that are outside the perceived best and worst criterion values, thus forming a secondary ideal and anti-ideal.

$$t_i^* = \sum_p \chi_{p,\gamma} t_{p,i}^*;\ t_i^- = \sum_p \chi_{p,\gamma} t_{p,i}^-(i);\ \ p = 1,2,\infty; \quad (3)$$

where $\chi_{p,\gamma}$ i $\sum_p \chi_{p,\gamma} = 1$ are the coefficients of the linear combination in the system of three metrics (t_1, t_2, t_∞), which represent the relative reliability of the function t_p for the dimension γ (e.g. γ is the number of criteria, variants, class, rankings, etc.) (Yoon, 1987, pp.283-284) or are chosen depending on the nature of the problem i.e. on what is required: a greater overall benefit $(p = 1)$, geometric proximity to the ideal $(p = 2)$ or smaller individual maximum deviations of the criteria values $(p = \infty)$ (Opricović, 1986, pp.45-48).

- Ideal similarity vector $S = \{s_i\}$ - similarity (closeness) of the variant V_i to the ideal solution V^* with elements (ideal similarity coefficients):

$$s_i = t_i^- / (t_i^* + t_i^-);\ 0 \le s_i \le 1. \quad (4)$$

- Rank of variants according to the criterion:

$$R(i) = max_i\{s_i\}. \quad (5)$$

The coefficient of similarity of ideal (4) is a quantitative indicator of the quality of the variant V_i at the same time according to all criteria and in relation to the ideal and the anti-ideal (or the degree of "goodness" of the variant). For $s_i > 0{,}5$ (when i $t_i^- > t_i^*$) the variant V_i has a greater influence on the variant and the variant is considered to be under the "control" of the ideal (the opposite is also true for $t_i^- < t_i^*$ the anti-ideal).

The similarity function of the variant to the ideal (similarity function) (4), for the constant criterion values $c_{ij} \in R$ (1) and one variant V_i (hereinafter the index "i" is implied), can be represented as a real function of *n* variables - weight $w_j \in (0;1)$ for each $j \in J$:

$$s(\underline{w}) = s_i(\underline{w});\ \underline{w} = \{w_j \in (0;1)\};\ \sum_{j=1}^{j=n} w_j = 1;\ \ for\ i \in I\ \ i\ \ j \in J\ , \quad (6)$$

where $\sum_{j=1}^{j=n} w_j = 1$ is the normalization condition. For the solved MADM problem, the weight components $\underline{w}$ are given in the intervals $\underline{w} = (w_j) \in [w_j^A, w_j^B]$, where w_j^A are the lower limits and w_j^B the upper limits of the interval of the values of the weight components (some components can be specified as discrete values). Interval weight estimates can be obtained in the process of group decision making on weights, when applying several objective methods of determining weights, as a consequence of incomplete information or uncertainty of decision-makers and the like. A set of initial weights is formed for each

VOJNOTEHNIČKI GLASNIK / MILITARY TECHNICAL COURIER, 2020, Vol. 68, Issue 3

criterion w_j^P and the lower w_j^{AP} and upper limit values w_j^{BP} are separated. The starting point of the weight $\underline{w}^{0P} = (w_j^{0P})$ has components $w_j^{AP} \leq w_j^{0P} \leq w_j^{BP}$ that can be the arithmetic means of several obtained weights (either modal or medial values) or at will chosen weight and for which it is generally $\sum_{j=1}^{j-n} w_j^{0P} \neq 1$. By normalizing these values, *the basic point of weights* $\underline{w}^0 = (w_j^0) \in [w_j^A , w_j^B]$ and $\sum_{j=1}^{j=n} w_j^0 = 1$ is obtained, with the limit weights w_j^A and w_j^B whose sums are $\sum_{j=1}^{j=n} w_j^A < 1$ and $\sum_{j=1}^{j=n} w_j^B > 1$. According to the basic point of weights $\underline{w}^0 = (w_j^0)$ and expressions (1-5), a *basic TOPSIS solution of the MADM problem* $(\underline{w}^0 ; s_p^0 = s_p (\underline{w}^0))$ is obtained or a variant $V_p , p \in I$ for $s_p (\underline{w}^0) = max_i \{ s_i (\underline{w}^0); i = \overline{1,m} \}$.

The function definition set $s(\underline{w})$ is a compact (closed and bounded) and convex set of points $\underline{w} \in \overline{E} \subseteq \Re^n$, such that $\overline{E} \subseteq \overline{F} \subseteq \Re^n$. A set $\overline{F}$ is an *n*-dimensional set bounded by *2n* hyperplanes, w_j^A and w_j^B, and $\underline{w} = (w_j) \in [w_j^A , w_j^B]$ is an *n*-dimensional point. The point $\underline{w} \in \overline{F}$, with the components $w_j > 0$ for each $j \in J$, not connected by the normalization condition $\sum_{j=1}^{j=n} w_j^0 = 1$, is the vertex of the set $\overline{F}$ only if each component has a value of $w_j = w_j^A$ or $w_j = w_j^B$. The vertex of the set $\overline{F}$ must contain *n* components: *p* components $w_{j_A}^A > 0$ for $j_A \in J_A \subset J$ and *q* components $w_{j_B}^B > 0$ for $j_B \in J_B \subset J$, so that $0 \leq p \leq n$, $0 \leq q \leq n$, $p + q = n$, $J_A \cup J_B = J$, and $J_A \cap J_B = \varnothing$; the total number of vertices is 2^n (variations with repetition). Since it is $\sum_{j_A} w_{j_A}^A + \sum_{j_B} w_{j_B}^B \neq 1$ in the general case and due to the normalization condition $\sum_{j=1}^{j=n} w_j = 1$, the set $\overline{E} \subseteq \overline{F}$ does not contain vertices, and thus not all points of boundaries (edges) and sides of the set $\overline{F}$.

A point $\underline{w} \in \overline{E} \setminus E$ is a *boundary point* of a set $\overline{E} \subseteq \Re^n$ only if there is $w_j = w_j^A$ or $w_j = w_j^B$ for at least one $j \in J$, and an *inner point* $\underline{w} \in E$ - only if there is $w_j^A < w_j < w_j^B$ for every $j \in J$, where E is the interior of the set $\overline{E}$. Each vertex of the set $\overline{E}$ contains *n* components: *p* components $w_{j_A}^A$, *q* components $w_{j_B}^B$ (where in $0 \le p \le n-1$, $0 \le q \le n-1$ and $p+q=n-1$) and a w_r component:

$$w_r = 1 - (\sum_{j_A} w_{j_A}^A + \sum_{j_B} w_{j_B}^B),\; w_r^A \le w_r \le w_r^B; \tag{7}$$

which is a condition for some combinations of the values $w_{j_A}^A$ and $w_{j_B}^B$ to form the vertex of the set $\overline{E}$. As it is $w_r^A \le (1 - \sum_{j_A} w_{j_A}^A - \sum_{j_B} w_{j_B}^B) \le w_r^B$, condition (7) in the general case cannot be fulfilled for all $2^{(n-1)}$ possible combinations of the values $w_{j_A}^A$ and $w_{j_B}^B$.

A set of function values $s(\underline{w})$ is a set $\overline{S} = \{ s \in [s^m ; s^M] \} \subseteq \Re$ limited with the values of the function for extreme solutions: *minimum* $(\underline{w}^m; s^m = s(\underline{w}^m))$ and *maximum* $(\underline{w}^M; s^M = s(\underline{w}^M))$. *Mapping* $s : \overline{E} \to \overline{S}\ (\Re^n \to \Re)$ is a surjection: there is at least one point $\underline{w} \in \overline{E}$ for which there is $s(\underline{w}) = C \in \overline{S}$ and for each point $\underline{w} \in \overline{E}$ there is only one value $s(\underline{w}) = C \in \overline{S}$: $(\forall s(\underline{w}) \in \overline{S})\ (\exists \underline{w} \in \overline{E})$; $(\forall \underline{w} \in \overline{E})\ (\exists !\, s(\underline{w}) = C \in \overline{S})$. The set of all solutions forms the *graph of the function* $\Gamma_s = \{ (\underline{w}; s) \in \Re^{n+1} \mid \underline{w} \in \overline{E}, s = s(\underline{w}) \in \overline{S} \}$.

The extremes of the function $s(\underline{w})$ are obtained as solutions of the NLP problem with a nonlinear objective function, *2n* linear constraints, the normalization condition and positive values of the variables:

$$(min/\,max)\ \ s(\underline{w});$$

$$w_j \ge w_j^A;\; w_j \le w_j^B;\; \sum_{j=1}^{j=n} w_j = 1;\; w_j > 0;\; j = \overline{1,n}. \tag{8}$$

The function $s(\underline{w})$ on a convex set $\overline{E}$ is continuous and twice differentiable, but it is not possible to unambiguously determine the convexity or concavity of the function on the whole set $\overline{E}$. For a special case and for a constant value $s(\underline{w}) = C$, function (4) can be written as $C = t^- / (t^* + t^-)$ or $C t^* - (1-C) t^- = 0$. Hence the assertion (Yoon, 1987, p.280) that a function $s(\underline{w})$ is convex for the subsets of points $\underline{w} \in \overline{E_1} \subseteq \overline{E}$ in which it is $s(\underline{w}) \ge 0.5$, and concave for subsets of points $\underline{w} \in E_2 = \overline{E} \setminus \overline{E_1}$ in which it is $s(\underline{w}) < 0.5$. Therefore, each *local extremum* is also a *global extremum*, that is, a function has extreme solutions at the boundary of the set $\overline{E}$, which are unique in terms of the values of the function and arguments. The convex function ($s(\underline{w}) \geq 0.5$) has a maximum, and the concave ($s(\underline{w}) < 0.5$) has a minimum at the vertex of the set $\overline{E}$ (Martić, 1978, pp.144-145) and these are *exact extreme solutions* that meet the *optimality criterion.* The minimum convex and maximum concave functions are at the boundary of the set (they can also be the vertices of the set $\overline{E}$), and if they are not the vertices of the set $\overline{E}$, then they are determined as *approximate extreme solutions* (incorrect, acceptable) according to the predefined criteria for function values and/or arguments according to real (*exact*) extreme solutions.

Nodes of the pairs of arguments (criteria)

Defining *the nodes of the pairs of arguments (criteria)* and their basic parameters is the most important phase of the presented method of solving the NLP problem. Nodes are formed for one variant V_i and each pair of criteria $r,t \in J; r \neq t$ and one point $\underline{w}^k$. In a narrower sense, *the node of the pair (two) of criteria (r,t) is the node of two different components w_j^k for $j = r,t$ of one point of weight $\underline{w}^k$: it represents a qualitatively new set of parameters arising from the mutual relations of characteristics (parameters) of current components w_r^k and w_t^k.*

The transition from the initial to a new solution is done by changing the starting point $\underline{w}^k$ to a new point of weights $\underline{w}^{k+1}$, where $k = 0,1,2,\ldots,$ is the mark of the iterative solution. The basic parameters of the point $\underline{w}^k$ are:

<u>*Active constraints of the criteria*</u> d_j^{Ak} and d_j^{Bk} (possible changes in weight components) at the point $\underline{w}^k$ for the intervals $[w_j^A, w_j^B]$:

$$d_j^{Ak} = w_j^k - w_j^A \geq 0;\ d_j^{Bk} = w_j^B - w_j^k \geq 0;\ d_j^{AB} = d_j^{Ak} + d_j^{Bk} = w_j^B - w_j^A,\ j \in J, \quad (9)$$

where $d_j^{Ak} \geq 0$ is the largest possible decrease, $d_j^{Bk} \geq 0$ is the largest possible increase in weight w_j^k, and $d_j^{AB} \geq 0$ is the size of the interval $[\underline{w}^A, \underline{w}^B]$. The values d_j^{Ak} and $d_j^{Ak} \geq 0$ and their sums $\sum_{j=1}^{j=n} d_j^{Ak}$ and $\sum_{j=1}^{j=n} d_j^{Bk}$ can be related by any sign (<, =,>).

<u>*The vector of change (increment) is the weight*</u> $\underline{v}^k$: when changing the point $\underline{w}^k$ to the point $\underline{w}^{k+1}$, the new point $\underline{w}^{k+1} = \underline{w}^k + \underline{v}^k$, where the

$\underline{v}^k = (v_j^k)$ *vector of change (increment) is the weight*. The values v_j^k can be $\neq 0$ or $= 0$, which is why non-negative values are introduced $v_j^{Ak}, v_j^{Bk} \geq 0$ ($v_j^{Ak} > 0$ reduction and $v_j^{Bk} > 0$ increase weight w_j^k):

$$a)\ v_j^{Ak} = -v_j^k \geq 0,\ v_j^{Ak} \in [0, d_j^{Ak}];\ \text{za}\ v_j^k \leq 0;$$

$$b)\ v_j^{Bk} = v_j^k \geq 0,\ v_j^{Bk} \in [0, d_j^{Bk}],\ \text{za}\ v_j^k \geq 0. \quad (10)$$

The values of the weight components at the new point $\underline{w}^{k+1}$ are[2]:

$$w_j^{k+1} = w_j^k + v_j^k = w_j^k + v_j^{Bk} - v_j^{Ak}. \quad (11)$$

where for each component w_j^k (11) at least one of the values v_j^{Ak} or v_j^{Bk} is equal to 0.

<u>The gradient of function:</u> from the development of function (6) into Taylor's polynomial of the first degree:

$$s(\underline{w}^{k+1}) = s(\underline{w}^k) + \nabla s(\underline{w}^k)(\underline{w}^{k+1} - \underline{w}^k) + R_1 = s(\underline{w}^k) + \sigma(\underline{w}^k) + R_1 \quad (12)$$

and for the value of the remainder $R_1 \approx 0$, the auxiliary function $\sigma^k = \sigma(\underline{w}^k)$ is equal to:

$$\sigma(\underline{w}^k) = \nabla s(\underline{w}^k)(\underline{w}^{k+1} - \underline{w}^k) = \nabla s(\underline{w}^k)(\underline{v}^{Bk} - \underline{v}^{Ak}); \quad (13)$$

where $\nabla s(\underline{w}^k) = \{\partial s(\underline{w}^k)/\partial w_j^k\}_{j=\overline{1,n}}$ the gradient of the function $s(\underline{w})$ is at the point $\underline{w}^k$. *Approximate values of the gradient components* $g_j^k = g_j(\underline{w}^k) \approx \partial s(\underline{w}^k)/\partial w_j^k$ can be calculated by the *method of double increment of variables* (Milovanović & Stanimirović, 2002, p.114):

$$g_j^k = [s(\underline{w}^{j,k+}) - s(\underline{w}^{j,k-})] / 2\delta;\ \delta > 0;\ j \in J, \quad (14)$$

where points $\underline{w}^{j,k+} = (w_1^k, \cdots, w_j^k + \delta, \cdots, w_n^k)$ and $\underline{w}^{j,k-} = (w_1^k, \cdots, w_j^k - \delta, \cdots, w_n^k)$, and $\delta > 0$ the increment is small (e.g. $\delta = 10^{-6}$ or less).

Node parameters

For the transition from the point $\underline{w}^k$ to the point $\underline{w}^{k+1}$ and with the normalization condition $\sum_{j=1}^{j=n} w_j^k = 1$, it is necessary to change the weights of at least two criteria $r, t \in J$ that form a *node* (r,t) with a unique value

---

[2] The index $k = 0,1,2,\ldots$, indicates the quantities in the point $\underline{w}^k$ (eg: s^k, σ^k, d_j^{Ak}, $d_{(r,t)}^k$, g_j^k, $g_{(r,t)}^k$) and the quantities that "come out" of it (eg: v_j^k, v_j^{Ak}, $z_{(r,t)}^k$, $\tau_{(r,t)}^k$).

of weight changes $v_{r(t)}^{Ak} = v_{t(r)}^{Bk} \geq 0$ and the direction of changes: $v_{r(t)}^{Ak}$ is the reduction of the weight w_r^k, and $v_{t(r)}^{Bk}$ is the increase of the weight w_t^k. The components $r,t \in J$ of the point $\underline{w}^{k+1}$ are equal to:

$$w_r^{k+1} = w_r^k - v_{r(t)}^{Ak};\ \ w_t^{k+1} = w_t^k + v_{t(r)}^{Bk};\ \ v_{r(t)}^{Ak} = v_{r(t)}^{Bk} \geq 0;\ \ r,t \in J, \tag{15}$$

while the other components are unchanged $w_j^{k+1} = w_j^k,\ \ j \in J \setminus \{r,t\}$. A set of nodes is formed for a known solution

$$\Theta^k = \{(r,t) \mid r,t \in J, r \neq t\} \tag{16}$$

with $n(n-1)$ elements in total. The basic characteristics of the nodes are:

<u>*Active constraints of nodes*</u> $d_{(r,t)}^k = d_{(r,t)}(\underline{w}^k)$ depend on a possible decrease in the *r*-component and on an increase of the *t*-component weight in nodes (9) (available resources):

$$d_{(r,t)}^k = \begin{cases} min(d_r^{Ak}; d_t^{Bk}) \geq 0;\ (r,t) \in \Theta \\ 0;\ \ r = t,\ [(r,t) \notin \Theta] \end{cases}, \tag{17}$$

where the matrix $D^k = (d_{(r,t)}^k)_{nxn}$ for $r,t \in J$.

<u>*Variables*</u> $z_{(r,t)}^k$: variables $z_{(r,t)}^k \geq 0$ are introduced, whose values show the change of the weight components in the nodes, whereby a square matrix $Z^k = (z_{(r,t)}^k)_{nxn}$ is formed, with the following elements:

$$a)\ \ z_{(r,t)}^k \begin{cases} \leq d_{(r,t)}^k \geq 0,\ (r,t) \in \Theta \\ = 0;\ \ r = t,\ [(r,t) \notin \Theta] \end{cases},$$

$$b)\ \ z_{(r,t)}^k = v_{r(t)}^{Ak} = v_{t(r)}^{Bk} \geq 0. \tag{18}$$

Since $v_{r(t)}^{Ak} = v_{t(r)}^{Bk}$, the values of the variables $z_{(r,t)}^k > 0$ are conditional and compensatory values of the weight changes in the node (r,t), and their summation in the nodes $(r,t) \in \Theta$ gives the total increase v_r^{Ak} or decrease v_t^{Bk} of each weight component:

$$a)\ \ j = r \rightarrow v_r^{Ak} = v_{r(1)}^{Ak} + \cdots + v_{r(n)}^{Ak} = \sum_{t=1}^{t=n} v_{r(t)}^{Ak} = \sum_{t=1}^{t=n} z_{(r,t)}^k \leq d_r^{Ak},$$

$$b)\ \ j = t \rightarrow v_t^{Bk} = v_{t(1)}^{Bk} + \cdots + v_{t(n)}^{Bk} = \sum_{r=1}^{r=n} v_{t(r)}^{Bk} = \sum_{r=1}^{r=n} z_{(r,t)}^k \leq d_t^{Bk},$$

$$c)\ \ \sum_{j=1}^{j=n} v_j^{Bk} - \sum_{j=1}^{j=n} v_j^{Ak} = 0. \tag{19}$$

The normalization condition is provided in each node and does not need to be considered further. The condition from the starting point of weights $\sum_{j=1}^{j=n} w_j^0 = 1$ (11) is also contained in the point $\underline{w}^1$ because of (19c): $\sum_{j=1}^{j=n} w_j^1 = \sum_{j=1}^{j=n} w_j^0 + \sum_{j=1}^{j=n} v_j^{B0} - \sum_{j=1}^{j=n} v_j^{A0} = 1$. The normalization condition is transformed into $\sum_{j=1}^{j=n} v_j^{Bk} - \sum_{j=1}^{j=n} v_j^{Ak} = 0$ or $\sum_{j=1}^{j=n} v_j^k = 0$ and is contained in each node (r,t) and for each point $\underline{w}^k \in \overline{E}$ in any iteration $k = 0,1,2,\ldots,$.

Gradient function in the node $g_{(r,t)}^k$: the increment of the value of the auxiliary function (13) for the node (r,t) is:

$$\sigma_{(r,t)}^k = (\partial s(\underline{w}^k)/\partial w_t^k) \cdot v_{t(r)}^{Bk} - (\partial s(\underline{w}^k)/\partial w_r^k) \cdot v_{r(t)}^{Ak}. \quad (20)$$

By changing $g_j^k \approx \partial s(\underline{w}^k)/\partial w_j^k$ for g_r^k and g_t^k (14) and $z_{(r,t)}^k = v_{r(t)}^{Ak} = v_{t(r)}^{Bk} \geq 0$ (19a, b) expression (20) becomes:

$$\sigma(z_{(r,t)}^k) \approx z_{(r,t)}^k (g_t^k - g_r^k) = z_{(r,t)}^k \cdot g_{(r,t)}^k, \; g_{(r,t)}^k = g(z_{(r,t)}^k), \quad (21)$$

where $g_{(r,t)}^k = g_{(r,t)}(\underline{w}^k)$ is the approximate value of the gradient function component $s(\underline{w})$ in the node $(r,t) \in \Theta^k$. The values $g_{(r,t)}^k$ for all nodes (r,t) form a square antisymmetric matrix $G^k = (g_{(r,t)}^k)_{nxn}$ with the elements:

$$g_{(r,t)}^k = \begin{cases} g_t^k - g_r^k; \; (r,t) \in \Theta^k \\ 0; \; r = t, \; [(r,t) \notin \Theta^k] \end{cases}, \quad (22)$$

where $g_{(r,t)}^k = -g_{(t,r)}^k$. The approximate total change in the value of the function $s(\underline{w}^k)$ for all nodes $(r,t) \in \Theta^k$, according to (21), is equal to:

$$\sigma(Z^k) = \sum_{(r,t)} g(z_{(r,t)}^k) z_{(r,t)}^k, \; (r,t) \in \Theta^k. \quad (23)$$

Possible changes in the function values by the nodes $\tau_{(r,t)}^k$ are derived values based on the values of the elements of the matrix D^k (18) and G^k (22). A matrix $T^k = (\tau_{(r,t)}^k)_{nxn}$ is formed, with the elements:

$$\tau_{(r,t)}^k = \begin{cases} g_{(r,t)}^k d_{(r,t)}^k \neq 0; \; za \; g_{(r,t)}^k \neq 0 \; i \; d_{(r,t)}^k > 0 \\ 0; \; za \; g_{(r,t)}^k = 0 \; ili \; d_{(r,t)}^k = 0 \end{cases}, \; (r,t) \in \Theta^k \quad (24)$$

of which there may be at most *n (n-1)* elements $\tau^k_{(r,t)} \neq 0$. This defines the basic characteristics of the nodes (r,t): $d^k_{(r,t)}$, $g^k_{(r,t)}$ and $\tau^k_{(r,t)}$ and the variables $z^k_{(r,t)}$, shown in Table 1.

Active nodes

The characteristic $\tau^k_{(r,t)} \neq 0$, as a derived quantity, is the most significant indicator of the possibility of changing the value of the function in the node (r,t) for the current point $\underline{w}^k$. Based on the values $\tau^k_{(r,t)} \neq 0$, the matrix T^k_- with the elements that are 0 or $\tau^k_{(r,t)} < 0$ and the matrix T^k_+ with the elements that are 0 or $\tau^k_{(r,t)} > 0$; this determines the subsets of *active nodes* Θ^k_- and Θ^k_+ at the point $\underline{w}^k$:

a) $\Theta^k_- = \{(r,t) \mid \tau^k_{(r,t)} < 0\} \subset \Theta^k$;

b) $\Theta^k_+ = \{(r,t) \mid \tau^k_{(r,t)} > 0\} \subset \Theta^k$. (25)

The active nodes in the point $\underline{w}^k$ are the nodes $(r,t) \in \Theta^k_- \cup \Theta^k_+$, and the *active gradient components* are only the components $g^k_{(r,t)} \neq 0$ in the active nodes (the nodes in which there are $g^k_{(r,t)} \neq 0$ and $d^k_{(r,t)} = 0$ are not active nodes). According to the influence on the value of the function (increase or decrease), i.e. for determining the extreme of the function (minimum, maximum), *active nodes* are the nodes $(r,t) \in \Theta^k_-$ for decreasing the value or determining the minimum of the function and the nodes $(r,t) \in \Theta^k_+$ for increasing the value or determining the maximum of the function. *Active gradient components* are only the components $g^k_{(r,t)} < 0$ (min) or $g^k_{(r,t)} > 0$ (max) in the active nodes ($\tau^k_{(r,t)} \neq 0$). The sum $\sum_{(r,t)} |\tau^k_{(r,t)}| = \sum_{(r,t)} |g^k_{(r,t)}| d^k_{(r,t)} \geq 0$ for the node $(r,t) \in \Theta^k_-$ is the largest possible decrease, and for the node $(r,t) \in \Theta^k_+$ the largest possible increase of the value of the function $s(\underline{w})$ is at the point $\underline{w}^k$. The value $\sum_{(r,t)} |\tau^k_{(r,t)}|$ can also be a criterion for accepting the achieved solution as an approximate extreme solution and for interrupting the iterative procedure if $\sum_{(r,t)} |\tau^k_{(r,t)}| \leq \varepsilon_\tau$ for $(r,t) \in \Theta^k_-$ (min) or $(r,t) \in \Theta^k_+$ (max), because the improvement of the function value in the next iteration cannot be greater than the defined value ε_τ (e.g. $\varepsilon_\tau \leq 5 \cdot 10^{-5}$).

The formation of the nodes $(r,t) \in \Theta^k$ ensures that the normalization condition $\sum_{j=1}^{j=n} w_j^k = 1$ (or $\sum_{j=1}^{j=n} v_j^k = 0$) is contained in each point $\underline{w}^k \in \overline{E}$ the non-negativity of the variables $z_{(r,t)}^k \geq 0$ and the independence of weight changes in a particular node $(r,t) \in \Theta^k$ from changes in the other nodes, with active limitations of criteria (18, 19).

Extreme solutions of the objective function (similarity functions)

The extremes of the function $s = s(\underline{w})$ (8) are determined by an iterative procedure starting from some feasible solution $(\underline{w}^k; s^k)$ which, in general, is not extreme. Improving the initial solution is possible only if there is at least one node $(r,t) \in \Theta_-^k$ (25a) (decrease in the value s^k) or only if there is at least one node $(r,t) \in \Theta_+^k$ (25b) (increase in the value s^k). According to expression (13), the current solution $(\underline{w}^k; s^k)$ is improved by increasing (decreasing) the value of the auxiliary function $\sigma(Z^k)$ (13, 23), when the nodes taken into account are only the nodes $(r,t) \in \Theta^k$ in which weight changes contribute to the improvement of the value of the auxiliary function $\sigma(Z^k)$.

The iterative procedure determines the boundary solutions $(\underline{w}^{k+1} \in \overline{E} \setminus E; s^{k+1})$ with the improved function $s(\underline{w})$ values, i.e. the boundary points $(\underline{w}^{k+1} \equiv \underline{w}^{k*}) \in \overline{E} \setminus E$ that will give an improved TOPSIS solution (2-4), while active constraints allow it. At the end of the procedure, a solution will be obtained at the point at the vertex of the set $\overline{E}$, which will be the exact extreme solution $\underline{w}^{k*} = (\underline{w}^m \vee \underline{w}^M) \in \overline{E} \setminus E$ or the initial solution for a further procedure and determination of the approximate extreme solution. In both cases, there is a single iterative procedure by which an admissible solution is obtained at the vertex of the set $\overline{E}$, from which no better solution can be obtained at any vertex of the set $\overline{E}$.

Exact extreme solutions

For the initial solution $(\underline{w}^k; s^k)$, usually k=0, it is convenient to form a table similar to Table 1 which contains the values of the active constraints d_j^{Ak} and d_j^{Bk} (9), the node characteristics (r,t) - the elements of the matrices D^k (17), G^k (22) and T^k (24) at the point $\underline{w}^k$, the partial sums $g_{(r,t)}^k$ and $\tau_{(r,t)}^k$ dependent on the active nodes Θ_-^k or Θ_-^k, the space for writing variables $z_{(r,t)}^k$ and their sums as the components of the vector $\underline{v}^k = (v_j^k)$.

The extremes of the function $s(\underline{w})$ (8) are determined as the solutions of the NLP problem with restrictions on the weight changes in the nodes $z_{(r,t)}^k \le d_{(r,t)}^k > 0$ (18) and according to the criteria $\sum_{t=1}^{t=n} z_{(r,t)}^k \le d_r^{Ak} \ge 0$ and $\sum_{r=1}^{r=n} z_{(r,t)}^k \le d_t^{Bk} \ge 0$ (19), that is, from the condition that the points of extremes are admissible, and, at the same time, the boundary points $\underline{w^{k+1} \in \overline{E} \setminus E}$.

The mathematical model NLP (8) was transformed according to the node parameters and a new model was formed containing the nonlinear objective function (due to the multiple differentiability of the function $s(\underline{w})$ and the nonlinearity of the function $g(z_{(r,t)}^k)$), $n(n+1)$ linear constraints (the normalization condition $\sum_{j=1}^{j=n} w_j = 1$ is contained in the nodes parameters) and for $n(n-1)$ variables $z_{(r,t)}^k \ge 0$, with indices as in Table 1:

$$\begin{aligned} &(min/\,max)\ \sigma(Z^k) = \textstyle\sum_{(r,t)} g(z_{(r,t)}^k)\, z_{(r,t)}^k\,, \\ &z_{(r,t)}^k \le d_{(r,t)}^k\,, \qquad n(n\text{-}1) \text{ constraints}, \\ &\textstyle\sum_{t=1}^{t=n} z_{(r,t)}^k \le d_r^{Ak}\,,\ \ n \text{ constraints}, \\ &\textstyle\sum_{r=1}^{r=n} z_{(r,t)}^k \le d_t^{Bk}\,,\ \ n \text{ constraints}, \\ &z_{(r,t)}^k \ge 0;\ (r,t) \in \Theta_-^k\ (min) \text{ or } (r,t) \in \Theta_+^k\ (max). \end{aligned} \tag{26}$$

The NLP task (8,26) is solved by applying an iterative procedure based on the first-order gradient method or the Cauchy method of the fastest drop (growth) of the value of the function $s(\underline{w})$[3] adapted for the application of node parameters. The direction of the antigradient $-\nabla s(\underline{w}^k)$ is also the direction of the fastest decrease in the value of the function $s(\underline{w})$ at the point $\underline{w}^k$, that is, it is the most favorable direction from the point $\underline{w}^k$ for determining the minimum (Vujičić et al, 1980, p.89); the direction of the gradient $\nabla s(\underline{w}^k)$ is the most favorable direction for determining the maximum.

Through the starting point $\underline{w}^k$, in addition to the most favorable direction, countless other favorable directions can be drawn that will contain the characteristics of one or more active nodes[4]. The aim is to determine the point $\underline{w}^{k+1} \in \overline{E}$ at which the TOPSIS value of the function s^{k+1} is better than the value s^k in the chosen favorable direction and in accordance with the limitations in model (26).

Solving problem (26) requires at least one known feasible solution $(\underline{w}^k; s^k)$ (basic TOPSIS solution $(\underline{w}^0; s^0)$ or any other feasible solution), for which there is at least one node $(r,t) \in \Theta_-^k$ (minimum) or at least one node $(r,t) \in \Theta_+^k$ (maximum) (25). Based on the values of all active components of the gradient at the point $\underline{w}^k$, the most favorable direction or the direction of the fastest fall (growth) of the objective function is set through it. Active nodes are determined depending on the required extreme: $(r,t) \in \Theta_-^k$ (min) or $(r,t) \in \Theta_+^k$ (max). The most $n(n-1)/2$ active nodes are possible for each required extremum, that is, it is the largest number of elements of the sets Θ_-^k and Θ_+^k for the inner point $\underline{w} \in E$. In the intersection of the most favorable direction and some, unknown in advance, hyperplane of the set $\overline{E}$ - w_j^A or w_j^B, there is the boundary point $(\underline{w}^{k*} \equiv \underline{w}^{k+1}) \in \overline{E} \setminus E$:

$$\underline{w}^{k*} = \underline{w}^k + \underline{v}^k = (w_j^k + v_j^k) = (w_j^k + v_j^{Bk} - v_j^{Ak}); \quad j \in J . \tag{27}$$

[3] Based on the gradient method of the fastest fall, several procedures and their modifications have been developed, which are not listed here, and some of them have been treated in the cited literature.

[4] Other favorable directions are applied in eliminating the degeneration of the procedure known as wedging and in determining the *basic solutions* for the required values of the function $s(\underline{w}) = C$ (shown below).

Table 1 – Parameters of the point $\underline{w}^k$ and the nodes (r, t) for the NLP model

Таблица 1 – Параметры точки $\underline{w}^k$ и узлов (r, t) для модели НЛП

Табела 1 – Параметри тачке $\underline{w}^k$ и чворова (r,t) за модел НЛП

$j \equiv t$		1	…	n	sums*
$j \equiv r$	$d_r^{Ak} \diagdown d_t^{Bk}$	d_1^{Bk}	…	d_n^{Bk}	
	$g_r^k \diagdown g_t^k$	g_1^k	…	g_n^k	
1	d_1^{Ak}	0	…	$d_{(1,n)}^k$	
	g_1^k	0	…	$g_{(1,n)}^k$	$\sum_{t=1}^{t=n} \lvert g_{(1,t)}^k \rvert$
	$\tau_{(r,t)}^k$	0	…	$\tau_{(1,n)}^k$	$\sum_{t=1}^{t=n} \lvert \tau_{(1,t)}^k \rvert$
	$z_{(r,t)}^k$	0	…	$z_{(1,n)}^k$	$\sum_{t=1}^{t=n} z_{(1,t)}^k = v_1^{Ak}$
⋮	⋮	⋮	⋮	⋮	
n	d_n^{Ak}	$d_{(n,1)}^k$	…	0	
	g_n^k	$g_{(n,1)}^k$	…	0	$\sum_{t=1}^{t=n} \lvert g_{(n,t)}^k \rvert$
	$\tau_{(r,t)}^k$	$\tau_{(n,1)}^k$	…	0	$\sum_{t=1}^{t=n} \lvert \tau_{(n,t)}^k \rvert$
	$z_{(r,t)}^k$	$z_{(n,1)}^k$	…	0	$\sum_{t=1}^{t=n} z_{(n,t)}^k = v_n^{Ak}$
sums*		$\sum_{r=1}^{r=n} \lvert g_{(r,1)}^k \rvert$	…	$\sum_{r=1}^{r=n} \lvert g_{(r,n)}^k \rvert$	
		$\sum_{r=1}^{r=n} \lvert \tau_{(r,1)}^k \rvert$	…	$\sum_{r=1}^{r=n} \lvert \tau_{(r,n)}^k \rvert$	$\sum_{(r,t)} \lvert \tau_{(r,t)}^k \rvert$
		$\sum_{r=1}^{r=n} z_{(r,1)}^k = v_1^{Bk}$	…	$\sum_{r=1}^{r=n} z_{(r,n)}^k = v_n^{Bk}$	

*sums $g_{(r,t)}^k$ and $\tau_{(r,t)}^k$ are determined in relation to $(r,t) \in \Theta_-^k$ or $(r,t) \in \Theta_+^k$

Minimum problem: The direction of the fastest fall is the direction of the antigradient $-\nabla s(\underline{w}^k)$, that is, the direction of the antigradient vector in the active nodes for the point $\underline{w}^k$ (the gradient vector is the sum of the gradient vectors $g_{(r,t)}^k < 0; (r,t) \in \Theta_-^k$ of the active components); the values of the variables $z_{(r,t)}^k > 0, (r,t) \in \Theta_-^k$ (18,19) have the same interrelationship (proportionality) as the values of the active components of the gradient[5]:

$$z^k_{(r,t)} = \mu^k |g^k_{(r,t)}|;(r,t) \in \Theta^k_-, \qquad (28)$$

where $\mu^k > 0$, *the unique coefficient (proportionality) of weight increment for all active nodes,* depends on the active constraints in the nodes ($d^k_{(r,t)} > 0$) and the criteria ($d^{Ak}_j > 0$ and $d^{Bk}_j > 0$); it is necessary to ensure, when passing the point $\underline{w}^k \in \overline{E}$ to the boundary point $\underline{w}^{k*} \in \overline{E} \setminus E$: a) that the point $\underline{w}^{k*}$ (27) is a feasible point; b) that $\underline{w}^{k*}$ is in the most favorable direction; and, c) that the *active constraints* of the nodes and the criteria are met to the maximum (to achieve the maximum possible changes in the weight components v^k_j). The values of the coefficient μ^k are obtained on the basis of the following considerations:

1) Active constraints in the nodes $z^k_{(r,t)} \le d^k_{(r,t)} > 0,(r,t) \in \Theta^k_-$ (18): for the boundary case $z^k_{(r,t)} = d^k_{(r,t)} > 0$ and $z^k_{(r,t)} = \xi^k_{(r,t)}|g^k_{(r,t)}| = d^k_{(r,t)};(r,t) \in \Theta^k_-$, where $\xi^k_{(r,t)} > 0$ is *the node coefficient*. The lowest value $\xi^k_{(r,t)} > 0$ in all nodes allows at least one resource $d^k_{(r,t)}$ - active constraint to be fully utilized and that $d^{k*}_{(r,t)} = 0$, based on which the *coefficient of active nodes* is determined $\xi^k > 0$:

a) $\xi^k_{(r,t)} = \begin{cases} d^k_{(r,t)} / |g^k_{(r,t)}| > 0; (r,t) \in \Theta^k_- \\ 0;\ (r,t) \notin \Theta^k_- \end{cases}$;

b) $\xi^k = min_{(r,t)}\{\xi^k_{(r,t)} > 0;(r,t) \in \Theta^k_-\}$. (29)

2) Active constraints of arguments (criteria) $\sum_{t=1}^{t=n} z^k_{(j,t)} \le d^{Ak}_j > 0$ and $\sum_{r=1}^{r=n} z^k_{(r,j)} \le d^{Bk}_j > 0$ for $(j = r; j = t) \in J$ (19a,b): to move to the point $\underline{w}^{k*} \in \overline{E} \setminus E$ at least one of the active constraints to the criteria, which have a positive value $d^{Ak}_j > 0$ or $d^{Bk}_j > 0$ at the point $\underline{w}^k$, should be fully

[5] In the following text, for a simpler presentation, the components of the gradient $g^k_{(r,t)} < 0;(r,t) \in \Theta^k_-$ and $g^k_{(r,t)} > 0;(r,t) \in \Theta^k_+$ are replaced by $|g^k_{(r,t)}| > 0$ for $(r,t) \in \Theta^k_-$ *(min)* or $(r,t) \in \Theta^k_+$ *(max)*.

utilized and there should be $d_j^{Ak*}=0$ or $d_j^{Bk*}=0$ at least for one $j=J$. The weight components for one criterion (27) are $v_j^k=v_j^{Bk}-v_j^{Ak}$, where in the final outcome $v_j^{Ak}=0$ or $v_j^{Bk}=0$. The change of the component v_j^k depends on partial changes in the row and column of the same index $j=r=t$ in the matrix G^k: changes in the row $j=r$ are $\sum_{t=1}^{t=n} z_{(r,t)}^k = v_j^{Ak} = \psi_j^k \sum_{t=1}^{t=n} |g_{(r,t)}^k| > 0$, and in the column $j=t$ they are $\sum_{r=1}^{r=n} z_{(r,t)}^k = v_j^{Bk} = \psi_j^k [\sum_{r=1}^{r=n} |g_{(r,t)}^k| > 0$, where $\psi_j^k > 0$ is the coefficient of proportionality for the *jth*-criterion. It follows that $v_j^k = \psi_j^k [\sum_{r=1}^{r=n} |g_{(r,j)}^k| - \sum_{t=1}^{t=n} |g_{(j,t)}^k|]$, where the sums in the parentheses [.] can be connected by any sign (<, =,>), when three cases are possible: a) $v_j^k < 0 v_j^{Ak}$, followed by $v_j^k = -v_j^{Ak}$ and $v_j^{Bk}=0$; b) $v_j^k>0$, followed by $v_j^k=v_j^{Bk}$ and $v_j^{Ak}=0$; and, c) $v_j^k=v_j^{Bk}=v_j^{Ak}=0$. For boundary cases, when $v_j^{Bk}=d_j^{Bk}>0$ or $v_j^{Ak}=d_j^{Ak}>0$, the *coefficients of the criteria* (ψ_j^k) and the *coefficient of all criteria* (ψ^k) are obtained:

$$a)\ \psi_j^k = \begin{cases} d_j^{Ak} \big/ (\sum_{t=1}^{t=n} |g_{(j,t)}^k| - \sum_{r=1}^{r=n} |g_{(r,j)}^k|) > 0; & for\ \sum_{t=1}^{t=n} |g_{(j,t)}^k| > \sum_{r=1}^{r=n} |g_{(r,j)}^k|; \\ d_j^{Bk} \big/ (\sum_{r=1}^{r=n} |g_{(r,j)}^k| - \sum_{t=1}^{t=n} |g_{(j,t)}^k|) > 0; & for\ \sum_{r=1}^{r=n} |g_{(r,j)}^k| > \sum_{t=1}^{t=n} |g_{(j,t)}^k|; \\ \to \infty; \ for\ \sum_{t=1}^{t=n} |g_{(j,t)}^k| = \sum_{r=1}^{r=n} |g_{(r,j)}^k|; \ (r,j),(j,t) \in \Theta_-^k; \end{cases}$$

$$b)\ \psi^k = min_j \{ \psi_j^k > 0;\ j \in J \}. \tag{30}$$

The transition from the point $\underline{w}^k \in \overline{E}$, which can be a boundary or an inner point, to the boundary point $\underline{w}^{k*} \in \overline{E} \setminus E$ in the direction of the fastest fall, is realized for the value of the *unique coefficient:*

$$\mu^k = min\{ \xi^k > 0; \psi^k > 0 \}, \quad for\ \Theta_-^k, \tag{31}$$

where the values ξ^k and ψ^k can be associated with any sign (<,=,>). Expressions (27-31) are key to determining exact extreme solutions using active node parameters.

In the further procedure, the values of the variables $z_{(r,t)}^k \ge 0$ are calculated (28) as well as the values of the weight increments $v_j^{Ak} = \sum_{t=1}^{t=n} z_{(j,t)}^k \ge 0$ (the sum $z_{(j,t)}^k$ in the rows of the matrix Z^k) and $v_j^{Bk} = \sum_{r=1}^{r=n} z_{(r,j)}^k \ge 0$ (the sum $z_{(r,t)}^k$ in the columns of the matrix Z^k) (19), together with the components of the point weight $\underline{w}^{k*}$ (27), and then the TOPSIS solution $(\underline{w}^{k*};s^{k*})$(2-4) is determined.

<u>Maximum problem:</u> Expressions (27-31) and (2-4) are used to determine the solution $(\underline{w}^{k*};s^{k*})$, so that the nodes $(r,t)\in\Theta_{-}^{k}$ (25a) are replaced by the nodes $(r,t)\in\Theta_{+}^{k}$ (25b), and the matrices T_{-}^{k} - by the matrices T_{+}^{k}.

<u>Optimality solution</u>: In the continuation of the examination procedure, the obtained solution $(\underline{w}^{k*};s^{k*})$ is obtained according to two criteria:

- *basic criterion:*

a) $s^{k*}<s^{k}$ *(min); b)* $s^{k*}>s^{k}$ *(max);* (32)

- *optimality criterion:*

a) $\tau_{(r,t)}^{k*}=g_{(r,t)}^{k*}d_{(r,t)}^{k*}\geq 0;\ \ for\ every\ (r,t)\in\Theta^{k*}$ *(min)*, or

b) $\tau_{(r,t)}^{k*}=g_{(r,t)}^{k*}d_{(r,t)}^{k*}\leq 0;\ \ for\ every\ (r,t)\in\Theta^{k*}$ *(max),* (33)

when three cases can occur:

1) criterion (32) is met and criterion (33) is not met: the obtained solution is not extreme, but it is the initial solution $(\underline{w}^{k*};s^{k*})\equiv(\underline{w}^{k+1};s^{k+1})$ for the *(k+1)* iteration, when the node parameters in Table 1 are calculated and the procedure is repeated (27-33); the procedure is repeated until solutions are obtained according to cases 2 or 3;

2) criteria (32) and (33) are met: the exact extreme solution was reached at the vertex of the set $\overline{E}$;

3) criteria (32) and (33) are not met: the solutions $(\underline{w}^{k};s^{k})$ and $(\underline{w}^{k*};s^{k*})$ are the initial solutions for the procedure of determining the approximate extreme solution (the case when (32) is not fulfilled, and when it is fulfilled, (33) is impossible).

For the starting inner point of the weights $w^{k=0}\in E$, the number of active nodes $(r,t)\in\Theta_{-}^{0}$ and $(r,t)\in\Theta_{+}^{0}$ is equal to $n(n-1)/2$. If there is an exact extreme solution $(\underline{w}^{m};s^{m})$ or $(\underline{w}^{M};s^{M})$ (33) and, during the procedure, in each iteration, $\xi^{k}\geq\psi^{k}>0$ and $\mu^{k}=\psi^{k}$ (31), and there is no degeneration - oscillation, then the solution is achieved after the iteration $k=n-1$. After each $k=1,2,\cdots$ iteration, the number of active nodes decreases and is equal to $(n-k)(n-k-1)/2$. At the end of the procedure and after iterations, there is only one active node, and at the point $\underline{w}^{k*}$ after $k=n-1$ iterations, there are no active nodes: $\Theta_{-}^{k}=\varnothing$ (min) or $\Theta_{+}^{k}=\varnothing$ (max). From the beginning of the procedure in each subsequent iteration, the value of the possible total weight change $\sum_{(r,t)}|\tau_{(r,t)}^{k}|$ in the active nodes decreases; for the exact extreme solution is $\sum_{(r,t)}|\tau_{(r,t)}^{k*}|=0$ and there is no possibility of further improvement of the function value. The number of iterations increases if oscillation or wedging (discussed below) appear "near" the hyperplane w_j^A or w_j^B.

Approximate extreme solutions

Determining approximate extreme solutions is necessary in the case when the extreme solution is not at the vertex of the set $\overline{E}$ and when criteria (32) and (33) are not met. One of possible solutions is the line search procedure[6], adjusted to node parameters, where the number of iterations should be as small as possible. The absence of an exact extreme solution is manifested in the iteration by which it would be obtained, when there is only one active node and when the value of the function s^{k*} is not better than the value s^k. Instead of $\sum_{(r,t)}|\tau_{(r,t)}^{k*}|=0$, new active nodes appear that did not exist previously[7]; this means that on the direction $[\underline{w}^k,\underline{w}^{k*}]$ there is a value of the function that is better than s^k and s^{k*} (it does not have to be an extreme value, because it can be located at the point $\underline{w}$ which is not on the current direction). First, the known segment of the direction $[\underline{w}^k,\underline{w}^{k*}]$ is examined, and if a solution

[6] Inaccurate linear search methods are widely discussed in the literature for nonlinear unconditional optimization problems (Zangvill, 1973; Bazaraa, et al., 2006; Luenberger & Ye, 2016) and they can also be applied to constraint problems or their adjustment is required. Although the procedures are known, due to the specific characteristics of the nodes, the whole procedure is given here.

[7] If, from the solution $(\underline{w}^{k*};s^{k*})$, which is not better than the solution $(\underline{w}^{k};s^{k})$, the already described procedure is continued by choosing the most favorable direction (27-31), due to the change of the gradient sign in previously active nodes, they will become inactive, and new active nodes will appear that did not exist at the beginning of the procedure - for the initial solution $(\underline{w}^{k};s^{k})$. For the obtained new solution, the value of the function may be even better than the value s^{k*}, but criterion (33) will not be met; then, a new solution is obtained from this solution, etc., until after several iterations, the solution $(\underline{w}^{k*};s^{k*})$ is obtained again, when the procedure begins to "circle" over the already obtained solutions. There does not have to be a solution $(\underline{w}^{k};s^{k})$ among these solutions.

that meets the set criteria is not found on it, then, by applying the procedure based on the direction of the fastest fall (growth), a new search segment is determined.

The segment of the direction $[\underline{w}^k, \underline{w}^{k*}]$ is divided into several equal parts (subsegments): $[\underline{w}^k \equiv \underline{w}^{k,l=0}, \underline{w}^{k*} \equiv \underline{w}^{k,l=n^k}]$, where $l = 0,1,2,..,n^k$ is the mark of the points on the segment of the direction, and $n^k \geq 4$ is both the *number of equal search steps* and the number of equal subsegments (integer) which provides search for a sufficient number of points for smaller subsegments. The following points are generated on a segment of the direction $[\underline{w}^{k,0}, \underline{w}^{k,n^k}]$:

$$\underline{w}^{k,l} = \underline{w}^{k,0} + l\,\alpha^k\,\underline{v}^k; \quad \textit{for } l = 1,2,...,n_k - 1; \tag{34}$$

where $\alpha^k \in (0;1/4)$ is the constant *size of the weight change step* in each of $n^k \geq 4$ equal steps in total; expression (34) is a linear combination of the points $\underline{w}^{k,0}$ and $\underline{w}^{k,n^k}$: $\underline{w}^{k,l} = (1 - l\,\alpha^k)\underline{w}^{k,0} + l\,\alpha^k\,\underline{w}^{k,n^k}$.

The criteria for accepting the approximate solution $(\underline{w}^{k,l}; s^{k,l})$ as an extreme solution and for stopping the iterative procedure are defined here in relation to the values of the function and the values of the arguments (criteria weights) for three consecutive iterative solutions:

- basic criterion:

$$a)\ s^{k,l-1} > s^{k,l} < s^{k,l+1};\ (min),$$

$$b)\ s^{k,l-1} < s^{k,l} > s^{k,l+1};\ (max); \tag{35}$$

- argument value criterion:

$$max_j\{|w_j^{k,l} - w_j^{k,l-1}|;|w_j^{k,l+1} - w_j^{k,l}|\} \leq \varepsilon_w; \tag{36}$$

- function value criterion:

$$max\{|s^{k,l} - s^{k,l-1}|;|s^{k,l+1} - s^{k,l}|\} \leq \varepsilon_s; \tag{37}$$

where $l = 1,2,...,n^k - 1$, and $\varepsilon_w, \varepsilon_s > 0$ are the parameters of small values.

The number of steps n^k and the size of the steps α^k are determined depending on the selected parameter ε_w (36):

$$n^k \geq (max_j\{|w_j^{k,n^k} - w_j^{k,0}|\}/\varepsilon_w) + 3 \ (n^k \textit{ - the first major integer}); \tag{38}$$

$$\alpha^k = 1/n^k, \quad \alpha^k \in (0;1/4). \tag{39}$$

whereby criterion (36) is met. The increments of the weight components $(\alpha^k v_j^k)$ are constant, and, with $n^k \geq 4$, it is ensured that at least three points $\underline{w}^{k,l}$ are determined on each segment $[\underline{w}^{k,0},\underline{w}^{k,n^k}]$ and the value of the limit parameter is achieved:

$$\varepsilon_w^k = max_j\{|w_j^{k,n^k} - w_j^{k,0}|\}/n^k) \le \varepsilon_w . \quad (40)$$

The choice of parameter values ε_w and ε_s can be based on the sensitivity of the value of the function to changes in the value of arguments in the extremum environment. Although the criteria for stopping the optimization process can be based on the norms of the arguments $||\underline{w}^{k+1} - \underline{w}^k|| / ||\underline{w}^k|| \le \varepsilon_w$ and the function values $|s(\underline{w}^{k+1}) - s(\underline{w}^k)| / s(\underline{w}^k) \le \varepsilon_s$ in two consecutive iterations, for the current NLP problem, the parallel application of criteria (36,37) in three iterations is favorable. Criterion (36) limits the largest individual weight changes via the parameter ε_w (40), so that the largest weight increment is $max_j\, \alpha^k v_j^k = \varepsilon_w^k \le \varepsilon_w$. *The sensitivity of the value of a function* (o_s^k), as a criterion for the selection of parameters ε_w and ε_s, can be defined as the ratio of changes in the value of the function and the maximum change of individual weights, i.e. as the ratio of the realized parameters $\varepsilon_w^k \le \varepsilon_w$ and ε_s^k for a certain subsegment: $o_s^k = \varepsilon_s^k / \varepsilon_w^k$. Numerical results for TOPSIS solutions show greater sensitivity of argument values (weight) than function values, because it is $o_s^k = \varepsilon_s^k / \varepsilon_w^k < 1$ or $\varepsilon_s^k < \varepsilon_w^k$, which should focus on the choice of the parameter ε_w. The parameters ε_w and ε_s can also be determined depending on the required accuracy of the values of arguments and functions: in order to round the values of weights and the function of the target to four exact decimal digits, it is enough to set $\varepsilon_w = 5 \cdot 10^{-5}$, which ensures $\varepsilon_s^k < 5 \cdot 10^{-5}$.

In the set of solutions $(\underline{w}^{k,l}, s^{k,l}; l = 1,2,...,n_k - 1)$, there does not have to be a solution for which $s^{k,l} < s^{k,0}$ *(min)* or $s^{k,l} > s^{k,0}$ *(max)*, because such a solution can also be in the first subsegment $[\underline{w}^{k,0}; \underline{w}^{k,l=1}]$. Therefore, for the sake of generality of the procedure, a point $\underline{w}^{k,a}$ is determined on the segment $[\underline{w}^{k,0},\underline{w}^{k,n^k}]$ in which the function has the value:

$$a)\ s^{k,a} = min_l\{s^k;\ l = 1,2,....,a-1,a,a+1,...,n^k - 1\}\ (min),$$

$$b)\ s^{k,a} = max_l\{s^k;\ l = 1,2,....,a-1,a,a+1,...,n^k - 1\}\ (max). \quad (41)$$

There is an improved solution on the subsegment $[\underline{w}^{k,a-1};\underline{w}^{k,a+1}]$: according to the selected ε_w and for $n^k \geq 4$ which provides at least four new intervals, determine the required parameters (38-40), search the subsegment and determine the TOPSIS solution according to the criteria (35,37).

The disadvantage of the procedure based on fulfilling criterion (36) is a large number of generated $\underline{w}^{k,l}$ points on the segment $[\underline{w}^{k,0},\underline{w}^{k,n^k}]$, especially for larger interval widths, when the values of the $s^{k,l}$ function and other required quantities need to be calculated for several hundred generated $\underline{w}^{k,l}$ points.

For the solved MADM problem procedure will satisfy criteria (35-37), knowing that due to the nonlinearity of the function gradient in the nodes $g(z^k_{(r,t)})$ and the appearance of new active nodes, the exact solution will be outside the direction $[\underline{w}^k;\underline{w}^{k*}]$. For the sake of generality of the procedure and reduction of error according to criteria (36,37), a two-phase procedure can be applied: a) linear search and determination of the best solution in the segment $[\underline{w}^k;\underline{w}^{k*}]$, it can also be the solution $[\underline{w}^{k+1}=\underline{w}^{k,a};s^{k,a}]$; and, b) determining a new segment between the obtained solution and the solution on the hyperplanes w^A_j or w^B_j. If the point $\underline{w}^{k+1}$ is where the best solution is achieved on the segment $[\underline{w}^k;\underline{w}^{k*}]$, a new direction of the fastest fall (growth) is set through it and a point $\underline{w}^{(k+1)*}$ is determined. On the new segment $[\underline{w}^{k+1};\underline{w}^{(k+1)*}]$, the value of the function is calculated at the newly generated points, etc. The two-phase procedure is repeated until criteria (35,37) are met. In general, an approximately extreme solution was obtained in two steps with a smaller error, but the procedure is much longer.

Procedure degenerations: wedging and oscillation

The presented procedure for determining a point on one hyperplane requires that in each iteration at least one component of weight w^k_j, which is different from the limit values $w^A_j < w^k_j < w^B_j$, have a value $w^{k*}_j = w^A_j$ or $w^{k*}_j = w^B_j$ at the new point $\underline{w}^{k*}$ and is in the direction of the fastest fall (growth). These requirements cannot be met if wedging occurs: starting from some *k*-th iteration and a point $\underline{w^k}$ that can be an inner or boundary point, through all subsequent iterations, the points "accumulate" "near" the hyperplane w_j^A or w_j^B and some expected boundary point $\underline{w^{k*}}$ which cannot be reached in a finite number of iterations. The expected point $\underline{w^{k*}}$ cannot be an extreme point, because wedging does not appear in the iteration in which the extreme solution is obtained; this iteration is preceded by only one active node, and for the occurrence of wedging there must be two or more active nodes, which facilitates the elimination of the problem. The possibility of wedging cannot be established at the initial stage of the proceedings.

Wedging occurs (but not necessarily) when the coefficient of active nodes ξ^k (29) is smaller than the coefficient of all criteria ψ^k (30): $\mu^k = \xi^k < \psi^k$ (31). As a consequence, none of the active constraints under criteria (19a, b) that had a positive value $d_j^{Ak} > 0$ or $d_j^{Bk} > 0$ in the point $\underline{w^k}$, will be fully utilized to achieve that $d_j^{Ak*} = 0$ or $d_j^{Bk*} = 0$ for at least one $j = J$. Through several iterations, the unique coefficient $\mu^k = \xi^k < \psi^k$ (31) decreases and $\mu^k \underset{k\to\infty}{\to} 0$, due to successive reduction $\xi^k = \xi^k_{(r,t)} > 0$. In each subsequent iteration, the values of the weight changes per node $z^k_{(r,t)} = \mu^k |g^k_{(r,t)}|$ decrease as well as the increment of the value of the objective function. When the process enters wedging, the number and indices of active nodes do not change, so that all the components of the direction vector that were active at the starting point $\underline{w^k}$ exist.

The $\mu^k = \xi^k < \psi^k$ disorder can disappear by the algorithm: if in some subsequent iteration in the second node (p,q) $\xi^k = \xi^k_{(p,q)} < \xi^k_{(r,t)}$ and $\xi^k_{(p,q)} \geq \psi^k_j$ are achieved, then the most favorable direction towards $\xi^k_{(p,q)}$ will be chosen, and the active node (r,t) will have no effect or will become an inactive node.

Unlike some possible ways to solve the problem of wedging, e.g. ε - *approximation* (Zangville, 1969) for the current problem of NLP and based on relative independence of active nodes, a procedure based on changing the direction can be applied: a new direction is chosen from a set of favorable directions which exclude individual active nodes. In any iteration after the occurrence of wedging, at the obtained point $\underline{w}^k$ close to the expected boundary point $\underline{w}^{k*}$, a new and less favorable direction is selected based on the characteristics of all active nodes except the node *(r, t)* which is the cause of wedging and is found to be $\mu^k = \xi^k_{(r,t)}$. By setting $g^k_{(r,t)} = 0$ for that node (current iteration only), the node (r,t) is excluded from the set of active nodes (25) and the new direction is selected in accordance with the characteristics of the remaining active nodes using expression (29-31). This does not disturb the procedure, because a favorable direction is chosen, but after obtaining a new boundary point $\underline{w}^{k*}$, the current value $g^{k+1}_{(r,t)} \neq 0$ must be returned to the procedure for the node (r,t), so that the node (r,t) can become an active node again if it satisfies conditions (25), when again the most favorable direction is chosen (29-31). There is a possibility that in several consecutive iterations the selected favorable directions must be changed and the number of active nodes successively reduced, until at some step it is obtained that it is $\mu^k = \psi^k \leq \xi^k > 0$, when the procedure continues by determining the $(\underline{w}^{k*}; s^{k*})$ solution, and the omitted nodes return to the procedure.

As the extreme solution does not depend on the initial solution or on the secondary solutions that are a consequence of choosing one of the favorable directions (based on the characteristics of all or only some active nodes), it gives the possibility to simplify the problem of wedging by: *always when* $\mu^k = \xi^k = \xi^k_{(r,t)} < \psi^k$, set the $g^k_{(r,t)} = 0$ for the node (r,t) and select another favorable direction, and in the *(k+1)* iteration, include the calculated value of $g^{k+1}_{(r,t)} \neq 0$ in the procedure of selecting the most favorable direction. This prevents the occurrence of wedging, that is, automates its removal, and the whole procedure is extended by several iterations at the most.

A special form of degeneration can be described as an *oscillation* of the value of the w^k_r component in the vicinity of a hyperplane. For example: in the *k*-th iteration for the *r*-th component of the point $\underline{w}^k$, the value $w^k_r = w^A_r$ is reached. In the normal course of the procedure, the already reached values on the hyperplane w_j^A or w_j^B do not change until the end of the procedure, which is not the case with oscillations: instead of $w_r^k = w_r^{k+1} = w_r^A$, the $w_r^{k+1} > w_r^A$ value close to w_r^A is obtained in the *(k+1)* iteration, while for some other component the boundary value $w_t^{k+1} = w_t^A$ or $w_t^{k+1} = w_t^B$ is reached. In one of the following iterations, the value of w_j^A is reached again for the r-th component, but wedging can also occur. The oscillation can also be repeated on the same hyperplane, when the $w_r^{k+1} - w_r^A$ differences also decrease. Apart from increasing the number of iterations, the oscillations do not affect the final solution, and the wedging is removed in the described way.

Partial stability of solutions

The stability of the MADM solution – the variant $V_p|(\underline{w};s_p(\underline{w}));p\in I$ *is defined in relation to all other variants* $V_q|(\underline{w};s_q(\underline{w});q\in I\setminus\{p\}$ *and represents the set of points* $\underline{w}\in E_p\subseteq \overline{E}$ *for which it is* $s_p(\underline{w})>s_q(\underline{w});p\in I;q\in I\setminus\{p\}$.

The partial stability of the solution $V_p|(\underline{w};s_p(\underline{w}))$ is determined in relation to one of the other variants $V_q;q\in I\setminus\{p\}$: *The solution* $V_p|(\underline{w};s_p(\underline{w}))$ *is stable in relation to the solution* $V_q|(\underline{w};s_q(\underline{w}))$ *for all points* $\underline{w}\in E_{pq}\subseteq\overline{E}$ *for which the function of partial stability is:*

$$h_{pq}(\underline{w})=s_p(\underline{w})-s_q(\underline{w})>0;\quad p,q\in I,p\neq q, \tag{42}$$

that is, if it is $s_p(\underline{w})/s_q(\underline{w})>1$. For $s_p^m>s_q^M$, the solution $(\underline{w};s_p(\underline{w}))$ is stable in relation to the solution $(\underline{w};s_q(\underline{w}))$ at each point $\underline{w}\in\overline{E}$ (Figure 1a) and therefore the determination of partial stability makes sense only if $\overline{S_P}\cap\overline{S_q}\neq\varnothing$, ie, if $s_p^M>s_q^m\wedge s_p^m<s_q^M$ (Figure 1: b,c,d,e). The function $h_{pq}(\underline{w})$ is concave or convex, continuous and differentiable on the convex set $\overline{E}$, and the local extreme is also the global extreme.

The set of values of the function is $\overline{S_{pq}}=\{h_{pq}\in[h_{pq}^m;h_{pq}^M]\}\subseteq\Re$ for $p,q\in I$ and $p\neq q$ or the line segment $\overline{h_{pq}^m;h_{pq}^M}$.

The extremes of the function $h_{pq}(\underline{w})$ follow from the function development $h_{pq}(\underline{w^{k+1}})=h_{pq}^{k+1}$ into the Taylor's polynomial of the first degree (12): $h_{pq}^{k+1}=(s_p^k-s_q^k)+\sigma_{pq}^k$, where $s_p^k-s_q^k=C$. The auxiliary function of σ_{pq}^k, according to (13,21), is equal to:

$$\sigma_{pq}^k=\sum_{(r,t)}(g_{p(r,t)}^k-g_{q(r,t)}^k)z_{(r,t)}^k=\sum_{(r,t)}g_{pq(r,t)}^k z_{(r,t)}^k;\ (r,t)\in\Theta. \quad (43)$$

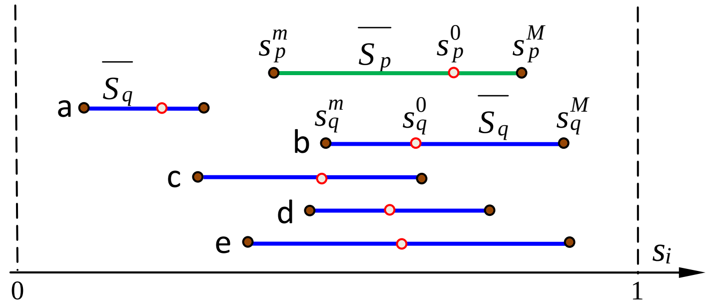

Figure 1 – Possible relations of the set of function values $s_i(\underline{w})$ of two variants

Рис. 1 – Возможные отношения множеств значений функций $s_i(\underline{w})$ двух вариантов

Слика 1 – Могући односи скупова вредности функција $s_i(\underline{w})$ две варијанте

The values of the function gradient components $h_{pq}(\underline{w})$ in the nodes $(r,t)\in\Theta$ are:

$$g_{pq(r,t)}^k=\begin{cases} g_{p(r,t)}^k-g_{q(r,t)}^k;\ (r,t)\in\Theta^k \\ 0;\ \ r=t,\ [(r,t)\notin\Theta^k] \end{cases} \quad (44)$$

and the elements are antisymmetric matrices $G_{pq}(\underline{w}^k)=G_{pq}^k=(g_{pq(r,t)}^k)_{nxn}$. To determine the extremes, it is sufficient to determine the points of weight $\underline{w}$ in which the nonlinear auxiliary function $\sigma_{pq}(\underline{w})$ (43) has extreme values, and then the corresponding TOPSIS solutions. Starting from an admissible solution (let that be the solution at the starting point $(\underline{w}^0;h_{pq}^0)$), by applying the presented procedure for determining the extremum of the function $s_i(\underline{w})$ (27-41) and by calculating the values $g_{pq(r,t)}^k$ (22, 44), d_r^{Ak}, d_t^{Bk} and $d_{(r,t)}^k$ (9, 17) in each iteration, the extreme solutions of $(\underline{w}^m; h^m_{pq} < 0)$ and $(\underline{w}^M; h^M_{pq} > 0)$ are obtained.

The separating hyperplane of the value set of the function $h_{pq} = C^R$ is defined by any value[8] of the $h = C^R | h^m < C^R < h^M$ function and divides the value set of the function $\overline{S} = \{ h \in [h^m; h^M]\} \subseteq \Re$ into two subsets: $\overline{S^-} = \{ h | h^m \le h \le C^R \} \subseteq \overline{S}$ and $S^+ = \{ h | h^M \ge h > C^R \} \subseteq \overline{S}$, where $\overline{S^-} \cup S^+ = \overline{S}$ and $\overline{S^-} \cap S^+ = \varnothing$. An acceptable approximate value of the function in the vicinity of the separating hyperplane of $h = C^R$ is:

$$h^C = C \in [C^R \pm \varepsilon_C]; \quad k = 0,1,2..., \tag{45}$$

where ε_C is a low value parameter (e.g. $\varepsilon_C = 5 \cdot 10^{-5}$ or less). The procedure for determining the set of solutions on the separating hyperplane of $(\underline{w}; h^C = C)$ has several phases, where it is determined: the set of *2n* boundary solutions and their extremes; basic boundary solutions for $h^C = C$ (if any) or basic solutions that are closest to the current hyperplane w^A_j or w^B_j; and, a set of solutions for $h^C = C$ on the set $\overline{E_C} \subseteq \overline{E}$. Accordingly, the partial stability of the variant V_p with respect to V_q is achieved for all points of $\underline{w} \in \overline{E}$ with the corresponding $(\underline{w}; (h > 0) \in S^+))$ solutions.

Boundary solutions

Boundary solutions are a set of solutions on one hyperplane of the set $\overline{E}$ (w^A_j or w^B_j). On the hyperplane w^A_j, these are $(\underline{w}^{a\lambda}; h^{a\lambda})$ solutions for the points $\underline{w}^{a\lambda} = (w^{a\lambda}_1, \cdots, w^{a\lambda}_\lambda = w^A_j, \cdots, w^{a\lambda}_n)$ (due to unambiguous indexing, additional $\lambda = \overline{1,n} \in J$ marks are introduced). If condition (7) is met, then there is at least one boundary point with the component $w^{a\lambda}_\lambda = w^A_\lambda$.

Based on the relative independence of the variables $z^0_{(\lambda,j)} \ge 0$ (18) and the built-in normalization condition (19) in each node, the $w^{a\lambda}_\lambda$

[8] In the following text, the *"pq"* indices were used only if it was necessary due to unambiguity.

component is determined on the basis of any starting point $\underline{w} \in \overline{E}$ - let that be the point $\underline{w}^0$: the choice of variables $z^0_{(\lambda,j)} \le d^0_{(\lambda,j)} > 0$ eliminates the active constraint of the λ-criterion $d^{A0}_\lambda > 0 \to d^{A1}_\lambda = 0$ and achieves the required condition: $\sum_{j=1}^{j=n} z^0_{(\lambda,j)} = d^{A0}_\lambda ;(\lambda,j) \in \Theta^0$. Nodes (λ,j) and the corresponding variables $z^0_{(\lambda,j)} \le d^0_{(\lambda,j)} > 0$ (the λ row of the matrix T^0) can be chosen at will until the specified condition is met, or preference can be given to a node in which $z^0_{(\lambda,j)} = d^0_{(\lambda,j)} = max_j\{d^0_{(\lambda,j)}\}$; if it is fulfilled that $z^0_{(\lambda,j)} = d^{A0}_\lambda$, then also $w^{a\lambda}_\lambda = w^A_\lambda$, otherwise the procedure should be continued by selecting a next node from the λ row of the matrix T^0 and by adding the necessary difference, until it is fulfilled that $\sum_{j=1}^{j=n} z^0_{(\lambda,j)} = d^{A0}_\lambda$.

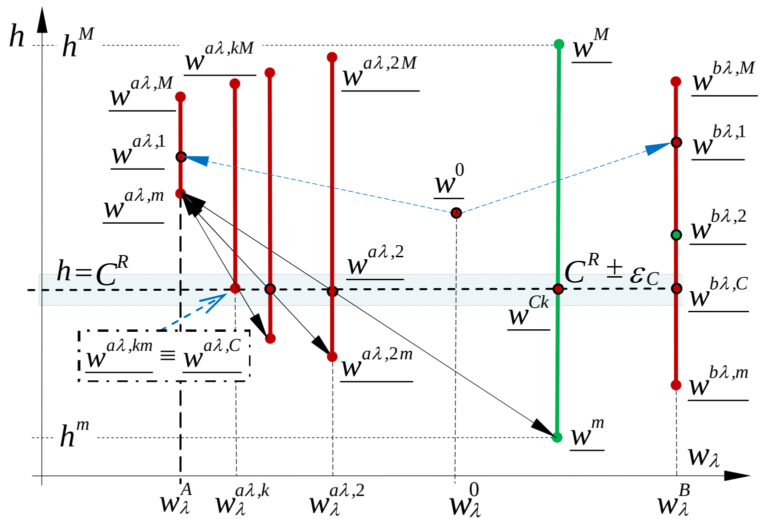

Figure 2 – Overview of the procedure for determining the basic solutions on hyperplanes
Рис. 2 – Обзор процедуры определения базовых решений на гиперплоскостях
Слика 2 – Приказ поступка одређивања основних решења на хиперравнима

Practically, in all rows of the matrix G^0 except in the λ row, $g^0_{(j1,j)} = 0; j \in J; j1 \in J \setminus \{\lambda\}$ should be set and in the active nodes (λ,j) the values of $z^0_{(\lambda,j)} \le d^0_{(\lambda,j)} > 0$ should be determined until the condition

$\sum_{j=1}^{j=n} z^0_{(\lambda,j)} = d^{A0}_\lambda$ is fulfilled. By applying expression (2-4) for the point $\underline{w^{a\lambda}} = \underline{w^{a\lambda,1}}$, the TOPSIS solution $(\underline{w^{a\lambda,1}}; h^{a\lambda,1})$ is obtained. In the same way, the solution of $(\underline{w^{b\lambda,1}}; h^{b\lambda,1})$ on the hyperplane w^B_j was obtained by eliminating the active constraint $d^{B0}_\lambda > 0 \rightarrow d^{B1}_\lambda = 0$ based on the choice of the variable $z^0_{(j,\lambda,} \leq d^0_{(j,\lambda)} > 0$ from which the $\sum_{j=1}^{j=n} z^0_{(j,\lambda)} = d^{B0}_\lambda$ (the λ column of the matrix T^0) was obtained.

Extreme solutions on the hyperplanes w^A_j and w^B_j (extreme boundary solutions) are the exact solutions at the vertex of the set $\overline{E}$ and are determined by applying the presented method for the extremes of the function $s(\underline{w})$. The starting point is the obtained solutions on the hyperplanes: e.g. for the hyperplane w^A_j, the initial solution is $(\underline{w^{a\lambda,1}}; h^{a\lambda,1})$; the component $w^{a\lambda,1}_\lambda = w^A_\lambda$ retains its value, which requires that the nodes that affect its value must become inactive.

From the starting point $\underline{w^{a\lambda,1}}$, the most favorable direction is chosen in accordance with the characteristics of the active nodes (the set Θ^1_- for the minimum or the set Θ^1_+ for the maximum) that are not in the λ row and the λ column of the matrix T^1: set $g^1_{(\lambda,j)} = g^1_{(j,\lambda)} = 0$ for all nodes *(r,t)* in the row of λ and the column of λ, and the further procedure for determining the extremes $(\underline{w^{a\lambda,m}}; h^{a\lambda,m})$(min) and $(\underline{w^{a\lambda,M}}; h^{a\lambda,M})$(max) is identical to the procedure shown for determining the exact extreme solutions of the function $s(\underline{w})$ (27-31). The interval of the value of the function $[h^{a\lambda,m}; h^{a\lambda,M}]$ on the hyperplane w^A_λ cannot be greater than the interval of the extremum of the function $h(\underline{w})$: $h^{a\lambda,M} - h^{a\lambda,m} \leq h^M - h^m$, Figure 2. In the same way, the extreme solutions on the hyperplane w^B_λ are determined. Extreme boundary solutions (maximum *4n* solutions), among which are the extreme solutions $h(\underline{w})$ of the function, are unique in terms of the corresponding points $\underline{w}$ and the values of the function $h(\underline{w})$. Not all extreme points ($\underline{w^{a\lambda,m}}$ and $\underline{w^{a\lambda,M}}$) are linearly independent; by eliminating the linearly dependent points, a set of points $\underline{w^v}$ is obtained which are the vertices of the set $\overline{E}$.

System of basic solutions for the separating hyperplane $h = C^R$

A *system of basic solutions* (SBS_C) is established for the value of the function $h = C$, which contains *2n* basic solutions: *n* solutions $(\underline{w^{a\lambda,C}}; h^{a\lambda,C} = C)$ and *n* solutions $(\underline{w^{b\lambda,C}}; h^{b\lambda,C} = C)$. These are the *basic boundary solutions* for the point $\underline{w^{a\lambda,C}}$ if $w_\lambda^{a\lambda,C} = w_\lambda^A$ (or $\underline{w^{b\lambda,C}}$ for $w_\lambda^{b\lambda,C} = w_\lambda^B$) or the *basic non-boundary solutions* that are closest to the current hyperplane w_λ^A or w_λ^B with $w_\lambda^{a\lambda,C} > w_\lambda^A$ or $w_\lambda^{b\lambda,C} < w_\lambda^B$:

a) On the hyperplane w_λ^B (or w_λ^A), there is an edge solution $(\underline{w^{b\lambda}}; h^{b\lambda} = C^R)$ (Figure 2, hyperplane w_λ^B) because it is $h^{b\lambda,m} \le C^R \le h^{b\lambda,M}$ and it is determined by repeatedly halving the segment $[\underline{w^{b\lambda,m}}; \underline{w^{b\lambda,M}}]$ until it is achieved that it is $h^{b\lambda,C} = C$. The segment $[\underline{w^{b\lambda,m}}; \underline{w^{b\lambda,M}}]$ is halved for the point $\underline{w^{b\lambda,2}} = 0.5\underline{w^{b\lambda,m}} + 0.5\underline{w^{b\lambda,M}}$ as well. The TOPSIS solution, in general, has the value $h^{b\lambda,2} \ne C$; in the next iteration, the segment of the interval in which $h = C^R$ ($[\underline{w^{b\lambda,m}}; \underline{w^{b\lambda,2}}]$ or $[\underline{w^{b\lambda,2}}; \underline{w^{b\lambda,M}}]$) is halved and the TOPSIS value is calculated, etc. The procedure is interrupted when $h^{b\lambda,k} = C^k \in [C^R \pm \varepsilon_C]$ is obtained in the k-th iteration and that solution is accepted as *the basic boundary solution* $[\underline{w^{b\lambda,C}}; h^{b\lambda,C}]$; for a larger number of iterations, a smaller absolute error $\varepsilon_C^k = |C^R - h^{b\lambda,C}| < \varepsilon_C$ was obtained.

b) On the hyperplane w_λ^A (or w_λ^B), there is no solution $(\underline{w^{a\lambda}}; h^{a\lambda} = C^R)$ because $C^R \notin [h^{a\lambda,m}; h^{a\lambda,M}]$. To achieve the $h = C$ value, the point $\underline{w^{a\lambda}}$ cannot have a value of $w_\lambda^{a\lambda} = w_\lambda^A$, but a value of $w_\lambda^{a\lambda} > w_\lambda^A$. These solutions are not boundary based on $w_\lambda^{a\lambda} = w_\lambda^A$, but are closest to the hyperplane w_λ^A (basic non-boundary solutions). The position of C^R can be $C^R < h^{a\lambda,m}$ (as in Figure 2) or $C^R > h^{a\lambda,M}$. For the situation in Figure 2, in order to determine the $w_\lambda^{a\lambda} > w_\lambda^A$ component, the point $w_\lambda^{a\lambda,2} > w_\lambda^A$ is first determined by iterative halving of the segment between two known points at which there is a solution with $h = C^R$ until the value $h^{a\lambda,k} = C$ is reached: for $h^{a\lambda,m} > C^R + \varepsilon_C$ value $h^{a\lambda,2} = C^R$ it is on the segment $[\underline{w}^m;\underline{w}^{a\lambda,m}]$, and for $h^{a\lambda,M}<C^R-\varepsilon_C$, on the segment $[\underline{w}^{a\lambda,M};\underline{w}^M]$. From the point $\underline{w}^{a\lambda,2}$, for the constant value $w_\lambda^{a\lambda,2}$ (in the row of λ and the column of λ the matrix G^2, set $g^2_{(\lambda,j)}=g^2_{(j,\lambda)}=0$) and determine the minimum $(\underline{w}^{a\lambda,2m};h^{a\lambda,2m})$. If the obtained solution does not satisfy condition (45) and if it is $h^{a\lambda,2m}<C^R-\varepsilon_C$, by repeatedly halving the new segment $[\underline{w}^{a\lambda,2m};\underline{w}^{a\lambda,m}]$, a new point $\underline{w}^{a\lambda,3}$ and a minimum $(\underline{w}^{a\lambda,3m};h^{a\lambda,3m}<C^S-\varepsilon_C)$ are obtained, etc. The procedure ends when the solution $(\underline{w}^{a\lambda,km};h^{a\lambda,km}=C)\equiv(\underline{w}^{a\lambda,C};h^{a\lambda,C}=C)$ is obtained in the *k*-th iteration, from which it is not possible to further move the point $\underline{w}^{a\lambda,km}$ towards the hyperplane w_λ^A provided that $h=C$, which determines the basic non-boundary solution $(\underline{w}^{a\lambda,km};h^{a\lambda,km}=C)\equiv(\underline{w}^{a\lambda,C};h^{a\lambda,C})$ (based on other weight components $w_j;\ j\in J\setminus\{\lambda\}$, these solutions can also be boundary)[9].

On the hyperplane w_λ^A, if $h^{a\lambda,M}<C^R-\varepsilon_C$, the procedure for determining the solution is similar: the segment $[\underline{w}^{a\lambda,M};\underline{w}^M]$ is considered; the relevant points are $\underline{w}^M$ and $\underline{w}^{a\lambda,kM}$; the non-boundary solution is $(\underline{w}^{a\lambda,kM};h^{a\lambda,kM}=C)\equiv(\underline{w}^{a\lambda,C};h^{a\lambda,C})$.

The presented procedure yields *n* solutions $(\underline{w}^{a\lambda,C};h^{a\lambda,C})$ and *n* solutions $(\underline{w}^{b\lambda,C};h^{b\lambda,C})$ that make up the SBS$_C$ for the value of the function $h=C^R\pm\varepsilon_C$. Due to the components λ of the points $\underline{w}^{a\lambda,C}$ and $\underline{w}^{b\lambda,C}$, the points of solution $\underline{w}$ in SBS$_C$ are mutually linearly independent.

A set of solutions for the separating hyperplane $h=C^R$: From SBS$_C$ linear combinations of the weight points $\underline{w}^{a\lambda,C}$ and $\underline{w}^{b\lambda,C}$, countless new

---

[9] In the numerical example, the solution $(\underline{w}^{b4};h^{b4,0}=0)$ is the basic non-boundary solution because $(w_4^{b4}=0.1681)<(w_4^B=0.1830)$ although $\underline{w}^{b4}\in\overline{E}\setminus E$ is a boundary point due to $w_1^{b4}=w_1^A=0.0990$.

weight points can be obtained based both on them and on the solutions with $h = C$:

$$\underline{w^{ab}} = \sum_{j=1}^{j=n} \beta_j^a \underline{w^{aj}} + \sum_{j=1}^{j=n} \beta_j^b \underline{w^{bj}}; \ \ \sum_{j=1}^{j=n} \beta_j^a + \sum_{j=1}^{j=n} \beta_j^b = 1; \ \ j \in J \ , \qquad (46)$$

where all coefficients $\beta_j^a, \beta_j^b \geq 0$ are not equal to 0, and can be selected according to different criteria. Due to the nonlinearity of the $h(\underline{w^{ab}})$ function, by using the points $\underline{w^m}$ and $\underline{w^M}$ and/or other known points, a satisfactory solution $(\underline{w^{ab,C}}; h^{ab,C})$ can be determined by the line search in the vicinity of the point $\underline{w^{ab}}$.

The procedure completely defines the set of all solutions of the function $h(\underline{w})$ (graph of the function): based on the most *4n* extreme boundary solutions (whose points $\underline{w}$ are not linearly independent), a set of linearly independent points $\underline{w^v}$ is singled out, which are also all vertices of the set $\overline{E}$. Other TOPSIS solutions can be determined on the basis of linear combinations of points on the vertices of the set $\overline{E}$. For each criterion $j \in J$ and any value $w_j \in [w_j^A, w_j^B]$, weight points can be determined for which the function $h_{pq}(\underline{w})$ has a maximum and minimum value, as well as points $\underline{w}$ for all values of the function from that interval. If some values of the weight point components are set to a predetermined and allowable value (maximum *n-2* values), it is possible to determine the solution for the required value of $h_{pq}(\underline{w}) = C$ based on the parameters of the remaining active nodes. By combining multiple SBS_C solutions for different $C^{\Re} \in [h_{pq}^m; h_{pq}^M]$ values, solutions with a range of $h_{pq} \in [C_1^{\Re}; C_2^{\Re}]$ values and stricter criteria for weight component values can be determined.

Numerical example

By applying the TOPSIS method to the MADM problem given by the initial matrix $C = \{c_{ij}; \ i = \overline{1,5}, \ j = \overline{1,6}\}$, for the weight point $\underline{w^0}$ and the coefficients of the linear combination $\chi_{p,6} = (0.5717; \ 0.2647; \ 0.1636)$ for $p = 1,2,\infty$, the basic solution was obtained: the variant V_2 $(\underline{w^0}; s_2^0 = 0.6209)$ and the rank $V_2 - V_3 - V_5 - V_1 - V_4$ (1-5) (Table 2).

Table 2 – Criteria Matrix, basic solution and extreme solutions
Таблица 2 – Матрица критериальных значений, базовые решение и экстремальные решения
Табела 2 – Матрица критеријумских вредности, основно решење и екстремна решења

j / i	criteria						$s_i(\underline{w}^0)$ (rank)	$s_i(\underline{w}^m)$	$s_i(\underline{w}^M)$
	$K_1(+)$	$K_2(-)$	$K_3(+)$	$K_4(-)$	$K_5(+)$	$K_6(-)$			
variants V_1	415	85	1112	60	1.42	11.9	0.4348 (4)	0.4107	0.4645
variants V_2	432	94	970	35	1.71	15.2	0.6209 (1)	0.5846	0.6518
variants V_3	405	77	1015	55	1.88	14.6	0.6058 (2)	0.5812	0.6366
variants V_4	352	62	1055	54	1.06	13.8	0.3522 (5)	0.3248	0.3838
variants V_5	328	78	1045	38	1.43	17.5	0.4997 (3)	0.4717	0.5214
$\underline{w}^A$	0.099	0.132	0.237	0.147	0.208	0.088	Set of function values $s_i(w)$ 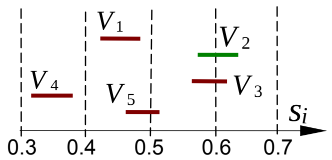		
$\underline{w}^B$	0.134	0.161	0.273	0.183	0.241	0.105			
$\underline{w}^0$	0.112	0.144	0.258	0.167	0.223	0.096			
d_j^{A0}	0.013	0.012	0.021	0.020	0.015	0.008			
d_j^{B0}	0.022	0.017	0.015	0.016	0.018	0.009			
d_j^{AB}	0.035	0.029	0.036	0.036	0.033	0.017			

Table 2 provides data for the weight range limits w_j^A and w_j^B, the initial active limits d_j^{A0} and d_j^{B0} (9) for $k=0$, and the extreme values of $s_i(\underline{w}^m)$ and $s_i(\underline{w}^M)$. Based on the characteristics of the formed nodes (Table 1), exact extreme solutions were obtained at the vertices of the set $\overline{E}$ (27-31, 2-4) when the optimality criterion (33) was met, regardless of the convexity or concavity of the function. The variant V_2 is slightly better than the variant V_3, but in the conditions of interval given weights, the ratio of their extreme values is $(s_2^M=0.6518)>(s_3^m=0.5812)$ and $(s_2^m=0.5846)<(s_3^M=0.6366)$, which shows that the sets of values of functions partially overlap and require testing the stability of solution $V_2|(\underline{w};s_2(\underline{w}))$ in relation to the solution $V_3|(\underline{w};s_3(\underline{w}))$.

The solution V_2 is stable with respect to V_3 for $h_{2,3}(\underline{w})=s_2(\underline{w})-s_3(\underline{w})>0$. For the function $h(w)$ (42), extreme solutions are determined (which are on the vertices of the set $\overline{E}$, in accordance with (7)), where, except for the component w_3, all other components w_j have values of one of the limits of the weight interval, Table 3. The set of values of the function is $\overline{S_{2,3}} = \{ h_{2,3} \in [-0.0298;\ 0.0557]\}$, in the point $\underline{w}^M$ the largest difference of TOPSIS values of the variants V_2 and V_3 $(h_{2,3}(\underline{w}^M) = 0.0557)$ is achieved, while in the point $\underline{w}^m$ the variant V_3 is "better" than the variant V_2 $(h_{2,3}(\underline{w}^m) = -0.0298)$.

Table 3 – Extreme solutions of the function $h_{2,3}(\underline{w})$

Таблица 3 – Экстремальные решения функции $h_{2,3}(\underline{w})$

Табела 3 – Екстремна решења функције $h_{2,3}(\underline{w})$

	w_1^0	w_2^0	w_3^0	w_4^0	w_5^0	w_6^0	$s_2(\underline{w})$	$s_3(\underline{w})$	$h_{2,3}(w)$
$\underline{w}^m$	0.0990	0.1610	0.2640	0.1470	0.2410	0.0880	0.6009	0.6307	-0.0298
$\underline{w}^M$	0.1340	0.1320	0.2550	0.1830	0.2080	0.0880	0.6425	0.5868	0.0557

For each hyperplane $w_j^A = w_\lambda^{a\lambda}$ and $w_j^B = w_\lambda^{b\lambda}$, boundary solutions and extreme boundary solutions ($4n = 24$ solutions) are determined, whereby the individual extreme boundary solutions are identical to each other or identical to the extreme solutions of the function $h(\underline{w})$. On the segments $[\underline{w}^{a\lambda,m}; \underline{w}^{a\lambda,M}]$ and $[\underline{w}^{b\lambda,m}; \underline{w}^{b\lambda,M}]$, the basic boundary solutions for the separating hyperplane $h^C = C \in [C^R + \varepsilon_C]$ (45) and for the reference value of the function $C^R = 0$ (if any) are determined, or the basic non-boundary solutions are determined. In order to determine only solutions with positive values of the function $h > 0$, due to partial stability and $S^+ = \{ h \mid h^M \geq h > C^R = 0 \} \subseteq \overline{S}$, a modified expression (45) was applied: $h^C = C \in [C^R + \varepsilon_C]$.

The obtained basic solutions are also boundary solutions based on the current hyperplane because $w_\lambda^{a\lambda,0} = w_\lambda^A$ or $w_\lambda^{b\lambda,0} = w_\lambda^B$, except for the solution for the point $\underline{w}^{b4,0}$ which is not a boundary solution based on the hyperplane w_4^B because $w_\lambda^{b\lambda,C} \neq w_\lambda^B$ (non-boundary basic solution) and $w_4^{b4,0} = 0.1681 < w_4^B = 0.1830$. In general, according to the definition of the boundary solution, the solution $\underline{w}^{b4,0}$ is a boundary solution based on other hyperplanes, because $w_1^{b4,0} = w_1^A = 0.990$ and $w_2^{b4,0} = w_2^B = 0.1610$ (Table 4)[10].

Table 4 – System of basic solutions for the separating hyperplane $h(\underline{w}) = 0$
Таблица 4 – Система базовых решений для разделения гиперплоскостей $h(\underline{w}) = 0$
Табела 4 – Систем основних решења за хиперраван раздвајања $h(\underline{w}) = 0$

$\underline{w}$ / *j*	$\underline{w}^{a1,0}$	$\underline{w}^{b1,0}$	$\underline{w}^{a2,0}$	$\underline{w}^{b2,0}$	$\underline{w}^{a3,0}$	$\underline{w}^{b3,0}$	$\underline{w}^{a4,0}$	$\underline{w}^{b4,0}$	$\underline{w}^{a5,0}$	$\underline{w}^{b5,0}$	$\underline{w}^{a6,0}$	$\underline{w}^{b6,0}$
1	0.0990	0.1340	0.1075	0.1106	0.1175	0.1053	0.1300	0.0990	0.1140	0.1073	0.1117	0.1116
2	0.1495	0.1532	0.1320	0.1610	0.1511	0.1503	0.1353	0.1610	0.1527	0.1489	0.1505	0.1505
3	0.2681	0.2418	0.2699	0.2509	0.2370	0.2730	0.2719	0.2482	0.2679	0.2528	0.2607	0.2438
4	0.1613	0.1567	0.1532	0.1644	0.1593	0.1603	0.1470	0.1681	0.1573	0.1620	0.1600	0.1600
5	0.2251	0.2263	0.2353	0.2250	0.2301	0.2232	0.2127	0.2404	0.2080	0.2410	0.2291	0.2291
6	0.0971	0.0880	0.1021	0.0880	0.1050	0.0880	0.1031	0.0881	0.1002	0.0880	0.0880	0.1050
$h(\underline{w})$	0.00002	0.00001	0.00004	0.00000	0.00003	0.00001	0.00003	0.00003	0.00004	0.00004	0.00000	0.00004
s_2=s_3	0.6091	0.6188	0.6238	0.6089	0.6174	0.6092	0.6139	0.6122	0.6007	0.6222	0.6150	0.6153

It is shown that the function $h(\underline{w})$ between the points of the weight of the basic solutions is concave or convex: between the points $\underline{w}^{a1,0}$ and $\underline{w}^{b1,0}$ the function is *convex*, and between the points $\underline{w}^{a2,0}$ and $\underline{w}^{b2,0}$ the function is *concave*. Due to the values of the λ weight components ($w_\lambda^{a\lambda}$ and $w_\lambda^{b\lambda}$), all points of the basic solutions $\underline{w}^{a\lambda,0}$ and $\underline{w}^{b\lambda,0}$ are linearly independent and their linear combinations give innumerable new weight points in the environment of the separating hyperplane. By applying expression (46) for $\beta_j^a = \beta_j^b = 1/2n = 1/12$, the solution is obtained:

$\underline{w}^{ab} = (0.1123;\ 0.1497;\ 0.2572;\ 0.1591;\ 0.2266;\ 0.0951)$;

$h_{2,3}^0(\underline{w}^{ab}) = 0.0003 < \varepsilon_C = 0.00005$ and $s_2(\underline{w}^{ab}) = s_3(\underline{w}^{ab}) = 0.6139$. The solution does not need to be corrected in accordance with other known

[10] For $\varepsilon_C = 5 \cdot 10^{-5}$ and the calculation of one basic boundary solution for which $w_j^A = w_\lambda^{a\lambda}$ or $w_j^B = w_\lambda^{b\lambda}$ about twenty iterations were required, and for the non-edge solution $\underline{w}^{b4}$ - about forty iterations.

points, for example in accordance with the extremes of the function or the boundary extreme solutions, because $h_{2,3}(\underline{w}^{ab}) < \varepsilon_C$ and the solution $(\underline{w}^{ab}; h_{2,3}^{ab})$ can be accepted in accordance with condition (45). The fulfilled condition (45) can also be a consequence of the concavity or convexity of the function on the segments between the points of the basic solutions.

Table 5 – Vertices of the set $\overline{E}$
Таблица 5 – Вершины множества $\overline{E}$
Табела 5 – Врхови скупа $\overline{E}$

$\underline{w}^v$	w_1	w_2	w_3	w_4	w_5	w_6	$h(\underline{w}^v)$
$\underline{w}^1$	0.0990	0.1610	0.2640	0.1470	0.2410	0.0880	-0.0298
$\underline{w}^2$	0.0990	0.1610	0.2470	0.1470	0.2410	0.1050	-0.0294
$\underline{w}^3$	0.0990	0.1610	0.2730	0.1470	0.2320	0.0880	-0.0283
$\underline{w}^4$	0.1090	0.1610	0.2370	0.1470	0.2410	0.1050	-0.0269
$\underline{w}^5$	0.1060	0.1610	0.2730	0.1470	0.2080	0.1050	-0.0216
$\underline{w}^6$	0.1340	0.1610	0.2370	0.1470	0.2330	0.0880	-0.0194
$\underline{w}^7$	0.1020	0.1320	0.2730	0.1470	0.2410	0.1050	-0.0111
$\underline{w}^8$	0.1340	0.1320	0.2730	0.1470	0.2090	0.1050	0.0040
$\underline{w}^9$	0.0990	0.1610	0.2370	0.1830	0.2303	0.0897	0.0207
$\underline{w}^{10}$	0.1230	0.1610	0.2370	0.1830	0.2080	0.0880	0.0337
$\underline{w}^{11}$	0.1190	0.1320	0.2370	0.1830	0.2410	0.0880	0.0416
$\underline{w}^{12}$	0.0990	0.1320	0.2730	0.1830	0.2080	0.1050	0.0467
$\underline{w}^{13}$	0.1160	0.1320	0.2730	0.1830	0.2080	0.0880	0.0512
$\underline{w}^{14}$	0.1340	0.1320	0.2370	0.1830	0.2090	0.1050	0.0550
$\underline{w}^{15}$	0.1340	0.1320	0.2380	0.1830	0.2080	0.1050	0.0554
$\underline{w}^{16}$	0.1340	0.1320	0.2550	0.1830	0.2080	0.0880	0.0557

Some of the weight components do not have to be given intervally but as discrete values (maximum *n-2* components), which also enables the determination of a set of solutions for a certain value of the function and the definition of the separating hyperplane. For example, if the weight point is $\underline{w} = (w_j)$ with the components $w_j = w_j^0$ for $j = 1,2,3$ and the components $w_j \in [w_j^A, w_j^B]$ for $j = 4,5,6$ (according to Table 2), and the required value is $h_{2,3}(\underline{w}) = 0.0500$ (to ensure a significant "advantage" of the variant V_2 over V_3), althhough $h_{2,3}(\underline{w}) < h_{2,3}^M = 0.0557$, such a solution does not exit because the maximum possible value of the function for these conditions is equal to $h_{2,3}(\underline{w}) = 0.0421$. For a smaller value, for example for $h_{2,3}(\underline{w}) = 0.0400$, there is a set of basic boundary solutions, and linear combinations of points of difficulty of these solutions determine other solutions that meet condition (45). One of these solutions is: $\underline{w^{ab}} = (0.1120;\ 0.1440;\ 0.2580;\ 0.1828;\ 0.2132;\ 0.0900)$; $h_{2,3}(\underline{w^{ab}}) = 0.0400$; $s_2(\underline{w^{ab}}) = 0.6278$ and $s_3(\underline{w^{ab}}) = 0.5878$.

From the set of points $\underline{w}$ for the extreme boundary solutions ($\underline{w^{a\lambda,m}}$, $\underline{w^{b\lambda,m}}$, $\underline{w^{a\lambda,M}}$ and $\underline{w^{b\lambda,M}}$), which are not all linearly independent, linearly independent points $\underline{w^v}$ are singled out and all vertices of the set $\overline{E}$ are determined by them (16 vertices of the set $\underline{w^v} \in \overline{E}$ are obtained, Table 5). This completely describes the set of definitions of the function $\overline{E}$, which with TOPSIS values of the function, represents a complete graph of the function $\Gamma_h = \{(\underline{w}; h_{2,3}) \in \Re^7 \mid \underline{w} \in \overline{E}, h_{2,3}(\underline{w}) \in \overline{S_{2,3}}\}$. Knowledge of function graphs enables determination of sets of solutions complying with specific requirements in accordance with the stated limitations, which exceeds the goal and scope of this work.

Conclusion

The initial idea of developing a concept for testing the stability of the solution of the MADM problem (best variant and the corresponding quantitative indicator of the quality of the variant according to the chosen MADM method) in relation to other solutions (variants) and variable criteria weights was operationalized only through the examination of partial stability in relation to some other solution - one variant. The problem of determining the set of solutions of partial stability is set as a problem of NLP with the aim of finding feasible solutions that meet the conditions from the definition of partial stability. The TOPSIS method with parameters and interval-given criteria weights was considered as a basis, which defined the reference function as nonlinear and differentiable, in the presence of a normalization condition for arguments (weight components).

The created NLP model contains a nonlinear objective function, linear constraints based on the nature of the arguments (values: from - to) and the normalization condition for the arguments. An appropriate method was not known for solving the set NLP task, and therefore an attempt was made to solve the problem by introducing the nodes of argument (criteria) pairs and by defining their parameters. This ensures the normalization condition in each node and for each feasible point, non-negativity of variables and independence of variables in nodes, within the limits of active constraints. Node parameters were applied to determine the extremes of the function, the extremes on the hyperplanes of the set of arguments and other feasible solutions needed to determine the partial stability of the MADM solution, as well as to eliminate the consequences of accompanying degeneration (wedging and oscillation of the solution).

The presented procedure for determining the extremes of a given NLP problem differs from the basic gradient method in applying nodes parameters, choosing favorable directions, determining improved solutions, as well as in the procedure of linear search for the point of difficulty for an improved TOPSIS solution. The well-known and applied line search procedure can be replaced by another, for example, the "golden ratio" procedure, if this would contribute to the reduction of the procedure.

The procedure can be applied to other MADM methods with a nonlinear reference function, as well as to the class of NLP problems with conditional optimization, in which the mathematical model contains a nonlinear and on the whole set of arguments differentiable objective function, natural linear constraints and the normalization condition for variables. The procedure is robust and requires a larger number of calculations, so adequate software support would increase the possibilities of application.

References

Bazaraa, M.S., Sherali, H.D., & Shetty, C.M. 2006. *Nonlinear Programming: Theory and Algorithms, 3rd Edition*. New Jersey: John Wiley & Sons, Inc. ISBN: 978-0-471-48600-8.

Hadley, G. 1964, *Nonlinear and dynamic programming.* Boston: Addison-Wesley Publishing Company Inc. ISBN 10: 0201026643, ISBN 13: 9780201026641.

Hwang, C.L., & Yoon, K. 1981. *Multiple Attribute Decision Making*, New York: Springer-Verlag. ISBN: 978-3-642-48318-9.

Luenberger, D.G., & Ye, Y. 2016. *Linear and nonlinear programming.* Basel: Springer International Publishing. ISBN: 978-0-387-74503-9.

Martić, Lj. 1978. *Višekriterijumsko programiranje.* Zagreb: Informator (in Serbian).

Milovanović, G.V. & Stanimirović, P.S. 2002. *Simbolička implementacija nelinearne optimizacije.* Niš: Elektronski fakultet (in Serbian).

Opricović, S. 1986. *Višekriterijumska optimizacija.* Belgrade: Naučna knjiga (in Serbian).

Petrić, J. 1979. *Nelinearno programiranje.* Belgrade: IŠRO „Privredni pregled" (in Serbian).

Vujičić, V., Ašić, M., & Miličić, N. 1980. *Matematičko programiranje.* Belgrade: Matematički institut (in Serbian).

Yoon, K. 1987. A Reconciliation Among Discrete Compromise Solutions. *Journal of the Operational Research Society*, 38(3), pp.277-286. Available at: https://doi.org/10.1057/jors.1987.44.

Zangwill, W.I. 1969. *Nonlinear programming.* Englewood Cliffs, N.J: Prentice-Hall. ISBN 10: 0136235794, ISBN 13: 9780136235798.

Zeleny, M. 1982. *Multiple Criteria Decision Making.* New York: McGraw-Hill.

ЧАСТИЧНАЯ УСТОЙЧИВОСТЬ МНОГОАТРИБУТИВНОГО ПРИНЯТИЯ РЕШЕНИЙ ПО ИНТЕРВАЛЬНО ЗАДАННОМУ ВЕСУ КРИТЕРИЯ − ПРОБЛЕМА НЕЛИНЕЙНОГО ПРОГРАММИРОВАНИЯ

Радомир Р. Джукич

независимый исследователь, г. Крушевац, Республика Сербия

РУБРИКА ГРНТИ: 27.00.00 МАТЕМАТИКА;
27.47.19 Исследование операций
ВИД СТАТЬИ: оригинальная научная статья

Резюме:

Введение/цель: В статье представлена разработанная процедура для решения класса задач нелинейного программирования (НЛП) с нелинейной и дифференцируемой целевой функцией, линейными естественными ограничениями и условием нормализации переменных (аргументов). Процедура была применена для определения частичной устойчивости решения задач многоатрибутивного принятия решений.

Методы: Основой процедуры является определение узлов пар аргументов и их параметров для допустимых многомерных точек. Параметры внедрены в примененном градиентном методе, методе возможных направлений и методе линейного поиска. При разработке процедуры были использованы основы метода TOPSIS как метода для многоатрибутивного принятия решений с интервально заданными критериями веса, в первую очередь из-за нелинейности в вызове функций.

Результаты: Также разработана процедура определения экстремальных и других допустимых решений при вызове функций (маргинальные и базовые решения) и всех вершин выпуклого множества определения функции. Таким образом сформирован полный график функции, т.е. определены требуемые решения из допустимого множества. Разработана процедура установления множества решений для определения разделяющей гиперплоскости множества значений функции; благодаря чему в отдельных случаях множество решений частичной устойчивости варианта определяется как решение многоатрибутивного принятия решений. Были предложены соответствующие процедуры для устранения отклонений в процедуре (заклинивание и колебание решений).

Выводы: Данное исследование является значительным вкладом в определение узлов аргументов и их параметров, которые обеспечивают условия нормализации в каждом узле и для каждой допустимой точки, неотрицательность переменных и независимость изменений аргументов в узлах в рамках активных ограничений. Разработана оригинальная процедура определения графов функций. Приведены соответствующие реальные числовые примеры.

Ключевые слова: веса критериев, узлы пар аргументов, градиентный метод, метод возможных направлений, система базовых решений, метод многоатрибутивного принятия решений, частичная устойчивость решений.

ПАРЦИЈАЛНА СТАБИЛНОСТ РЕШЕЊА ВИШЕАТРИБУТНОГ ОДЛУЧИВАЊА ЗА ИНТЕРВАЛНО ЗАДАТЕ ТЕЖИНЕ КРИТЕРИЈУМА – ПРОБЛЕМ НЕЛИНЕАРНОГ ПРОГРАМИРАЊА

Радомир Р. Ђукић

самостални истаживач, Крушевац, Република Србија

ОБЛАСТ: математика, нелинеарно програмирање
ВРСТА ЧЛАНКА: оригинални научни рад

Сажетак:

Увод/циљ: У раду је приказан пројектовани поступак за решавање класе задатака нелинеарног програмирања (НЛП) са нелинеарном и диференцијабилном функцијом циља, линеарним природним ограничењима и нормирајућим условом за променљиве (аргументе). Поступак је примењен за одређивање парцијалне стабилности решења проблема вишеатрибутног одлучивања (ВАО).

Методи: Основ поступка представља дефинисање чворова парова аргумената и њихових параметара за допустиве вишедимензионалне тачке. Параметри се имлементирају у градијентни метод, метод повољних праваца и метод линијског тражења. У развоју поступка коришћени су основи метода ТОПСИС за ВАО са интервално задатим тежинама критеријума, првенствено због нелинеарности референтне функције.

Резултати: Разрађен је поступак одређивања екстремних и других допустивих решења референтне функције (рубна и основна решења) и свих врхова конвексног скупа дефинисаности функције. Тиме је формиран потпуни график функције, на основу којег се могу одредити захтевана решења из допустивог скупа. Развијен је поступак одређивања скупа решења за дефинисање хиперравани раздвајања скупа вредности функције. На тај начин се, као специфичан случај, дефинише и скуп решења парцијалне стабилности варијанте као решења ВАО. За отклањање дегенерације поступка (заклињавање и осциловање решења) предложене су адекватне процедуре.

Закључак: Најзначајнији допринос овог рада јесте дефинисање чворова аргумената и њихових параметара којима се осигурава нормирајући услов у сваком чвору и за сваку допустиву тачку, ненегативност променљивих и независност промена аргумената у чворовима, у границама активних ограничења. Такође, развијен је оригиналан поступак за одређивање графика функције и представљен одговарајући реалан нумерички пример.

Кључне речи: тежине критеријума, чворови парова аргумената, градијентни метод, метод повољних праваца, систем основних решења, вишеатрибутно одлучивање, парцијална стабилност решења.

Paper received on / Дата получения работы / Датум пријема чланка: 10.06.2020.
Manuscript corrections submitted on / Дата получения исправленной версии работы / Датум достављања исправки рукописа: 06.07.2020.
Paper accepted for publishing on / Дата окончательного согласования работы / Датум коначног прихватања чланка за објављивање: 08.07.2020.

DEVELOPMENT OF A METHOD FOR DETERMINING THE SIZE OF CLEARANCE IN SLIDING BEARINGS

Nikola P. Žegarac
Serbian Academy of Inventors and Scientists,
Belgrade, Republic of Serbia,
e-mail: zegaracnikola@vektor.net,
ORCID iD: https://orcid.org/0000-0002-1766-8184

DOI: 10.5937/vojtehg68-26107; https://doi.org/10.5937/vojtehg68-26107

FIELD: Mechanical Engineering, Energetics, Shipbuilding
ARTICLE TYPE: Original Scientific Paper

Abstract:

Introduction/purpose: The purpose of this paper is to present the importance of applying a new diagnostic method with a monitoring system and its capability to reliably determine when and where the problem will occur related to the wear of plain bearings in further operation of the plant, to offer a quality assessment of how the system will continue to function over time, to predict causes of failures and how to eliminate them as well as to provide time for planned maintenance of technical systems.

Method:The new method solves the problem of sliding bearing diagnostics by measuring the dynamic trajectories (orbit) of the sleeve in the sliding bearing. Modern methods of technical diagnostics based on the measurement of dynamic parameters and electrical quantities and their analysis enable the support of measuring systems and measurement sensors from different manufacturers.

Results: Measurements of the dynamic trajectories of sleeves in sliding bearings determine the values characterizing: normal condition, initial clearance size, further clearance increase, bearing clearance sizes, the moment when the state parameters are close to the upper limit of the allowable clearance, and the specific clearance size when further plant exploitation can cause system failure.

Conclusion: The new diagnostic method and monitoring systems can be widely applied in all technical fields: internal combustion engines, hydroelectric power plants, thermal power plants, process plants, and in many other areas. Many monitoring systems, compatibility of devices and equipment of different manufacturers are supported by hardware and software. The calculations of theoretical and experimental dynamic parameters were verified. The method has a wide range of possibilities of application.

Keywords: sliding bearing, bearing clearance, bearing wear, bearing sleeve, dynamic trajectory.

Introduction

The new procedure and measuring systems (hereinafter referred to as monitoring systems) for determining the clearance size, i.e. the degree of wear of sliding bearings, is a new diagnostic method in the technical field. It is is characterized by the following: it allows direct measurement of the movement parameters of the sleeve in the sliding bearing, thus enabling automatic quality control of plants in which sliding bearings are built into. The monitoring system has an almost unlimited lifetime, has no transferable and wear-exposed elements, does not depend on the speed of rotation and overload of a plant, in the case of internal combustion engines, and does not depend on the engine type and stroke. The new method is used as a precautionary measure to prevent possible system crashes. The monitoring system can be built into machinery during production, so there is no limit if it is installed on a plant already in operation. Monitoring systems can be implemented in the on-line version, i.e. as a constant monitoring system or in the off-line version, i.e. as an occasional monitoring system, depending on the plant type and the requirements of the plant user (Černej et al, 1986).

Theoretical settings, dynamics of sliding bearings, and the calculation of dynamic parameters

There is a range of impacts such as defective lubrication, dirty and diluted lubricating oil, incorrect bearing geometry due to manufacturing and assembly errors, or large bearing deformations caused by dynamic forces during plant operation, which causes damage to sliding bearings. High temperatures in sliding bearings are most often due to:

- transient mixed friction with a longer duration, mixed friction in a larger zone along the bearing range or due to mixed friction of higher intensity,
- lack of lubricating oil for a certain period of time or a permanent lack of oil in the sliding bearing.

The causes of mixed friction may be different or a combination of multiple impacts, such as (Ličen & Zuber, 2003):

- mistakes in making liners and sleeves,
- small and large bearing clearances,
- excessive mounting or working deformation of the bearing,
- clogging of oil channels with dirt in the lubrication system,
- small lubricant pump capacity,

- transmission of dynamic forces, and
- filtration and cooling of lubricating oil.

Fatigue of the material in the sliding bearing occurs if the limit of the dynamic endurance of the bearing material exposed to cyclically variable pressures in the oil film is exceeded. Today's limits, with regard to fatigue and bearing wear, are (Černej et al, 1986):

- minimum oil film thickness obtained by calculation - 2 μm,
- maximum pressure in the oil film up to 250 MPa,
- maximum temperature in the oil film up to 140°C, and
- hydrodynamic specific friction force in the bearing up to 0.15 W/mm^2.

The bearing pressure of the bearing lubricating oil is determined by the bearing capacity characteristic and is in the range from 90° to 130° of the bearing circularity. In the rest of the clearance, the lubricating oil pressure is approximately equal to the oil supply pressure in the sliding bearing.

Knowledge of the parameters of the dynamic orbit of the sleeve in the sliding bearing leads to quality indicators about the relative performance of certain drive and design parameters such as: bearing dimension, the size of the clearance in the bearing, speed of rotation, viscosity of lubricating oil, and the like.

The dynamic orbit (trajectory) parameters of the sleeve in the bearing are determined by:

- the minimum thickness of the oil film, which is closely related to the bearing load,
- maximum pressure in the oil film,
- the friction magnitudes in the bearing (energy losses) depending on the bearing temperature regime, and
- the amount of oil flow in the bearing.

In order to theoretically obtain the dynamic trajectory of the sleeve in the sliding bearing, the input data requires a dynamic load force of the bearing and the angle at which it acts. The basis for obtaining the dynamic trajectory is based on the balance of the dynamic force (F) loading the sleeve and the hydrodynamic forces due to the pushing of the sleeve (Fp) and turning the sleeve in the bearing (Fo), (Figure 1), (Žegarac, 1989).

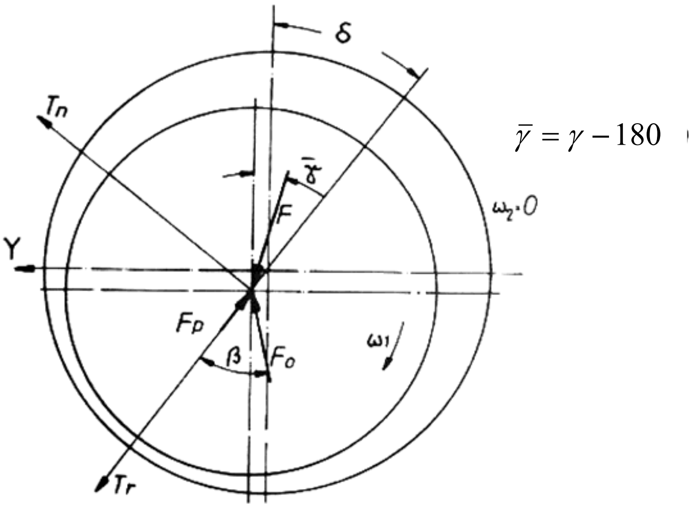

Figure 1 – Schematic presentation of a cylindrical sliding bearing and the equilibrium position of dynamic forces
Рис. 1 – Схематическое изображение цилиндрического подшипника скольжения и положение равновесия динамических сил
Слика 1 – Шематски приказ цилиндричног клизног лежаја и равнотежног положаја динамичких сила

Based on the balance of dynamic forces, the exact position of the sleeve motion in the sliding bearing is obtained at each moment of the plant cycle time.

For realistic operating conditions and different directions of rotation of the sleeve in the bearing in Figure 2, possible positions of the non-stationary loaded bearing (Lang & Steinhilper,1978) are shown.

From equation (1), the value for the dynamic force is obtained:

$$F_p = F\left[\cos(\delta-\gamma) - \frac{sign(\delta-\gamma)\sin(\delta-\gamma)}{tg\beta}\right] sign(\beta - |\delta-\gamma|) \quad (3)$$

From equation (2), the value for the dynamic force is obtained:

$$F_0 = F\frac{sign(\delta-\gamma)\sin(\delta-\gamma)}{\sin\beta} \quad (4)$$

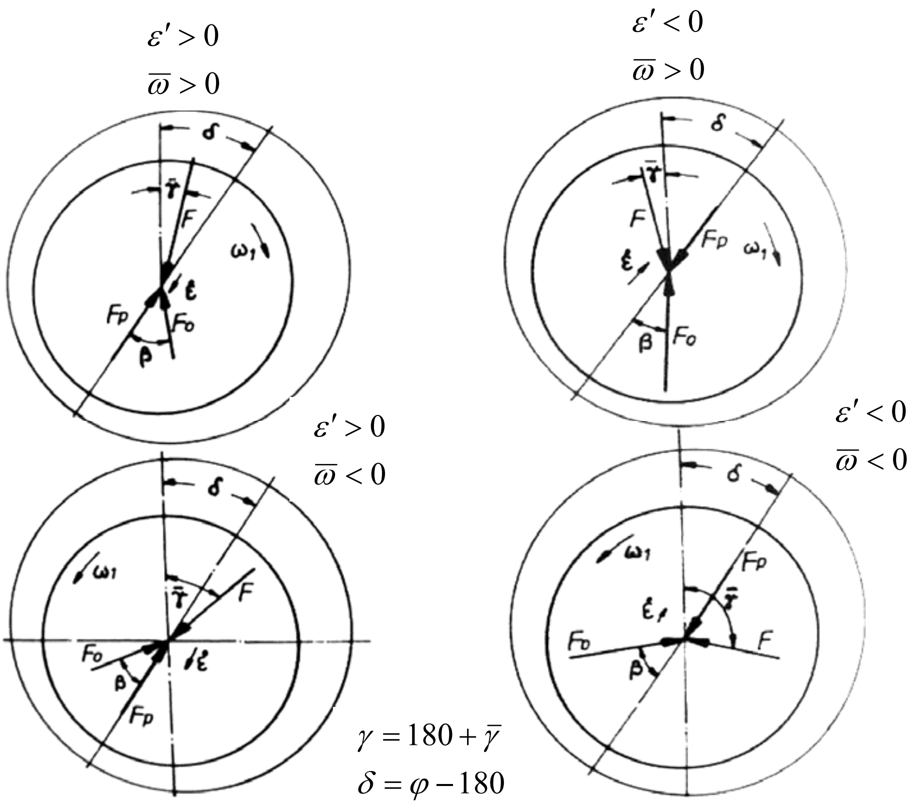

Figure 2 – Possible balance positions of the sleeve of a non-stationary loaded sliding bearing
Рис. 2 – Возможные положения равновесия рукава нестационарно нагруженного подшипника скольжения
Слика 2 – Могући положаји равнотеже рукавца нестационарног оптерећеног клизног лежаја

By introducing known ratios for Sommerfeld's bearing characteristics for components due to the rotation and thrusting of the sleeve, the parameters of the dynamic trajectory of the angular velocity of the sleeve in the bearing are obtained (Lang & Steinhilper,1978):

$$So_0 = \frac{F_0 \psi^2}{BD\eta|\overline{\omega}|} \tag{5}$$

$$So_p = \frac{F_p \psi^2}{BD\eta|\dot{\varepsilon}|} \tag{6}$$

The effective angular velocity of the sleeve $\left|\bar{\omega}\right|$ is given by equation (7):

$$\left|\bar{\omega}\right| = \left|\bar{\omega}^{*} - \omega_{sp}\right| = \left|\omega_1 + \omega_2 - 2\dot{\delta}\right| , \tag{7}$$

where is:
ω_1 - angular velocity of the sleeve,
ω_2 - angular bearing speed (ω_2 = 0, in the case of the non-rotating main sleeve bearing),
$\left|\bar{\omega}^{*}\right|$ - relative angular velocity of the sleeve in the bearing,
$\omega_{sp} = -2\frac{d\delta}{dt}$ - is a hydrodynamic effect in the bearing, stopping the sleeve and causing it to rotate in the opposite direction,
$\left|\dot{\delta}\right|$ - angular velocity of the minimum thickness of the oil film,
ψ - relative bearing clearance calculated according to equation (8):

$$\psi = \frac{R - r}{r} = \frac{Z}{r} , \tag{8}$$

where is:

R - bearing radius,
r - bearing sleeve radius, and
Z - radial bearing clearance.

Finally, the value for $\left|\bar{\omega}\right|$:

$$\left|\bar{\omega}\right| = \left|\bar{\omega}^{*} - 2\dot{\delta}\right| = \frac{sign(\delta - \gamma)F\sin(\delta - \gamma)\psi^2}{BDSo_0\eta\sin\beta} \tag{9}$$

The value for the radial velocity of the sleeve center ($\dot{\varepsilon}$) is obtained from equation (10), (Lang & Steinhilper,1978):

$$\dot{\varepsilon} = \frac{F\psi^2}{BD\,\eta S_{op}}\left[\cos(\delta-\gamma) - \frac{\sin|\delta-\gamma|}{tg\beta}\right] \quad (10)$$

The value for the angular velocity of the minimum thickness of the oil film ($\dot{\delta}$), is obtained from equation (11):

$$\dot{\delta} = \frac{1}{2}\left[\bar{\omega}^{*} - \frac{F\psi^2}{BD\,\eta So_0}\frac{\sin(\delta-\gamma)}{\sin\beta}\right] \quad (11)$$

An internal combustion engine of the type 6ASL-25D, manufactured by Jugoturbina - Karlovac, licensed by Sulzer company, Switzerland, was chosen as an example of modeling and calculating dynamic parameters in order to determine the size of clearance in the sliding bearing.

Determining clearance in sliding bearings of internal combustion engines is very complex. In this case, the main bearings of the engine crankshaft were the subject of investigation.

Figure 3 shows the kinetostatic model of the motor mechanism, on the basis of which the calculation of all dynamic parameters will be performed: the speed of the parts of the motor mechanism, acceleration, the dynamic forces that load the sliding bearing and the calculation of the parameters of the dynamic orbit, on the axis, which will determine the clearance size, i.e. bearing wear. A dynamic calculation was performed in a completely new way. The results of the calculations were obtained by the help of the software developed for this purpose (Žegarac, 1989).

Figure 4 shows the change in the intensity of the dynamic loading force (F) acting on the sleeve of the 1st main bearing, depending on the rotation angle of the crankshaft (α = 0° to 720°), during the engine operating cycles, (Žegarac, 1989).

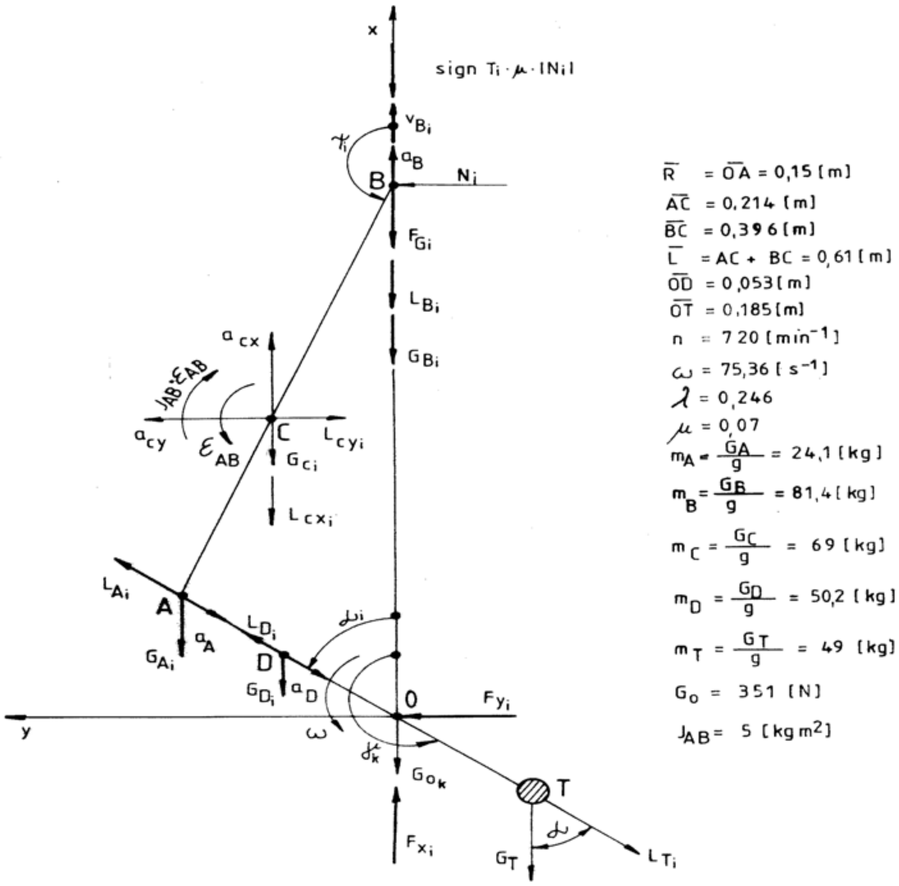

$L_{A_i} = m_A \cdot a_A$ $\quad L_{cx_i} = m_c \cdot a_{cx}$ $\quad L_{T_i} = m_T \cdot R \cdot \omega^2$

$L_{B_i} = m_A \cdot a_A$ $\quad L_{cy_i} = m_c \cdot a_{cx}$ $\quad L_{D_i} = m_D \cdot a_D$

Figure 3 – Kinetostatic model of an internal combustion engine

Рис. 3 – Кинетостатическая модель двигателя внутреннего сгорания

Слика 3 – Кинетостатички модел моторног механизма са унутрашњим сагоревањем

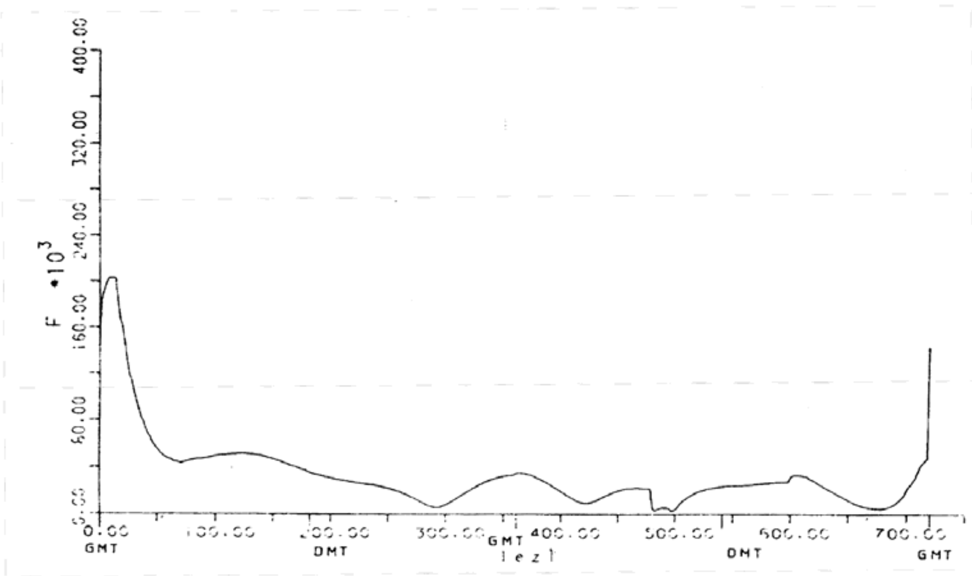

Figure 4 – Changing the intensity of the dynamic force (F) acting on the sleeve of the 1st main bearing depending on the angle of rotation of the crankshaft engine (α=0° to 720°)

Рис. 4 – Изменение интенсивности динамической силы (F), действующей на рукав первого главного подшипника, в зависимости от угла поворота коленчатого вала двигателя (α=0° до 720°),

Слика 4 – Промена интензитета динамичке силе (F) која делује на рукавац првог главног лежаја у зависности од угла заокрета коленастог вратила мотора (α=0° до 720°)

Figure 5 shows the change in the angle (γ) at which the load force (F) acts on the main bearing sleeve depending on the crankshaft rotation angle (α = 0° to 720°):

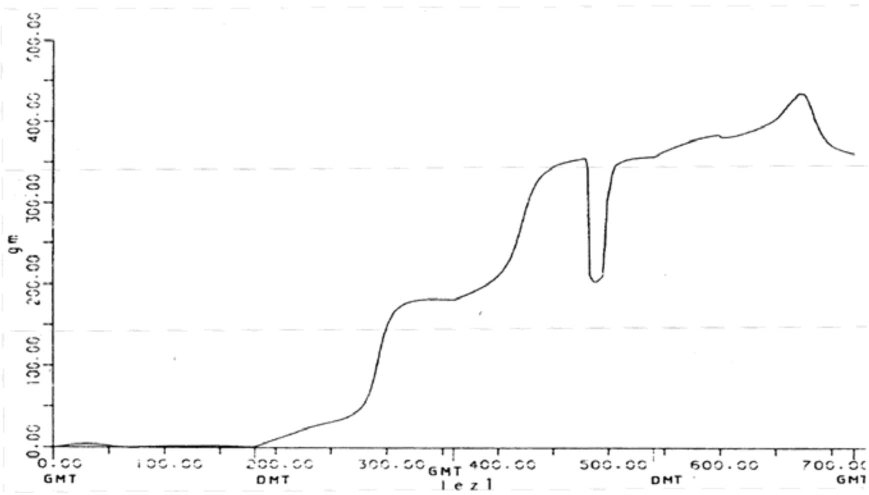

Figure 5 – Changing the angle (γ) at which the force (F) acting on the main bearing sleeve depends on the the crankshaft rotation angle (α=0° to 720°)

Рис. 5 – Изменение угла (γ), под которым сила (F), действующая на рукав главного подшипника, зависит от угла коленчатого вала двигателя (α=0° до 720°)

Слика 5 – Промена угла (γ) под којим сила (F) делује на рукавац главног лежаја у зависности од угла заокрета коленастог вратила мотора (α=0° до 720°)

Figure 6 shows the hydrodynamic forces (Fo) and (Fp) depending on the crankshaft rotation angle (α) on the 1st main bearing of the engine. It presents the sum of the forces (ΣFy), (ΣFx), the influence of the dynamic forces from all engine cylinders on the 1st main bearing of the engine in the horizontal axis (y) and the vertical axis (x).

The radial clearance in the bearing is Z = 124 μm, (Žegarac, 1989):

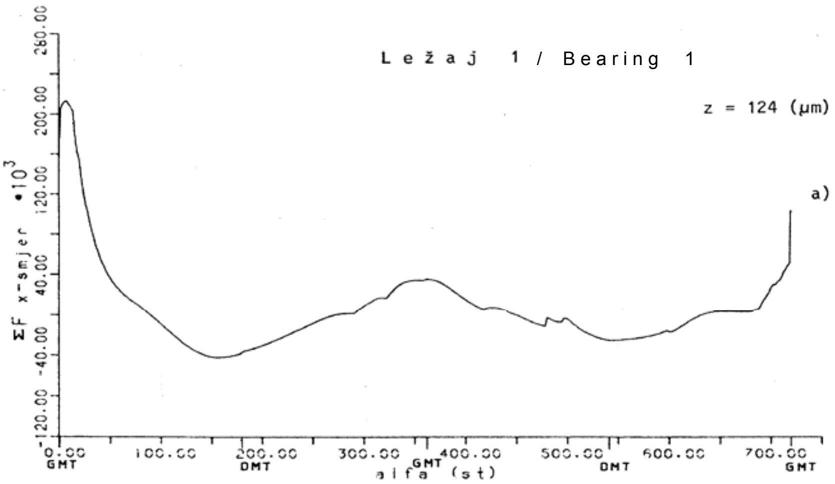

a)

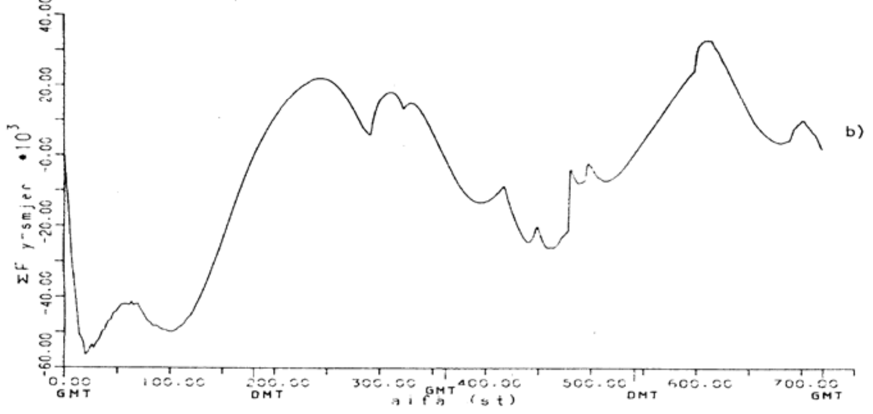

b)

Figure 6 – Changing the intensity of the hydrodynamic forces ΣFx, ΣFy depending on the the crankshaft rotation angle (α = 0° do 720°)
a) vertical axis of the motor, b) horizontal axis of the motor

Рис. 6 – Изменение интенсивности гидродинамических сил ΣFx, ΣFy, в зависимости от угла поворота коленчатого вала (α = 0° do 720°)
а) вертикальная ось двигателя, б) горизонтальная ось двигателя

Слика 6 – Промена интензитета хидродинамичких сила ΣFx и ΣFy у зависности од угла заокрета (α = 0° до 720°) коленастог вратила мотора:
а) вертикална ос мотора, б) хоризонтална ос мотора

Figure 7 shows the calculated dynamic trajectory of the sleeve on the 1st main bearing of the crankshaft, at 100% engine load and an engine speed of n = 720 min^{-1} when the value of the radial clearance is Z = 124μm. In the dynamic trajectory, the crankshaft rotation angle (α = 0° to 720°) is indicated. The angle value (α = 0°) indicates the start of the expansion in the engine, (Žegarac, 1989).

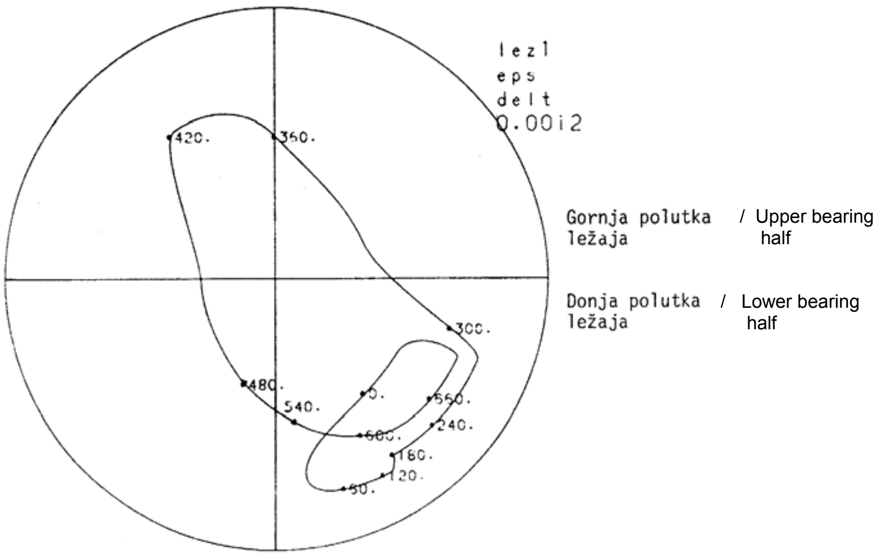

Figure 7 – View of the calculated dynamic trajectory of the main sleeve on the 1st main bearing on the engine crankshaft
Рис. 7 – Изображение измеренной динамической траектории главного рукава в первом главном подшипнике двигателя коленчатого вала
Слика 7 – Приказ прорачунате динамичке путање главног рукавца на првом главном лежају коленастог вратила мотора

Experimental research

The experimental studies were performed on a marine diesel engine type 6ASL-25D, manufactured by Jugoturbina - Karlovac, licensed by Sulzer company, Switzerland, at different engine modes and engine speeds up to a maximum speed of n = 720 min^{-1}. All the preparations for the measurement were made, the operating parameters of the engine were adjusted, the monitoring system was installed and the measurement system calibrated (Easy-Laser, 2020), (Žegarac,1993).

If the plant is in operation and there is a need to install a new monitoring system, the installation and centering of contactless encoders to measure the center displacement of the sleeve center can be performed with a laser centering system of the sleeve center relative to the bearing center (Žegarac, 2016), (Ličen & Zuber, 2003).

Dynamic trajectories were measured in the unladen mode, up to a maximum speed of $n = 720\ min^{-1}$.

Dynamic trajectories at partial engine loads were also measured, up to a maximum engine speed of $n = 720\ min^{-1}$.

Figure 7 shows the measured dynamic trajectories of the main sleeve on the 1st main bearing of the crankshaft engine at 100% engine load and a speed of $n = 720\ min^{-1}$.

The size of the radial clearance in the sliding bearing is $Z = 124\mu m$.

The figure also shows the size (e) that represents the displacement of the sleeve center relative to the bearing center, i.e. the eccentricity of the sleeve center, which is directly related to the bearing clearance (Z).

In order to compare the calculated and measured sizes of the bearing clearance, the term of so-called relative eccentricity (ε) was introduced and determined by the equation:

$$\varepsilon = \frac{e}{Z} \tag{12}$$

Figure 8 shows the angle (δ) of the minimum thickness of the oil film.

On the basis of the measured values (e) and (δ), the clearance in the sliding bearing and the assessment of further plant exploitation are determined in order not to cause a plant failure.

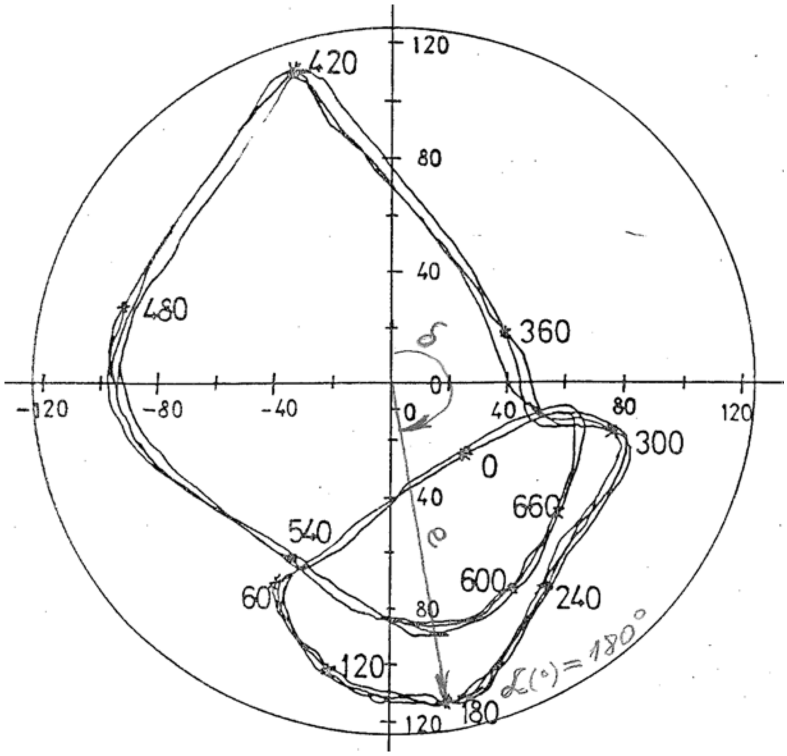

Figure 8 – Display of the measured dynamic sleeve trajectory on the 1st main bearing of the crankshaft, at the engine load of 100%, n = 720 min^{-1}, and the bearing clearance Z=124 (μm)

Рис. 8 – Изображение измеренной динамической траектории рукава в первом главном подшипнике двигателя коленчатого вала, при нагрузке на двигатель (100%), n = 720 мин$^{-1}$, зазор подшипника Z = 124 (μm)

Слика 8 – Приказ измерене динамичке путање рукавца на првом главном лежају мотора коленастог вратила мотора при оптерећењу мотора (100%), n = 720 min^{-1}, зазор лежаја Z=124 (μm)

Figure 9 displays the measured dynamic trajectory of the sleeve on the 1st main bearing of the crankshaft engine at the load of 0%,n = 720 min^{-1}, and the bearing clearance Z = 124(μm):

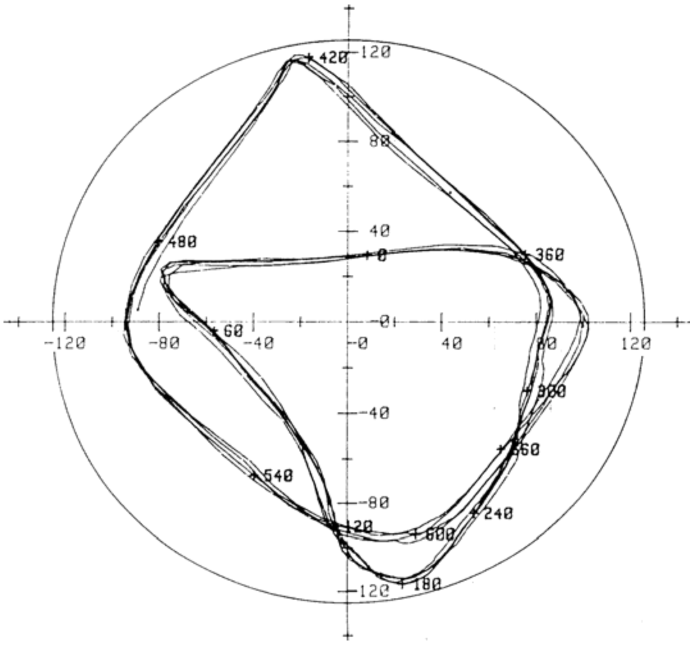

Figure 9 – Display of the measured dynamic trajectory of the sleeve on the 1st main bearing of the crankshaft , at the engine load of 0%, n = 720 min^{-1}, and the bearing clearance Z = 124 (μm)
Рис. 9 – Изображение измеренной динамической траектории рукава в первом главном подшипнике двигателя коленчатого вала, при нагрузке на двигатель (0%), n = 720мин$^{-1}$, зазор подшипника Z = 124 (μм)

Отображение измеренной динамической траектории втулки на 1-м главном подшипнике коленчатого вала при нагрузке двигателя 0%, n = 720 мин-1 и зазоре подшипника Z = 124 (μm)
Слика 9 – Приказ измерене динамичке путање рукавца на првом главном лежају мотора коленастог вратила мотора, при оптерећењу мотора (0 %), n=720min^{-1}, зазор лежаја Z=124 (μm)

Based on the results of measuring the displacement of the center of the sleeve (e) for this engine type, the dependence (Z) of (e) was determined (Žegarac, 1989):

$$Z = 1.01 \cdot e + 7{,}48 \pm 4 \quad (13)$$

The results are presented in Figure 10.

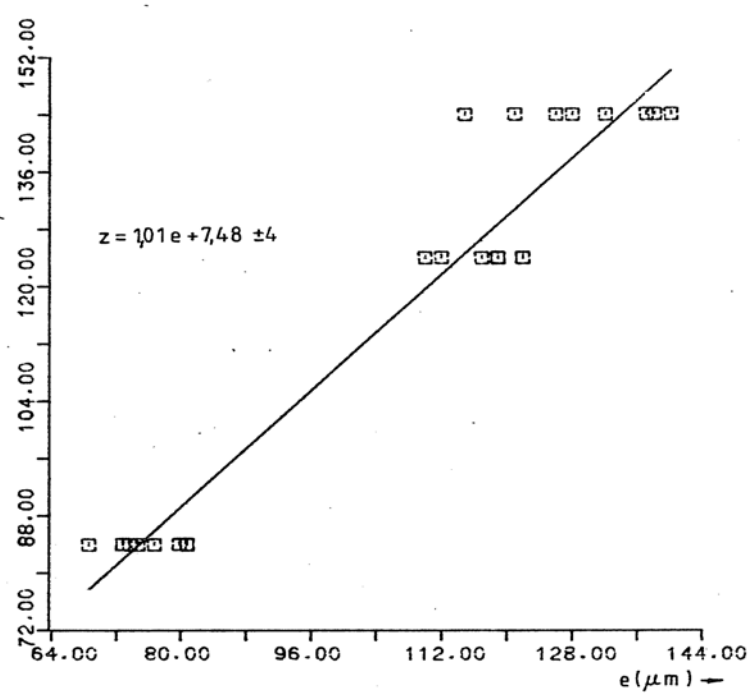

Figure 10 – Graphic depiction of the clearance size (Z) and the displacement of the center of the sleeve (e) for different rotation speeds and engine loads

Рис. 10 – Графическое изображение размера зазора (Z) и смещения центра рукава (е) для разных скоростей вращения и нагрузок на двигатель

Слика 10 – Графички приказ зависности величине зазора (Z) и помака средишта рукавца (е), за различите бризине вртње и оптерећења мотора

Comparison of the theoretical calculation results and the experimental research results

Figure 11 gives a graphic representation of the calculated and measured values of the sleeve eccentricity (e) depending on the angle of rotation of the crankshaft (α) for various bearing wear degrees, at a rotation speed of n = 720 min^{-1} and at 100% engine load, (Žegarac, 1993):

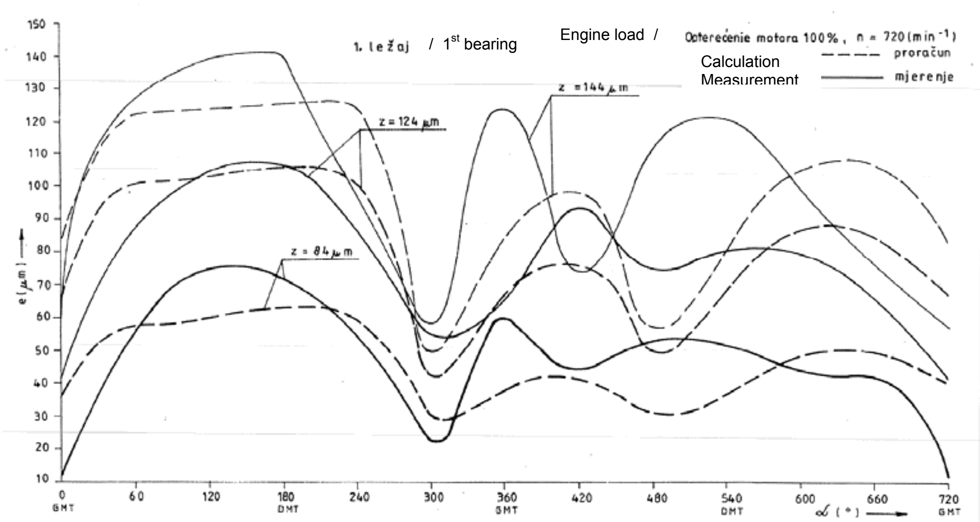

Figure 11 – Display of the calculated and measured eccentricities of the sleeve (e) on the 1st main bearing depending on the crankshaft rotation angle (α) for different sizes of bearing clearance Z=84 (μm), Z=124(μm), Z=144 (μm), engine speed n = 720 min^{-1} and 100% engine load

Рис. 11 – Изображение рассчитанных и измеренных эксцентриситетов рукава (e) первого главного подшипника, в зависимости от угла поворота коленчатого вала (α) при разных размерах зазора подшипника Z = 84 (μm), Z = 124(μm), Z = 144 (μm), частота вращения двигателя n = 720 мин$^{-1}$ и нагрузка на двигатель 100%

Слика 11 – Приказ прорачунатих и измерених ексцентричности рукавца (e) на првом главном лежају у зависности од угла заокрета коленастог вратила мотора (α) за различите величине зазора у лежају: Z=84 (μm), Z=124(μm), Z=144 (μm), брзини вртње мотора n =720 min^{-1} и оптерећењу мотора 100%

In Figure 12, there is a graphic representation of the measured values of the sleeve eccentricity (e) depending on the angle of rotation of the crankshaft (α) for various bearing wear degrees Z=84 (μm), Z=124 (μm), Z=144 (μm), at different speeds of rotation, without loading the engine.

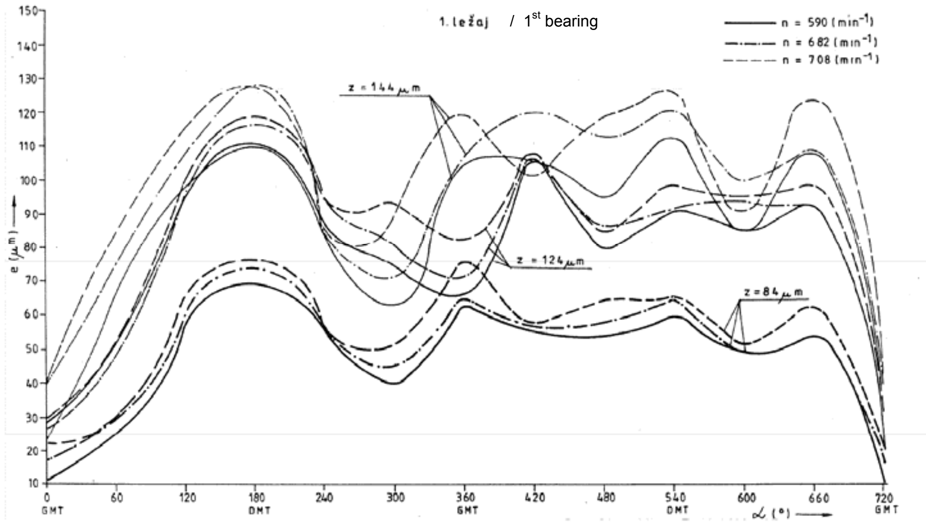

Figure 12 – Display of the measured eccentricities of the sleeve (e) on the 1st main bearing, depending on the crankshaft rotation angle (α) for different sizes of the clearance in the bearing Z=84(μm), Z=124 (μm), Z=144 (μm) and speed, no engine load

Рис. 12 – Изображение измеренных эксцентриситетов рукава (е) первого главного подшипника в зависимости от угла поворота коленчатого вала (α) при разных величинах зазора в подшипнике Z = 84 (μm), Z = 124 (μm), Z = 144 (μm) и скорость, без нагрузки на двигатель

Слика 12 – Приказ измерених ексцентричности рукавца (е) на првом главном лежају, у зависности од угла заокрета коленастог вратила (α), за различите величине зазора у лежају: Z=84(μm), Z=124 (μm), Z=144 (μm) и брзинама вртње, без оптерећења мотора

Figure 13 gives a graphic representation of the calculated and measured values of the eccentricity angle of the bearing hose (δ) depending on the angle of rotation of the crankshaft of the engine (α) for various bearing wear degrees, at 100% engine load and the engine speed of n = 720 min^{-1} (Žegarac, 1993):

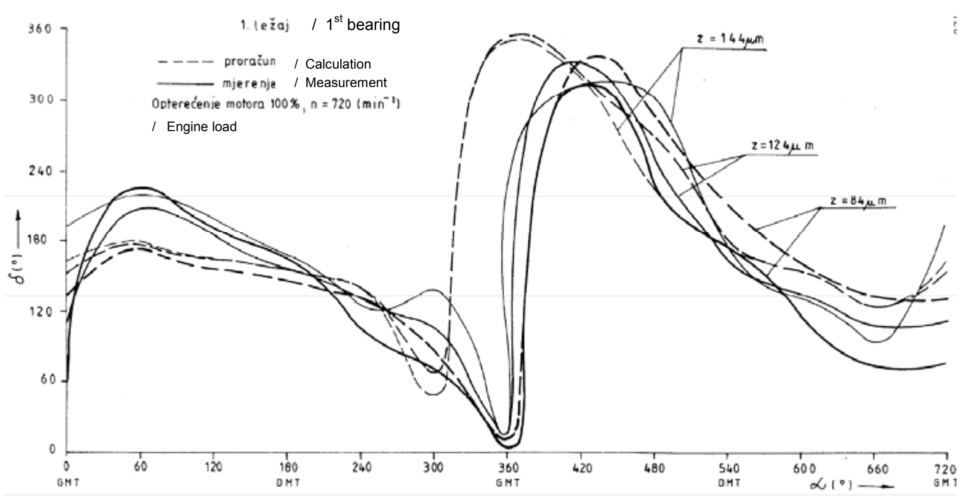

Figure 13 – Display of the calculated and measured values of the angle of eccentricity of the bearing hose (δ) depending on the crankshaft rotation angle (α) for various bearing wear degrees, 100% engine load, speed of rotation engine n = 720 min^{-1}

Рис. 13 – Изображение расчетных и измеренных значений угла эксцентриситета рукава подшипника (δ) в зависимости от угла поворота коленчатого вала двигателя (α) при различном износе подшипника, при 100% нагрузке на двигатель, скорости вращения двигателя n = 720 мин$^{-1}$

Слика 13 – Приказ прорачунатих и измерених вредности угла ексцентричности руквца лежаја (δ) у зависности од угла заокрета коленастог вратила мотора (α) за разна истрошења лежаја, при 100% оптрећењу мотора, брзини вртње мотора n=720 min^{-1}

Based on the comparison of the calculated dynamic sizes and the measurement results, it can be concluded that the correspondence of the results of the calculations and measurements is in the domain of 5%, which is completely acceptable. The repeatability of the measurement values during the measurement was obtained.

The method of calculation and measurement of the functional parameters of the new diagnostic method has been completely verified.

Diagnostics of sliding bearings can be carried out for all modes, rotation speeds and plant loads.

The author of this scientific paper has spent many years of research on many projects related to technical diagnostics of machine and electrical plants, development, research, design and implementation of monitoring systems (Žegarac, 1994), (Žegarac, 2019).

Conclusion

The application of the new diagnostic method and the monitoring system gives an opportunity to reliably determine when and where the problem will arise related to the wear of sliding bearings in further plant operation, to offer a quality assessment of how the system will continue to function over time, as well as to predict the causes of failures and how to remedy them, and to provide time for routine maintenance of technical systems. Modern methods of technical diagnostics based on the measurement of dynamic parameters and electrical sizes and their analysis allow the support of measuring systems and measurement sensors from different manufacturers. The capabilities of a very advanced program configuration for system diagnostics and monitoring are presented. The values of the functional parameters were measured and software processed as well as their limit values and alarms displayed in different ways.

There are options for remote control and monitoring, shutting off particular parts from further exploitation to prevent damage to various plants where vital machine elements are installed. High accuracy and reliability of measurements of all relevant measuring sizes are ensured, on the basis of which the technical correctness of the plant can be qualitatively determined. Multi-channel, modular, software-hardware monitoring, control and protection systems allow the optimization of plant operating parameters. The new diagnostic method and monitoring systems can be widely applied in all technical fields: internal combustion engines, hydropower plants, thermal power plants, process plants, and in many other areas. Many systems for monitoring, compatibility of devices and equipment from various manufacturers are supported by hardware and software. Mechanical and electrical sizes measured on different types of plants are very important for further operations of drive systems. In this paper, a special attention is given to the diagnostics of sliding bearings.

The new method of diagnostics of sliding bearings, by measuring the dynamic trajectory of the sleeves in the bearing, does not depend on the plant type, and can be applied to all types of internal combustion engines and various other plants. The author of this very important project proposes that this new method and its accompanying monitoring systems be installed in drive systems. In the past, many important systems did not have similar monitoring systems in place, and many problems arose. For system installations used since the 1950s, simpler systems for monitoring basic functions were designed, which was not enough, especially in recent times, as the development of new techniques has progressed.

New plant monitoring systems have alarm functions. The alarm can be visual or accoustic or in the form of SMS notifications. The field of technical diagnostics is a very interesting field for many scientists (Braut et al, 2008), (Ličen & Zuber, 2003). This area is under-researched, as is the area of medical diagnostics.

References

Braut, S., Žigulić, R., & Butković, M. 2008. Numerical and experimantal analysis of a shaft bow influence on a rotor to stator contact dynamics. *Strojniški vestnik-Journal of Mechanical Engineering,* 54(10), pp.693-706 [online]. Available at: https://www.sv-jme.eu/article/numerical-and-experimantal-analysis-of-a-shaft-bow-influence-on-a-rotor-to-stator-contact-dynamics/ [Accessed: 7 April 2020].

Černej, A., & et al. 1986. Radni uslovi podmazivanja ležaja dizel motora. *Goriva i maziva*, 26(5-6), pp.229-236 (in Serbian).

-Easy-Laser. 2020. *Laser measurement & alignment systems. Technical documentation.* Damalini, Sweden: Easy-Laser.

Lang, O.R, & Steinhilper, W. 1978. *Gleitlager*. Berlin, Heidelberg: Springer-Verlag. Available at: https://doi.org/10.1007/978-3-642-81225-5.

Ličen, H., & Zuber, N. 2003. Vibrodiagnostics as an element for quality and reliabilty assurance: SPIDER 8 – universal measuring device, concept and application. In: *Quality 2003: 3rd Research/expert conference with international participation,* Zenica, Bosnia and Herzegovina, pp.299-306. November 13-14 [online]. Available at: http://www.quality.unze.ba/zbornici/QUALITY%202003/045-R-037.pdf (in Serbian) [Accessed: 7 April 2020].

Žegarac, N. 1989. *Dijagnostika kliznih ležajeva u dizel motoru* (in Serbian). Ph.D. thesis. Zagreb: University of Zagreb, Faculty of Mechanical Engineering and Naval Architecture.

Žegarac, N. 1993. *Postupak dijagnostike ležajeva merenjem dinamičkih putanja glavnih rukavaca, kolenastog vratila.* Serbian Patent number P-640/93.

Žegarac, N. 1994. Analysis of the wear of vital parts of turbocharged engines of high specific power. *Scientific Technical Review*, 44(6), pp.14-24.

Žegarac, N. 2016. Experience in the development of the invention from the aspect of scientific verification and market creation. *Vojnotehnički glasnik/Military Technical Courier*, 64(1), pp.92-109 Available at: https://doi.org/10.5937/vojtehg64-9315 (in Serbian).

Žegarac, N. 2019. The Application of Modern Diagnostic Systems on Machine and Electric Power Plants. *Tehnika*, 74(1), pp.73-87. Available at: https://doi.org/10.5937/tehnika1901073Z.

РАЗРАБОТКА МЕТОДА ОПРЕДЕЛЕНИЯ ВЕЛИЧИН ЗАЗОРОВ В ПОДШИПНИКАХ СКОЛЬЖЕНИЯ

Никола П. Жегарац

Сербская академия изобретателей и ученых,
г. Белград, Республика Сербия

РУБРИКА ГРНТИ: 55.00.00 МАШИНОСТРОЕНИЕ; 55.45.00 Судостроение, 44.00.00 ЭНЕРГЕТИКА
ВИД СТАТЬИ: оригинальная научная статья

Резюме:

Введение/цель: Цель данной статьи заключается в представлении важности применения нового метода диагностики и системы мониторинга, возможности надежного определения времени и точного места возникновения проблемы, связанной с износом подшипников скольжения при дальнейшей эксплуатации установки, а также качественного прогноза при продолжении работы системы с течением времени, предусмотрение причин отказа и способов их устранения, а также планировки регулярного технического обслуживания системы.

Метод: Новый метод решает проблему диагностики подшипников скольжения путем измерения траекторий перемещения (орбита) вала в подшипнике скольжения. Современные методы технической диагностики, основанные на измерении динамических параметров и электрических величин и их анализе позволяют поддерживать измерительные системы и датчики от различных производителей.

Результаты: Измеряя траектории передвижения (орбиты) валов в подшипниках скольжения, определяется значения, которые характеризуют: нормальное состояние, начальную величину зазора, его дальнейшее увеличение, величину зазора подшипника, когда параметры приближаются предельно допустимой величине зазора и определяется величина зазора, в случае если дальнейшая эксплуатация установки может привести к отказу системы.

Вывод: Новый метод диагностики и системы мониторинга может иметь широкое применение во всех технических областях, таких как: двигатели внутреннего сгорания, гидроэлектростанции, тепловые электростанции, технологические установки и пр. Аппаратное и программное обеспечение поддерживает множество систем мониторинга, контроля совместимости устройств и оборудования от разных производителей. Проведена верификация расчета *теоретических и экспериментальных динамических параметров. Метод имеет широкий спектр применения.*

Ключевые слова: подшипник скольжения, зазор подшипника, износ подшипника, вал подшипника, траектория перемещения.

РАЗВОЈ МЕТОДЕ ЗА УТВРЂИВАЊЕ ВЕЛИЧИНЕ ЗАЗОРА У КЛИЗНИМ ЛЕЖАЈЕВИМА

Никола П. Жегарац
Српска академија изумитеља и научника, Београд, Република Србија

ОБЛАСТ: машинство, енергетика, бродоградња
ВРСТА ЧЛАНКА: оригинални научни рад

Сажетак:

Увод/циљ: У раду је представљена примена нове дијагностичке методе и мониторинг система. Приказана је могућност да се поуздано утврди када и где ће се појавити проблем који се јавља при трошењу клизних лежајева у даљој експлоатацији постројења. Поред тога, оцењује се како ће систем наставити да функционише током времена, предвиђају се узроци кварова и начин њиховог отклањања, као и време за планско одржавање техничких система.

Метода: Нова метода решава проблем дијагностике клизних лежајева мерењем динамичких путања рукавца у клизном лежају. Савремене методе техничке дијагностике, засноване на мерењу динамичких параметара и електричних величина и њихове анализе, омогућавају подршку мерних система и сензора за мерење разних произвођача.

Резултати: Мерењем динамичких путања (трајекторије) рукаваца у клизним лежајима утврђују се величине које карактеришу: нормално стање, почетну величину зазора, његово даље повећавање, величине зазора лежаја, када су параметри стања близу горње границе дозвољеног зазора, и утврђивање величине зазора када даља експлоатација постројења може проузроковати хаварију система.

Закључак: Нова дијагностичка метода и мониторниг система могу се широко применити у свим техничким областима: моторима са унутрашњим сагоревањем, хидроелектранама, термоелектранама, процесним постројењима и многим другим областима. Хардверски и софтверски подржавају се многи системи за надгледање и проверава компатибилност уређаја и опреме разних произвођача. Извршена је верификација прорачуна *теоријских и експерименталних динамичких параметара. Метода има широке могућности примене.*

Кључне речи: клизни лежај, зазор лежаја, истрошење лежаја, рукавац лежаја, динамичка путања.

Paper received on / Дата получения работы / Датум пријема чланка: 12.04.2020.
Manuscript corrections submitted on / Дата получения исправленной версии работы / Датум достављања исправки рукописа: 18.05.2020.
Paper accepted for publishing on / Дата окончательного согласования работы / Датум коначног прихватања чланка за објављивање: 20.05.2020.

ELECTRICALLY CONDUCTIVE FIBERS IN CLUSTER BOMBLETS WHICH TARGETED THE ELECTRIC POWER SYSTEM OF FR YUGOSLAVIA IN 1999

Mirjana N. Anđelković-Lukić[a], *Mirjana* D. Stojanović[b]

[a] Military Technical Institute, Belgrade, Republic of Serbia;
Government of the Republic of Serbia, Interagency Coordination Body, Belgrade, Republic of Serbia,
e-mail: mirjana.andjelkovic.lukic45@gmail.com, **corresponding author**,
ORCIDiD: https://orcid.org/0000-0002-5076-4901

[b] Institute for Technology of Nuclear and Other Mineral Raw Materials, Belgrade, Republic of Serbia,
e-mail: mira1412@gmail.com,
ORCIDiD: https://orcid.org/0000-0003-4509-391X

DOI: 10.5937/vojtehg68-27231; https://doi.org/10.5937/vojtehg68-27231

FIELD: Chemical technology
ARTICLE TYPE: Original scientific paper

Abstract:

Introduction/purpose: The paper presents the mode of operation of the CBU-102(V) 2/B cluster bomb, weighing about 340 kg and containing bomblets with electrically conductive fibers for disabling power plants.

Methods: Physical and chemical analyses of the fibers were performed. The following test methods were used for fiber characterization: a binocular microscope for determining fiber thickness and a qualitative XRF analysis performed on an XRF-MiniPal spectrometer, PANalytical. The XRFanalysis aimed at qualitative detection of the present elements, which was confirmed by a quantitative chemical analysis.

Results: The semi-quantitative XRF analysis determined the content of gallium (0.007%), the peak of which was detected on the spectrum. Gallium nitride is a material that can be used as a semiconductor. The chemical analysis was performed on an atomic absorption spectrophotometer Analyst 300, Perkin Elmer.

Conclusion: The instrument for differential thermal analysis and thermogravimetry (DTA/TG), NETZCH STA 409 EP (operational range from 20°C to 1000°C), confirmed that the sample was of 50% silicate origin, non-toxic and with heavy metal content in traces. The rest of the *sample is aluminum whose presence in soil can cause decline in soil fertility thus leading to decline in crop yields.*

Keywords: chemical warfare, cluster bomb, electrically conductive fibers, energy system, chemical analysis, thermochemical analysis, silicate, aluminum, environmental impact, soil, declined fertility, reduced yield.

Introduction

The attack on FR Yugoslavia began with a combined action of tomahawk cruise missiles (BGM-109 TLM) and AGM-86-ALCM launched from V-52N strategic bombers, which took off from RAF Fairford base (Great Britain) and from the southern Adriatic sea from submarines and ships of the Sixth fleet, USA Navy. A total of 78 projectiles were launched in the first raid. At the same time, about 300 planes took off from the aircraft carriers from the Sixth fleet and bases in Italy, Germany and Turkey, 100-200 out of which were fighters, armed with the most modern guided munitions (air bombs and air-to-ground and air-to-air missiles). They deployed air attacks with the aim of destroying and neutralizing vital facilities of the Yugoslav Army, and especially the Air Force (RV) and the Air Defense (PVO), with a quick operation. After the war, the Pentagon publicly stated that the focus of the operation was the destruction and neutralization of the air defense system of FR Yugoslavia (Anđelković-Lukić, 2015, p.36).

Military doctrines in the world's largest countries hold the view that war conflicts, such as those in Iraq, Bosnia and Herzegovina, Chechnya and Yugoslavia, can be successfully resolved by selective attacks on vital enemy targets using high-precision weapons from a distance. Such aggressions are carried out by mass attacks with cruise missiles and aviation on airports, positions of missile units and air defense radars, command posts, telecommunication systems, but also on the country's economic infrastructure in order to immediately overcome resistance and endanger the existence of the population. For this purpose, CBU-102/B cluster bombs with BLU-114/B bomblets were deployed against electric power facilities. At the same time, cluster bombs with high-explosive bomblets were used against civilian targets such as residential buildings, hospitals, schools, etc. (reference) All missiles dropped on FR Yugoslavia during the bombing, in terms of their effect and purpose, can be classified into three general groups:

- high-explosive (HE), guided and unguided, of various calibers, (missiles, air bombs and cluster bombs),

- anti-tank, armour-piercing, filled with depleted uranium, and
- non-lethal, which do not have the effect of an explosion at the target, but cause serious damage, so-called "soft bombs" or "blackout bombs".

The paper will present the properties and action of bombs for incapacitation of electric power facilities and the physico-chemical analysis of electrically conductive fibers contained in cluster bomblets within cluster bombs and containers. (Anđelković-Lukić, 2015, p.36).

Electrically conductive fibers are intended to create blackouts, to disable the power grid of a state, leaving it without electricity. This includes hospitals, industrial plants, schools, colleges, etc.

They were first used over Iraq, but their chemical structure was that of graphite fibers, an allotropic modification of carbon, which is also highly conductive. Therefore, all such bombs containing electrically conductive fibers are popularly called graphite bombs, and, despite the difference in their composition, they all work in the same way: they disrupt the electricity supply in the attacked country. (Jeler & Roman, 2016, pp.13-18)

The fibers dropped on FR Yugoslavia were the product of highly sophisticated technology, a product of the fourth generation, and they work by causing short circuits on transmission lines.

Cluster bombs with electrically conductive fibers targeting the electrical grid of FR Yugoslavia

Depending on the model, cluster bombs (CBUs - Cluster Bomb Units) consist of the body of the SUU-65/B or SUU-66/B (Stores Release and Suspension Unit) air bomb loaded with 202 BLU-114/B bomblets. The CBU-102/B cluster bomb weighs about 340 kg and bomblets, 1 kg each, are filled with spools of conductive filaments. It was developed for the US Air Force to be dropped from the altitudes of 600m - 6000m at a speed of 460 up to 1.200 km/h. It is released from aircraft and covers an elliptical surface measuring approximately 150×360 m. This bomb was developed in 1994, and became operational in the US Armed Forces in the late 1990s. (Anđelković-Lukić, 2015, pp.57-58)

Bombs with electro-conductive fibers (which contains BLU-114/B bomblets, produced in the USA) were used in the NATO aggression on FR Yugoslavia (1999), when more than 70% of the electricity in the national power grid was disabled.

In less than 24 hours, experts from Serbia managed to restore the operability of the electrical system, so that the used bombs with electrically conductive fibers did not give the expected results. (Jeler & Roman, 2016, pp.15)

In the territory of FR Yugoslavia (Republic of Serbia), the power transmission system in 1999 consisted of:

1) Overhead lines (transmission lines) a total of 449 in the length of 9,408 km, by voltage levels:

- 400 kV - 37, in the length of 1,626 km;
- 220 kV - 48, in the length of 1,917 km;
- 110 kV - 358, in the length of 5,804 km;
- 35 kV - 6, in the length of 141 km;

2) Underground lines (cables) of voltage level 110 kV, 2 in total, in the length of 6.1 km;

3) Transformer stations (TS) a total of 30, total installed capacity 15.396 MVA, by voltage levels:

- 400/H kV/kV - 14, total installed capacity 9,750 MVA;
- 220/H kV/kV - 13, total installed capacity 5,343 MVA;
- 110/H kV/kV - 3, total installed capacity 303.5 MVA and

4) Distribution plants (DP) a total of 8, by voltage levels, as follows:
- 400 kV - 4;
- 220 kV -1,
- 110 kV - 4. (Energy Agency of the Republic of Serbia, 2017, p.8)

Cluster bombs targeted overhead lines, transformer stations and switchyards.

The electric power system of the FR of Yugoslavia was targeted with cluster air bombs with BLU-114/B bomblets from the beginning to the end of May 1999:

- May 2, 1999, at 9.45 pm, the substations TS 400/200 kV "Obrenovac", TS 220/35 kV "Bajina Bašta", TS 2400/220/110kV "Niš", TS 400/220/110kV "Novi Sad" and distribution plant RP 400kV "Drmno".

- May 7, 1999, at 9.21 pm, the substations TS 400/220 kV "Belgrade 8", TS 220/110 kV "Belgrade 5", TS 400/220 kV "Obrenovac" and TS 220/110 "Belgrade 3".

- May 13, at 10.40 pm, distribution plants RP 400 kV "Drmno" and RP 10/35 kV TPP "Kolubara" and the substations TS 400/220/110 kV "Niš 2", TS 400 and 110 kV "Novi Sad 3".
- May 22, at 2.18 p.m, the substations TS 400/220 kV "Drmno", TS 400/220 kV "Belgrade 8", TS 400/220/110 kV "Niš 2", TS 220/35 kV "Bajina Bašta" and the plant 110 kV TPP "Kostolac A". (Dveri srpske, pp.68-69)

Due to a small mass of fibers, winds occasionally carried conductive fibers from uncleaned parts of facilities and their surrounding areas, which then fell on the already cleaned parts of the electrical system and short circuits and power outages occurred repeatedly.

Engineers from the Military Technical Institute with colleagues from the Faculty of Technology and Metallurgy in Belgrade successfully solved the lifting of conductive fibers from the ground, using a certain procedure, by which thin threads were glued to the ground and there was no possibility for their re-lifting.

Their lifting into the air and causing short circuits again was thus prevented. When the enemy realized that Serbian electric power grid workers were successfully repairing the damage from conductive fibers and that there was practically no damage to the electric power system, they started firing HE bombs at transformer stations. This resulted in subsequent soil contamination, because transformer oil leaked from the hit transformer stations and went into the water and into the soil (Anđelković-Lukić, 2015, p.104).

How the CBU-102/B cluster bomb works

The CBU-102/B cluster bomb has a timer fuze with an altimeter which at a given height from the ground activates a detonation blade that cuts off the front and the rear of the bomb with the stabilizer, and the container is cut along its length to three parts at an angle of 120º (Figure 1) thus releasing cluster bomblets under the action of air current and centrifugal force. Spools are made of silicon fiber covered with a molecular layer of aluminum probably applied by a special process, evaporation under vacuum, or by a nanotechnological process. (Anđelković-Lukić, 2015, p.55)

Figure 1 – Parts of an activated CBU-102/B cluster bomb (in Figures 1 and 2, inactivated BLU-114/B bomblets are marked with the arrows) (Serbian Armed Forces, 1999)
Рис. 1 – Части активированной кассетной бомбы CBU-102/B (на рисунках 1 и 2 стрелками отмечены неактивированные бомбы BLU-114/B) (Serbian Armed Forces, 1999)
Слика 1 – Делови активиране касетне бомбе CBU-102/B (на сликама 1 и 2 стрелицама су обележене неактивиране бомбице BLU-114/B) (Serbian Armed Forces, 1999)

Figure 2 – Content of the BLU-114/B cluster bomblet (Serbian Armed Forces, 1999)
Рис. 2 – Содержание кассетной бомбы BLU-114/B (Serbian Armed Forces, 1999)
Слика 2 – Садржај касетне бомбице BLU-114/B (Serbian Armed Forces, 1999)

Table 1 shows the technical characteristics of the CBU-102/B cluster bomb, and Figure 3 shows the arrangement of spools in the cluster bomblet shell, top view.

Table 1 – Technical characteristics of the CBU-102/B cluster air bomb
Таблица 1 – Технические характеристики кассетной авиационой бомбы CBU-102/B
Табела 1 – Техничке карактеристике касетне авио-бомбе CBU-102/B

Purpose and the name	CBU-102/B cluster air bomb for disabling electric power facilities
Total weight	340 kg
Charge	BLU-114/B bomblets (202 pieces, individual weight of about 1 kg)
Dimensions of the BLU-114/B bomblet	Length 16.7 cm, diameter 6.7 cm
Number of spools	147 pieces
Weight of a spool	2 g
Length of a filament in a spool	150 m
Material	Glass fibers with aluminum coating
Manufacturer	USA

CBU-102/B cluster bombs are carried by F-117 aircraft and manufactured in the USA (Jeler & Roman, 2016, pp.13-18).

Figure 3 – Arrangement of spools in the bomblet, top view (Serbian Armed Forces, 1999)
Рис. 3 – Расположение катушек в бомбе малого калибра, вид сверху (Serbian Armed Forces, 1999)
Слика 3 – Распоред калемова у бомбици, изглед са горње стране (Serbian Armed Forces, 1999)

Figure 4 shows an open bomblet and a mechanism for opening the shell.

Figure 4 – Parts of an open cluster bomblet with spools and an ejection mechanism (Serbian Armed Forces, 1999)
Рис. 4 – Части открытой кассеты с катушками и механизмом выбрасывания (Serbian Armed Forces, 1999)
Слика 4 – Делови отворене касетне бомбице са калемовима и избацним механизмом (Serbian Armed Forces, 1999)

After being dispersed from bomblets, spools unwind and conductive filaments fall on high-voltage lines of the power system and form electrically conductive lines which cause short circuits and electrical discharges. Unwound filaments have a length of about 150 m, and while they fall, they unwind into a number of thinner ones creating a net at the point of impact, covering large areas. Such a net has higher strength than individual filaments. Figure 5 shows unwound electrically conductive filaments on transmission lines.

A short circuit is accompanied by filament evaporation, ionization of the air and the formation of an intensive current flow between the wires of the transmission line, i.e. the appearance of electric arcs, with accompanying manifestations: temperatures above 4000°C and strong flashes of whitish light. Not only does the power system break down, but also high temperatures can cause fires and explosions. (Anđelković-Lukić, 2015, p.58).

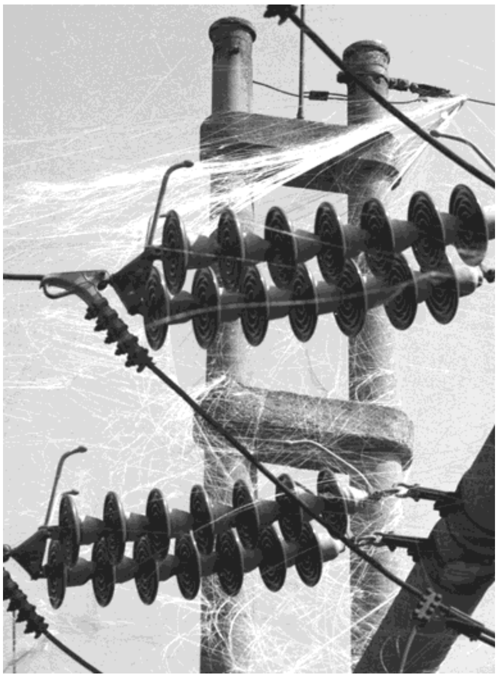

Figure 5 – Electrically conductive filaments on power transmission lines (Serbian Armed Forces, 1999)
Рис. 5 – Электропроводящие волокна на линиях электропередачи (Serbian Armed Forces, 1999)
Слика 5 – Електропроводљива влакна на далеководима (Serbian Armed Forces, 1999)

Characterization of electrically conductive fibers

In order to characterize electrically conductive fibers, a qualitative XRF analysis, a (DTA/TG) analysis and a chemical quantitative analysis were performed. The analyses were performed at the Institute for Technology of Nuclear and Other Mineral Resources in Belgrade and represent the first test for the Commission for Investigating the Consequences of NATO Bombing in 1999, formed by a Government decision in June 2018.

The analysis sample was taken from one spool from an inactivated BLU-114/B cluster bomblet. Figure 6 shows a spool sample for a fiber analysis.

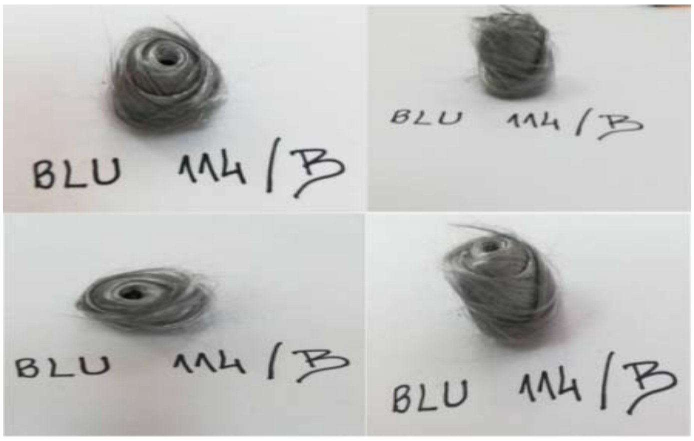

Figure 6 – Samples for the analysis – a separate spool of fibers from a cluster bomblet (Serbian Armed Forces, 1999)
Рис. 6 – Образцы для анализа – извлеченная из кассетной бомбы волоконная катушка (Serbian Armed Forces, 1999)
Слика 6 – Узорци за анализу – издвојен намотај влакана из касетне бомбице (Serbian Armed Forces, 1999)

Figure 7 shows a BLU-114/B fiber magnified on a binocular microscope.

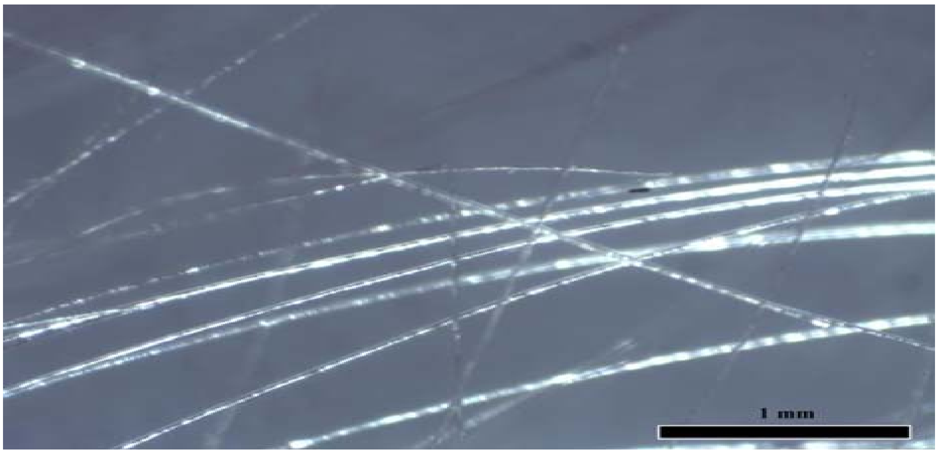

Figure 7 – External appearance of a conductive fiber from the BLU-114/B, magnified on a binocular microscope (size - 1 mm) (Serbian Armed Forces, 1999)
Рис. 7 – Вид проводящего волокна из BLU-114/B, увеличенный под бинокулярным микроскопом (размер - 1 мм) (Serbian Armed Forces, 1999)
Слика 7 – Спољни изглед проводљивог влакна из BLU-114/B, увећан на бинокуларном микроскопу (размера : 1 mm) (Serbian Armed Forces, 1999)

The qualitative XRF analysis was performed on the XRF-MiniPal, PANalytical spectrometer, and the XRF spectrum of the fibers is shown in Figure 8 (the energy in KeV is represented on the x-axis, and the relative intensity of the peak on the y-axis).

The spectrum was recorded using a sodium filter that reduces the intensity of interfering lines and background noise. The XRF analysis aimed at qualitative detection of the present elements, which was confirmed by a quantitative chemical analysis. The semi-quantitative XRF analysis determined the content of gallium (0.007%), the peak of which was detected on the spectrum. Gallium nitride is a material that can be used as a semiconductor.

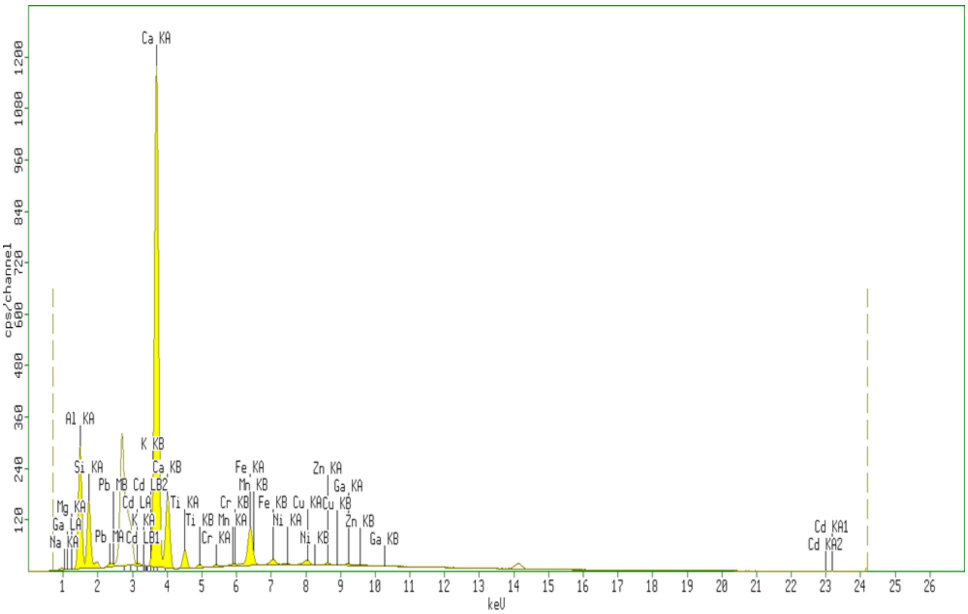

Figure 8 – XRF spectrum of a conductive fiber (with a sodium filter)
Рис. 8 – Рентгенофлуоресцентный спектр провода (с натриевым фильтром)
Слика 8 – XRF спектар проводљивог влакна (са натријумским филтером)

The chemical analysis was performed on the atomic absorption spectrophotometer Analyst 300, Perkin Elmer (Table 2). The sample was dissolved in HCl (1: 1) and the insoluble residue was alkaline.

Table 2 – Chemical analysis of the sample of conductive fibers from the BLU-114/B bomblet
Таблица 2 – Химический анализ образца проводящих волокон из бомбы BLU-114/B
Табела 2 – Хемијска анализа узорка проводљивих влакана из бомбице BLU-114/B

Element	Al	SiO_2	CaO	MgO	Fe_2O_3	Na_2O	K_2O	TiO_2
%	51.400	31.640	13.260	1.606	0.495	1.132	0.104	0.329
Element	Pb	Zn	Cu	Cd	Cr	Ga	Ni	MnO
%	0.029	0.015	0.006	<0.001	0.002	0.007	<0.001	0.003

Based on the chemical analysis of the conductive fibers, it is concluded that these are glass fibers coated with aluminum, which is in accordance with the literature data. Fang et al. (2010), write about the usage of ordnance with conductive fibers/filaments which can consist of carbon filaments or glass filaments with metal coating.

Filaments have a characteristic of creating a compulsively sequential arc that leads to a short circuit in the contact between two electrical phases or the phase and the ground.

The sum of all determined inorganic oxides that are part of the glass fiber is 48.5686%, the content of heavy metals (Pb, Zn, Cu, Cd, Ni) is 0.0522%, the content of Ga 0.0074% and the content of aluminum is 51.400%. The analysis of the acid-soluble part of the fiber detected all elements except Si which remained in the insoluble residue and after melting was transferred to the solution. This information is important from the point of view of the solubility of aluminum and its potential harmful effect on soil contamination and inclusion in the food chain.

The device for a thermal (DTA/TG) analysis is NETZCH STA 409 EP (operating range of 20-1000 °C, with a heating rate of ΔT = 10 °C/min). The experiments were performed in an air atmosphere. The differential thermal analysis, DTA, (Figure 9) indicates an endothermic peak at 659 ºC, which corresponds to the melting point of aluminum, which according to the literature is 660.3 °C. The TGA, thermogravimetric analysis, indicates that there was no change in mass. The TGA of the sample resulted in melting of the metal without loss of mass.

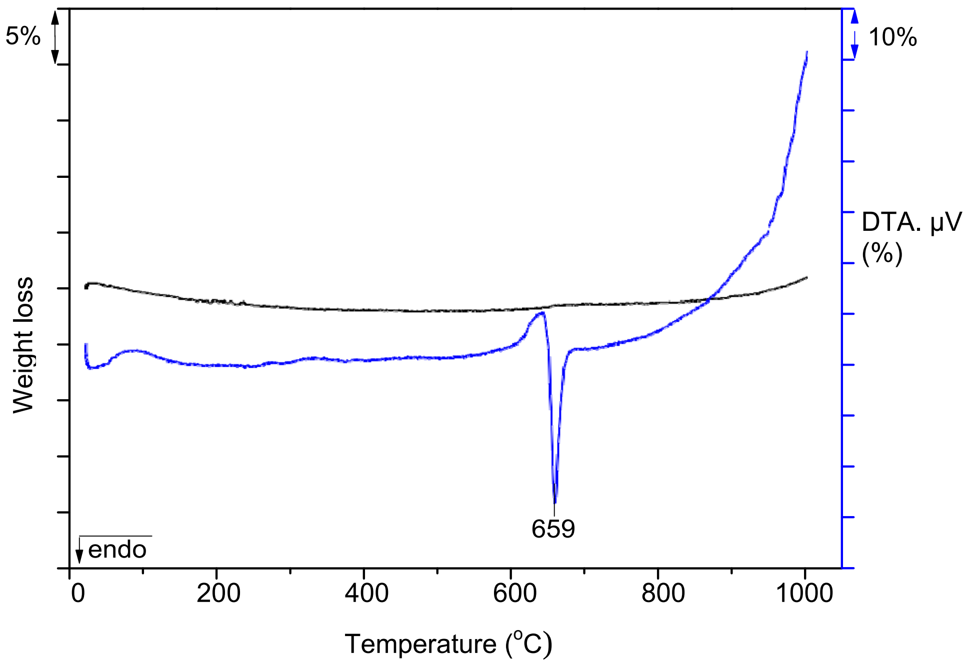

Figure 9 – Thermal analysis (DTA/TG) of a sample of conductive fibers
Рис. 9 – Термический анализ (ДТА/ТГ) образца проводящих волокон
Слика 9 – Термијска анализа (DTA/TG) узорка проводљивих влакана

This is obviously a non-toxic sample that is about 50% of silicate origin.

Ecological aspects of the impact of aluminum on arable land

Aluminum makes up 51.40% of the fiber sample (Table 2). Its presence in the soil can cause the decline in soil fertility, which leads to the reduction in the yield of cultivated crops. The phyto-toxicity of aluminum in acidic soils has been the subject of numerous studies in the country and in the world. It is known that the harmful effects of aluminum depend on its concentration and form, the pH value, organic and inorganic ligands in the solution, the ionic strength, and the plant genotype. Aluminum binds strongly to phosphates, sulfates, and silicates, and its desorption from negatively charged soil colloids is difficult, given the highly positive charge (Mrvić et al, 2012, pp.257-262).

Hydrogen and aluminum cations are responsible for soil acidity. Below pH 6, the substitution acidity of the soil, aluminum is the main source of H + ions, due to the dissociation of Al from clay minerals. Aluminum becomes more soluble at lower pH values. Very acidic soils with the pH value below 4 are not suitable for agricultural production. Leachate from acid soils can contain substances, especially aluminum, which have a detrimental effect on the quality of surface water and groundwater and a negative effect on plants, animals, especially fish in watercourses and lakes. Research in recent decades indicates the harmful effect of Al on human health, with an emphasis on its role in Alzheimer's disease. (Rondeau et al, 2000, pp.59-66)

Conclusion

During the aggression on FR Yugoslavia in 1999, CBU-102/B cluster bombs with BLU-114/B bomblets filled with electrically conductive fibers were dropped on electric power facilities of FR Yugoslavia. Cluster bombs with high-explosive bomblets targeted civilian objects such as residential buildings, hospitals, schools, etc.

The qualitative XRF analysis of conductive fibers from BLU-114/B bomblets was performed on an XRF-MiniPal spectrometer, PANalytical. Spectrum recording was done using a sodium filter that reduces the intensity of interfering lines and background noise. The XRF analysis aimed at qualitative detection of the present elements, which was confirmed by a quantitative chemical analysis. The semi-quantitative XRF analysis determined the content of gallium (0.007%), the peak of which was detected on the spectrum. Gallium nitride is a material that can be used as a semiconductor.

Based on the chemical analysis of the conductive fibers, it is concluded that they are glass fibers with aluminum coating, which is in accordance with the literature data (Fang et al, 2010).

The differential thermal analysis (DTA) indicates an endothermic peak at 659 ºC, which corresponds to the melting point of aluminum, which is, according to literature data, 660.3 ° C.

It is obvious that this is a sample that is about 50% of silicate origin, non-toxic in nature, and with the content of heavy metals in traces, which is important from the point of view of environmental protection.

The rest of the sample consists of aluminum, the presence of which in the soil can cause the decline in soil fertility, resulting in a lower yield of cultivated crops. The phyto-toxicity of aluminum in acidic soils has been the subject of numerous studies in the country and in the world.

Unfortunately, no study has been done after the aggression to determine the degree of degradation, i.e. decline in soil fertility due to residual electrically conductive fibers near the affected electric power facilities by analysing the content of accessible forms of aluminum, as forms that are easily adsorbed in plant organs and included in the food chain.

References

Anđelković-Lukić, M. 2015. *Darovi milosrdnog anđela - Ekološko razmatranje rata NATO protiv SR Jugoslavije, 2. dopunjeno izdanje.* Novi Sad: Balkanija (in Serbian).

-Dveri srpske. 2009. Nato genocid. *Dveri srpske,* 10(41), pp.68-69 (in Serbian).

-Energy Agency of the Republic of Serbia. 2017. *Document number: 312-3/2016-C-1*, January 26, p.8. Belgrade: Energy Agency of the Republic of Serbia (in Serbian).

Fang, W., Shunshan, F., Wenxuan, W. & Fuwang, L. 2010. Analysis of action mechanism of graphite bombs and reaction method of power system. In: *International Conference on Power System Technology (POWERCON 2010)*, Zhejiang, China, pp.1-6, October 24-28. Available at: https://doi.org/10.1109/POWERCON.2010.5666135

Jeler, G.E. & Roman, D. 2016. The Graphite Bomb: An Overview of its Basic Military Applications. *Review of the Air Force Academy*, 14(1), pp.13-18. Available at: https://doi.org/10.19062/1842-9238.2016.14.1.2.

Mrvić, V., Čakmak, D., Sikirić, B., Nikoloski, M., Delić, D., Belanović, S. & Beloica, J. 2012. Effect of acidification on the content of water-soluble aluminium in pseudogleys. *Ratarstvo i povrtarstvo*, 49(3), pp.257-262 (in Serbian). Available at: https://doi.org/10.5937/ratpov49-2293.

Rondeau, V., Commenges, D., Jacqmin-Gadda, H. & Dartigues, J-F. 2000. Relation between Aluminum Concentrations in Drinking Water and Alzheimer's Disease: An 8-year Follow-up Study. *American Journal of Epidemiology*, 152(1), pp.59-66. Available at: https://doi.org/10.1093/aje/152.1.59.

-Serbian Armed Forces (SAF). 1999. *General Staff Archive.* Belgrade: Serbian Armed Forces (SAF).

ЭЛЕКТРОПРОВОДЯЩИЕ ВОЛОКНА В КАССЕТНЫХ БОМБАХ, СБРОШЕННЫХ НА ОБЪЕКТЫ ЭЛЕКТРОЭНЕРГЕТИЧЕСКОЙ СИСТЕМЫ СОЮЗНОЙ РЕСПУБЛИКИ ЮГОСЛАВИЯ В 1999 ГОДУ

Мирьяна Н. Анджелкович-Лукич[а], **корреспондент,** *Мирьяна* Д. Стоянович[б]

[а] Военно-технический институт, г. Белград, Республика Сербия; Правительство Республики Сербия, Межведомственный координационный орган, г. Белград, Республика Сербия

[б] Институт технологий ядерных и других минеральных ресурсов, г. Белград, Республика Сербия

РУБРИКА ГРНТИ: 78.00.00 ВОЕННОЕ ДЕЛО;
78.25.12 Химическое, биологическое и зажигательное оружие. Вооружения и средства радиационной, химической и биологической защиты,
61.00.00 ХИМИЧЕСКАЯ ТЕХНОЛОГИЯ. ХИМИЧЕСКАЯ ПРОМЫШЛЕННОСТЬ;
61.01.94 Охрана окружающей среды
ВИД СТАТЬИ: оригинальная научная статья

Резюме:

Введение/цель: В статье представлен способ функционирования кассетной бомбы CBU-102(V) 2/B, массой около 340 кг, содержащей бомбы малого калибра с электропроводящими волокнами, который был применен для выведения из строя электростанций.

Методы: В ходе исследования был выполнен физический и химический анализ волокон. Для определения характеристик волокна использовались следующие методы: бинокулярный микроскоп для определения толщины волокна и качественный рентгенофлуоресцентный анализ, выполненный на спектрометре XRF-MiniPal, PANalytical. Рентгенофлуоресцентный анализ был выполнен с целью качественного обнаружения присутствующих элементов, которое было подтверждено количественным химическим анализом.

Результаты: Полуколичественный рентгенофлуоресцентный анализ выявил содержание галлия (0,007%), пик которого был обнаружен на спектре. Нитрид галлия является материалом, который можно использовать в качестве полупроводника. Химический анализ проводили с помощью атомно-абсорбционного спектрофотометра Analyst 300, Perkin Elmer.

Выводы: Прибор для дифференциального термического анализа и термогравиметрии (ДТА/ТГ), NETZCH STA 409 EP (рабочий диапазон от 20 ° C до 1000 ° C), подтвердил, что образец *содержал 50% нетоксичного силиката и следы тяжелых металлов. Остальная часть образца содержала алюминий, присутствие которого в почве может вызвать снижение плодородия почвы, что как следствие приводит к снижению урожайности.*

Ключевые слова: химическая война, кассетная бомба, электропроводящие волокна, энергетическая система, химический анализ, термохимический анализ, силикат, алюминий, воздействие на окружающую среду, почва, снижение плодородия, снижение урожайности.

ЕЛЕКТРОПРОВОДЉИВА ВЛАКНА У КАСЕТИЦАМА БОМБИ КОЈИМА ЈЕ НАПАДНУТ ЕЛЕКТРОЕНЕРГЕТСКИ СИСТЕМ СР ЈУГОСЛАВИЈЕ 1999. ГОДИНЕ

Мирјана Н. Анђелковић Лукић[а], **аутор за преписку**, *Мирјана* Д. Стојановић[б]

[а] Војнотехнички институт, Београд, Република Србија;
Влада Републике Србије, Међуресорно координационо тело, Београд, Република Србија

[б] Институт за технологију нуклеарних и других минералних сировина, Београд, Република Србија

ОБЛАСТ: хемијске технологије
ВРСТА ЧЛАНКА: оригинални научни рад

Сажетак:

Увод/циљ: У раду је приказан начин функционисања касетне бомбе CBU-102(V) 2/B, масе око 340 kg, у којој се налазе бомбице са електропроводљивим влакнима којима су онеспособљавана електроенергетска постројења.

Методе: Извршене су физичке и хемијске анализе влакна. За анализу влакана коришћене су следеће методе испитивања: бинокуларни микроскоп за одређивање дебљине влакна, квалитативна XRF анализа урађена на спектрометру XRF-MiniPal и PANalytical. Циљ XRF анализе био је да се квалитативно детектују присутни елементи, што је потврђено и квантитативном хемијском анализом.

Резултати: Семиквантитативном XRF анализом одређен је садржај галијума (0,007%), чији је пик детектован на спектру. Галијум-нитрид је материјал који се може користити као полупроводник. Хемијска анализа урађена је на атомско-абсорпционом спектрофотометру Analyst 300, Perkin Elmer.

Закључак: На уређају за диференцијално-термијску анализу и термогравиметрију (ДТА/ТГ), NETZCH STA 409 EP (опсег рада 20–1000°C), потврђено је да се ради о узорку који је око 50%

силикатног порекла, нетоксичног карактера, са садржајем тешких метала у траговима. Остатак узорка чини алуминијум чије присуство у земљишту може да утиче на смањење плодности, што доводи до смањења приноса гајених култура.

Кључне речи: хемијски рат, касетна бомба, електропроводљива влакна, енергетски систем, хемијска анализа, термохемијска анализа, силикат, алуминијум, еколошки утицај, земљиште, смањење плодности, смањење приноса.

Paper received on / Дата получения работы / Датум пријема чланка: 24.06.2020.
Manuscript corrections submitted on / Дата получения исправленной версии работы / Датум достављања исправки рукописа: 17.07.2020.
Paper accepted for publishingon / Дата окончательного согласования работы / Датум коначног прихватања чланка за објављивање: 18.07.2020.

MODULATION TRANSFER FUNCTION IN THE ANALYSIS OF ELECTRO-OPTICAL SYSTEM PERFORMANCE

Nedeljko S. Pađen[a], *Dragana* B. Perić[b], *Branko* G. Livada[c], *Milan* M. Milosavljević[d]

[a] Vlatacom Institute, Belgrade, Republic of Serbia; Singidunum University, Department for Electrical Engineering and Computing, Belgrade, Republic of Serbia, e-mail: nedeljko.padjen@vlatacom.com, **corresponding author**, ORCIDiD: https://orcid.org/0000-0002-5556-7552

[b] Vlatacom Institute, Belgrade, Republic of Serbia, e-mail: dragana.peric@vlatacom.com, ORCIDiD: https://orcid.org/0000-0002-2556-8212

[c] Vlatacom Institute, Belgrade, Republic of Serbia, e-mail: branko.livada@vlatacom.com, ORCIDiD: https://orcid.org/0000-0002-7257-4842

[b] Singidunum University, Department for Electrical Engineering and Computing, Belgrade, Republic of Serbia, e-mail: mmilosavljevic@singidunum.ac.rs, ORCIDiD: https://orcid.org/0000-0001-9630-804X

DOI: 10.5937/vojtehg68-26985; https://doi.org/10.5937/vojtehg68-26985

FIELD: Electro-optics, Electronics, Mathematics
ARTICLE TYPE: Original scientific paper

Abstract:

Introduction/purpose: The Modulation Transfer Function (MTF) is a useful tool for an imaging system performance analysis. It is used in Electro-Optical (EO) system design, verification of targeted system parameters, but also in optimization tasks for systems under test. This methodology based on the linear systems theory allows the performance analysis of complicated EO systems to be divided into subsystems. In this paper, the MTF methodology will be presented and explained, followed by the measurements performed in the electro-optical laboratory. The MTF measurements were performed on three types of cameras in different spectral bands, after which the results were compared to the model expectations and theoretical limits for the imaging system. For one of the sensors, the limiting frequency was also measured using the USAF 1951 test target which allowed the comparison between the methods.

NOTE: The previous version of this paper was presented at Sinteza 2019 International Scientific Conference on Information Technology and Data Related Research (Pađen, 2019).

Methods: Laboratory measurements and theoretical mathematical calculations.

Results: Based on the laboratory and theoretical results, the measurement results were further analyzed.

Conclusion: The measurements have proven that the calculated cutoff frequency and the MTF curve represent the limit for the real measured system performance. Therefore, this study has confirmed that the MTF can be convenient for finding system limitations and bottlenecks and for increasing the overall performance of the system.

Key words: MTF-Modulation Transfer Function, USAF 1951 test, electro-optics.

Introduction

Border security in the modern society has become an increasingly important task for countries in order to prevent illegal immigration, smuggling and cross-border criminal, but also to answer to the recent needs for border lockdowns due to the pandemic health crisis (McDaniel et al, 2006), (Dufour, 2013). As borders are vast, usually not easily accessible areas, the task of their protection requires centralized control and integration of various types of sensors such as radars, cameras, motion sensors, and unmanned aerial vehicles. One of the key roles in these systems is the one of Multi-Sensor Imaging Systems (MSIS) which are sets of different sensors covering the visible spectral band (Holst, 2008) - VIS (0.4-0.7 μm), but also the Near Infrared – NIR (0.7-1.1 μm), Shortwave Infrared - SWIR (1.1-2.5 μm), Midwave Infrared – MWIR (2.5-7 μm) and Longwave Infrared - LWIR (7-15 μm) ones. The goal of these systems is to provide all-day, all-weather visibility, which is achieved by integrating high quality detectors working in different spectral bands and powerful lenses, for long range and high resolution systems (Perić et al, 2019). Based on their main role in the system, MSIS can be designed for various tasks such as detection, recognition, and identification of different type of objects (vehicles, trucks, pedestrians, etc.).

This paper will analyze one such multi-sensor imaging system consisting of a visible camera, an SWIR and an MWIR camera with lenses whose specifications will be listed in Chapter 5 of this paper. The performance assessment of this system was done in an electro-optical laboratory by measuring the system Modulation Transfer Function and, for one of the sensors, the resolution using the USAF 1951 resolution test chart.

In Chapter 2, we will describe the basics of the electro-optical (EO) imaging system performance and its main models. Chapter 3 gives an overview of the theory behind the MTF analysis and its contribution in the overall performance analysis of one imaging system, followed by Chapter 4 where the methodology uncertainties and biases are listed.

The laboratory environment, the equipment used for the measurements and the procedures and methods used in this process are described in Chapter 5.

Chapter 6 presents the measurement results for all three sensors and discusses them in relation to the theoretical expectation.

The alternative measurement of system limiting resolution is presented in Chapter 7.

The real-environment outdoor camera performance is presented in Chapter 8 where the system potential to perform detection, recognition and identification of objects is tested on the scene 12 km far from the EO system position.

Finally, the last chapter offers the conclusions on the conducted testing and proposes some possible guidelines for further optimization of electro-optical imaging systems.

Electro-optical imaging system performance

The analysis of the electro-optical imaging system performance is a complex process that must cross-reference the results and information gathered in different environments, as depicted in Figure 1.

Besides the necessity of taking measurements/predictions in various environments, one must take into consideration all the elements of the system, from the scene, to the observer (Holst, 2008).

Figure 2 depicts one such system, and the elemets which are affecting the creation of an image to be presented to the observer.

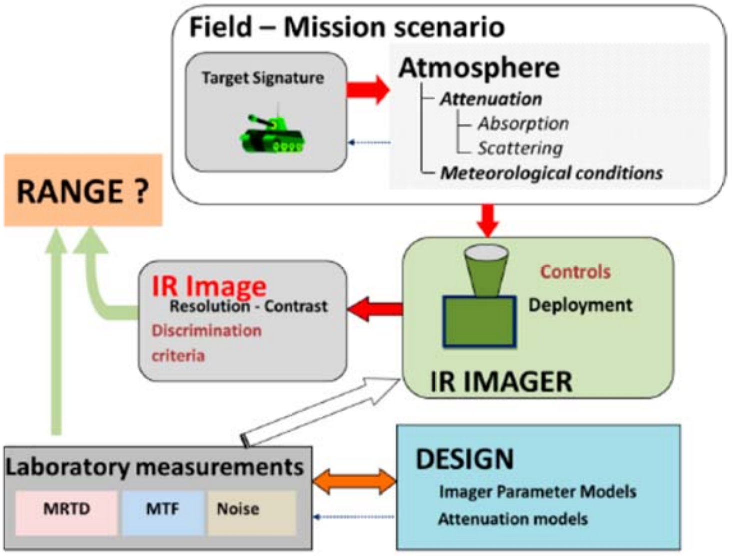

Figure 1 – Relationship between different system predictions and measurements, for an infrared imager (Perić et al, 2019)
Рис. 1 – Отношениемежду различными прогнозами и измерениями системыдля инфракрасной томографии (Perić et al, 2019)
Слика 1 – Однос између различитих предикција и мерења система за инфрацрвену камеру (Perić et al, 2019)

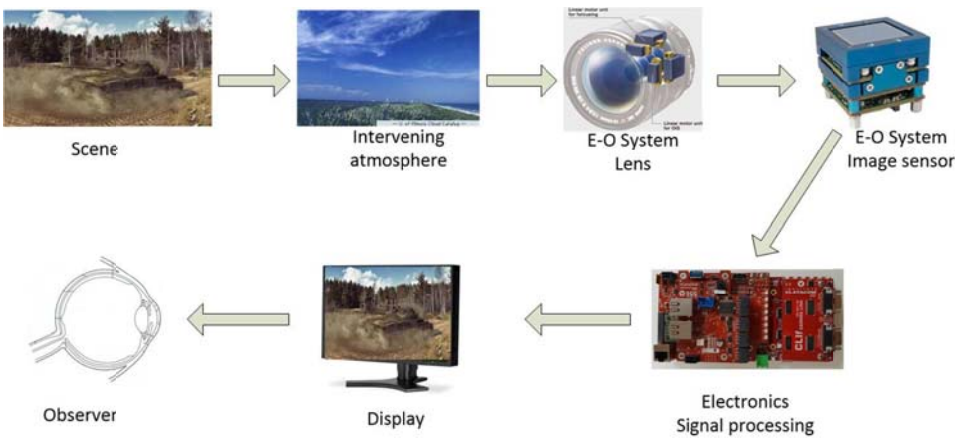

Figure 2 – Electro-optical imaging chain
Рис. 2 – Электрооптическая цепочка изображений
Слика 2 – Електрооптички ланац слике

The major elements that contribute to the resulting image quality are the following (Holst, 2008):

- The scene content - target and background characteristics, clutter, motion
- Intervening atmosphere - rain, haze/fog, transmittance, dust
- Electro-optical system – Lens and Sensor system - Minimum Resolvable Temperature Difference (for infrared systems), Minimum Resolvable Contrast (for visible systems), resolution, sensitivity, noise,
- Electronics – Signal processing
- Display - distance to the observer, luminance, contrast, and finally,
- Observer - his experience, fatigue, training, and workload.

In order to relate these various measurable system design parameters with their operational performance, different models were developed and used. Three levels of models are best answering to these requirements (Shumaker & Wood, 1988), (Fiete, 2010):

- Component/phenomenology models – These models find the MTF of the whole system (MTFSYS) by finding the MTF of individual components, listed in the paragraph above. The MTFSYS is then used as an input parameter for the next-level system modeling;
- System performance models – Built on component models, they describe the total system performance for some controlled tasks;
- Operational models – These models focus only on the overall operational system functionality, where they are used to calculate detection, recognition and identification ranges of the whole system.

The focus of our analysis will be limited to the component model, where the Modulation Transfer Function will be used to describe the signal transfer characteristics of the whole system, and of some of its subsystems.

The MTF methodology and its main characteristics as well as limitations are described in more detail in the following two chapters.

MTF analysis

The MTF analysis is one of the primary parameters used in electro-optical system design, sub-system specification and performance analysis (Holst, 2011).

This methodology carries out the analysis of the total impulse response of the system from the spatial (time) domain to the frequency domain by the means of Fourier analysis. The benefit of this is the replacement of the complex time domain mathematics, involving two-dimensional convolutions, with much simpler multiplications between elements (Boreman, 2001).

The imaging channel response is described by the Optical Transfer Function (OTF), where the Modulation Transfer Function represents the modulus of OTF, i.e. the magnitude response of our optical system to the sinusoidal input signals of various frequencies.

The MTF analysis is applicable only for linear shift invariant (LSI) systems which should modify only amplitude and phase of the target (Holst, 2011). In order to achieve this, four conditions must be met: 1. signal processing is linear; 2. the radiation is incoherent; 3. the image is spatially invariant; and 4. the system mapping is single valued. While these conditions are generally not fulfilled, especially on a microscale, the MTF analysis is a very useful tool in a system performance analysis and comparison and, as such, very much in use in the system design and choice of adequate optical elements (Perić et al, 2018).

The MTF methodology connects two important aspects of the image – its modulation depth (or contrast) and resolution - through the concept of spatial frequency.

The modulation depth is actually a measure of visibility of an image. The finite-size impulse response of the electro-optical system (i.e. not the delta function) decreases the modulation depth of the image, compared to that one of the object (Daniels, 2018).

In image processing applications, a system performance is often described in terms of spatial frequency, defined in the number of *line pairs per mm* (or *cycles per mm*, or cycles per miliradian), where one line pair (or one cycle) represents the closest spacing of black and white bars that can be resolved by the system.

Figure 3 presents the USAF 1951 resolution test chart which is one of the most commonly used targets for evaluating system spatial frequency (United States Department of Defense, 1950). The basis of the chart is a group of three vertical and three horizontal lines organized by groups and elements. A higher group/element number gives a higher number of black and white line-pairs per millimeter, i.e. higher spatial freqency. The chart clearly shows that by increasing spatial frequency (increasing the number of black and white line-pairs per millimeter, noted with a higher group/element number in the figure), it becomes more difficult to distinguish the lines.

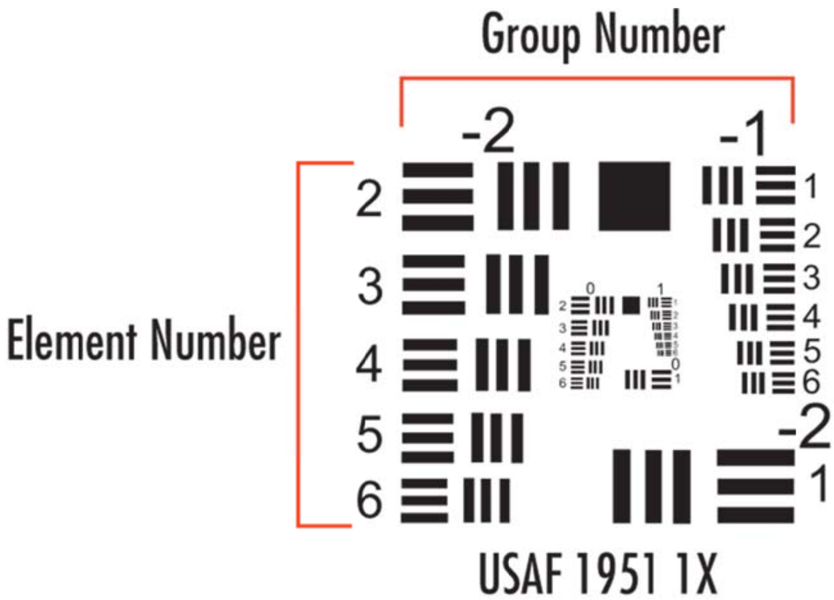

Figure 3 – USAF 1951 resolution test chart, where the group of bars with ahigher group/element number have higher spatial frequencies
Рис. 3 – Тестовая цель ВВС США 1951 года, где группа линий с большим числом групп / элементов имеет более высокую пространственную частоту
Слика 3 – Тестна мета УСАФ 1951, где група линија са већим бројем групе/елемената има већу просторну фреквенцију

The concept of spatial frequency will be additionally explained later in the document, where the system resolution will be evaluated by using the USAF 1951 test chart.

The following figure depicts how the increase of spatial frequency of the object (the upper graph) affects the modulation depth of the image (middle graph), resulting in the degradation of the MTF function (lower graph).

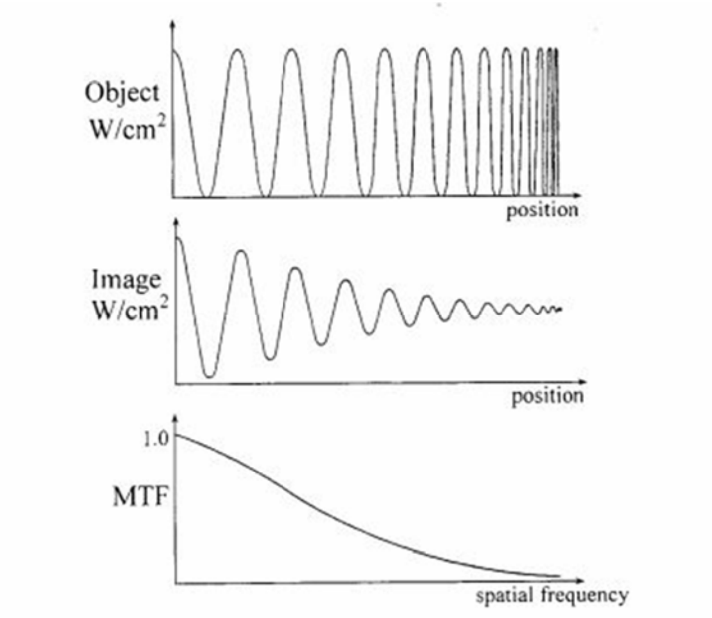

Figure 4 – MTF as a function of spatial frequency (Boreman, 2001)
Рис. 4 – MTF как функция пространственной частоты (Boreman, 2001)
Слика 4 – MTF као функција просторне учестаности (Boreman, 2001)

To summarize, by moving to the spectral domain, instead of convoluting the independent impulse responses of the system components, we will simply multiply their separately calculated MTFs, resulting in the overall system modulation transfer function (MTFSYS). Figure 5 illustrates typical MTF shapes of some of the system components. The x-axis, noted with ξ, represents normalized spatial frequency, i.e. spatial frequency divided with cutoff frequency (detector, or optical cutoff, depending on the type of the system, as explained in Table 1 of this paper).

The MTFs presented in Figure 5 do not conclude the list of the elements affecting the final shape of the MTF system graph, where jitter, defocus and noise also influence the final result. The more components are analysed, the better result (result closer to real measurements) will be achieved. As a rule of thumb, it can be considered that the quality of the optical system is better if the area below the curve is greater. Nonetheless, there is no ultimate way to evaluate which MTF shape is the best (Boreman, 2001), due to non-linearity of the human eye which does the task of reconstruction filtering.

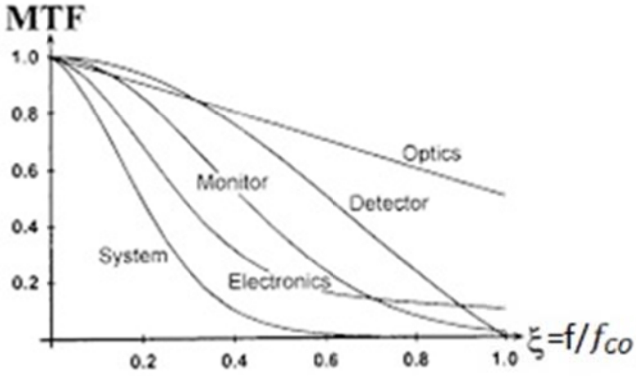

Figure 5 – System MTF as a result of components MTFs, where ξ denotes normalized spatial frequency (Boreman, 2001)
Рис. 5 – Система MTF какрезультат компонентов MTF, где ξ обозначает относительную пространственную частоту (Boreman, 2001)
Слика 5 – Систем MTF као резултат MTF-a појединачних компоненти, где ξ означава релативну просторну учестаност (Boreman, 2001)

The parameter that uniquely defines the shape of the electro-optical system modulation transfer function is given by the expression $F_{\#}\lambda/d$, where $F_{\#}$ is the focal ratio (F-number), λ is the wavelength, and d is the detector size (Holst, 2011).

The following table gives the relation between the value of the expression and its representation in the spatial and frequency domain.

Table 1 – Optics-limited versus detector-limited system performance (Holst, 2011)
Таблица 1 – Оптико-ограниченная эффективность системы по сравнению с детектором (Holst, 2011)
Табела 1 – Поређење система ограничених детектором, односно оптиком (Holst, 2011)

$F_{\#}\lambda/d$	System performance	Spatial domain	Frequency domain
<1	Detector-limited	Airy disc smaller than the detector	Optical cutoff greater that detector cutoff
>1	Optics-limited	Airy disc larger than the detector	Detector cutoff greater than optical cutoff

This ratio also reveals the systems prone to aliasing, boresome artefacts of the signal under-sampling, which occur for the ratios below the value of 2.

While the MTF measurement brings a lot of benefits in system design and analysis, this methodology also has its uncertainties, described in the following chapter.

MTF methodology uncertainties

The MTF laboratory measurement process suffers from various uncertainties or biases, mostly caused by the fact that the methodology requirement for the LSI system is not achieved. This results in differences in measuring which can be categorized into four groups (Haefner, 2018):

- Data corruption,
- Equipment and experimental selection,
- Operator selection, and
- System under test effects.

Data corruption is the reason of the most severe errors in the MTF measurement, which can make the whole process unusable and meaningless. The main reasons of data corruption can be found in:

- Saturation, where multiple input values are mapped to the same output value,
- Quantization, where low signal quantization levels can lead to significant variations in signal output uncertainties, and
- Non-linear response.

Equipment and experimental variations are the reason why the MTF results for the same system, measured in different laboratories, will give different results. These variations are caused by:

- Target angle variations - as the system is not diffraction-limited, the MTF is rotationally dependent

Operator selection, where one needs to select:

- Region of Interest (ROI) - real systems are not spatially invariant, so the choice of ROI will influence MTF measurements,
- Focus adjustment, where results obtained even by highly trained technicians will vary due to selected focuses which will affect measurement results.

System under test effects, such as:

- Non-uniformity, caused by detectors imperfections, poor optics, or fixed patter nnoise, and
- System noise.

While all these challenges in MTF measuring are well documented, with defined best practices how to mitigate these uncertainties, results from the laboratory must be accompanied with the ones from tests performed in real environment, to enhance the evaluation of the system and give clear guidelines for its improvement.

MTF measurement setup

The MTF characteristics measurements were done in an electro-optical laboratory equipped with a collimator station, illustrated in the following Figure:

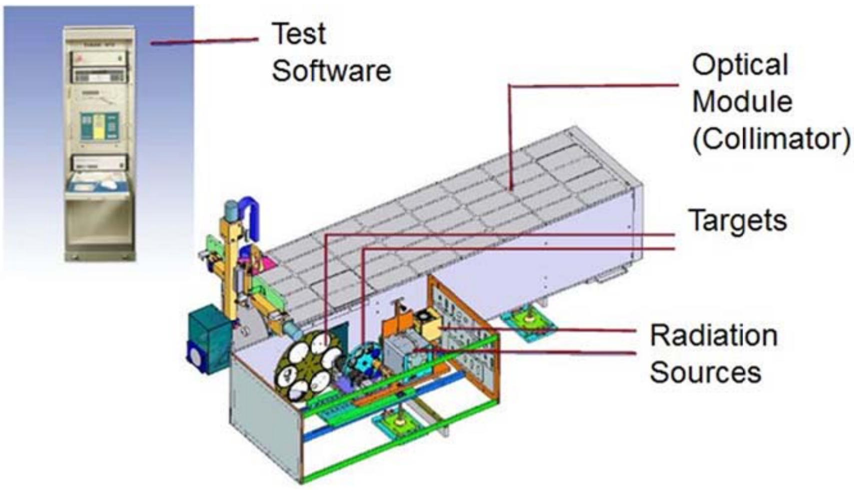

Figure 6 – Electro-optical modular test station (CI Systems, 2012)
Рис. 6 – Электрооптическая модульная испытательная станция (CI Systems, 2012)
Слика 6 – Модуларна електрооптичка тест-станица (CI Systems, 2012)

The test system has the following characteristics (CI Systems, 2012): the collimator's effective focal length (EFL) is 3,025mm (120 inches), with a clear aperture of 355.6mm (14 inch) and a field of view of 1.0º. The radiation source is VIS/SWIR integration sphere with a spectral range of 0.44-2.2 μm, and a blackbody source (absolute temp. range 0°C to 125°C, resolution 0.001°C), which is used for MWIR and LWIR measurements.

The characteristics of the cameras under the test are as follows:

- SWIR – resolution 640 x512 pixels, detector pixel size 15 μm. The lens has a declared waveband of 0.9-1.7 μm, and a variable focal length (f_l) of up to 2500mm. The measurements were made on f_l = 2500mm, with $F_{\#}$=16

- Visible camera – resolution 1920x1080 pixels, detector pixel size 5 µm. The lens has a declared waveband of 0.4–0.7 µm, and a variable focal length of up to 2000mm (with extender). The measurements were made on f_l = 2000mm, with $F_{\#}$=16
- MWIR - resolution 640x512 pixels, detector pixel size 15 µm. The lens has a declared waveband of 3–5 µm, an anticipated waveband central wavelength of λ=4 µm, and a variable focal length of up to 825 mm. For the purpose of measurements, we set the focal length to f_l = 784mm, to provide enough room for fine focusing.

There are different methods to determine the system MTF, using the imaging lines, points, or even imagery from a system of well-known MTF values (Schowengerdt et al, 1985).

In this case, the MTF measurements were performed with a step-target, depicted in Figure 7. The MTF measurement procedure with the step target is described in the following lines.

Figure 7 – Step-target, used in the MTF measurement
Рис. 7 – Целевой тест, используемыйпри измерении MTF
Слика 7 – Тест-мета која се користи за мерење МТФ-а

The measurement process begins by selecting and placing the slanted step target with an almost perfect edge in the target wheel, switching on the integration sphere and setting the intensity. The edge spread function (ESF) is the system response to a high contrast edge (Kohm, 2004). Images in a number of consecutive frames are taken, and averaging is done over all recorded frames. The derivative of the ESF produces the line spread function (LSF), which is the system response to a high contrast line. While the target has an almost perfect edge, its image gets distorted as a result of the system imperfection, resulting in the LSF.

From the LSF, by means of Fast Fourier transformation (FFT), the MTF graph is derived, presenting all frequencies up to cut-off frequency.

The above described procedure measured the MTF of the whole system, which was compared with the MTF curves for the detector (determined by the size of the pixel and the focal length of the lens) and the optics system (which is limited by the optical diffraction), calculated from formulas (1) to (5) (Holst, 2008).

The MTF curve for the detector is calculated as the magnitude of the following formula

$$OTF_{detector}(f_x)=\mathrm{sinc}(\pi\alpha_d f_x) = \frac{\sin(\pi\alpha_d f_x)}{\pi\alpha_d f_x} = \frac{\sin\left(\pi \frac{f_x}{f_{DCO}}\right)}{\pi \frac{f_x}{f_{DCO}}}, \tag{1}$$

$$\alpha_d = \frac{1}{f_{DCO}} = \frac{\mathrm{d}}{f_l} = \frac{detector\ pixel\ size}{effective\ focal\ length}, \tag{2}$$

The diffraction (optical) MTF was calculated by the following formula:

$$OTF_{diff}(f_x) = \frac{2}{\pi}[cos^{-1}\left(\frac{f_x}{f_{OCO}}\right) - \left(\frac{f_x}{f_{OCO}}\right)\sqrt{1-(\frac{f_x}{f_{OCO}})^2}], \quad for\ f_x \le f_{OCO}, \tag{3}$$

$$OTF_{diff} = 0\ , for\ f_x > f_{OCO}\ , \qquad where \tag{4}$$

$$f_{OCO} = \frac{f_l}{\lambda F_\#}\ and\ F_\# = \frac{f_l}{D} = \frac{1}{2NA} \tag{5}$$

The parameters used in the formulas (and in the tables in the following chapter) are

- λ – central wavelength,
- d – detector pixel size,
- f_l – focal length,
- D – diameter of the lens aperture,
- $F_\#$ – F-number, a function of the focal length and the lens aperture,
- f_{DCO} – detector cutoff frequency,
- f_{OCO} – optical (diffraction) cutoff frequency,
- NA – Numerical aperture, and
- f_N – Nyquist frequency, which is half of detector cutoff frequency, as per the sampling theorem.

Measurement results

The measurement parameters and the calculated cutoff frequencies are summarized in Table 2 for the visible camera, in Table 3 for the short-wave infrared (SWIR) camera, and in Table 4 for the mid-wave infrared (MWIR) camera.

Table 2 – Calculated cutoff frequencies for the visible camera
Таблица 2 – Рассчитанные предельные частоты для камеры видеонаблюдения
Табела 2 – Израчунате граничне фреквенције за видљиву камеру

λ [μm]	Detector size d[μm]	Focal length f_l[mm]	F-number $F_{\#}$	Detector cutoff frequency f_{DCO} [cy/mrad]	Nyquist frequency f_N [cy/mrad]	$F_{\#}$λ/d	Optical cutoff frequency f_{OCO} [cy/mrad]
0.5	5	2000	16	400.00	200.00	1.60	250

Table 3 – Calculated cutoff frequencies for the SWIR camera
Таблица 3 – Рассчитанные предельные частоты для SWIR камеры
Табела 3 – Израчунате граничне фреквенције за SWIR камеру

λ [μm]	Detector size d[μm]	Focal length f_l[mm]	F-number $F_{\#}$	Detector cutoff frequency f_{DCO} [cy/mrad]	Nyquist frequency f_N [cy/mrad]	$F_{\#}$λ/d	Optical cutoff frequency f_{OCO} [cy/mrad]
1.5	15	2500	16	166.67	83.33	1.60	104.1667

Table 4 – Calculated cutoff frequencies for the MWIR camera
Таблица 4 – Рассчитанные предельные частоты для MWIR камеры
Табела 4 – Израчунате граничне фреквенције за MWIR камеру

λ [μm]	Detector size d[μm]	Focal length f_l[mm]	F-number $F_{\#}$	Detector cutoff frequency f_{DCO} [cy/mrad]	Nyquist frequency f_N [cy/mrad]	$F_{\#}$λ/d	Optical cutoff frequency f_{OCO} [cy/mrad]
4	15	784	4	52.27	26.13	1.07	49

These values were then used to calculate and plot the graphs for the MTF of the detector, the MTF of the diffraction, and the resulted MTF of the system (MTF product) using formulas (1-5), given in the previous chapter. The graph X-axes are all plot up to the Nyquist frequency (which is one half of the sampling frequency), as that is the highest frequency which can be faithfully reconstructed, as per the sampling theorem (Holst, 2008).

Figure 8 presents the graphs of the calculated MTFs and the measured MTF for the visible camera with the extender (f_l =2000mm).

Figure 9 gives the graphs of the calculated MTFs and the measured MTF for the SWIR camera with a focal length of 2500mm.

Finally, Figure 10 shows the MTF calculations and measurements for the MWIR camera with a zoom lens with the maximum focal length of 825mm, which was set on 784mm for these measurements.

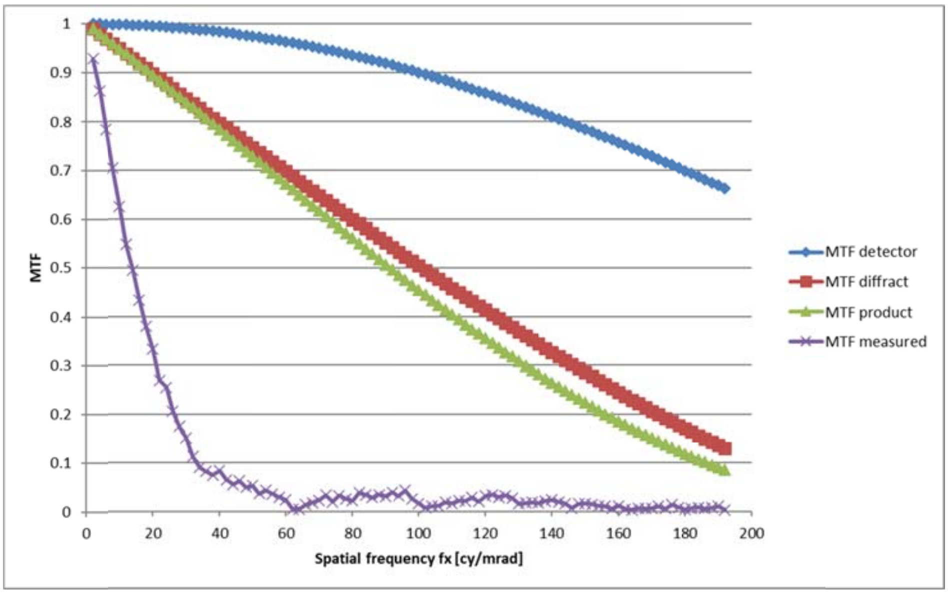

Figure 8 – MTF for the visible camera, f_l=2000mm
Рис. 8 – MTF для камеры видеонаблюдения, f_l =2000mm
Слика 8 – MTF за видљиву камеру, f_l =2000 mm

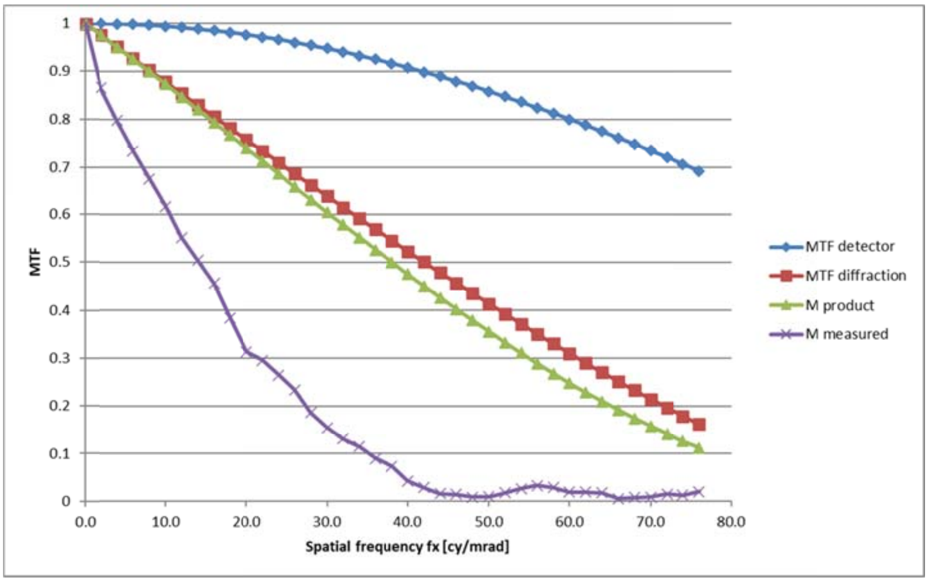

Figure 9 – MTF for the SWIRcamera, f_l =2500mm
Рис. 9 – MTF для SWIR камеры, f_l =2500mm
Слика 9 – MTF за SWIR камеру, f_l =2500 mm

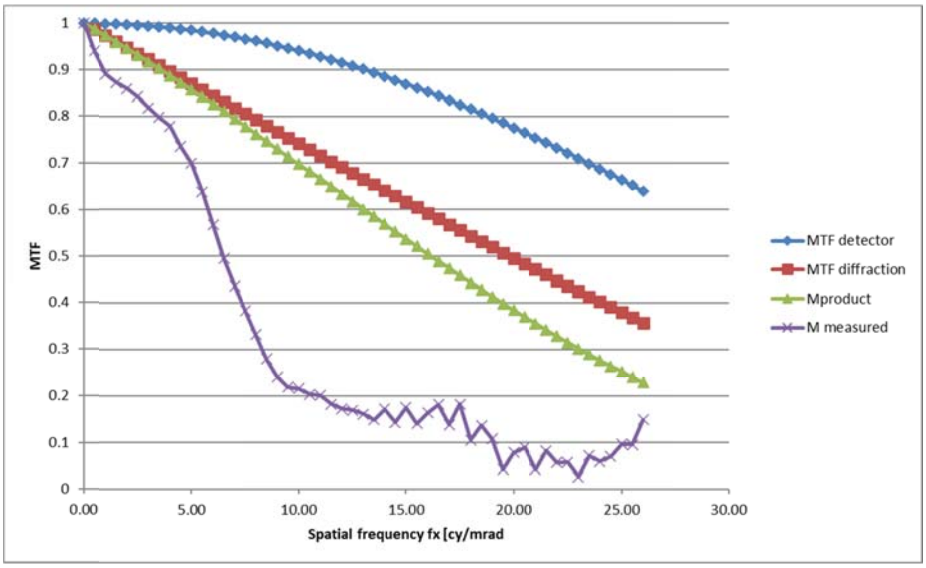

Figure 10 – MTF for the MWIR camera, f_l =784mm
Рис. 10 – MTF для MWIR камеры, f_l =784mm
Слика 10 – MTF за MWIR камеру, f_l =784 mm

A. Visible camera, with the extender (f_l =2000mm)

By analyzing Figure 8, we can conclude that the measured result (the MTF measured curve) has lower cutoff frequency than the one expected by the theory (the MTF product curve). The deviation of the measured MTF from the theoretical one, reflected in the steeper decline of the MTF curve, can be explained by the effect of the elements which were not measured in this case, such as focus, electronics for video processing, display, etc. We can also conclude that the limiting factor in this case is the diffraction of the lens system (f_{OCO}), as the MTF diffract graph is below the MTF detector. While the calculated diffraction of the lens system is at 250 cy/mrad, we can see that the measured MTF is falling below 0.2 already for the spatial frequencies at a one tenth of the optical cutoff. This can be explained by using the optical extender (to achieve the targeted focal length) which has also introduced the deviations caused by the aberrations (imperfection) of the optical extender elements.

B. SWIR camera, a focal length of 2500mm

This measurement, performed by the short-wave infrared camera with a narrow field of view (NFOV), reveals that again we are dealing with an optics-limited system, which is obvious from the graph (where the MTF diffraction is lower than the MTFdetector line), from the values of $f_{DCO}$and f_{OCO}, but also from the value of $F_{\#}$λ/d expression, as per the limits defined in Table 1 of this paper. The MTF measured curve is also below the MTF product one but, compared to the visible camera in the scenario A, the measured curve is less steep. In this scenario, the measured MTF drops below 20% approximately at a value of 26 cy/mrad, which is around 25% of the optical cutoff. Based on this, it is safe to conclude that the SWIR lens has better optical characteristics than the one used with the visible camera. Having this in mind, we expect better identification in SWIR images which will be tested with images taken from a real scenario.

C. MWIR camera, a focal length of 784mm

Unlike the first two scenarios where the system was clearly residing in the diffraction (optics) limited part, here the cutoff frequencies (detector, and optical) are much closer, resulting in closer MTF detector and MTF diffraction graphs, compared to the first two scenarios. What is also readable from the graph is that the measured MTF is above 10% for most of the values up to the Nyquist limit, which is a general indication of a well-designed system and better image quality (Boreman, 2001) (although the system performance can be really evaluated only through the prism of frequency specific range of interest). What also must be commented is the measured results for the frequencies above 22-23 cy/mrad, reflected in the incline of the graph-line. As this have no explanation in physics of the system, this behavior can be explained by system non-linearity, signal processing, measurement setup, and other aspects which are described in Chapter 4 of this paper and have the effect on the MTF measurements.

Other methods for measuring EO system resolution

The MTF analysis and measurements, presented in the previous chapters, offers a lot of information to the viewer, by describing the system behavior on the whole spectrum of frequencies, up to the limiting, cutoff frequency. There are other methods to measure optical resolution: the United States Air-Force (USAF) 1951 resolution test chart, being one of the most popular ones, is given in Figure 11 of this document.

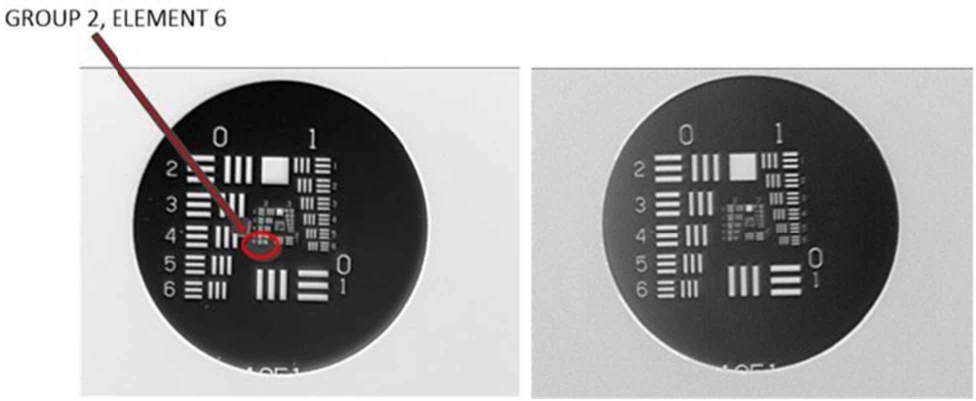

Figure 11 – USAF resolution target, imaged with the MWIR camera described in Chapter 6. The left image was taken with a good focus, the right one with a bad focus.
Рис. 11 – Цель разрешения ВВС США, полученная с помощью камеры MWIR, описанной в главе VI. Левое изображение было получено прихорошей фокусировке, правое приплохой фокусировке.
Слика 11 – USAF-ова резолуциона мета снимљена MWIR камером описаном у поглављу VI. Слика лево снимљена је са добрим фокусом, а слика десно са лошим фокусом.

This target consists of a group of elements, each element consisting of three vertical and three horizontal bars of precise width. The observer task is to visually identify which group of bars can still be distinct without blurring into one another. By identifying the number of that last resolvable element, which is in our case group 2, element 6, the resolution limit can be calculated from the formulas:

$$Resolution\left(\frac{lp}{mm}\right) = 2^{Group+\frac{element-1}{6}} = 2^{2\frac{5}{6}} = 7.13\,\frac{lp}{mm} \qquad (6)$$

$$Resolution\left(\frac{cy}{mrad}\right) = Collimator\ EFL\ [mm] * 10^{-3} * Resolution\left(\frac{lp}{mm}\right) = 21.56\ \frac{cy}{mrad} \qquad (7)$$

where the Collimator Effective Focal Length (EFL) is 3,025mm, as previously mentioned.

Having in mind that the human visual system can work with contrast which is above 5% (although this cannot be taken as a hard fact, as it depends on the human visual system properties), by analyzing again Figure 10, we can see that the value of the MTF is falling to 5% somewhere around the spatial frequency of 20 cy/mrad, which is similar to the limiting resolution found with the USAF 1951 test target (formula 7).

The USAF target, as shown, is an effective method to quickly estimate the system resolution, but it suffers from some challenges. The most important one is in the fact that the process heavily depends on the observer (and his decision on what target is resolvable), but also on some other things, such as the image focus, which can seriously affect the measurement, as shown in Figure 11.

While the MWIR system and the focal length forming the target image were the same for both images, the focus of the object (target) for the right image was not done properly. As a result, the limiting resolution derived from this image is lower than previously estimated. While the matter of the focus is also affecting the MTF calculations (Holst, 2008), (Haefner, 2018), in this case of the USAF1951 test target, it will give a completely wrong picture of the system capability.

Real scenario images

In order to illustrate the image performance of the multi-sensor imaging system (MSIS) in a real scenario, the system tested in the laboratory (a Visible and an SWIR camera, without an MWIR sensor) was installed outdoors and set to monitor the scene approximately 12 kilometers apart from the MSIS position.

Figure 12 – Visible camera image
Рис. 12 – Изображение с камеры видеонаблюдения
Слика 12 – Слика снимљена видљивом камером

Figure 13 – SWIR camera image
Рис. 13 – Изображение с SWIR камеры
Слика 13 – Слика снимљена SWIR камером

What is clearly distinguishable in the pictures are vehicles, buses, pedestrians and the general background characteristics (buildings, trees, etc.). Since this type of system is generally designed to perform detection, recognition and identification of objects, it is safe to say that the system is performing well for the purpose it was built for. Comparing the images in VIS and SWIR, we can conclude that the SWIR image is richer in detail, which is expectable regarding the comments stated earlier in the paper. During the tests, we also noticed remarkable advantage of the SWIR image in the presence of fog.

Conclusions

The theoretical analysis and laboratory measurements of electro-optical system performance have demonstrated that the MTF can be an effective analytical tool.

Theoretical calculations have shown that the increase of the focal length results in the increase of the F-number ($F_{\#}$), and for that reason the diffraction of the lens system becomes the dominant limitation factor compared to the detector limitation. In that way, we have identified the maximal frequency for our system.

The MTF measurements in the electro-optical laboratory have given some valuable information. Besides a visual confirmation on the system limiting elements (where the lower diffraction lines prove they limit the system, and not the detector), the comparison of the curves for VIS, SWIR and MWIR cameras has shown that the SWIR and MWIR lenses have supreme optical characteristics compared to those of the VIS camera. In addition, the visualization of the results in the form of graphs has clearly shown the areas where the system non-linearity and various forms of data corruption caused the graph to behave unexpectedly.

The resolution measurement using the USAF target has presented the alternative ways to analyze the system performance, although less accurate compared to the MTF measurement methodology.

With the real scenario images, we have confirmed the expectation from the laboratory measurements that the SWIR camera gives a better (richer in detail) image compared to the Visible camera. This was especially obvious for the tests conducted in the degraded environmental conditions (fog).

Taking into account the considerable distance, it can also be concluded that the whole EO system performs well, for the purpose it was built for (detection, recognition and identification of objects). This leads to a general guideline in the design and optimization of EO systems – the key of success is to fully understand the system requirements and the use-cases (Hobbs, 2000), since no system can be designed to provide perfect resolution, contrast, brightness and color fidelity, for any object distance, in all possible environmental conditions. Therefore, the best systems are the ones designed for the exact purpose. Then, through a careful selection of system elements (lens, detector, etc.) and the system parameter optimization, we can influence the system performance.

To further prove the value of the MTF analysis, future efforts will be made to include in the calculations the effects of other system elements such as focus, jitter, and image processing MTFs. It is expected this will provide better matching of measured and calculated MTF results as well as give some additional direction for further EO system optimization.

References

Boreman, G.D. 2001. *Modulation Transfer Function in Optical and Electro-Optical Systems*. Bellingham, WA: SPIE Press. PDF ISBN: 9780819480453, Print ISBN: 9780819441430. Available at: https://doi.org/10.1117/3.419857.

-CI Systems. 2012. *METS - Modular Electro-Optical Test System. Cat. No. 607-5610H.* Carrollton, TX, USA: CI Systems.

Daniels, A. 2018. *Field Guide to Infrared Systems, Detectors, and FPAs, Third Edition*. Bellingham, WA: SPIE Press. ISBN: 9781510618640.

Dufour, J.-Y. 2013. *Intelligent Video Surveillance Systems*. New Jersey, USA: John Wiley & Sons, Inc. Print ISBN:9781848214330, Online ISBN:9781118577851. Available at: https://doi.org/10.1002/9781118577851.

Fiete, R.D. 2010. *Modeling the imaging chain of digital cameras*. Bellingham. WA: SPIE Press. PDF ISBN: 9780819483362, Print ISBN: 9780819483393. Available at: https://doi.org/10.1117/3.868276.

Haefner, D.P. 2018. MTF measurements, identifying bias, and estimating uncertainty. In: *Proc. SPIE 10625, Infrared Imaging Systems: Design, Analysis, Modeling, and Testing XXIX - SPIE Defense + Security,* Orlando, FL, US, 1062506, April 26. Available at: https://doi.org/10.1117/12.2303974.

Hobbs, P.C.D. 2000. *Building Electro-Optical Systems: Making it All Work*. New Jersey, USA: John Wiley & Sons, Inc. Print ISBN: 9780471246817, Online ISBN: 9780471224297. Available at: https://doi.org/10.1002/0471224294.

Holst, G.C. 2008. *Electro-optical imaging system performance, 5th edition*. Winter Park, FL: JCD Publishing. ISBN: 9780970774965.

Holst, G.C. 2011. Imaging system fundamentals. *Optical Engineering*, 50(5), 052601. Available at: https://doi.org/10.1117/1.3570681.

Kohm, K. 2004. Modulation transfer function measurement method and results for the Orbview-3 high resolution imaging satellite. In: *ISPRS Archives, XXth ISPRS Congress Technical Commission I*, Istanbul, Turkey, 35, pp.7-12, July 12-23 [online]. Available at: https://www.isprs.org/proceedings/XXXV/congress/comm1/papers/2.pdf. [Accessed: 07 July 2020].

McDaniel, R., Hughes, R. & Seibel, E. 2006. EO/IR sensors enhance border security applications. In: *Proceedings Volume 6203, Optics and Photonics in Global Homeland Security II - Defense and Security Symposium*, Orlando, FL, US, 620304, May 5. Available at: https://doi.org/10.1117/12.673678.

Pađen, N., Perić, D. & Milosavljević, M. 2019. Imaging System Performance Analysis Using Modulation Transfer Function. In: *Sinteza 2019 - International Scientific Conference on Information Technology and Data Related Research*, Novi Sad, Serbia, pp.567–574, April 20. Available at: https://doi.org/10.15308/Sinteza-2019-567-574.

Perić, D., Livada, B., Perić, M., & Vujić, S. 2019. Thermal Imager Range: Predictions, Expectations, and Reality. *Sensors*,19(15), 3313. Available at: https://doi.org/10.3390/s19153313.

Perić, D., Livada, B., Radisavljević, M. & Vujić, S. 2018. Performance Comparison of SWIR Vision Systems Using MTF Analysis. In: *Proceedings of Papers – 5th International Conference on Electrical, Electronicand Computing Engineering, IcETRA*N, Palić, Serbia, pp.762-765, June 11-14. ISBN: 978-86-7466-752-1 [online]. Available at: https://www.etran.rs/common/Zbornik%20ETRAN%20IC%20ETRAN-18-final.pdf. [Accessed: 07 July 2020].

Schowengerdt, R.A., Archwamety, C. & Wrigley, R.C. 1985. Landsat Thematic Mapper image-derived MTF. *Photogrammetric Engineering and Remote Sensing,* 51(9),pp.1395-1406 [online]. Available at: https://www.asprs.org/wp-content/uploads/pers/1985journal/sep/1985_sep_1395-1406.pdf [Accessed: 07 July 2020].

Shumaker, D.L. & Wood, J.T. 1988. Overview Of Current IR Analysis Capabilities And Problem Areas. In: *Proceedings Volume 0890, Infrared Systems and Components II,* Los Angeles, CA, US, pp.74-80, May 3. Available at: https://doi.org/10.1117/12.944272.

-United States Department of Defense. 1950. *MIL-STD-150A: Military Standard Photographic Lenses*. Washington D.C: Armed Forces Supply Support Center.

ФУНКЦИЯ МОДУЛЯЦИИ ПЕРЕДАЧИ ПРИ АНАЛИЗЕ ЭЛЕКТРООПТИЧЕСКИХ СИСТЕМ

Неделько С. Пайжен[аб], **корреспондент**, *Драгана* Б. Перич[а], *Бранко* Г. Ливада[а], *Милан* М. Милосавлевич[б]

[а] Институт «Влатаком», г. Белград, Республика Сербия

[б] Университет «Сингидунум», кафедра электротехники и вычислительной техники, г. Белград, Республика Сербия

РУБРИКА ГРНТИ: 47.00.00 ЭЛЕКТРОНИКА. РАДИОТЕХНИКА;
47.57.00 Инфракрасная техника,
47.57.29 Приборы ночного видения.
27.00.00 МАТЕМАТИКА;
27.35.00 Математические модели естественных наук и технических наук. Уравнения математической физики,
27.35.47 Уравнения переноса.

ВИД СТАТЬИ: оригинальная научная статья

Резюме:

Введение/цель: Функция модуляции передачи (MTF) является полезным инструментом для анализа эффективности системы формирования изображений. Она используется при разработке электрооптических систем (ЕО), проверке целевых параметров системы, а также в задачах оптимизации тестируемой системы. Данная методология основана на теории линейных систем и обеспечивает возможность разделения анализа эффективности сложных систем ЭО на подсистемы. В настоящей статье представлена и объяснена методология MTF, а также приведены примеры измерений, произведенных в электрооптической лаборатории. Измерения MTF проводились с помощью трех видов камер в разных спектральных диапазонах, после чего результаты сравнивались с прогнозируемыми моделями и теоретическими пределами системы формирования изображения.

Методы: Лабораторные измерения и теоретическая математическая статистика.

Результаты: Результаты измерений были дополнительно проанализированы на основании проведенных лабораторных и теоретических результатов.

Выводы: Проведенные измерения показали, что рассчитанная предельная частота и кривая MTF представляют собой границу реальных измеренных характеристик эффективности системы. Таким образом, исследование подтвердило, что MTF может способствовать выявлению системных ограничений и узких мест, а также повышению общей эффективности системы. Разработаны рекомендации по дальнейшей оптимизации систем формирования изображений.

Ключевые слова: функция модуляции передачи, тестовая цель USAF 1951, электрооптика.

МОДУЛАЦИОНА ФУНКЦИЈА ПРЕНОСА У АНАЛИЗИ ПЕРФОРМАНСИ ЕЛЕКТРООПТИЧКИХ СИСТЕМА

Недељко С. Пађен[аб], **аутор за преписку**, *Драгана* Б. Перић[а], *Бранко* Г. Ливада[а], *Милан* М. Милосављевић[б]

[а] Институт Влатаком, Београд, Република Србија

[б] Универзитет Сингидунум, Катедра за електротехнику и рачунарство, Београд, Република Србија

ОБЛАСТ: електрооптика, електроника, математика
ВРСТА ЧЛАНКА: оригинални научни рад

Сажетак:

Увод/циљ: Модулациона функција преноса (MTF) користан је алат за анализу перформанси система за обраду слике. Користи се у дизајнирању електрооптичких (ЕО) система, при провери циљаних параметара система, али и у задацима оптимизације тестираних система. Ова методологија, заснована на теорији линеарних система, омогућава да се анализа перформанси сложених ЕО система подели на подсистеме. MTF методологија најпре је представљена и објашњена, а затим је приказано мерење извршено у електрооптичкој лабораторији. MTF мерења изведена су на три типа камера, у различитим спектралним опсезима, након чега су резултати упоређени са очекиваним моделима и теоријским ограничењима система за обраду слике.

Методе: Лабораторијска мерења и теоријска математичка израчунавања.

Резултати: На основу лабораторијских и теоријских резултата додатно су анализирани резултати мерења.

Закључак: Мерења су доказала да израчуната гранична фреквенција и кривуља MTF представљају границу за стварне перформансе система. Потврђено је да MTF може бити погодан за проналажење ограничења и уских грла система, као и за побољшање укупних перформанси система.

Кључне речи: модулациона функција преноса, тестна мета УСАФ 1951, електрооптика.

Paper received on / Дата получения работы / Датум пријема чланка: 09.06.2020.
Manuscript corrections submitted on / Дата получения исправленной версии работы / Датум достављања исправки рукописа: 10.07.2020.
Paper accepted for publishing on / Дата окончательного согласования работы / Датум коначног прихватања чланка за објављивање: 11.07.2020.

INFLUENCE OF PRE-PROCESSING ON ANOMALY-BASED INTRUSION DETECTION

Danijela D. Protić
Serbian Armed Forces, General Staff,
Department for Telecommunication and Informatics (J-6),
Center for Applied Mathematics and Electronics,
Belgrade, Republic of Serbia,
e-mail: adanijela@ptt.rs,
ORCID iD: https://orcid.org/0000-0003-0827-2863

DOI: 10.5937/vojtehg68-27319; https://doi.org/10.5937/vojtehg68-27319

FIELD: Computer Sciences
ARTICLE TYPE: Original scientific paper

Abstract:

Introduction/purpose: The anomaly-based intrusion detection system detects intrusions based on a reference model which identifies the normal behavior of a computer network and flags an anomaly. Machine-learning models classify intrusions or misuse as either normal or anomaly. In complex computer networks, the number of training records is large, which makes the evaluation of the classifiers computationally expensive.

Methods: A feature selection algorithm that reduces the dataset size is presented in this paper.

Results: The experiments are conducted on the Kyoto 2006+ dataset and four classifier models: feedforward neural network, k-nearest neighbor, weighted k-nearest neighbor, and medium decision tree. The results show high accuracy of the models, as well as low false positive and false negative rates.

Conclusion: The three-step pre-processing algorithm for feature selection and instance normalization resulted in improving performances of four binary classifiers and in decreasing processing time.

Key words: anomaly-based intrusion detection, machine learning, Kyoto 2006+.

Introduction

Intrusion detection systems (IDSs) monitor computer network behavior to perform diagnostics of the security status and protect the network from malicious activities or various anomalies. Intrusion detection systems can be divided into two basic groups. Misuse or signature based IDSs detect malware based on knowledge accumulated from known attacks. Anomaly based IDSs detect deviations from a model of usual network behavior. The goal of anomaly detection is to build a statistical model of normal network behavior and look for activities which deviate from the created model (Protić & Stanković, 2020, p.7). The main disadvantage of the signature based IDS is a difficulty to detect unknown attacks. The biggest challenge in anomaly detection is to identify what is considered normal. Machine learning (ML) based binary classifiers can detect anomalies with a high accuracy of prediction. In supervised learning, the number of training instances collected over a period of time can be large, which makes the evaluation of the models computationally expensive. Feature selection reduces the training set, which speeds up the processing time and increases the accuracy of the classifiers. This paper shows the results of the experiments of the three-step feature selection and instances normalization pre-processing algorithm conducted on the Kyoto 2006+ dataset and four machine learning models, namely: feedforward neural network (FNN), k – nearest neighbor (k-NN), weighted k-NN (wk-NN), and medium decision tree(DT). Accuracy (ACC), false positive rate (FPR), false negative rate (FNR), and processing time are given.

Feature selection and instances normalization: Three-step pre-processing algorithm

One of the major issues in supervised ML is a large number of instances in the training set. The aim of feature selection is to reduce the dataset size and remove irrelevant features. Furthermore, raw data have to be pre-processed before being fed to the input of the model so that effects of one feature cannot dominate the others. In this paper, a three-step pre-processing algorithm for feature selection is presented. The algorithm is given as follows:

1 Identify and discard all irrelevant features;
2 Remove features which cannot be normalized into the range [-1,1];
3 Normalize instances into the range [-1,1] by applying the hyperbolic tangent function:

$$\tanh(n) = \frac{2}{1+e^{2n}} - 1, \quad (1)$$

where *n* is the number of instances in the dataset.

Feature selection improves performances of the classifier, saves memory space and decreases processing time. Additionally, instances normalization speeds up the model training and reduces the domination of one feature over the other ones.

Data collection: The Kyoto 2006+ dataset

The Kyoto 2006+ dataset contains records of real network traffic data collected from November 2006 to December 2015 at five different computer networks inside and outside the Kyoto University (Takakura, 2020) (Protić, 2018, pp.587-589). During the observation period, over 50 million sessions of normal traffic, 43 million sessions of known attacks and 426 thousand sessions of unknown attacks were recorded (Protić & Stanković, 2018, p.44). The dataset consists of 14 statistical features derived from the KDD Cup '99 dataset (Table 1) and 10 additional features which enable more efficient investigation (Table 2) (Ashok Kumar & Venugopalan, 2018), (Song et al, 2011, pp.29-36).

Table 1 – The Kyoto 2006+ Dataset – first 14 features
Таблица 1 – Набор данных Kyoto 2006+ - 14 первых функций
Табела 1 – Kyoto 2006+ база података – првих 14 атрибута

No	Feature	Description
1	Duration	The length of the connection (seconds).
2	Service	The connection's server type (dns, ssh, other).
3	Source bytes	The number of data bytes sent by the source IP address.
4	Destination bytes	The number of data bytes sent by the destination IP address.
5	Count	The number of connections whose source IP address and destination IP address are the same to those of the current connection in the past two seconds.
6	Same_srv_rate	% of connections to the same service in the Count feature.
7	Serror_rate	% of connections that have 'SYN' errors in the Count feature.
8	Srv_serror_rate	% of connections that have 'SYN' errors in the Srv_count (% of connections whose service type is the same to that of the current connections in the past two seconds) feature.
9	Dst_host_count	Among the past 100 connections whose destination IP address is the same to that of the current connection, the number of connections whose source IP address is also the same to that of the current connection.
10	Dst_host_srv_count	Among the past 100 connections whose destination IP address is the same to that of the current connection, the number of connections whose service type is also the same to that of the current connection.
11	Dst_host_same_src_port_rate	% of connections whose source port is the same to that of the current connection in the Dst_host_count feature.
12	Dst_host_serror_rate	% of connections that have 'SYN' errors in the Dst_host_count feature.
13	Dst_host_srv_serror_rate	% of connections that have 'SYN' errors in the Dst_host_srv_count feature.
14	Flag	The state of the connection at the time the connection was written (tcp, udp).

Table 2 – The Kyoto 2006+ Dataset – additional 10 features
Таблица 2 – Набор данных Kyoto 2006+ - 10 дополнительных функций
Табела 2 – Kyoto 2006+ база података – додатних 10 атрибута

No	Feature	Description
1	IDS_detection	Reflects if IDS triggered an alert for the connection; '0' means any alerts were not triggered and an arabic numeral means the different kind of alerts. The arenthesis indicates the number of the same alert.
2	Malware_detection	Indicates if malware, also known as malicious software, was observed at the connection; '0' means no malware was observed, and string indicates the corresponding malware was observed at the connection. The parenthesis indicates the number of the same malware.
3	Ashula_detection	Means if shellcodes and exploit codes were used in the connection; '0' means neither shellcode nor exploit code were observed, and an arabic numeral means the different kinds of the shellcodes or exploit codes. The parenthesis indicates the number of the same shellcode or exploit code.
4	Label	Indicates whether the session was attack or not; '1' means normal. '-1' means a known attack was observed in the session, and '-2' means an unknown attack was observed in the session.
5	Source_IP_Address	Means the source IP address used in the session. The original IP address on IPv4 was sanitized to one of the Unique Local IPv6 Unicast Addresses. Also, the same private IP addresses are only valid in the same month; if two private IP addresses are the same within the same month, it means their IP addresses on IPv4 were also the same, otherwise are different.
6	Source Port Number	Indicates the source port number used in the session.
7	Destination IP Address	It was also sanitized.
8	Destination Port Number	Indicates the destination port number used in the session.
9	Start Time	Indicates when the session was started.
10	Duration	Indicates how long the session was being established.

The proposed algorithm discards all categorical features as well as features for further investigation, excluding the Label feature (step 1), cuts all features containing instances that cannot be normalized into the range [-1,1] (step 2) and normalize the rest of instances (step 3). Out of 24 features of the Kyoto 2006+ data set, 17 features are left after the first pre-processing algorithm step and nine features (5-13) are left after the pre-processing is done. The Label feature is used for the detection of anomalies. Scaled instances not only reduce the effects of one feature to the others but speed up the FNN since the network training is more efficient if normalization is performed on inputs. If the number of inputs is ≥3, the sigmoid functions used in the hidden layer become easily saturated. If the saturation happens at the beginning of the training, the gradients will be small which may slow down the network training (Protić & Stanković, 2020, p.9).Also, instances are scaled due to the fact that distances in the wk-NN model lose accuracy because of a small difference between the farthest and the nearest neighbors.

Classifier Models

In supervised machine learning, classifiers can be divided into two groups. Lazy learners, such as the k-NN and the wk-NN, do not focus on constructing a general model, but store the training data and weight until a test set appears. Eager learners, such as the FNN, construct a classification model before getting data for predictions.

k-Nearest Neighbor

The k-NN stores all instances corresponding to the training data into the *n*-dimensional space. Classification is computed on a simple majority vote of the k-NN of each point, based on the Euclidean distance measure given with (Protić & Stanković, 2020, p.9):

$$d\left(x_i, y_i\right) = \sqrt{\sum_{s=1}^{p} \left(x_{is} - y_{is}\right)^2} \; . \qquad (2)$$

The prediction speed of the k-NN is medium as well as memory usage. Interpretability of the classifier is hard. In the experiments, the distinction between classes is medium, and the number of neighbors is set to 10 (Protić & Stanković, 2018, p.48).

Weighted k-Nearest Neighbor

The main idea of the wk-NN is to extend the k-NN so that the instances within the training set which are particularly close to the new instance should get a higher weight in the decision than more distant ones (Tsigkritis et al, 2018, pp.70-84). The distances are transformed into the weights as follows:

$$w = \frac{1}{d\left(\mathbf{x}, \mathbf{y}\right)^2} \; . \qquad (3)$$

The wk-NN classifier adapts as the new training data is collected, which allows the algorithm to respond quickly to changes in the input during real-time use. In contrast with the fast training stage, the algorithm requires expensive testing. All the cost of the algorithm is in the processing time. All characteristics of the classifier are the same as for the k-NN model except flexibility which is also medium (medium distinctions between classes using a distance weight) (Protić & Stanković, 2018, p.48).

Medium Decision Tree

The Decision Tree is one of the graph-like algorithms which use branching methods to illustrate every possible outcome of decisions, where nodes represent features, links represent decision rules and leafs represent outcomes. The Iterative Dichotomy 3 algorithm (ID3) calculates entropy and information gain to build a tree (Protić & Stanković, 2020, p.9). Entropy is a measure which controls how the tree decides to split the data. If the target feature can take on *k* different values, then the entropy of the *S* relative to this *k*-wise classification is given as follows:

$$Entropy\ (S) = -\sum_{i=1}^{k} p_i \log_2 (p_i), \tag{4}$$

where p_i represents the proportion of *S* belonging to the class *i*. The information gain represents the expected reduction in entropy based on the decrease in entropy after the dataset is split on the feature (See Eq.5).

$$Gain\ (S, A) = Entropy\ (S) - \sum_{v \in avlues\ (A)} \frac{|S_v|}{|S|} \cdot Entropy\ (S_v). \tag{5}$$

The feature with the highest information gain will split first. The *Gain*(*S*,*A*) of a feature *A* relative to a collection of examples *S* provides information about the target function value; given the value of some other feature *A* that splits *S* into the subsets S_v (Protić & Stanković, 2020, p.10).The characteristics of the medium DT classifier are: fast prediction speed, low memory usage, easy interpretability and medium model flexibility, i.e. medium number of leaves for finer distinctions between classes. The maximum number of splits is 20 (Protić & Stanković, 2018, p.48).

Feedforward Neural Network

The objective of the FNN is to minimize an output error in accordance with the back-propagation algorithm. The FNN transfer function used in the experiments is given with Eq. 6.

$$y_i(\mathrm{w}, \mathrm{W}) = F_i\left(\sum_{j=1}^{q} W_{ij} f_j\left(\sum_{l=1}^{m} w_{ji} x_l + w_{j0}\right) + W_{f0}\right). \tag{6}$$

where x_l are inputs, y_i are outputs, **w** and **W** are weight matrices, f_j and F_i denote the transfer functions of hidden and output layers, *m* represents the number of inputs, *q* represents the number of outputs, and w_{j0} and W_{f0} denote biases. The objective of the FNN presented in this paper is to minimize the output error in accordance with the Levenberg-Marquardt (LM) algorithm (Levenberg, 1944, pp.164-168) (Marquardt, 1963, pp.431-441).The LM algorithm performs a combined training process: around the area with complex curvature, the LM switches to the gradient descent (GD) algorithm until the local curvature is proper to make a quadratic approximation. Then it approximately becomes the Gauss-Newton(GN) algorithm which can speed up the convergence (Kwaket al, 2011, pp.327-340). The structure of the FNN presented in this paper is 9 inputs, 9 weights in the hidden layer and one output. The transfer function in the hidden layer is tangent hyperbolic while the output layer's transfer function is linear.

Experiments

A key criterion which differentiates classification techniques is prediction accuracy which represents the ratio of the number of instances correctly classified to the total number of instances (See Eq. 7).

$$ACC = \frac{TP + TN}{TP + TN + FP + FN}, \tag{7}$$

where TP (true positive) represents the number of positive samples correctly predicted by the classifier, FN (false negative) represents the number of positive samples wrongly predicted as negative, FP (false positive) represents the number of negative samples wrongly predicted as positive and TN represents the number of negative samples correctly predicted by the model (Ambedkar & Kishore Babu, 2015, pp.25-29). Additionally, processing time (t), false positive rate (FPR) and false negative rate (FNR) are also measurement criteria (Nguyen & Armitage, 2008, p.56). Processing time (t) is a sum of the training and testing time. FPR represent the fraction of negative samples predicted as a positive class (See Eq. 8).

$$FPR = \frac{FP}{TN + FP}. \tag{8}$$

FPR is a measure of accuracy for a test. It is defined as the probability of rejecting the null hypothesis, i.e. it is a probability that a false alarm will be raised; a positive result will be given when the true value is negative (Split, 2020). Ideally, FPR should be low (0.1 or less). A low FPR indicates that the classifier does not classify many irrelevant examples as relevant (Shirabad et al, 2007, p.198).

FNR represent the fraction of positive samples predicted as a negative class (Eq.9):

$$FNR = \frac{FN}{TP + FN} . \quad (9)$$

FNR is the probability that a true positive will be missed by the classifier.

The experiments presented here are conducted on three pre-processed daily records from the Kyoto 2006+ dataset (See Table 3) and performed using Intel(R), Core(TM) i7-2620M CPU 2.7GHz processor, with 16GB RAM Installed memory.

Table 3 – Daily records – number of instances
Таблица 3 – Количество экземпляров в день
Табела 3 – Број инстанци по дану

Day	**N*umber* of instances**
03/02/2007	57278
14/02/2007	58317
27/02/2007	57278

All classifiers are trained so that 70% of daily records are used for training and 30% are used for testing. The results on accuracy, FPR, FNR, and processing time are given in Figures 1-4, respectively.

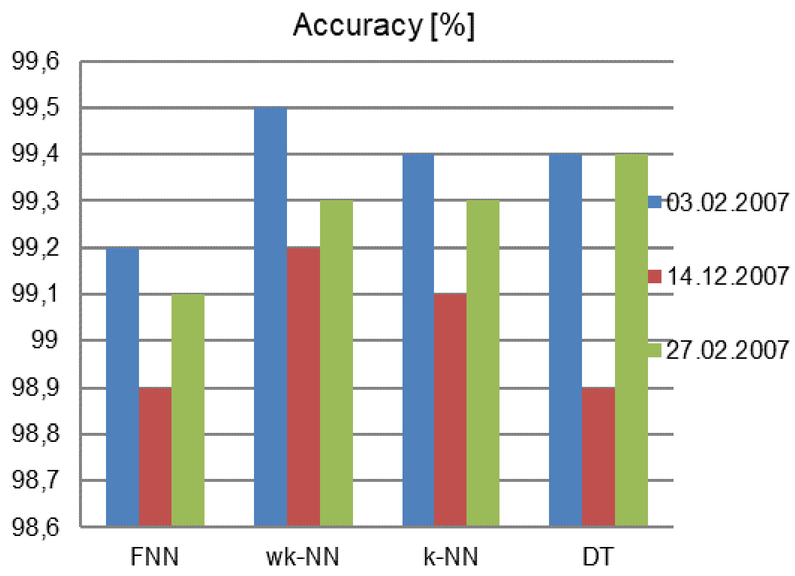

Figure 1– Accuracy
Рис. 1 – Точность
Слика 1 – Тачност

As it can be seen from Figure 1, the wk-NN has the highest accuracy of all of the models (up to 99.5%). However, the accuracies of both k-NN and DT are also high (99.4%). The FNN is less accurate than the other models but its accuracy is still very high (99.2%).

Low FPR (see Figure 2) indicates that the models classify a small number of relevant examples as irrelevant, so the probability a false alarm will be raised is very low. Although all models show a low probability of false alarm, the k-NN model classifies the highest number of irrelevant examples as relevant.

FNR has the highest value for the DT model, trained on the 14.02.2007 dataset. The lowest value of FNR gives the FNN trained on the 27.02.2007 dataset. However, FNRs of all classifiers are lower than 0.8%, and lower than 0.2% if DT is not considered as relevant.

As it is expected, the processing time is high for the lazy learners (the k-NN and the wk-NN) and exceeds 50s. The FNN and the DT show significantly shorter processing time (more than 10 times).

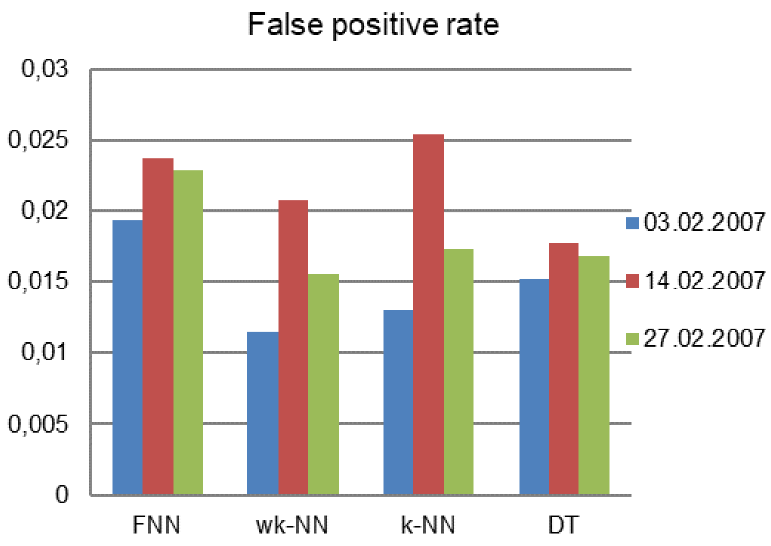

Figure 2 – False positive rate
Рис. 2 – Ложноположительный показатель
Слика 2 – Мера лажно позитивних детекција

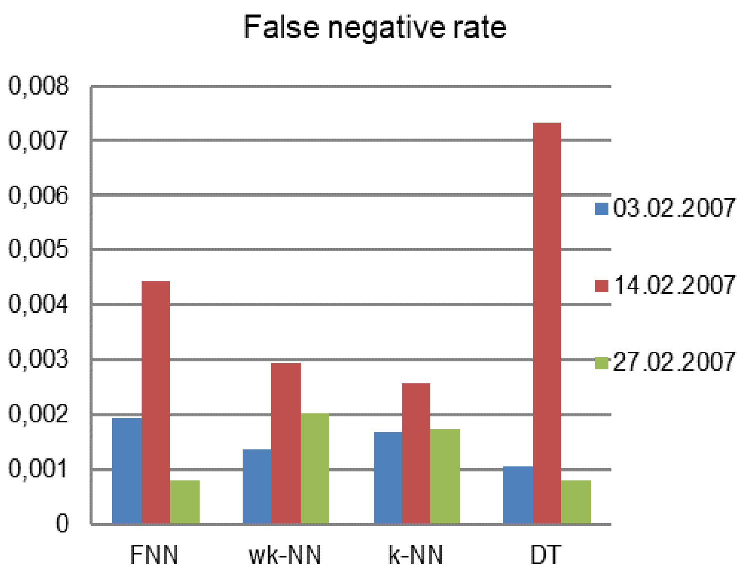

Figure 3 – False negative rate
Рис. 3 – Ложноотрицательный показатель
Слика 3 – Мера лажно негативних детекција

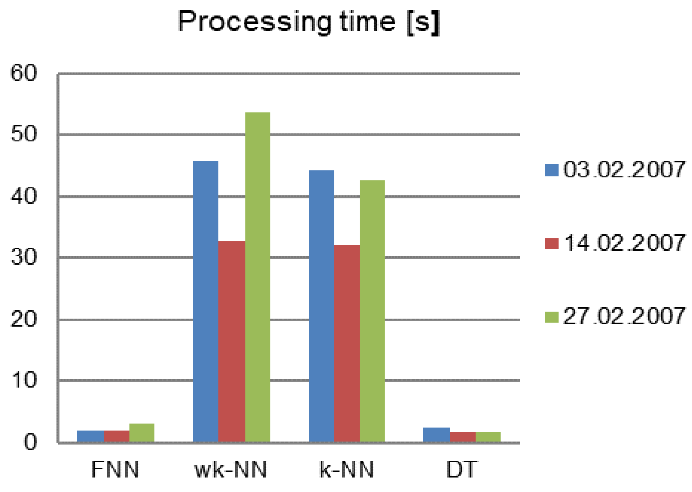

Figure 4 – Processing time
Рис. 4 – Время обработки
Слика 4 – Време обраде

Conclusion

The three-step pre-processing algorithm for feature selection and instance normalization resulted in improving performances of four binary classifiers and in decreasing processing time.

The algorithm reduced three training sets derived from the Kyoto 2006+ dataset. Accuracy, false positive rate, false negative rate, and processing time are given as measures of the performances of the classifiers.

The results show the highest accuracy of the wk-NN model. Low false positive rates indicate that the models classify a small number of relevant examples as irrelevant. FNR is significantly higher for the DT model than for FNN, k-NN, and wk-NN models.

The processing time of the lazy learners is significantly higher than the processing time of eager learners.

References

Ambedkar C. & Kishore Babu, V.2015. Detection of Probe Attacks Using Machine Learning Techniques. *International Journal of Research Studies in Computer Science and Engineering*, 2(3), pp.25-29 [online]. Available at: https://www.arcjournals.org/pdfs/ijrscse/v2-i3/7.pdf [Accessed: 29 June 2020].

Ashok Kumar, D. & Venugopalan, S.R. 2018.*A Novel algorithm for Network Anomaly Detection using Adaptive Machine Learning*. Singapore: Springer Singapore.

Kwak, Y.T., Hwang, J.W., & Yoo, C.J. 2011. A new damping strategy of Levenberg-Marquardt algorithm for multilayer perceptrons. *Neural Network World*, 21(4), pp.327-340. Available at: https://doi.org/10.14311/NNW.2011.21.020.

Levenberg, K. 1944. A method for the solution of certain problems in least squares. *Quarterly of Applied Mathematics*, 2, pp.164-168 Available at: https://doi.org/10.1090/qam/10666.

Marquardt, D.W. 1963. An Algorithm for Least-Squares Estimation of Nonlinear Parameters. *Journal of the Society for Industrial and Applied Mathematics*, 11(2), pp.431-441 [online]. Available at: https://www.jstor.org/stable/2098941?seq=1 [Accessed: 29 June 2020].

Nguyen, T.T.T. & Armitage, G. 2008. A Survey of Techniques for Internet Traffic Classification using Machine Learning. *IEEE Communications Surveys & Tutorials*, 10(4), pp.56-76. Available at: https://doi.org/10.1109/SURV.2008.080406.

Protić, D.D. 2018. Review of KDD CUP '99, NSL-KDD and KYOTO 2006+ Datasets. *Vojnotehnički glasnik/Military Technical Courier*, 66(3), pp.580-596. Available at: https://doi.org/10.5937/vojtehg66-16670.

Protić, D. & Stanković, M. 2018. Anomaly-Based Intrusion Detection: Feature Selection and Normalization Influence to the Machine Learning Models Accuracy. *European Journal of Formal Sciences and Engineering*, 2(3), pp.101-106. Available at: http://dx.doi.org/10.26417/ejef.v2i3. p101-106.

Protić, D. & Stanković, M. 2020. Detection of Anomalies in the Computer Network Behavior. *European Journal of Formal Sciences and Engineering*, 4(1), pp.7-13. Available at: http://dx.doi.org/10.26417/ejef.v4i1. p7-13.

Song, J., Takakura, H., Okabe, Y., Eto, M., Inoue, D. & Nakao, K. 2011. Statistical Analysis of Honeypot Data and Building of Kyoto 2006+ Dataset forNIDS Evaluation. In: *Proc. 1st Work-shop on BADGES - Building Anal. Datasets and Gathering Experience Returns for Security*, Salzburg, pp.29-36, April 10-13. Available at: https://doi.org/10.1145/1978672.1978676.

-Split. 2020. *What is false positive rate?* [online]. Available at: https://www.split.io/glossary/false-positive-rate/ [Accessed: 29 June 2020].

Shirabad, J.S., Lethbridge, T.C. & Matwin, S. 2007. Modeling Relevance Relations Using Machine Learning Techniques. In: Zhang, D. & Tsai, J.J.P. (Eds.) *Advances in Machine Learning Applications in Software Engineering*, *Chapter VIII*, pp.168-207. Hershey, PA: Idea Group Pub. (IGI Global research collection). Available at: https://doi.org/10.4018/978-1-59140-941-1.ch008.

-Takakura. 2020. *Traffic Data from Kyoto University's Honeypots* [online]. Available at: http://www.takakura.com/kyoto_data/ [Accessed: 29.06.2020].

Tsigkritis, T., Groumas G. & Schneider M. 2018. On the Use of k-NN in Anomaly Detection. *Journal of Information Security*, 9(1), pp.70-84. Available at: https://doi.org/10.4236/jis.2018.91006.

РОЛЬ ПРЕДВАРИТЕЛЬНОГО ПРОЦЕССИРОВАНИЯ ПРИ ОБНАРУЖЕНИИ АТАК, ОСНОВАННЫХ НА АНОМАЛИЯХ

Даниела Д. Протич

Вооруженные силы Республики Сербия, Генеральный штаб,
Управление информатики и телекоммуникаций (J-6),
Центр прикладной математики и электроники,
г. Белград, Республика Сербия

РУБРИКА ГРНТИ: 20.00.00 ИНФОРМАТИКА;
20.15.05 Информационные службы, сети, системы в целом
ВИД СТАТЬИ: оригинальная научная статья

Резюме:

Введение/цель: Система обнаружения атак, основанных на аномалиях, выявляет вторжение в компьютерную сеть, основываясь на эталонной модели, которая идентифицирует нормальное поведение компьютерной сети, детектируя аномалию. Модели машинного обучения классифицируют вторжения или злоупотребления по двум группам: нормальный трафик или аномалия. Оценка моделей классификаторов является достаточно сложным процессом, так как в сложных компьютерных сетях большое количество обучающих записей.

Методы: В данной статье представлен алгоритм выбора атрибутов, который уменьшает множество данных.

Результаты: Эксперименты проведены на множестве данных Kyoto 2006+ базы и на четырех моделях классификаторов, с помощью следующих методов: метод нейронной сети с прямой связью, метод k-ближайшего соседа, метод взвешенных k-ближайших соседей и метод дерева принятия решений. Результаты проведенных экспериментов показали высокую точность моделей.

Выводы: Трехступенчатый алгоритм предварительной обработки для выбора атрибутов и нормализации экземпляров обеспечил улучшение характеристик четырех бинарных классификаторов и сократил время обработки данных.

Ключевые слова: обнаружение аномалий, машинное обучение, KYOTO 2006+.

УТИЦАЈ ПРЕПРОЦЕСУИРАЊА НА ДЕТЕКЦИЈУ НАПАДА ЗАСНОВАНИХ НА АНОМАЛИЈАМА

Данијела Д. Протић

Војска Србије, Генералштаб, Управа за телекомуникације и информатику (J-6), Центар за примењену математику и електронику,
Београд, Република Србија

ОБЛАСТ: рачунарске науке, информационе технологије
ВРСТА ЧЛАНКА: оригинални научни чланак

Сажетак:

Увод/циљ: Систем за детекцију упада који се заснива на детекцији аномалије открива напад на рачунарску мрежу на основу референтног модела који идентификује нормално понашање рачунарске мреже и детектује аномалију. Модели машинског учења класификују упаде или злоупотребе у две групе: групу нормалног саобраћаја и групу аномалија. У сложеним рачунарским мрежама број инстанци у обучавајућем скупу може бити велики, што евалуацију модела класификатора чини тешком.

Методе: У раду је приказан алгоритам за избор атрибута који смањује величину скупа података.

Резултати: Експерименти су изведени на скупу података из Kyoto 2006+ базе и на четири модела класификатора: моделу feedforward неуронска мрежа, моделу к-најближих суседа, моделу пондерисаних к-најближих суседа и моделу стабла одлучивања. Резултати показују високу тачност модела.

Закључак: Препроцесуирање трокорачним алгоритмом за избор атрибута и нормализацију инстанци резултирало је побољшањем перформанси четири бинарна класификатора и смањило време процесуирања.

Кључне речи: детекција аномалија, машинско учење, Kyoto 2006+.

Paper received on / Дата получения работы / Датум пријема чланка: 30.06.2020.
Manuscript corrections submitted on / Дата получения исправленной версии работы/ Датум достављања исправки рукописа: 11.07.2020.
Paper accepted for publishing on / Дата окончательного согласования работы / Датум коначног прихватања чланка за објављивање: 13.07.2020.

СТРУЧНИ РАДОВИ

ПРОФЕССИОНАЛЬНЫЕ СТАТЬИ

PROFESSIONAL PAPERS

APPLICATION OF GEOINFORMATION TECHNOLOGY IN THE ARMED FORCES IN THE REPUBLIC OF KAZAKHSTAN

Erlan S. Zakiev[a], *Serikhan* K. Kozhakhmetov[b]

[a] National Defence University named after the First President of the Republic of Kazakhstan - Elbasi, Faculty of Digital Technology and Security of Information Systems, Department of Simulation and Information Systems, Nur-Sultan, Republic of Kazakhstan,
e-mail: zakiev-astana@bk.ru, **corresponding author**,
ORCID iD: https://orcid.org/0000-0002-4518-3985

[b] National Defence University named after the First President of the Republic of Kazakhstan - Elbasi, Faculty of Logistics Troops, Department of Logistics, Nur-Sultan, Republic of Kazakhstan,
e-mail: skozhahmetov@bk.ru,
ORCID iD: https://orcid.org/0000-0001-9038-8165

DOI: 10.5937/vojtehg68-26559; https://doi.org/10.5937/vojtehg68-26559

FIELD: IT, Geoinformation Technology
ARTICLE TYPE: Professional Paper

Abstract:

Introduction / purpose: This article is written in order to acquaint readers with geoinformation technology in the process of organizing topographic and geodetic support, as well as to make recommendations and suggestions that will enable the formation of an effective and comprehensive system of geoinformation support for the Armed Forces, other troops and military units of the Republic of Kazakhstan.

Methods: The analytical approach was used in the analysis of the causes of local warfare, armed conflicts and use of high-precision weapons in combat operations where sophisticated reconnaissance, geoinformation systems and communications are involved. The conclusions were also drawn on the basis of the analysis of the historical development of geoinformation technologies.

Results: The article provides a brief overview of geospatial support systems using geoinformation technologies in foreign countries and the topographic service of the Armed Forces of the Republic of Kazakhstan.

Conclusions: Creating a unified state geoinformation space is of high importance since technologies are developing in the direction of the *distribution of geoportals, cloud services and the development of service-oriented architecture systems that will allow the creation of distributed GIS of various kinds. Integration of geographic information systems with rapidly developing systems of remote sensing of the Earth will dramatically increase the capabilities of modern GIS, allowing real-time updating of spatial information, especially in the field of important decision-making.*

Keywords: geoinformation technology, geoinformation support, geoinformation, geoinformation system, geospatial support systems, topographic service, remote sensing systems, Armed Forces of the Republic of Kazakhstan.

Introduction

Analyses of local wars and special operations show that, in the era of high-precision weapons and maneuverable combat operations, the highest importance is given to sophisticated reconnaissance equipment, topographic and geodetic and navigational support and communications. They provide timely detection and recognition of targets, command and control, accuracy and timeliness of strikes. Moreover, they allow all this to be done in real time.

The process of organizing topographic support for military operations in modern conditions, taking into account the experience of counter-terrorism operations in Chechnya, Afghanistan and Iraq, necessarily includes the following aspects:

- timely and complete provision of command and control bodies with topographic and special maps, early production of topographic plans of cities;
- preparation of initial astronomical and geodetic data on the positions of missile forces and artillery and passing them to appropriate command and control bodies;
- providing staff and troops with additional information about the terrain in the form of special photo documents of the terrain, with other reference materials made in direct preparation for combat and during engagement in it;
- provision of appropriate systems for command and control, reconnaissance and guidance by digital electronic maps, digital terrain models;
- organization and timely communication to the troops of the results of topographic reconnaissance of the terrain and the enemy (Evglevsky & Morozov, 2005, p.40).

Topographic-geodetic and cartographic support is one of the main types of ensuring the effective development of economy, strengthening the country's defense and security and is a combination of managerial, production, scientific and educational measures for the creation, storage and communication of cartographic-geodetic data to consumers, including the territory and zones of the economic interests of the Republic of Kazakhstan and territories of foreign states.

The creation and use of cartographic and geodetic data is one of the most important factors contributing to the solution of key tasks of the state policy of the Republic of Kazakhstan, the creation of “Digital Kazakhstan”, an increase in the share of digital products for command and control, a means in automated control systems.

All this dictates the need to take a fresh look at the problem of ensuring the country's security and fully sets the task of maintaining a high level of combat readiness of the Armed Forces, other troops and military units of the Republic of Kazakhstan, their comprehensive support, implementation of measures to develop operational (combat) support in modern conditions.

One of the types of operational (combat) support is topographic and geodetic support, which consists of the supply of geospatial information to the headquarters of the Armed Forces, other troops and military units of the Republic of Kazakhstan, for the effective management and use of weapons.

Nowadays, geographic information systems (GIS) are considered as an effective tool for analyzing various types of data in the study of regional development and the development of integrated solutions. Currently, GIS occupy one of the leading places among various information technologies in the field of management and planning.

As was the case in the Gulf War, technology aspects are at odds with each other. Sometimes with technology, expectations become directly opposite without any kind of warfare. And sometimes a war ends in a very short time due to technology.

One of the most important parts of all types of wars is intelligence and operational information about the enemy and his units, reliable and obtained in a very short time.

The accuracy of the data in this article was proven in the conduct of hostilities by coalition forces in Iraq. In the article “Electronics today; November 1996” Major General Gurbaksh Singh says: “Lessons learned from military history show that victory over the enemy lies in being one step ahead of him in terms of the timeliness of providing information, managing subordinate units, and also the use of information systems.

Information systems and weapon control systems can warn the attack time, and assume the enemy's position with high probability and fairly accurately, in which case it is easier to take the necessary disposition before the enemy and destroy him" (Satyanarayana & Yogendran, 2009).

The preparation and conduct of warfare is impossible without reliable information about the terrain, which is reflected in the combat manuals of the armed forces of many countries of the world, including the United States.

Currently, the United States production facilities provide the creation of more than 300 types of geographic information documents not only for its Armed Forces, but also for the military contingents of the countries participating in joint operations with the American army. So, after the collapse of Yugoslavia, in military cooperation with the American army, military units of 33 countries used the American state standards in the field of cartography and information documents on the terrain created by topographers and surveyors of the United States (Azov, 2003).

According to the United States Ministry of Defense, in armed conflicts and local wars of the new century, the one who will win will be the one who is able to quickly collect multifaceted, constantly changing data on the course of the battle, analyze them, draw the right conclusions, make the right decision and quickly pass it to subordinates. For a guaranteed victory, it is necessary to achieve the so-called information superiority over the enemy, which makes it possible to forestall him in assessing the rapidly changing situation on the battlefield, making the right decision and planning the course of the operation (military operations). The description of the current situation should be large-scale, covering all aspects of the battle, sufficiently generalized and intuitive to decision-makers (Kulabukhov, 2007, pp.13-15).

The development of the modern army, as well as the development of modern society as a whole, is based on the introduction and development of information technology. The most important component of most technologies is the processing of digital terrain information in conjunction with diverse data about the enemy and their troops.

Now that the world is entering the new millennium with an understanding of the benefits of digital imaging, sound and communications, topographic and geodetic support simply cannot be left out of technological progress.

It becomes obvious that geoinformation support is the topographic and geodetic support of the 21st century. It includes aerospace, optical-electronic reconnaissance, satellite communications, digital computer technology, and classical methods of geodesy, cartography, and photogrammetry. An analysis of the tasks solved by the topographic services of the associations of the Armed Forces of the Republic of Kazakhstan in the preparation and during operations and combat operations, as well as the means and methods of solving them, indicates that there is a serious lag in these issues in comparison to the armies of developed countries.

A Geographic Information System (GIS) is a hardware-software human-machine complex that provides for the collection, processing, display and distribution of spatial coordinate data, the integration of information and knowledge about the territory for their effective use in solving scientific and applied problems associated with inventory, analysis, modeling, forecasting, environmental management and territorial organization of a society (Kulabukhov, 2007, pp.13-15).

Geoinformation support involves the circulation of terrain data through channels connected to databases of geographical information systems (GIS). Actually, they are the basis of geoinformation support.

At its core, a GIS is a combination of a geographic or topographic map and an extensive array of digitally expressed heterogeneous information, systematized and linked to the corresponding point in the cartographic image. Digital information about the terrain can be presented in the form of an electronic topographic, geographic, aviation map, city plan, diagram, electronic photographic plan, elevation matrix, matrix of terrain properties, etc.

A GIS performs two important functions: creating a digital map of the area, integrated with an expanded database, and turning a digital map into electronic - visualization - with the possibility of interactive work with the user. Many other functions are based on these two functions implemented with GIS (Goodchild & Kemp, 1990).

The term “geographic information system” (GIS), which appeared in the early 60s of the last century, underwent quite a lot of changes in its meaning, and for a long time did not have a clear and unambiguous interpretation. The number of existing definitions is almost equal to the number of authors who wrote on this topic. And since specialists from the most diverse branches of knowledge and practice (literally from geology to sociology) turned to GIS, considering them from their positions, the definitions of the essence of systems differ quite significantly.

With the development of science, knowledge about the earth, natural resources, geology and geography, geoinformatics in many countries of the world previously understood “a specialized section of computer science that deals with geography” (Ivanov & Markus, 1999, pp.36-37).

By area of the territory subject to cartographic and geodetic support, the countries closest to the Republic of Kazakhstan are: Russia, the USA, Canada and China. RK takes the 9th place in the world.

Historical aspects of the formation and development of a geoinformation system

The emergence and rapid development of GIS was predetermined by the rich experience of topographic and, especially, thematic mapping, successful attempts to automate the cartographic process, as well as revolutionary achievements in the field of computer technology, computer science and computer graphics.

Of particular note are the ideas and experience of integrated thematic mapping, which convincingly demonstrated the effect of systematic use of diverse data to extract new knowledge about geographical objects. Complexity and integrability are still the most important GIS properties that attract users.

Technological support for geo-mapping projects was implemented in the style of Automatic Design Systems. It is this approach that underlies modern geographic information systems. In the history of the development of GIS, the following main periods can be distinguished:

1. Pioneer period (late 1950s - early 1970s).

This is the time of researching the fundamental possibilities of creating GIS, accumulating knowledge, developing empirical experience, and creating the first large projects.

2. The period of state initiatives (early 1970 - early 1980).

This period was characterized by the development of large geoinformation projects supported by the state, the formation of state institutions in the field of GIS, and the reduction of the role and influence of individual researchers and small groups.

3. The period of commercial development of GIS (beginning of 1980 - end of 1990).

This was the period of creating a wide market for GIS software, creating desktop GIS, expanding their scope by integrating them with non-spatial data bases, the emergence of non-professional GIS users, and the emergence of distributed geodatabases.

4. User period (1990 - present)

This period has been characterized by increased competition among commercial manufacturers of GIS shells, the discovery of software systems that allowed users to adapt and upgrade the shell to their tasks, and the beginning of the formation of a global geographic information infrastructure (Baranov et al, 1999, p.14).

There are a few words to be said about organizations, projects and researchers who played a key role in the development of GIS.

The beginnings of GIS in Canada

The first geoinformation technologies were developed in the late 1950s - 1960s in Canada, the USA and Western Europe. Among the main achievements of this period in the GIS theory is the determination of the fundamental capabilities of geographic information systems; in the practical sphere, the development of the first large GIS. The largest and most successful of these was the Canada Geographic Information System (CGIS), developed under the guidance of renowned English geographer Roger Tomlinson.

The objectives of this GIS were to map the lands of Canada with their subsequent classification. It was decided to transfer tens of thousands of cartographic information storage units to computer media, to organize databases intelligently and to create software managing all this. Taken together, all this was to form a GIS.

What is fundamentally new to the creators of the Canada GIS in the formation and development of GIS technology?

1. The use of scanning to automate the process of entering geodata.

2. The division of cartographic information into thematic layers and the development of a conceptual solution about “attribute data tables”, which made it possible to separate the planned (geometric) geo-information files about the location of objects and files containing thematic (meaningful) information about these objects.

3. Functions and algorithms for overlay operations with polygons, calculation of areas and other cartometric indicators, and much more .

The advent of GIS in the USA

The US National Census Bureau, one of the organizations that played a key role in the development of geographic information systems, developed GBF-DIME (Geographic Base File, Dual Independent MapEncoding) format in the late 60s.

The history of GBF-DIME began in February 1967 when the US Census Bureau began experimenting with computer mapping. Bureau programmers struggled with inefficiency and redundancy when converting printed paper cards to digital cards. The problem was that in those days, every intersection of streets (in the US cities, there is often a trellis system when the streets form a grid of streets and avenues) was entered exactly eight times. According to Donald Cooke, who was a Bureau programmer at that time and became famous, in particular, for statements like “paper cards lead to fires but perform decorative functions well,” the problem was overcome thanks to the principles of cartographic topology proposed by Bureau's mathematician James Corbett.

Thus, the encoding scheme, later known as DIME, was discovered. The main idea was to renumber nodes (in this case, intersections of streets) and squares (blocks). In the summer of 1967, innovations showed their effectiveness in practice - they dramatically increased the efficiency of digitization and error detection and became the basis for mapping census results.

From the beginning of the 1970s to the beginning of the 1980s, the design of geographic information systems proved to be very costly, and the role of individual researchers in this area decreased markedly. At the same time, the role of state-funded large institutions increased. A number of large-scale geoinformation projects were implemented (Mishin, 2014).

The most famous of them is the census of the US National Census Bureau in 1970 using a special topological approach containing a mathematical method for describing the spatial relationships between objects, to organize the management of geographical information based on the presentation format of DIME map data.

This was a revolutionary innovation. The GBF-DIME format was later transformed into TIGER.

During the 70s, GBF-DIME cards were created for all US cities. This technology is still used by many modern geographic information systems.

The creation, state support and updating of DIME-files also stimulated the development of experimental work in the field of GIS based on the use of databases on street networks:

- automated navigation systems;
- systems for the removal of municipal waste and garbage;
- movement of vehicles in emergency situations, etc.

At the same time, based on this information, a series of atlases of large cities was created containing the results of the 1970 Census, as well as a large number of simplified computer maps for marketing, retail planning, etc.

That is, in this period of the beginning of the 70s, a phenomenon such as raster computer mapping appeared. Points, lines and areal objects on the map were represented by many symbols. These data could be displayed on the plotter in various scales and projections. All attention and efforts at that time were focused on the map itself and then the foundations of modern GIS technology were laid.

The obvious advantage of computer mapping was the ability to select a site on the map and quickly draw it, while it took weeks to introduce changes to the map before introducing computer mapping. In the 80s, the foundations of modern computer cartography were laid. At this time, the attention and efforts of researchers were mainly focused on creating a high-quality digital map using graphic objects (points, lines and polygons) represented by a variety of coordinates. The obvious advantage of electronic cartography was the ability to select a plot on the map, change the scale, and display it on the plotter in various scales and projections. However, the cost of hardware and software was not available to all specialists. In this regard, opinions were even expressed about not promising and inexpedient development of GIS technology due to a very high price of the final product.

The oldest companies, founded in 1969, which are, to this day, the largest GIS developers, are ESRI (Redlands, California) and Intergraph (Huntsville, Alabama). These two companies are the producers of the most popular geographic information systems in the USA and in the world - for example, together they produce exactly half of the GIS used in the USA.

The largest contribution to the development of GIS and GIS technologies during this period was made by ESRI. The first ESRI commercial product, ArcInfo, was released in 1981. In the same year, the first ESRI user conference was held, bringing together 18 people. As new operating systems and new hardware emerged, ArcInfo quickly moved to new platforms. Deliveries of the latest version of the system - ArcInfo 8 - began a few months ago.

ESRI later focused on developing fundamental GIS ideas and applying them to real-world projects, such as developing a Baltimore reconstruction plan or helping MobilOil select a site in Reston.

Digital terrain models in the form of an irregular triangulation network were built at Simon Fraser University, which carried out the order of the US Defense Department. The main objective of the project was to solve the problem of matching the real hypsometric profile of a certain territory (in other words, the elevation profile) with the model embedded in the computer. In other words, it was the military task of accurately guiding missiles at a target.

Widespread GIS and their active development led to a significant increase in competition in the market of geoinformation products, the intensification of research on their further improvement. At the same time, the processes of globalization of the geographic information infrastructure began.

The so-called "Age of Maturity" of GIS coincided in time with the intensive development of computer networks, which played a positive role in supplying geographic information systems with a wide variety of information. At this time, the demand for thematic information made us pay attention to the problem of data collection. The idea of an integrated information environment was formed when the data of space and aerial photographs coexisted peacefully in one system with a digital topographic base, various database tables, graphs, etc.

And finally, in the 90s, intelligent information systems appeared, using both visual and sound images, a variety of multimedia features. One of the latest achievements in the field of GIS is the construction of virtual worlds, while GIS provides three-dimensional visualization (Ivanov & Markus, 1999).

The GIS is currently a multimillion-dollar industry that involves millions of people around the world. Many experts call this period the user period, since the market for geographic information products has turned into the so-called customer market, when increased competition leads to the fact that the buyer, his preferences and needs begin to play a major role in the market.

During this period, an example of a new attitude towards users was shown by the developers and owners of the geographic information software GRASS (Geographic Resources Analysis Support System) for workstations created by the American military specialists (Army Corpsof Engineers) for the tasks of environmental management and land management.

They opened GRASS for free use (public-domain), including the removal of copyrights to the source code of programs. As a result, users and programmers can create their own applications, integrating GRASS with other software products.

Currently, GRASS Version 4.1, created in 1993, including the source code of the programs, system and reference documentation, a training manual for users, a number of data sets as examples, is openly distributed on the Internet.

An example of Army Corpsof Engineers was followed by ESRI, which opened its ArcView 1 forWindows software product in 1994 for unlimited free use (also available on the Internet).

Currently, the leaders in global GIS are the products of two firms - this is the ArcFM system of the American company ESRI, and it provides users with a variety of tools. ESRI has strengthened its position as a leading provider of GIS software products; in 2017, it accounted for more than a third (more precisely, $ 736.7 million, or 36%) of total sales of GIS software.

Intergraph Corporation (Huntsville, Alabama) took the second place in terms of sales of GIS software products. According to Daratech estimates, in 2017 this corporation delivered software for $ 246.8 million, which is 9% of the total sales in the industry (in 2008 its share was 16%), (Gorno-Altayskiy Gosudarstvennyy Universitet, 2020).

The saturation of the market with GIS software tools, especially those designed for personal computers (Desktop GIS), has dramatically increased the scope of GIS technologies. This required substantial sets of digital geodata, as well as the need to form a system of training and education for GIS specialists. The GIS is studied in schools, colleges and universities.

Unfortunately, Kazakhstan and the former USSR did not participate in the global development of geographic information technologies until the mid-1980s. Nevertheless, our country has its own experience in the development of geographic information systems and technologies (Gorno-Altayskiy Gosudarstvennyy Universitet, 2020).

GIS history in Europe

In general, the achievements of the United States overshadow the achievements of Europe, and indeed the rest of the world. Nevertheless, Europe has also made a significant contribution to the process. The situation with computer mapping in Europe had certain differences, which led to the fact that Europe went its own way in the process of developing GIS.

It is interesting that one of the first successful experiments using the principle of complexing (combining and superimposing) spatial data using an agreed set of maps dates back to the 18th century! The French cartographer Louis-Alexandre Berthier used the transparent layers superimposed on the base map to show the movement of troops in the battle of Yorktown (Kulabukhov, 2007, pp.13-15).

The fact is that almost every European country has its own national cartographic agency.

Thus, about 30 organizations produce maps in Europe on a scale of 1:25 000 and higher, while in the United States there are only two such organizations - the civilian US Geological Survey and the military Defense Mapping Agency. In addition, the national cartographic agencies of European countries had more responsibilities and were engaged in both cadastres and land information systems - that is, they did the part of the work that universities or private campaigns did in the USA.

Some of the European agencies started experimenting with computerized inventory databases (for example, in Sweden and Austria) very early. Ordnance Survey in England, IGN in France and the national mapping agency of Germany quite successfully mastered the new technology. There were other pioneers. Alas, their heyday never came.

Unfortunately, the European companies that worked with GIS were not as successful as their American counterparts. So, approximately at the same time as ESRI and Intergraph, the English Ferranti and the Swiss Contraves were founded (a little later the Norwegian Koninglike Wappenfabriek and the German Messerschmidt-Boelkow-Bluehm joined them).

Ferranti offered a geographic information system for cadastral mapping in the late 70s, but soon disappeared from the market. Why did it stop developing? There is still no answer to this question.

Much can be gleaned from collections of reports at early GIS conferences. Survey companies such as Wild and Kern (which later merged with Leica) took up GIS under the influence of a successful project in Basel. The companies went in different ways - one of them adapted American products for the European market, the other developed its own product. Siemens, Laser-Scan (recently celebrated its thirtieth birthday) and Smallworld are European companies founded in the years of the GIS and still operating. True, you will not immediately remember which GIS each of them proposed.

It is believed that many of the differences between European and American GIS histories are caused, firstly, by the difference in the education system, and secondly, by the fact that people from various professions were involved in the creation of GIS on different sides of the Atlantic. In Europe (especially in Germany) they were mainly surveyors, in the USA - geographers. Programmers played a big role on both continents. In addition, the good old European conservatism influenced the development of GIS. Nevertheless, the exchange of ideas between Europe and America was very effective.

History of development of topogeodesic support in the Republic of Kazakhstan

The history of mapping of Kazakhstan is inextricably linked with the mapping of the territory of the USSR. Until 1945, all topographic and geodetic and cartographic work was carried out by the topographic and geodetic teams of the Central Asian Airborne Geodetic Enterprise and by the topographic teams of the West Siberian Airborne Geodetic Enterprise Figure 1.

Figure 1 – Mapping the territory of Kazakhstan
Рис. 1 – Картографирование территории Казахстана
Слика 1 – Мапирање територије Казахстана

In order to prepare personnel for the tasks of mapping the territory of Kazakhstan, by order of the USSR Minister of Education and the head of the Main Directorate of Geodesy and Cartography under the Council of Ministers of the USSR No. 64/195 of July 3, 1946, the Semipalatinsk Topographic College was opened. In the period from 1960 to 1985, the military department of the Semipalatinsk Topographic College carried out training with the qualifications of technician-geodesist, technician-aerial photo-geodesist, cartographer, and a military rank of sublieutenant.

Officers graduating from the topographic college served in the vast expanses of the Soviet Union - in Central, Central Asia, Volga, North-West, Siberian, Ural and Far Eastern districts, and also performed international duties in Afghanistan, Africa and other countries.

After the independence had been gained, graduates of the topographic college continued their service in the ranks of the topographic service of the Armed Forces of the Republic of Kazakhstan, namely: Lieutenant Colonels Myrzabaev K.S., Yaudenov B., Boyandinov A.B., Kozlov AV., majors Shipilin Yu.V., Akishbaev S.S., foreman Konakpaev S.K., sergeant Acheulov A.A., and many others.

Some graduates of the topographic college (not having the military rank of sublieutenant) decided to connect their fate with the army and graduated from the Leningrad Higher Military Topographic Command School named after Army General Antonov (later the St. Petersburg Higher Military Topographical Command School, 2003; Military Topographical Institute of the F.M. Mozhaysky Military Space Academy): reserve colonel Mausymbekov E.Z., master, colonel Zakiev E.S. and colonel Dzhanpeisov M.E.

From 1984 to 2005, only 5 officers graduated from the Leningrad Higher Military Topographic Command School named after the Army General Antonov (reserve colonel Karabalaev N., Zh., reserve lieutenant colonel Kenzebekov B.K., Lahanov K.T. colonel Baizanov A.L. (PhD) and colonel Maykhiev D.K.).

From 1990 to 2003, 7 officers (reserve colonel K.S. Bayashev, master colonel E. Zakiev, colonels S. Zholdybaev, S. Ashirov, P. P. Goncharenko, and reserve captains Kemerbaev N.T. and Mikhailovsky P.V.) graduated from the St. Petersburg Higher Military Topographical Command School (Zakiev & Gerasimov, 2017, pp.94-100).

They held various positions in the topographic service of the Armed Forces of the Republic of Kazakhstan. During 28 years of the existence of the topographic service of the Armed Forces of the Republic of Kazakhstan, it has undergone a number of transformations and changes in the organizational structure.

1992-1998

The Military Topographic Directorate of the General Staff of the Armed Forces of the Republic of Kazakhstan - creation and establishment of a topographic service.

1998-2001

The topographic service of the main operational management of the General Staff of the Armed Forces of the Republic of Kazakhstan during this period created the Republic State Enterprise *Kazakhstan GIS Center* with modern equipment to create topographic maps for the aircraft.

2001-2007

The Main Directorate of New Technologies of the Armed Forces of the Republic of Kazakhstan developed the "Concept for the creation of a geoinformation system of the Armed Forces of the Republic of Kazakhstan", which defines the main directions for the development and implementation of a geoinformation system in the command and control system.

In order to implement the Law of the Republic of Kazakhstan “On Geodesy and Cartography” and the Concept for the creation of a geographic information system of the Armed Forces of the Republic of Kazakhstan, an order was issued by the Chairman of the Committee of Heads of Staff - First Deputy Minister of Defense of the Republic of Kazakhstan No. 288 dated July 6, 2005 “On the implementation of a geographic information system and software MapInfo Professional in the Armed Forces Republic of Kazakhstan".

In addition, the Kazakhstan GIS Center joint stock company in the MapInfo Professional program for the Armed Forces of the Republic of Kazakhstan created digital (vector) topographic maps of the territory of the Republic of Kazakhstan on a scale of 1: 1,000,000, 1: 500000, 1: 200000, 1: 100000, and the creation of digital topographic maps with scale updates of 1: 50,000 (Zakiev, 2012).

2007-2010

With the withdrawal of the Military Topographic Directorate from the DPO (Department for Operational Planning of the Republic of Kazakhstan) and its transformation into an independent structural unit, certain measures were taken to improve the structure of the existing topographic support system.

In implementation of the provisions of the Military Doctrine on the self-sufficiency of groupings of troops, the provision of topographic and geodetic information to formations, military units and institutions is carried out on the basis of territorial affiliation from regional map stores.

The positions of chiefs of topographic services and topographical officers were introduced in the types of armed forces, military branches, regional commands, and constant readiness formations. Thus, a command and control structure was created from the tactical to the strategic level. In January 2010, the Military Topographical Directorate withdrew from the DPO. In 2008, the achievements in the field of digital cartography were demonstrated to the Supreme Commander-in-Chief of the Armed Forces of the Republic of Kazakhstan - the President of the Republic of Kazakhstan.

The topographic service participated at the joint exercises of the CRRF CSTO (Collective Rapid Reaction Force of Collective Security Treaty Organization) Interaction-2009.

The training of reserve officers of topographic and geodetic specialties began in the Military Department of the S. Seifullin Kazakh Agro Technical University.

2010-2014

During this period, the Military Topographic Directorate of the General Staff of the Armed Forces of the Republic of Kazakhstan acquired modern topographic and geodetic instruments for performing topographic and geodetic work, Figure 2.

Figure 2 – Production of the terrain models by topographers of the Armed Forces of the Republic of Kazakhstan in 2010
Рис. 2 – Изготовление макета местности топографами ВС РК 2010 г.
Слика 2 – Модел терена који су израдили топографи Оружаних снага Републике Казахстан 2010. године

At the joint exercises of the Shanghai Cooperation Organization Peace Mission-2010, the topographic service produced layouts of the area and completely restored the points of the state network and the points of the artillery network at the Matybulak training ground and at other military training grounds in the Republic.

In 2012, at the National University of Defense, a new course - Geoinformation Systems - was introduced at the Faculty of General Staff and subsequently for all specialties at the master's program, Figure 3.

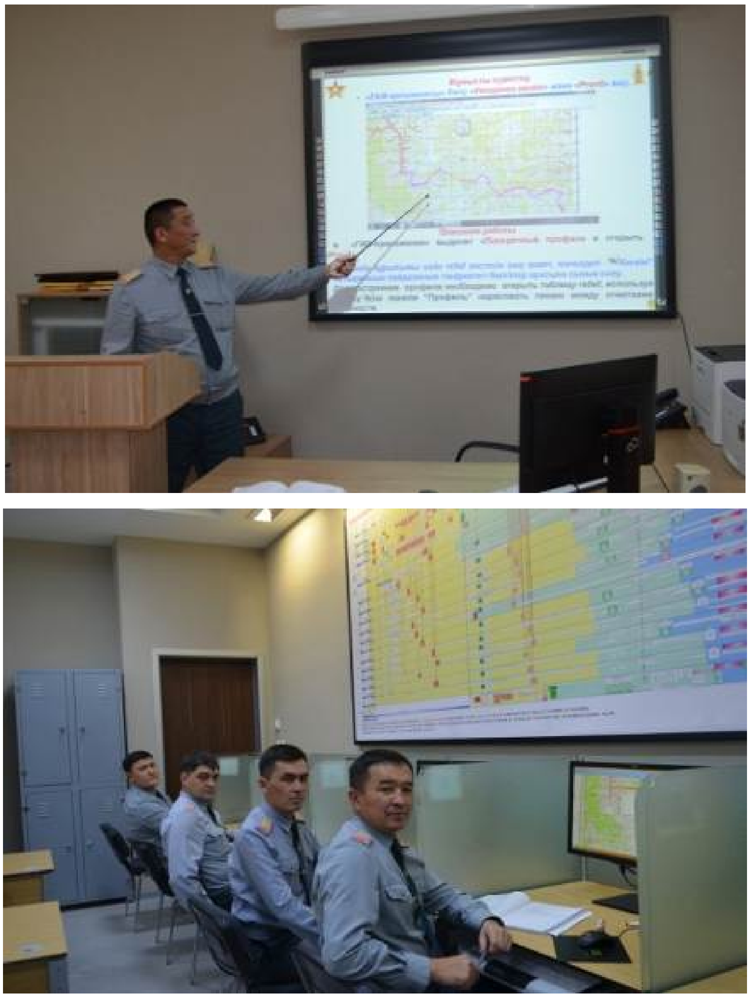

Figure 3 – Lesson with undergraduates in the GIS course
Рис. 3 – Занятие с магистрантами по дисциплине «ГИС»
Слика 3 – Предавање из предмета ГИС постдипломцима

2014-2017

During this period, the Department of Geoinformation Support of the Main Directorate of Armed Forces of the Republic of Kazakhstan purchased a mobile navigation and geodetic complex for the topographic part intended for the operational solution of tasks related to topographic and geodetic training of areas for combat use of troops, topographic and geodetic reference (control of the accuracy of topographic and geodetic reference) of the elements of military combat units, and topographic reconnaissance, Figure 4.

Figure 4 – Mobile navigation and geodetic complex
Рис. 4 – Подвижный навигационно-геодезический комплекс
Слика 4 – Мобилна навигација и геодетски комплет

At the National University of Defense named after the first president, Elbasy, a new subject named Topogeodesic Support of Troops was introduced in September 2016 and a unified program for the Military Topography subject is being developed together with the Defense Ministry of Kazakhstan for all military institutes of the Armed Forces of the Republic of Kazakhstan.

As a result of studying the discipline, undergraduates of the National University of Defense named after the First President of the Republic of Kazakhstan - Elbasy should be informed:

- about the principles, tasks and systems of topographic and geodetic support;
- about the organizational structure of the topographic service of the Armed Forces of the Republic of Kazakhstan;
- about the system of providing troops with topographic maps, initial astronomical and geodetic data, special maps and photo documents of the area;
- on the purpose, armament and capabilities of the units of topographic and geodetic support;
- about the features of the tasks of topographic and geodetic support in various conditions;
- about modern concepts of the development of geographic information technology.

They should know:

- the content of measures of topographic and geodetic support of military operations of troops;
- organization of topographic and geodetic support;
- about geographic information technologies and their use in the command and control system;
- about the capabilities of geographic information systems and their development trends in the leading countries of the world.

They should be able to:

- plan and organize events for topographic and geodetic support of troops;
- perform stock calculations of topographic maps and special works;
- develop a plan for topographic and geodetic support and orders;
- work in a geographic information system with software (input, manipulation, management, query and analysis, visualization);
- identify and relate GIS problems to other sciences;
- apply GIS on command post exercises and in everyday performance.

The should familiarize themselves:

- with the purpose of geographic information technology in the processing of digital information about the area and its use;
- with the main directions of the development of geographic information technology in the state and the Armed Forces.

From 2013 to the present, undergraduates have been lectured in the discipline of Geoinformation Systems by years: 2013 - 60 people; 2014 - 83 people; 2015 - 113 people; 2016 - 137 people; 2017 - 149 people; 2018 - 121 people, 2019 - 113 people, which is total of 776 people.

2017-2019

The Directorate of Geographic Information Support of the Center for Military Space Programs of the Ministry of Defense of the Republic of Kazakhstan.

The problem of using unified geoinformation data arose due to the heterogeneity of geospatial information used in the Armed Forces, other troops and military units. Issues within departmental information interaction and analytical decision support based on geoinformation data were implemented using various software tools.

Currently, the ArcGIS software platform has partially created geospatial data:

- in the Ministry of Internal Affairs of the Republic of Kazakhstan as part of the deployment of the module of the geographic information system of the Operations Management Center and
- in the CoES of the Ministry of Internal Affairs of the Republic of Kazakhstan as part of the deployment of the GIS subsystem of the corporate information and communication system.

From 2002 to 2016, a large volume of cartographic materials in the Mapinfo format has been created in the Ministry of Defense of the Republic of Kazakhstan. By the order of the Ministry of Defense of the Republic of Kazakhstan, plans and topographic maps were produced in analog and electronic formats on a scale of 1:10 000 - 1: 1000 000 on the territory of the Republic of Kazakhstan, border states, military training grounds, as well as on the territory of regional centers and large cities, covering 8034 nomenclature sheets.

In addition, single materials of large-scale topographic maps were produced on the territory of military training grounds in the ArcGIS format on 164 nomenclature sheets.

At the same time, the conversion of geospatial data from one format to another is carried out with a loss of quality of materials (Zakiev et al, 2020, pp.356-382).

At the same time, ESRI GIS refers to the relevant order of the Department of Foreign Assets Control of the US Department of the Treasury and the Bureau of Industry and Security of the US Department of Commerce.

To address all of the above aspects, officers of the National Defense University named after the First President of the Republic of Kazakhstan, the Leader of the Nation, took part in a competition for grant funding for the project *Development of the geographic information system in the Armed Forces, other troops and military units of the Republic of Kazakhstan*.

The purpose of the project is improving the quality of geoinformation information and increasing the effectiveness of planning and decision-making in combat operations and operations in the Armed Forces, other troops and military units of the Republic of Kazakhstan.

The tasks are:

- to develop the principles and requirements for the system of preparation and accumulation of unified geographic information and support in peacetime and wartime, and
- to develop recommendations for improving the system of transmission and control of geographic information of the Armed Forces, other troops and military units of the Republic of Kazakhstan.

2019 - until now

The Department of Geoinformation Support of the General Staff of the Armed Forces of the Republic of Kazakhstan plans to adopt in 2021 a Special Geoinformation Platform (hereinafter - the SGIP) created as part of the implementation of the scientific and scientific-technical program as part of targeted funding for the scientific and scientific-technical program (hereinafter - the program) “Development of a special GIS platform for the defense and security of the Republic of Kazakhstan.”

The SGIP allows organizing the accumulation, storage, accounting, search and provision of interested consumers with geospatial information in real time on the principle of geographically distributed data banks.

Such information will be available in the electronic form to various categories of users through geoportals, both through secure and open channels of the Ministry of Defense data transmission system to other troops and military units in the Republic of Kazakhstan.

To date, navigation support in the Armed Forces of other troops and military units, related services and technical equipment has developed separately by braches and arms without close mutual coordination of organizational structures and coordination of technical policies for the creation of navigation equipment and systems. This entailed a number of organizational and technical problems.

The creation of a single special geographic information platform will allow the formation of a functional, organizational and technical unity of all weapon systems. Its concept is based on the principle of centralized management in combination with a rational distribution of powers and responsibilities between military command and control bodies.

Conclusion

Spatial data is crucial for a military commander in a battle, as he is responsible for making decisions in operation planning and developing. The Ministry of Defense in any country collects data on routing, filtering, analysis and presentation of information for decision-making. Regional conflicts, rapid deployments, and flexible responses place a heavy burden on military commanders, their staff, and auxiliary systems to maintain the situation on the ground with regard to enemy operations. Visualizing raw tabular data in a spatial structure has many advantages. Therefore, digital mapping and GIS are central to such diverse activities as battlefield simulation, mission briefing and communications planning, logistics management and team management.

The analysis of geospatial support systems made it possible to identify their main features and directions for future development. In particular, technologies are developing in the direction of the distribution of geoportals, cloud services and the development of service-oriented architecture systems that will allow the creation of distributed GIS of various kinds. Integration of geographic information systems with rapidly developing remote sensing systems of the Earth will dramatically increase the capabilities of modern GIS, allowing real-time updating of spatial information, especially in the field of important decision-making. It can be suggested that the three main categories of data collection used to create GIS databases include: field data collection and GPS, aerial reconnaissance, and satellite reconnaissance.

Thus, the Unified Special Geographic Information Platform will provide full and current cartographic and other specialized information about the navigation situation to all control units, which completely eliminates duplication and significantly reduces the time it is brought to the troops.

References

Azov, V.Yu. 2003. Kontseptsiya sozdaniya yedinoy informatsionno-upravlyayushchey struktury VS SSHA. *Zarubezhnoye voyennoye obozreniye*, 1 (in Russian) [online]. Available at: http://pentagonus.ru/publ/3-1-0-72 [Accessed: 10 May 2020]. (In the original: Азов, В.Ю. 2003. Концепция создания единой информационно-управляющей структуры ВС США. *Зарубежное военное обозрение*, №1)

Baranov, Yu.B., Berljant, A.M., Kapralov, E.G., Koshkarev, A.V., Serapinas, B.B., & Filippov, Yu.A. 1999. *Geo-Informatics. Explanatory dictionary of basic terms.* Moscow: GIS Assotiation (in Russian). ISBN: 5-89227-019-X [online]. Available at: http://www.geokniga.org/bookfiles/geokniga-berlyant-amkoshkarev-avgeoinformatikatolkovyy-slovarmgis-associaciya1999.pdf [Accessed: 10 May 2020]. (In the original: Баранов, Ю.Б., Берлянт, А.М., Капралов, Е.Г., Кошкарев, А.В., Серапинас, Б.Б., Филиппов, Ю.А. 1999. *Геоинформатика. Толковый словарь основных терминов*. Москва: ГИС Ассоциация. ISBN: 5-89227-019-X).

Evglevsky, I.V., & Morozov, N.N. 2005. Opyt TGO boyevykh deystviy voysk v 21 veke. *Nauka i voyennaya bezopasnost,* 2, pp.39-43 (in Russian). (In the original: Евглевский, И.В., Морозов, Н.Н. 2005. Опыт ТГО боевых действий войск в XX веке. *Наука и военная безопасность,* №2, с.39-43).

Goodchild, M.F. & Kemp, K.K. 1990. *NCGIA Core curriculum in GIS* [e-book]. Santa Barbara, CA: National Center for Geographic Information and Analysis, University of California. Available at: https://ibis.geog.ubc.ca/courses/klink/gis.notes/ncgia/ [Accessed: 10 May 2020].

-Gorno-Altayskiy Gosudarstvennyy Universitet. 2020. *Istoriya razvitiya geoinformatsionnykh sistem* (in Russian) [online]. Available at: http://e-lib.gasu.ru/eposobia/gis/2.html [Accessed: 10 May 2020]. (In the original: Горно-Алтайский государственный университет. 2020. *История развития геоинформационных систем* [онлайн]. Доступно по адресу: http://e-lib.gasu.ru/eposobia/gis/2.html).

Ivanov, V., & Markus, A. 1999. Topograficheskaya karta 21 veka. *Armejskij sbornik*, 9, pp.42-45 (in Russian). (In the original: Иванов, В., Маркус, А. 1999. Топографическая карта XXI века. *Армейский сборник*, № 9, с.42-45).

Kulabukhov, A.N. 2007. Primeneniye sovremennykh informatsionnykh tekhnologiy v khode planirovaniya boya. *Voyennaya mysl*, 9, pp.13-15 (in Russian) [online]. Available at: http://militaryarticle.ru/voennaya-mysl/2007-vm/10046-primenenie-sovremennyh-informacionnyh-tehnologij-v [Accessed: 10 May 2020]. (In the original: Кулабухов, А.Н. 2007. Применение современных информационных технологий в ходе планирования боя. *Военная мысль*, № 9, с.13-15).

Mishin, E.I. 2014. *Geograficheskiye informatsionnyye sistemy: Uchebnoye posobiye.* Smolensk: Smolensk State Agricultural Academy (in Russian) [online]. Available at: http://www.sgsha.ru/sgsha/biblioteka/Geograf_vet.pdf [Accessed: 10 May 2020]. (In the original: Мишин, Е.И. 2014. *Географические информационные системы: Учебное пособие.* Смоленск: ФГОУ ВПО «Смоленская ГСХА»).

Satyanarayana, P., & Yogendran, S. 2009. Military applications of GIS. *Geospatial World,* 9 January [online]. Available at: https://www.geospatialworld.net/article/military-applications-of-gis/ [Accessed: 10 May 2020].

Zakiev, E.S. 2012. *Geoinformatsionnaya sistema v VS RK: Uchebno-metodicheskoye posobiye*. Shchuchinsk: Izdatelskiy tsentr NUO (in Russian). (In the original: Закиев, Е.С. 2012. *Геоинформационная система в ВС РК: Учебно-методическое пособие.* Щучинск: Издательский центр «НУО»).

Zakiev, E.S., & Gerasimov, S.V. 2017. 25-let topograficheskoy sluzhbe Vooruzhennykh Sil Respubliki Kazakhstan. In: *Proceedings of International scientific-practical conference Professionalization of the army - a reliable guarantor of ensuring the military security of the state,* Astana, pp.94-100 (in Russian). (In the original: Закиев, Е.С., Герасимов, С.В. 2017. 25-лет топографической службе Вооруженных Сил Республики Казахстан. В: *Сборник материалов международной научно-практической конференции «Профессионализация армии – надежный гарант обеспечения военной безопасности государства»*, Астана,с.94-100).

Zakiev, E.S., Pankov, S.V., & Kalabay, K.B. 2020. Application of geoinformation systems in the armed forces and other military formations in the Republic of Kazakhstan. *Vojnotehnički glasnik/Military Technical Courier*, 68(2), pp.356-382. Available at: https://doi.org/10.5937/vojtehg68-25830.

ПРИМЕНЕНИЕ ГЕОИНФОРМАЦИОННЫХ ТЕХНОЛОГИЙ В ВООРУЖЕННЫХ СИЛАХ РЕСПУБЛИКИ КАЗАХСТАН

Ерлан С. Закиев[а], **корреспондент**, *Серикхан* К. Кожахметов[б]

[а] Национальный университет обороны имени Первого Президента Республики Казахстан − Елбасы,
Факультет цифровых технологий и безопасности информационных систем,
кафедра имитационного моделирования и информационных систем,
г. Нур-Султан, Республика Казахстан

[б] Национальный университет обороны имени Первого Президента Республики Казахстан − Елбасы,
Факультет материально-технического обеспечения войск,
кафедра тылового обеспечения,
г. Нур-Султан, Республика Казахстан

РУБРИКА ГРНТИ: 36.00.00 ГЕОДЕЗИЯ. КАРТОГРАФИЯ;
36.29.00 Топография. Фототопография
36.29.33 Топографические и специализированные карты и планы. Цифровые модели местности
ВИД СТАТЬИ: профессиональная статья

Резюме:

Введение/цель: Данная статья написана с целью ознакомления читателей с геоинформационной технологией в процессе организации топогеодезического обеспечения, а также с выработкой рекомендаций и предложений, которые позволят сформировать эффективную и полноценную систему геоинформационного обеспечения Вооруженных Сил, других войск и воинских формирований Республики Казахстан.

Методы: Применяя аналитический подход при исследовании причин локальных войн и вооруженных конфликтов с использованием высокоточного оружия и маневренных боевых действий с помощью видовых средств разведки, геоинформационных систем и связи. Выводы были сделаны и на основании анализа исторических аспектов становления и развития геоинформационной технологии.

Результаты: В статье приведен краткий обзор систем геопространственного обеспечения с использованием геоинформационных технологий в зарубежных государствах и топографической службе Вооруженных Сил Республики Казахстан.

Выводы: Создание единого государственного географического информационного пространства является весьма важным фактором, так как технологии развиваются в направлении распространения геопорталов, облачных сервисов и развитие систем сервисноориентированной архитектуры, которые обеспечат создание ГИС различной направленности. Интеграция геоинформационных систем с быстро развивающимися системами дистанционного зондирования Земли резко увеличит возможности современных ГИС, позволяя в режиме реального времени актуализировать пространственную информацию, особенно в области принятия важных решений.

Ключевые слова: геоинформационные технологии, геоинформационное обеспечение, геоинформация, геоинформационная система, системы геопространственного обеспечения, топографическая служба, системы дистанционного зондирования, вооруженные силы Республики Казахстан.

ПРИМЕНА ГЕОИНФОРМАЦИОНЕ ТЕХНОЛОГИЈЕ У ОРУЖАНИМ СНАГАМА РЕПУБЛИКЕ КАЗАХСТАН

Ерлан С. Закијев[а], **аутор за преписку**, *Серикхан* К. Кожахметов[б]

[а] Народни универзитет одбране „Први председник Републике Казахстан – Елбаси",
Факултет информационих технологија и безбедности информационих система,
Катедра симулационог моделовања и информационих система,
Нур-Султан, Република Казахстан

[б] Народни универзитет одбране „Први председник Републике Казахстан – Елбаси",
Факултет војне логистике, Одељење логистике,
Нур-Султан, Република Казахстан

ОБЛАСТ: информационе технологије, геоинформационе технологије
ВРСТА ЧЛАНКА: стручни рад

Сажетак:

Увод/циљ: Циљ чланка је да упозна читаоце са геоинформационом технологијом у процесу организовања топографске и геодетске подршке, као и да дâ препоруке и предлоге који ће омогућити формирање ефикасног и свеобухватног система геоинформационе подршке за оружане снаге, остале трупе и војне јединице Републике Казахстан.

Методе: При методу анализе узрока локалних ратова, оружаних сукоба и употребе високо-прецизног оружја у вођењу борбених операција у којима се примењују софистицирана средства за извиђање, као и савремени географски информациони системи и комуникације, коришћен је аналитички приступ. Закључци су изведени и на основу анализе историјског развоја географских информационих технологија.

Резултати: Укратко су приказани системи геопросторне подршке који користе геоинформационе технологије, како у страним земљама, тако и у топографској служби Оружаних снага Републике Казахстан.

Закључак: Стварање јединственог државног геоинформационог простора је од велике важности, будући да се технологије развијају у правцу дистрибуције геопортала, ка услугама путем cloud-а и системима рачунарске архитектуре усмереним на услуге, који ће омогућити стварање разноврсних геоинформационих система. Интегрисање географских информационих система са системима даљинске детекције Земље који се брзо развијају драстично ће повећати могућности модерног ГИС-а, омогућавајући ажурирање просторних информација у реалном времену, посебно у области доношења важних одлука.

Кључне речи: геоинформационе технологије, геоинформациона подршка, геоинформације, геоинформациони систем, системи геопросторне подршке, топографска служба, системи даљинске детекције, оружане снаге Републике Казахстан.

Paper received on / Дата получения работы / Датум пријема чланка: 11.05.2020.
Manuscript corrections submitted on / Дата получения исправленной версии работы / Датум достављања исправки рукописа: 24.06.2020.
Paper accepted for publishing on / Дата окончательного согласования работы / Датум коначног прихватања чланка за објављивање: 26.06.2020.

HYPERLEDGER FRAMEWORKS WITH A SPECIAL FOCUS ON HYPERLEDGER FABRIC

Marija S. Krstić[a], *Lazar* J. Krstić[b]

Academy of Vocational Studies Southern Serbia,
Department of Business Studies, Leskovac, Republic of Serbia

[a] e-mail: krstic.marija@vpsle.edu.rs, **corresponding author,**
ORCID iD: https://orcid.org/0000-0003-3009-8400

[b] e-mail: krstic.lazar@vpsle.edu.rs,
ORCID iD: https://orcid.org/0000-0001-9131-6876

DOI: 10.5937/vojtehg68-26206; https://doi.org/10.5937/vojtehg68-26206

FIELD: IT
ARTICLE TYPE: Professional Paper

Abstract:

Introduction/purpose: The Blockchain market is a developing market, and many industries are increasingly aware of the importance of having and implementing Blockchain due to changing business conditions. After an introductory consideration of the Blockchain concept, the article focuses on the projects under the Linux Hyperledger Initiative, with particular reference to Hyperledger Fabric, notably on the concepts, architecture, organizational focus, private channels and smart contracts, as well as flow of transactions in the Hyperledger Fabric network. In the last, practical part of the paper, we presented a simulation of a business network and created a simple application for money exchange using the Hyperledger Fabric framework. The aim of the paper is to present the Hyperledger frameworks and highlight all the details of Hyperledger Fabric in order to determine whether its application in practice is justified.

Methods: Basic methods (analysis, synthesis, deduction, induction, concretization, generalization) as well as general-scientific methods (analytical-deductive and comparative) were used.

Results: All relevant features of Hyperledger Fabric were considered, a blockchain business network based on it was built, and an application for cash exchange through the network was created.

Conclusion: Hyperledger Fabric is the most comprehensive and the most flexible Hyperledger framework with the largest number of use cases.

Key words: Blockchain, Hyperledger, Hyperledger Fabric.

Introduction

Blockchain technology is considered a suitable catalyst for transformation and has the potential to become a digital trend in the near future. This modern technology provides data duplication on all devices participating in the network. Blockchain is suitable for end users because the data cannot be changed after storage in a chain of blocks. Namely, each data update is correctly recorded, which facilitates the process of recording transactions and tracking assets in the business network.

Using open source tools, we strive to create Blockchain techniques available to a wide range of people. One such tool is Hyperledger, a set of technologies used to create new blockchains. The application of Hyperledger Blockchain technologies in business processes improves transparency, enhances accountability and algorithmically guarantees trust between business partners. The technologies created within the Hyperledger projects are increasingly called Third Generation Blockchain systems, where the first generation is considered to be Bitcoin, and the second Ethereum.

The paper presents research on the topic of Hyperledger projects with special reference to Hyperledger Fabric. The first part is an introduction to the basic concepts and principles of Blockchain technology, which enables a decentralized way of data storage. After giving the basics of the Blockchain technology, the research continues in the direction of the Hyperledger initiative of the Linux Foundation in the second part of the paper. The third part is dedicated to Hyperledger Fabric, i.e. concepts, architecture, organizational focus, private channels, smart contracts and transactions in the Hyperledger Fabric network. In the last, practical part of the paper, a simulation of a business network is given and a simple application for money exchange is created, with the aim of a simpler understanding of the Hyperledger Fabric working principle.

Blockchain technology

Blockchain technology is a distributed replicated database. It is organized in the form of a single-linked list (chain), where nodes are blocks with data on transactions, protected by cryptographic methods after grouping. Hence the name Blockchain. It is a system that enables the realization of digital transactions without intermediaries. It is based on the P2P architecture, where the nodes that participate in the implementation of the service have a copy of all records, and constantly communicate with each other and synchronize records (Minović, 2017).

To support consistent updating of information and to enable a full range of functions in the general ledger (transactions, queries, etc.), the Blockchain network uses smart contracts to provide controlled access to the ledger. Smart contracts are not only a key mechanism for encapsulating information and maintaining online simplicity, but can also be drawn up to allow participants to automatically execute certain aspects of transactions. The process by which general ledger transactions are synchronized online, to ensure that the general ledger is updated only when the transactions are approved by the respective participants and that the transactions remain in the same order when updating the general ledger, is called consensus.

The consensus mechanism can be said to represent a predefined cryptographic validation method that ensures the correct sequencing of transactions on Blockchain. The consensus algorithm defines the rules, i.e. the ways in which network participants can reach an agreement on transaction validation. The most commonly used algorithms are Proof of Work (PoW) and Proof of Stake (PoS).

Proof of Work is the most widespread way of reaching consensus, which is based on mining. To validate a transaction, each node must perform a complex mathematical calculation. That is why the device consumes certain resources: electricity and processing power. On the other hand, for successful validation, a node (miner) is rewarded with a certain monetary value in cryptocurrency. The more processing power it has, the faster the node will complete the mathematical calculation and get the reward, that is, will earn more. Proof of Stake does not involve mining, some nodes validate transactions and others confirm them, and everyone keeps part of their money in a virtual safe and whoever tries to cheat the system loses money (Pavlović, 2018).

Blockchain can be classified into three types: public, private and allowed Blockchain. The classification is based on the node's ability to access or add a new block to the network. Public blockchain networks are widely available, any node can join the network, participate in transactions and create blocks. The examples of public blockchain are Bitcoin, Ethereum, Dash and Litecoin. On the other hand, with private Blockchain networks, only invited members are allowed to join the network and there is no anonymity of participants, as with public networks. The identity of each participant is known and cryptographically authenticated, on the basis of which the execution of transactions is monitored. Access rights to executed transactions may be granted to anyone or restricted in some way. The examples of private Blockchain are Hydrachain Ripple, Monaco and Multichain. The third type of Blockchain, which is the middle ground between private and public Blockchain, is known as a consortium or allowed Blockchain. In this type of blockchain, the network is controlled by a group of nodes. The examples of the consortium Blockchain network are Hyperledger Fabric and Corda (Nasir et al, 2018).

Blockchain can also be said to be a collaborative data registry. Each time the data is accessed and modified, the change is recorded and confirmed, followed by encryption that cannot be subsequently edited. All changes are saved and added to the total record, and each subsequent change requires a repetition of the entire process, with the data being stored in a new block that is encrypted and attached to the previous block. Blockchain requires a lot of processing power due to the complex cryptography that computers have to solve in order to enable storage and access to data. Six basic qualities of Blockchain can be singled out, which together form a functional system (Piljan et al, 2018):

- Decentralization: Blockchain is a distributed database located on all users' computers around the planet, i.e. on the Internet. Thus, there is no central database that can be attacked, hacked or forged. Also, there is no need for an intermediary - information, money, securities or something else can be sent without the need for a broker or a third party (PayPal, Western Union).

- Encryption: Blockchain is encrypted, it uses an advanced encryption technique using private and public keys providing virtually complete security in the authenticity of the transmitted data.

- Transparency: Blockchain is public. All users have access to the database and no one can hide an individual transaction.

- Inclusiveness: Blockchain does not require special technical preconditions for participation, the protocol is designed in such a way that it can be implemented on practically any computer or mobile device, thus providing the possibility of use to practically the entire Internet population.

- Immutability: after a transaction has been executed, verified and placed in a block, it is linked to the previous transaction or block. This structure is marked with a unique code and timestamp, which prevents the possibility of subsequent changes.

- Historicity: there is no way to steal a transaction or data about a block, because that would mean rewriting the entire Blockchain, or all transactions ever performed in it. This means that Blockchain at all times contains all transactions that have been executed since the chain was created.

Hyperledger

Hyperledger is an open source project founded by the Linux Foundation. The initiative was launched in December 2015 in order to advance and promote Blockchain technologies and expand the possibilities of their application in the business world. Members of the Hyperledger initiative are many of the world's leading companies in the fields of information and high technologies, finance and banking, production and distribution of products (supply chain), such as: Intel, IBM, Cisco, Airbus, Daimler, JP Morgan, American Express, Deloitte, PWC, BNP Paribas, Baidu, SAP, Huawei, as well as many others, including the domestic company GameCredits (Gajić, 2018).

Hyperledger is not a unique Blockchain technology, but a collection of technologies included by member companies. Although there is a long-term goal of greater integration between projects, most Hyperledger projects still operate independently. Hyperledger has never issued its cryptocurrency, and according to its founders, it will continue to do so in the future. Concrete technologies can be said to be explicitly designed and built for enterprise use cases, not for public markets.

The active development of Hyperledger projects took place at the beginning of 2016, and it implies the development of a larger number of frameworks and tools. Hyperledger frameworks, i.e. distributed ledger technology (DLT) technologies include Fabric, Sawtooth, Iroha, Indy and Burrow, while tools are being developed from Composer, Cello and Explorer (Dhillon et al, 2017).

Each of the Hyperledger technologies has its own specific advantages in certain applications. Some of the mentioned technologies have advanced in the development phases and are actively applied (Fabric, Sawtooth, Iroha), while others are still in the incubation phase (Burrow, Indy). As far as tools are concerned, the most developed is Composer.

Hyperledger projects follow a design philosophy that includes a modular extensible approach, interoperability, an emphasis on highly secure solutions, a token-based approach without a native cryptocurrency, and the development of a rich and simple application user interface. The modular approach allows developers to experiment with creating different types of components. They can create components that can be combined, in order to develop distributed general ledger solutions that meet different requirements. Hyperledger recognizes that security is a fundamental aspect of distributed general ledgers, as many use cases involve large-value transactions or sensitive data. In the future, many different Blockchain networks will have to communicate and exchange data in order to form more complex and powerful networks. A high degree of interoperability will provide support for a growing application of Blockchain. Also, Hyperledger projects provide rich and simple application user interfaces that support interoperability with other systems. However, the design philosophy includes the ability to create tokens used to manage digital objects which can represent currencies.

The Hyperledger Architecture Working Group has singled out the following business components of Blockchain (Hyperledger, 2018):

- Consensus Layer - Responsible for creating an order agreement and validating the set of transactions that make up the block.
- Smart Contract Layer - Responsible for processing transaction requests and determining the validity of transactions by applying business logic.
- Communication layer - Responsible for peer-to-peer transmission of messages between nodes participating in a common general ledger.
- Data Warehouse Abstraction - Allows different data warehouses to be used in other modules.
- Crypto Abstraction - Allows you to replace different crypto algorithms or modules without affecting other modules.
- Identity Services - Allows you to establish trust roots during Blockchain instance setup, enroll and register identities or system entities during network operation, and manage changes. They also provide authentication and authorization.
- Access Services - Responsible for managing various approaches specified in the system, such as the validation approach, the consensus approach, or the group management approach. They connect and depend on other modules to implement different approaches.
- Application User Interfaces - Allows clients and applications to connect to Blockchain.
- Interoperability - Interoperability between different Blockchains is supported.

Hyperledger goals

Hyperledger provides a neutral space for software collaboration between companies that are traditionally competitors. It also provides a neutral space for cross-sectoral cooperation. Blockchains in Hyperledger are allowed and are specifically designed to be business solutions. Because it is a system that requires permission, only those authorized can join the network. This makes it more secure, as the administrator can restrict access to Blockchain. In addition, instead of making all transactions available to everyone online, they are only shown to the relevant parties. Hyperledger's goals include (Hyperledger, 2020d):

- Creating acceptable working environments, i.e. distributed open source ledger technologies as well as code bases to support business transactions.
- Providing a neutral, open community-based infrastructure supported by business and technical management.
- Creating technical communities to develop Blockchain and use cases.
- Educating the public about market opportunities for Blockchain technology.
- Promoting the community using access to tools with many platforms and frameworks.

Hyperledger frameworks

Each of the Hyperledger technologies of the distributed general ledger has its own specific advantages in certain applications. The Hyperledger frameworks are used to build business blockchains for a consortium of organizations. Hyperledger incubates and promotes a range of business blockchain technologies, including (Blockstuffs, 2018):

- distributed general ledger frameworks,
- smart contracts,
- graphical interfaces,
- library client,
- service libraries, and
- simple applications.

The Hyperledger strategy encourages the reuse of common blocks, enables rapid component innovation, and promotes interoperability between projects. As already mentioned, five Hyperledger Blockchain frameworks can be singled out (Suprunov, 2018):

- Hyperledger Fabric,
- Hyperledger Iroha,
- Hyperledger Indy,
- Hyperledger Sawtooth, and
- Hyperledger Burrow.

Hyperledger Fabric is the basis for developing applications or solutions with a modular architecture. It allows components, such as consensus and Membership Services Providers (MSP), to be plug-and-play.

Iroha Hyperledger is designed to be simple and easy to engage in infrastructure projects that require distributed general ledger technology. Hyperledger Iroha has a simple construction, modern C++ domain-based design, and it emphasizes the development of mobile applications, as well as a new, chain-based, Byzantine Fault Tolerance consensus algorithm, called Sumeragi (IBM Global Business Services, 2019).

Hyperledger Indy is a distributed general ledger, built for a decentralized identity. Indy provides tools, libraries, and components that can be reused to create and use independent digital identities based on Blockchain or other distributed general ledgers. These identities are interoperable across administrative domains, applications, and all other parts of organizations. The key characteristics of Indy are (Blockstuffs, 2018):

- Independence - Indy keeps identity artifacts in the general ledger with distributed ownership. These artifacts can include public keys and evidence of existence, and no one but the rightful owner can change or remove the identity.
- Privacy - Indy maintains privacy by default, as any identity owner can operate without any risk of correlation or trace.
- Verifiable requirements - Identification requirements may resemble known credentials such as birth certificates, driver's licenses, passports, etc. They can be combined and transformed using methods that reveal only certain information to allow selective disclosure of only the data needed in a particular context.

Hyperledger Sawtooth is a modular platform for building, implementing, and managing distributed general ledgers. Distributed general ledgers provide a digital record (such as property ownership) that is maintained without central management or implementation. In addition to enabling organizations to organize, build, implement, and run complex distributed books, this platform includes a new consensus algorithm, Proof of Elapsed Time (PoET), that targets large distributed populations of validators with minimal resource consumption (Hyperledger, 2020b). Sawtooth contains several technical innovations, such as dynamic consensus, proof of elapsed time, compatibility with Ethereum contracts, parallel transaction execution, and private transactions. Dynamic consensus allows a consortium to change consensus algorithms on a running blockchain by simply starting a transaction. Proof of Elapsed Time is a consensus algorithm with proven usability in operation, but without high energy consumption. Smart contract abstraction is also enabled, allowing users to create smart contracts in the language of their choice. In terms of private transactions, Sawtooth node clusters can be easily used with separate permissions, ensuring privacy and confidentiality among participants in that particular chain.

Hyperledger Burrow is a modular Blockchain client with a permitted smart contract interpreter that is partially done in the Ethereum Virtual Machine (EVM) specification (Hyperledger, 2020a). It can be said that Burrow is a smart contract machine that requires a license. Monax originally developed and proposed this machine to Hyperledger. Burrow provides an extremely deterministic, smart blockchain design that focuses on contracts. The components that Burrow encompasses are the consensus mechanism, the Application Blockchain Interface (ABCI), the smart contract mechanism, and the gateway. The consensus mechanism maintains a network stack between nodes and ordered transactions that will be used by applications. The ABCI application interface provides an interface specification for connecting the consensus mechanism and the application. The smart contract mechanism provides developers with an extremely deterministic mechanism for managing complex industrial processes. The gateway provides a programming interface for system integrations and user interfaces.

Hyperledger tools

Tools, such as software that facilitate deployment, debugging, and design, can make a huge difference in the ease of use of any system, for both developers and users. Hyperledger is constantly investing in building great support tools. There are several tools that allow easy and efficient access to Blockchain. The most used among the tools are Hyperledger Composer, Hyperledger Cello, Hyperledger Explorer and Hyperledger Caliper.

Hyperledger Composer is the most developed and most powerful Hyperledger tool. It can be said that it is a framework for Hyperledger Fabric. Using Composer brings simpler concepts for Hyperledger Fabric, called Business Network Definitions (BND). These are source code packages that define a business network. This includes permissions, queries, participants, assets and transaction definitions, as well as the implementation of different types of transactions. GNI should be applied to all nodes of the Hyperledger Fabric network. Hyperledger Fabric is implemented with Hyperledger Composer as a platform and infrastructure (Verhoelen, 2018). Hyperledger Composer is written in

JavaScript and is the most active tool for development activity. It is a tool for building business blockchain networks, and is designed to accelerate the integration of block applications and smart contracts with existing business models. This tool is a framework that accelerates the development of applications developed through Hyperledger Fabric.

Hyperledger Cello enables easy hosting of Blockchain, connected components and infrastructure according to external sites. It is a module-based Blockchain tool and a service system. Also called Blockchain as a Service (BaaS), it allows the user to maintain a Blockchain network and infrastructure (Blockstuffs, 2018). BaaS is an offer that allows users to leverage cloud-based solutions to build, host and use their Blockchain applications, smart contracts and Blockchain-based features, while a cloud-based service provider manages all necessary infrastructure maintenance tasks and activities. Hyperledger Cello also provides tracking and analytics capabilities.

Hyperledger Explorer provides a control panel for viewing block information, node logs, statistics, smart contracts, transactions, and all other information stored in Blockchain. Users can query for specific blocks or transactions to see complete details. Hyperledger Explorer can integrate with any authentication or authorization platform, commercial or open source, to provide features that match user privileges.

Hyperledger Caliper allows users to measure the performance of a particular Blockchain implementation with a set of predefined use cases. Hyperledger Caliper allows you to create reports that contain a number of performance indicators, such as Transactions Per Second, Transaction delays, and resource usage (Kuhrt, 2019). Hyperledger Caliper is a performance testing tool for Hyperledger blockchain solutions such as Fabric, Composer, Iroha, and others. Using Caliper, the team working on Blockchain applications can take continuous measurements while building smart contracts and transaction logic and use those measurements to track performance changes. Caliper is compatible with Sawtooth, Indi and Fabric Blockchain systems.

Hyperledger Fabric

Hyperledger Fabric, as a Hyperledger framework, is the most advanced in development. It is interesting to note that, as part of the Hyperledger project, it originated from IBM. This work environment offers a modular architecture in which components such as consensus algorithms and membership service providers can be modified on a plug-and-play basis.

Hyperledger Fabric is a platform for software solutions that use a distributed general ledger (database). It is a private, permissive blockchain infrastructure that provides a modular architecture with delineating roles between nodes within the Blockchain system, executing smart contracts, and configurable consensus and membership services. Its advantages are: identity management, channel privacy and confidentiality, efficient data transmission processing, chaincode functionality, and modular design.

Hyperledger Fabric is designed to be a company-oriented Blockchain solution that is extremely modular and adaptable. Hyperledger Fabric is private and requires permission. This means that it is understood that Hyperledger Blockchains are not available to the general public and do not have tokens that can be exchanged. Blockchain users must have verified identities and join Blockchain using a Membership Service Provider (MSP). Membership service providers are configured in the system, and there may be more than one, but all members must be accessible by one or more membership service providers. Hyperledger Fabric also has a number of special tools that make it particularly well equipped (Hill et al, 2018).

Hyperledger Fabric technology distributed general ledgers profit from the advantages of container technologies for working with smart contracts, which in this context are called a program code chain and which realize the application logic of the system using the Go programming language. The specific mechanism of private channels that exists in Hyperledger Fabric allows the sharing of confidential information between individual participants in the Blockchain network. The key features that set Hyperledger Fabric apart as a comprehensive and customizable Blockchain solution are (Hyperledger-fabricdocs Documentation, 2019):

- Assets - Definitions of assets allow the exchange of almost anything that has monetary value over the network, from food through old cars to the currencies of the future.

- Chaincode - Chaincode execution is separate from transaction handling, limiting required levels of trust and verification across nodes, and optimizing network scalability and performance.

- General Ledger Features - A fixed, shared book that encodes the entire transaction history for each channel and includes the ability to ask SQL like queries for more efficient audit and dispute resolution.

- Channel privacy - Channels enable multilateral transactions with a high degree of privacy and confidentiality required by competing companies and industries that exchange assets through a common network.

- Security and Services for Members - Membership that requires permission provides a reliable Blockchain network, where participants know that all transactions can be detected and monitored by authorized regulators and auditors.

- Consensus - A unique approach to consensus provides the flexibility and usability that a company needs.

Another important feature introduced by Hyperledger Fabric is confidentiality when performing transactions on the same network of nodes. Hyperledger Fabric adopts the following terminology related to its workflow: Blockchain "application" through the interface manages the user and the network. Smart contracts are also called chain codes and are provided using the Node SDK, Java SDK and command line interface - as development tools (Belotti et al, 2019).

Features of architecture

Hyperledger Fabric is designed with several key features and use cases that are considered important for business users. It is basically a general ledger. The general ledger is a set of blocks, and each block contains a set of transactions. A transaction is anything that changes/updates the state of a Blockchain. Transactions, in turn, are performed using smart contract codes installed on Blockchain. The general ledger records the status of data and transactions, and each node in the network has a replicated copy of the general ledger. There are two basic components to a general ledger:

- World state database in which the current values of general ledger data are recorded. It provides fast and efficient access to current values, instead of searching transaction logs. Data is stored by key-value structure, and this database is characterized by frequent additions, updates and deletions.

- A transaction log that records all changes over the world state database, and once recorded, data cannot be changed or deleted.

The blocks are arranged sequentially, and within each block there is a set of transactions. These transactions are also stored as events in a specific sequence. Unlike other Blockchains, the creation of a transaction and the resulting string does not necessarily occur at the same time or on the same computer. This is because ordering transactions is separate from executing transactions. In Hyperledger Fabric, computers used to manage Blockchain can be included in three different ways (node types), and these are (Hill et al, 2018):

- Client: The client acts on behalf of the Blockchain user and submits actions and events to the network as part of the application.
- Peers: Peers process incoming validation transactions and update status changes as a result of transactions and chain code applications. When they make a transaction, they broadcast the result to the network so that the transaction can be done by the customer.
- Client: While the peer nodes execute transactions, the client nodes review all executed transactions and decide on the final order that is considered to have occurred in the Blockchain. The nodes that ordered the service decide on the final sequence of events and thus decide on the final set of events to be printed on the next block of the Blockchain.

There is a possibility that one computer performs the function of all three types of nodes on the Hyperledger Fabric Blockchain. While it is possible for the same computer on the Hyperledger network to execute transactions and determine their sequence, Hyperledger is able to evolve even further by providing them as separate services.

Figure 1 shows how applications communicate with peers to access the general ledger. The general ledger query involves a simple three-step dialogue between the application and the node, while updating the general ledger is a little more complicated and includes two additional steps. Applications connect to nodes whenever they need access to general ledgers and chain codes. Nodes, in collaboration with customers, ensure that the general ledger updates changes to all nodes in the network.

In a specific example (Figure 1), the application A connects to the node P1 and calls the chain S1 to query or update the general ledger L1. P1 invites S1 to generate a response to a proposal that contains the result of a query or a proposed general ledger update. The application A receives a response to a proposal and the query process ends. For updates, the application A builds a transaction from all responses, which it sends to the client O1. It collects transactions over the network in blocks and distributes them to all nodes, including P1. P1 confirms the transaction before it is applied to L1. When L1 is updated, P1 generates an event, received by A, to indicate completion (Hyperledger, 2020c).

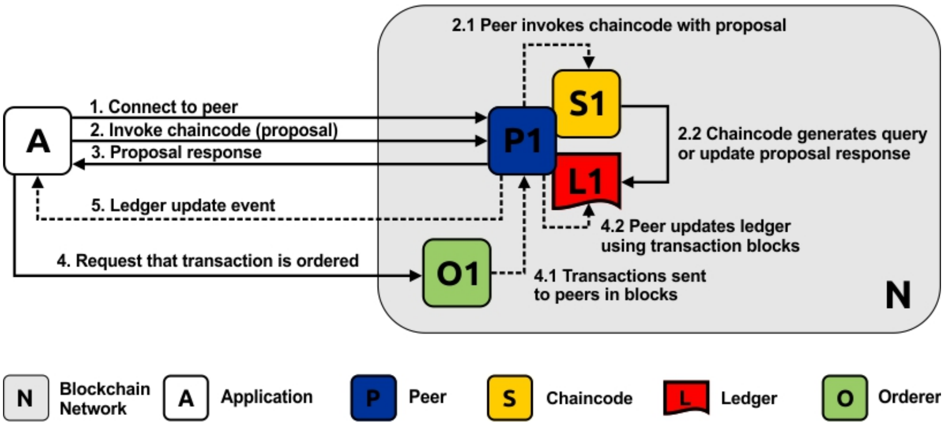

Figure 1 – Query and update of the general ledger
Рис. 1 – Запрос и обновление главной книги
Слика 1 – Постављање упита и ажурирање главне књиге

Organizational focus

Blockchain networks are managed by a set of organizations, not a single organization. Nodes are key to building this type of distributed network. They are the property of organizations and their network connection points. As a business-oriented system, Hyperledger Fabric distinguishes between peers, customers and the organization that owns them. It is intended to create networks between organizations, and the clients who run Blockchain do so as agents of that organization.

Each node on the network uses the Blockchain network on behalf of the participating organization. This is different from networks such as Ethereum and Bitcoin, where a network is created by a set of computers that independently contribute resources to the network, or the network perceives it to do so independently, regardless of who owns them. At Hyperledger Fabric, the organizations that create the general ledger are the ones that contribute to the network by contributing resources in the form of peers and clients. The difference is subtle but crucial. In most public networks, the idea is to allow computers to coordinate, but in Hyperledger Fabric, the idea is to allow companies to coordinate. Organizations give each of their peers a signed digital certificate proving their membership in a particular organization. This certificate then allows each subscriber to connect to the network through a membership service provider, giving them access to network resources. The focus on organizations versus the focus on private computers leads to another feature of Hyperledger Fabric that is focused on companies, and which is necessary due to a larger number of business requirements, i.e. private channels (Hill et al, 2018).

Private channels

There are different types of nodes with different roles in the network: endorser peer, anchor peer, and orderer peer. After receiving the request to call the transaction from the client application, the endorser peer confirms the transaction, which means checking the details of the certificate and the role of the applicant, and then executes the chain code and simulates the outcome of the transaction, but does not update the general ledger. The anchor peer receives updates and transmits updates to other nodes in the organization. The order peer is considered the central communication channel in the Hyperledger Fabric network. The order peer is responsible for the consistency of the general ledger status online. It creates blocks and delivers them to all nodes (Mamun, 2018).

A channel is a private "subnet" of communication between two or more specific network members to perform private and confidential transactions. The communication within the channel is isolated and protected, and transactions and data on the channel are visible only to channel members.

The channel is defined by members (organizations), anchor peers, general ledger, application chain(s), and ordering service. Every online transaction is executed on a channel, where each party must be verified and authorized to perform transactions on that channel. Each node that joins the channel has its own identity assigned to it by the membership service provider, which confirms the authenticity of each node to other nodes within the channel and services. Although nodes may belong to a number of channels, information on transactions, general ledger status, and channel membership is limited to nodes within each channel (Boaventura, 2018). If an organization has access to the Blockchain network, it has the ability to create and maintain a private channel with certain other members. Members (organizations) define and structure a channel to allow certain nodes to run private and confidential transactions, which other members of the same network cannot see and access. Each channel includes nodes, a common general ledger, chain codes on the channel, and one or more ordering services.

Smart contracts

In the Hyperledger Fabric network, smart contracts are also called the chaincode. Unlike Ethereum, the Hyperledger Fabric chain is not built directly into the general ledger itself. Instead, the chain code is installed on each node and interacts with the general ledger to read and update resource status information. Because the chaincode is signed and approved by all nodes, and because each node that uses part of the chaincode must acknowledge any change in the general ledger, this system still uses distributed contracts to allow a distributed and reliable consensus.

Transaction flow

In a distributed general ledger system, a consensus is the process of reaching agreement on the appropriate set of transactions to be added to the general ledger. In Hyperledger Fabric, the consensus involves three different steps (Kulkarni, 2019):

- transaction approval,
- ordering, and
- validation.

These steps ensure that network policies are followed. The implementation of these steps can be considered through the execution of the transaction flow. Otherwise, transactions must be executed, endorsed and then approved, because only such transactions can have an impact on the change of balance. The approval is guided by the policy according to which the participants approve the transaction. The endorsment policy defines which nodes must execute the transaction, and then agree on the results before recording the transaction. The ordering phase accepts the approved transactions and agrees to the request for the transaction to be recorded in the general ledger. Validation takes a block of transactions and confirms the accuracy of the results, including the approval check.

Creating a Blockchain business network and cash exchange application using the Hyperledger Fabric framework

The process of creating a Blockchain business network and a simple application for exchanging funds from one client's account to another's account, as well as the transaction process itself, will be presented in order to better understand the working principle of Hyperledger Fabric. In order to realize the above, the software for virtualization of operating systems, VirtualBox, was used, on which the Linux OS Ubuntu 18.04.2 LTS was installed and configured. The reason for choosing the mentioned operating system is the possibility of Hyperledger Fabric functioning only on Unix-based operating systems.

Installing the necessary prerequisites, local work environment and Hyperledger Fabric

Running the Hyperledger Composer and Hyperledger Fabric development tools requires certain prerequisites to be properly installed and configured. The prerequisites include:

- Docker Engine - basic client-server technology that builds and runs containers using Docker components and services;
- Docker Compose - a tool for initializing and running Docker applications consisting of multiple containers;
- Node - a platform, created using JavaScript, suitable for creating fast real-time applications;
- npm - an online repository of JavaScript modules, many of which are written specifically for Node;
- git - a free open source version control system designed to handle small or large projects with a focus on speed and efficiency;
- Python 2.7.x - interpreted, interactive, object-oriented high-level programming language.

Creating a local work environment requires the installation of the following tools:

- composer-cli - basic CLI tools for performing administrative, operational and development tasks;
- composer-rest-server - a utility for starting a REST server on a machine to represent a business network as a RESTful API;
- composer-playground - user interface for configuration, implementation and testing of business network;
- generator-hyperledger-composer - a tool for generating applications.

The Hyperledger Fabric installation procedure involves:

- creating and selecting a new directory;
- downloading and extracting downloaded tools needed to install Hyperledger Fabric;
- specifying the desired version of Hyperledger Fabric;
- launching Hyperledger Fabric;
- generating a PeerAdmin card (Figure 2).

The PeerAdmin card is analogous to real business cards, and gives the cardholder the authority to deploy, delete, and manage business networks in a Hyperledger Fabric environment.

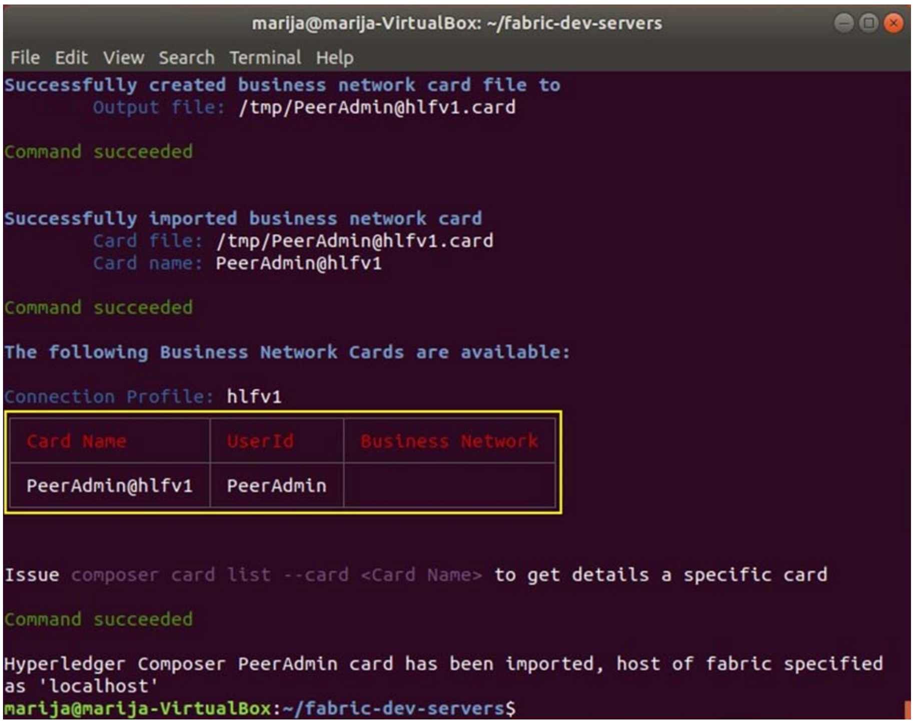

Figure 2 – Successfully generated PeerAdmin card
Рис. 2 – Успешно созданная карта PeerAdmin
Слика 2 – Успешно генерисана картица PeerAdmin

Generating a business network

After successful installation of the Hyperledger Fabric environment, it is necessary to generate a business network (Figure 3). The generated business network consists of data models, transaction logic and access control rules. The data model and access control rules are programmed in a domain-specific language, while the transaction logic is programmed in JavaScript.

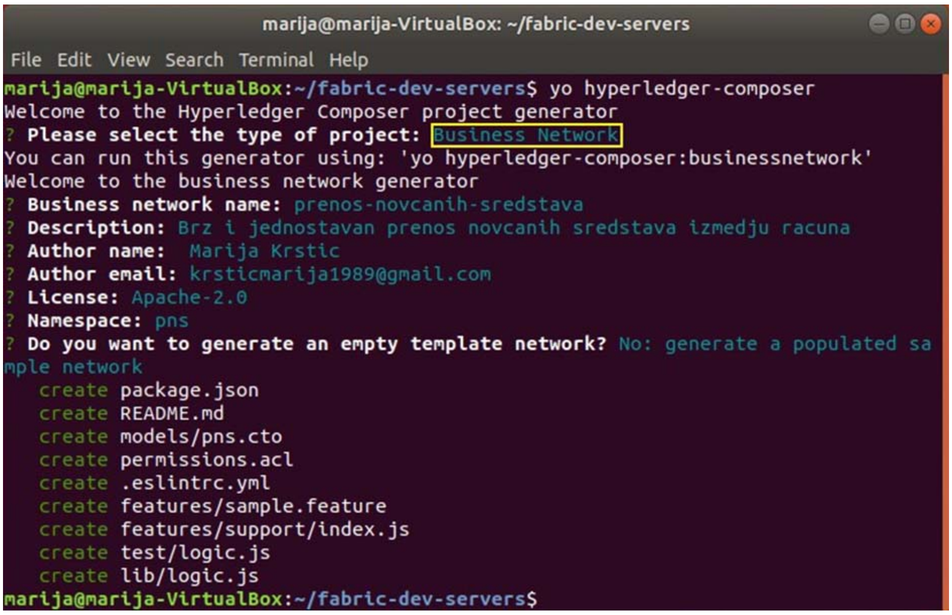

Figure 3 – Successfully generated business network
Рис. 3 – Успешно созданная бизнес-сеть
Слика 3 – Успешно генерисана пословна мрежа

Generating application

In order to make transactions as easy as possible for clients, it is necessary to create client software. In this regard, there is a utility to start the REST server on the machine to represent the business network as a RESTful API.

The Hyperledger composer generator, in addition to generating a business network, also enables generating application. Figure 4 shows a successfully generated application, while Figure 5 presents the balance on customer accounts after the transaction.

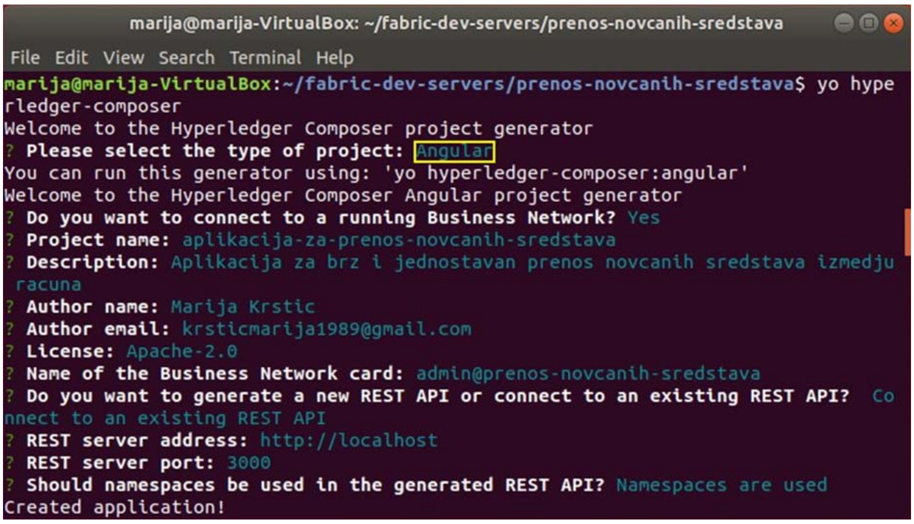

Figure 4 – Successfully generated application
Рис. 4 – Успешно созданное приложение
Слика 4 – Успешно генерисана апликација

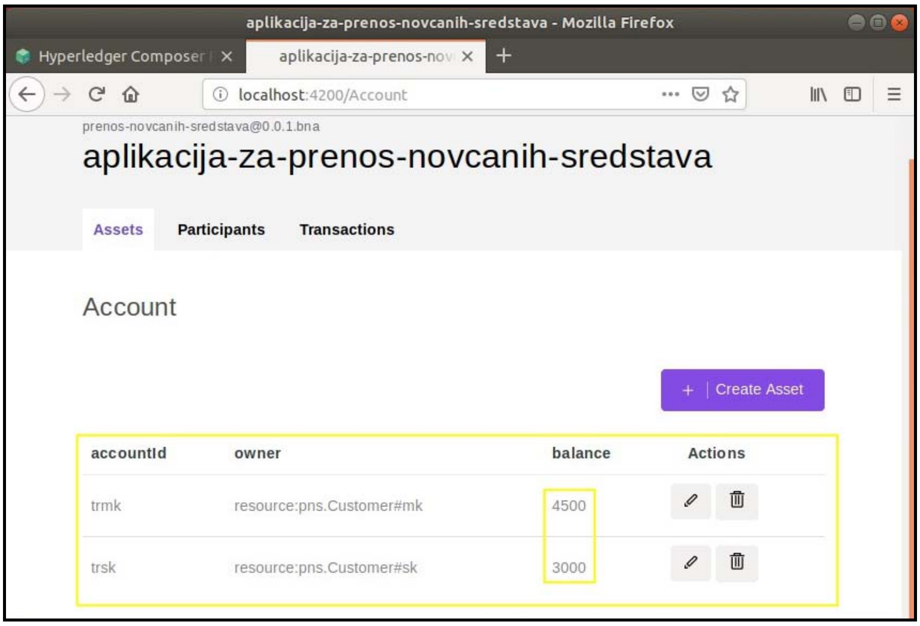

Figure 5 – Balance on the client accounts after a transaction
Рис. 5 – Сальдо по счетам клиентов после транзакции
Слика 5 – Салдо на рачунима клијената након трансакције

Conclusion

Organizations whose business is based on the application of Blockchain technology have a bright future, and the reason lies in the fact that it is a promising new technology for secure online transactions. This technology creates the opportunity to establish accountability based on reliable real-time information exchange between organizations involved in a multi-party business structure. It can offer practical and efficient solutions that can be applied in the system creation, which can bring competitive advantages to organizations in technological and operational terms.

Blockchain technology is increasingly used in systems whose characteristics such as distribution, accessibility, security and trust are among the main qualities of the services and products they offer. In this regard, and in order to develop the best possible stand-alone or integrated Blockchain solutions, the Hyperledger project was created, within which numerous platforms and tools for the development of various Blockchain systems were developed. The Hyperledger family consists of six projects and a set of support tools, all with subtly different focuses and benefits to suit different needs. Hyperledger' s main goal is to take business transactions to a whole new level that includes major global processes.

The most voluminous and flexible project, designed with the largest number of use cases, is Hyperledger Fabric. Responding to business needs, Hyperledger Fabric has evolved significantly in recent years and now accounts for most of the features that businesses can rely on.

Hyperledger Fabric is designed for corporate use from the start. It is the most active of all other Hyperledger projects, and the community gathered around the platform is constantly growing. As such, it has already been successfully implemented in many areas such as banking, finance, retail, and healthcare. This open-source Blockchain is supported by a consortium of large technology companies such as IBM, Cisco, SAP, Intel, and Oracle.

References

Belotti, M., Božić, N., Pujolle, G., & Secci, S. 2019. A Vademecum on Blockchain Technologies: When, Which and How. *IEEE Communications Surveys & Tutorials*, 21(4), pp.3796-3838. Available at: https://doi.org/10.1109/COMST.2019.2928178.

-Blockstuffs. 2018. *Introduction of Hyperledger, its projects and tools* [online]. Available at: https://www.blockstuffs.com/blog/introduction-of-hyperledger-its-projects-and-tools [Accessed: 02 April 2020].

Boaventura, A. 2018. *Getting to know Oracle Autonomous Blockchain Cloud Service - Part 1 -Working with Provisioning Interface* [online]. Available at: https://medium.com/oracledevs/getting-to-know-oracle-autonomous-blockchain-cloud-service-working-with-provisioning-interface-fb3be5179daf [Accessed: 05 April 2020].

Dhillon, V., Metcalf, D., & Hooper, M. 2017. *Blockchain Enabled Applications: Understand the Blockchain Ecosystem and How to Make it Work for You*. New York, NY: Apress.

Gajić, D., 2018. *Šta je Hyperledger i kako vam može pomoći u razvoju Blockchain aplikacija* [online]. Available at: https://startit.rs/sta-je-hyperledger-i-kako-vam-moze-pomoci-u-razvoju-Blockchain-aplikacija/ (in Serbian) [Accessed: 21 March 2020].

Hill, B., Chopra, S., & Valencourt, P. 2018. *Blockchain Quick Reference*. Birmingham, UK: Packt Publishing.

-Hyperledger. 2018. *Hyperledger Architecture, Volume II Smart Contracts*. 2018. [online]. Available at: https://www.hyperledger.org/wp-content/uploads/2018/04/Hyperledger_Arch_WG_Paper_2_SmartContracts.pdf [Accessed: 21 March 2020].

-Hyperledger. 2020a. *Hyperledger Burrow* [online]. Available at: https://www.hyperledger.org/projects/hyperledger-burrow [Accessed: 29 March 2020].

-Hyperledger. 2020b. *Hyperledger Sawtooth* [online]. Available at: https://www.hyperledger.org/projects/sawtooth [Accessed: 29 March 2020].

-Hyperledger. 2020c. *Peers* [online]. Available at: https://hyperledger-fabric.readthedocs.io/en/release-1.4/peers/peers.html [Accessed: 04 April 2020].

-Hyperledger. 2020d. *Hyperledger Blockchain Technologies for Business* [online]. Available at: https://www.hyperledger.org/wp-content/uploads/2018/10/Hyperledger_DataSheet_10.18_Web-2.pdf [Accessed: 04 April 2020].

Hyperledger-fabricdocs Documentation. 2019. [e-book]. Hyperledger. Available at: https://buildmedia.readthedocs.org/media/pdf/hyperledger-fabric/release-1.2/hyperledger-fabric.pdf [Accessed: 04 April 2020].

-IBM Global Business Services. 2019. *Blockchain: Emerging Use Cases for Insurance* [online]. Available at: https://www.the-digital-insurer.com/wp-content/uploads/2019/02/1409-Blockchain-Emerging-Use-Cases-for-Insurance.pdf [Accessed: 29 March 2020].

Kuhrt, T. 2019. *Hyperledger Caliper* [online]. Available at: https://wiki.hyperledger.org/display/caliper/Hyperledger+Caliper [Accessed: 02 April 2020].

Kulkarni, S. 2019. *Exploring Transaction Flow in Hyperledger Fabric* [online]. Available at: https://opensourceforu.com/2019/01/exploring-transaction-flow-in-hyperledger-fabric/ [Accessed: 07 April 2020].

Mamun, M. 2018. *How does Hyperledger Fabric works* [online]. Available at: https://medium.com/coinmonks/how-does-hyperledger-fabric-works-cdb68e6066f5 [Accessed: 04 April 2020].

Minović, M. 2017. Blockchain technology: usage beside cripto currencies. In: *Infotech 2017: ICT conference & exhibition*, Arandjelovac, Serbia, June 7-8. Available at: http://infotech.org.rs/pdf/011.pdf (in Serbian) [Accessed: 02 April 2020].

Nasir, Q., Qasse, I.A., Abu Talib, M., & Nassif, A.B. 2018. Performance Analysis of Hyperledger Fabric. *Security and Communication Networks Platforms*, 2018, Article ID 3976093. Available at: https://doi.org/10.1155/2018/3976093.

Pavlović, R. 2018. New Tendencies of Blockchain Technology in Insurance with a Potential Greater Than Bitcoin Mining. In: *SorS 2018: 29. susret osiguravača i reosiguravača*, Sarajevo, B&H, pp.239-255, June 6-8. Available at: https://brankopavlovic.rs/documentation/SORS2018.pdf (in Serbian) [Accessed: 02 April 2020].

Piljan, T., Piljan, I., & Cogoljević, D. 2018. Uticaj Blockchain tehnologije na osiguranje. *Vojno delo*, 70(2), pp.360-373 (in Serbian). Available at: https://doi.org/10.5937/vojdelo1802360R.

Suprunov, P. 2018. 5 *Hyperledger Projects In Depth* [online]. Available at: https://medium.com/practical-blockchain/5-hyperledger-projects-in-depth-3d14c41f902b [Accessed: 27 March 2020].

Verhoelen, J. 2018. *An overview of Hyperledger blockchain projects* [online]. Available at: https://blog.codecentric.de/en/2018/03/blockchain-project-hyperledger/ [Accessed: 30 March 2020].

ПРОГРАММНАЯ ПЛАТФОРМА HYPERLEDGER С ОСОБЫМ АКЦЕНТОМ НА БЛОК-СХЕМУ HYPERLEDGER FABRIC

Мария С. Крстич, **корреспондент,** *Лазар* Й. Крстич

Академия профессионального образования Южная Сербия,
Департамент бизнес-образования,
г. Лесковац, Республика Сербия

РУБРИКА ГРНТИ: 20.00.00 ИНФОРМАТИКА;
20.15.05 Информационные службы, сети, системы в целом
ВИД СТАТЬИ: профессиональная статья

Резюме:

Введение/цель: Развивающийся рынок блокчейнов с каждым днем становится все интереснее для многих отраслей, которые вследствие изменения условий ведения бизнеса, стали лучше понимать насколько важно иметь и пользоваться блокчейнами.

После вступительного ознакомления с концепцией Blockchain в статье представлены проекты в рамках инициативы компании Linux Foundation, с особым акцентом на деятельность Hyperledger Fabric ее концепциях, архитектуре, организационной направленности, частных каналах и умных-контрактах, а также на потоке транзакций в сети Hyperledger Fabric. В последней практической части статьи представлены бизнес-симуляция и разработанное простое приложение для обмена денежных средств с помощью системы Hyperledger Fabric. Целью данной статьи является представление рабочих условий Hyperledger и выявление всех деталей Hyperledger Fabric, для того чтобы можно было понять насколько применение системы Hyperledger на практике является обоснованным.

Методы: В работе применялись основные методы (анализ, синтез, дедукция, индукция, конкретизация, обобщение), а также общенаучные методы (аналитико-дедуктивный и сравнительный).

Результаты: Были рассмотрены все релевантные характеристики Hyperledger Fabric, создана бизнес-сеть блокчейнов и разработано приложение для обмена денежных средств в сети.

Выводы: Hyperledger Fabric – это самая масштабная и гибкая Hyperledger программная платформа с наибольшим количеством пользователей.

Ключевые слова: Blockchain, Hyperledger, Hyperledger Fabric.

РАДНА ОКРУЖЕЊА HYPERLEDGER СА ПОСЕБНИМ ОСВРТОМ НА HYPERLEDGER FABRIC

Марија С. Крстић, **аутор за преписку,** *Лазар* Ј. Крстић

Академија струковних студија Јужна Србија, Одсек за пословне студије, Лесковац, Република Србија

ОБЛАСТ: информационе технологије
ВРСТА ЧЛАНКА: стручни рад

Сажетак:

Увод/циљ: Мада је Blockchain тржиште у развоју, многе индустрије, услед променљивих услова пословања, све више разумеју важност његовог постојања и примене. Након уводног разматрања појма Blockchain-а, истраживање се наставља у правцу упознавања са пројектима у оквиру иницијативе Hyperledger фондације Linux, са посебним освртом на Hyperledger Fabric, где ће бити речи о концептима, архитектури, организационом фокусу, приватним каналима и паметним *уговорима, као и току трансакција у мрежи Hyperledger Fabric. У последњем практичном делу рада приказана је симулација пословне мреже и креиране су једноставне апликације за размену новчаних средстава применом радног окружења Hyperledger Fabric. Циљ рада јесте упознавање са радним окружењима Hyperledger и истицање свих појединости Hyperledger Fabric-а ради утврђивања оправданости његове примене у пракси.*

Методе: Коришћене су основне методе (анализа, синтеза, дедукција, индукција, конкретизација, генерализација), као и опште научне методе (аналитичко-дедуктивна и компаративна).

Резултати: Сагледане су релевантне карактеристике Hyperledger Fabric-а, његовом применом изграђена пословна мрежа Blockchain и креирана апликација за размену новчаних средстава посредством изграђене мреже.

Закључак: Hyperledger Fabric представља најобимније и најфлексибилније радно окружење Hyperledger са највећим бројем случајева употребе.

Кључне речи: Blockchain, Hyperledger, Hyperledger Fabric.

Paper received on / Дата получения работы / Датум пријема чланка: 28.04.2020.
Manuscript corrections submitted on / Дата получения исправленной версии работы / Датум достављања исправки рукописа: 22.05.2020.
Paper accepted for publishing on / Дата окончательного согласования работы / Датум коначног прихватања чланка за објављивање: 24.05.2020.

САВРЕМЕНО НАОРУЖАЊЕ И ВОЈНА ОПРЕМА
СОВРЕМЕННОЕ ВООРУЖЕНИЕ И ВОЕННОЕ ОБОРУДОВАНИЕ
MODERN WEAPONS AND MILITARY EQUIPMENT

Модернизација московског антиракетног штита[1]

У току је велика модернизација московског ракетног штита, односно ракетног система А-135.

Противракетни силос прекривен снегом (у позадини се види транспортер ракета 53Т6)

Током шездесетих и седамдесетих година совјетски инжењери закључили су да није могуће направити ефикасан противракетни штит против масовног ракетног удара са постојећим нивоом научног и технолошког знања.

Тражили су да се развијају информационе компоненте ракетне одбране, система за рано упозорење и фокусирање на оружја за одбијање ограниченог удара. Наведено је да би се на тај начин могла бранити престоница од једноструког, случајног или провокативног удара или удара ограниченог броја балистичких ракета које би лансирале треће државе или подморнице на којима је изгубљена командна структура.

[1] www.airrecognition.com, 10 април 2020

Током 1969. године војни врх се сложио да се изгради слојевити ватрени прстен који би укључивао два пресретачка ешелона: ешелон дугог домета (ван атмосфере) и ешелон мањег домета (атмосферског) који би могли штитити главни објекат против ракета које би пробиле ракетни штит.

Десетог јуна 1971. године почео је рад на пројектовању система А-135, пресретача дугог домета под називом *Amur*.

Данас А-135 подразумева командно и рачунарско место са контролом над ракетном одбраном, А-295, пресретачку ракету дугог домета за пресретање циљева у горњим деловима атмосфере и изнад атмосфере (домет 600 км, аеродинамичке контроле за пресретање у атмосфери и ротационе моторе за пресретање ван атмосфере), пресретачку ракету другог ешелона (за блиско пресретање), атмосферски пресретач великих брзина 53Т6 или PRS-1/PRS-1M са гасним динамичким контролама, четворострани радар Don-2N у месту Sofrino за праћење свемирских објеката дијаметра 5 дм на раздаљинама од 1500 км, нуклеарних пуњења за противракетне ракете и ракетних силоса. На располагању се налази преко стотину противракетних ракета. Силоси нису под камуфлажом, али су солидно заштићени од директног удара или терористичког напада.

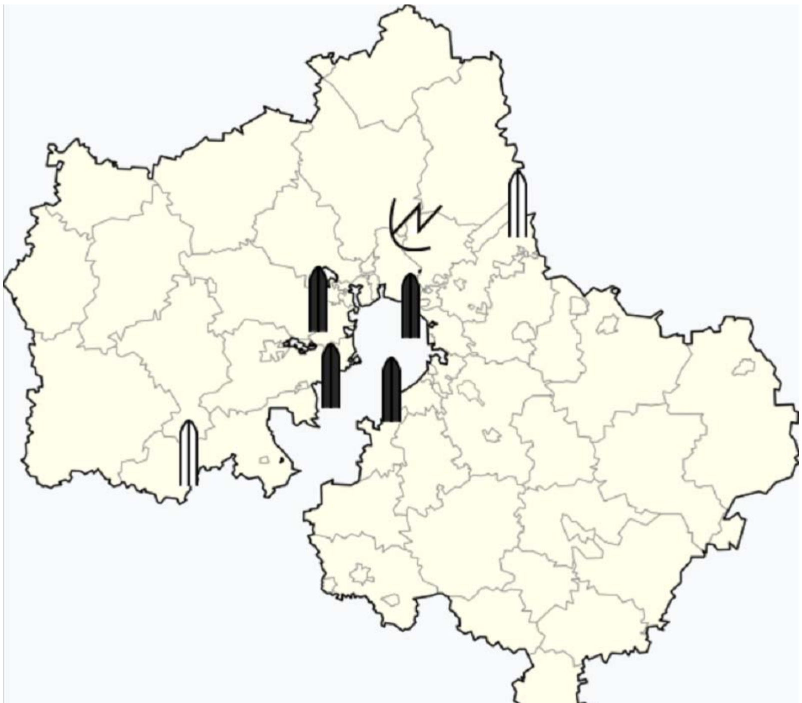

Противракетни систем А-135 у московској области. Црне ракете су оперативне 53Т6, беле представљају неоперативне ракете 51Т6, а тањир је радар Don-2N

Vučković, D., SAVREMENO NAORUŽANJE I VOJNA OPREMA / MODERN WEAPONS AND MILITARY EQUIPMENT, pp.664-679

Систем А-135 има велике могућности. Он открива балистичке ракете на даљинама до 1500 км, док је даљина откривања свемирских објеката од 600 до 1000 км. Такође, А-135 може симултано пратити 100 софистицираних балистичких мета и упутити десетине противракетних ракета на њих. Пошто је израђен пре неколико деценија, потребна му је модернизација – нове електронске компоненте, нови компјутери, као и савремене противракетне ракете.

Радари за рано упозорење система А-135

На почетку модернизације дошло је до неочекиваних резултата. Пошто су нови електронски елементи по величини и тежини мањи, испоставило се да четворострани радар у Софрину има много више празног простора.

Модернизација противракетног пројектила 53Т6 била је компликована. Пробе ракете PRS-1М почеле су током новембра 2017. године. Изгледа да је нови, модерни противракетни пројектил много бржи и убојити од свог претходника. Вишеканални ватрени комплекс Amur-P тестиран је у комплексу Sary-Shagan ради тестирања московске противракетне одбране А-135.

Amur-P састоји се од вишенаменског радара Don-2NPr, командног места 5К80Р повезаног са компјутером Elbrus, лансирних места за блиско пресретање противракетним пројектилима смештеним у силосима, техничке позиције за припрему противракетних пројектила и за пренос података и система 5Ya67, лоцираног на раздаљини од 100 км. Систем Amur-P налази се на позицијама 7, 8, 35, 6/52, а противракетне ракете се лансирају са позиције 35.

Радарски систем Don-2NP

Радарски систем Don-2NP са својом фазираном антенском решетком део је московског радарског система Don-2N базираног у месту Софрино. Он открива, прати циљеве и противракетне ракете, преноси команде противракетним ракетама и прима повратне информације. Затим, систем Amur лансира једностепене противракетне ракете типа PRS-1M за блиско пресретање са одвајајућом вођеном бојевом главом дизајна Novator.

Драган М. Вучковић (*Dragan* M. Vučković),
e-mail: draganvuckovic64@gmail.com,
ORCID iD: http://orcid.org/0000-0003-1620-5601

Турска одабрала украјински активни систем заштите *Zaslon*[2]

Основни недостатак система активне заштите *Zaslon* јесте што је потенцијално смртоносан за пешадију која наступа уз тенк, што проузрокује велике проблеме у случају да пешадија напада непријатељски положај уз блиско садејство тенкова.

Због тога је америчка војска дуго оклевала да их монтира на своје тенкове. На крају је одлучено да се монтира система са усмереним дејством.

[2] The National Interest, May 9, 2020

Vučković, D., SAVREMENO NAORUŽANJE I VOJNA OPREMA / MODERN WEAPONS AND MILITARY EQUIPMENT, pp.664-679

Сарадња турске и украјинске одбрамбене индустрије значајно је напредовала током последњих година. Наиме, Турска све интензивније развија своје оклопне и противоклопне технологије са великим ослонцем на украјинска решења. Један од интересантних примера је и украјински систем активне заштите *Zaslon* који турска војска монтира на своје тенкове М60, а који по лиценци израђује турска компанија *Aselsan.*

Турски тенкови М60 на којима се монтира систем Zaslon

Zaslon спада у ред „сирових" активних система заштите на тржишту. Ослања се на вишеструке експлозивне „цеви" које су увучене у странице возила. Када се возило налази у опасној зони, цеви се извлаче, а радар који је у цеви се активира, тражећи мету. Када се циљ детектује, цев се активира, детонира, стварајући ударни талас фрагмената који уништавају или оштећују пројектил. Конструктори система тврде да је ефикасан и против кинетичких пројектила, што није много вероватно.

Међутим, конструкција система *Zaslon* идеална је за унапређење постојећих возила. *Zaslon* не захтева додатне модуле на куполи већ се они монтирају на трупу, тако да не постоји додатно оптерећење саме куполе као у случају усмереног система активне заштите система *Trophy* на тенку *M1 Abrams*. Украјински извори такође наводе да је време реаговања једноставнијег система заштите *Zaslon* брже у односу на системе усмераваног дејства као што је *Trophy,* јер не постоји потреба за усмеравањем система према циљу.

Међутим, постоји велика опасност по пешадију која наступа поред тенка. Америчка војска је збогтога дуго оклевала са монтажом активних система заштите. Будући да је *Zaslon* смртоносан за своју пешадију, смртоносан је и за непријатељску пешадију, јер се може користити и као последња мера одбране од непријатељских снага.

Нажалост, нема никаквих података о успешности система *Zaslon* који су монтирани на турским тенковима М-60Т за време недавних офанзива, јер је већина употребљених тенкова била нека од варијанти тенка *Leopard 2* за које ће, вероватно, бити одабран неки софистициранији систем.

Zaslon-L

Турска варијанта система Zaslon разликује се од оригинала који је опремљен са два пресретача. Турски систем заснован је на систему Zaslon-L који садржи само један пресретач. То га чини врло осетљивим на ситуације у којима долази до засићења система одбране нападом са више пројектила одједном, јер онај угао са којег је испаљен пресретач остаје без одбране од следећег пројектила или ракете. Систем може бити ефикасан у пресретању појединачних противтенковских ракета, али када је у питању напад са више пројектила одједном ефикасна одбрана је под знаком питања.

Драган М. Вучковић (*Dragan* M. Vučković),
e-mail: draganvuckovic64@gmail.com,
ORCID iD: http://orcid.org/0000-0003-1620-5601

Нова шведска подморница[3]

Пројекат нових подморница започет је почетком деведесетих година под називом U-båt 2000 и требало је да буде завршен крајем деведесетих и почетком двехиљадитих година. Са крајем хладног рата и нестанком претње Совјетског Савеза чинило се да је престала потреба за новом класом подморница. Пројекат је био заустављен до половине двехиљадите године, када је потреба за заменом подморница класе Södermanland

[3] The National Interest, May 20, 2020, .navyrecognition.com

Vučković, D., SAVREMENO NAORUŽANJE I VOJNA OPREMA / MODERN WEAPONS AND MILITARY EQUIPMENT, pp.664-679

постала неопходна. Првобитно је била предвиђена сарадња скандинавских земаља ради пројектовања и производње подморница класе *Viking,* али је та идеја одбачена након што се Данска повукла из пројекта, што је значило да компанија Kockums (касније SAAB) мора сама да настави пројекат.

Током марта 2015. године поново је започет рад на пројекту након што је шведска влада поручила изградњу две подморнице класе А-26 за максимални износ од око 840 милиона америчких долара. Очекује се да ће подморнице бити завршене до 2022. године, а припадаће класи *Blekinge* под називима *HMS Blekinge* и *HMS Skåne*.

Подморница класе А-26

Шведске подморнице су мале и прилагођене балтичком подморју, али су изузетно аутоматизоване, што подразумева мали број чланова посаде. Ове подморнице опремљене су новим модерним погоном независним од ваздуха (AIP Air Independent Propulsion) и лаким торпедима, пречника 400 мм, који су жично вођени и могу бити испаљивани у салвама.

Систем *Stirling* функционише тако што се ствара неопходна топлота у одвојеним коморама за сагоревање у којима гори мешавина течног кисеоника и дизела чији се гасни продукт шаље у затворени део системског погона који затим покреће клипове у цилиндрима, претварајући топлотну енергију у механичку. Погон *Stirling* је енергетски ефикасан и има врло ниску акустичку и инфрацрвену слику.

Аутономија подморнице А-26 само уз *Stirling* погон мери се недељама, а зависи од укрцаних залиха кисеоника и дизела. За то време подморница не мора израњати на површину.

Подморницу А-26 могу да користе и специјалне снаге. Опремљена је великим хангаром између торпедних цеви (под називом вишенаменски портал) и са два контејнера са опремом испод самог хангара. Када се налази на дну мора рониоцима специјалних снага омогућен је излаз и улаз преко хангара, а постоји и могућност њиховог изласка и док подморница плута на одређеној дубини.

Нове подморнице користе напредну технологију која их чини невидљивим путем равнотеже различитих звучних одраза. Ове технологије омогућавају да их непријатељ не може детектовати, класификовати и лоцирати. Шведска има дугу историју пројектовања таквих подморница. Подморница А-26 је израђена од великих еластичних материјала и преграда ради смањивања замора материјала и постојећих звукова, али и апсорпције удара. Ради даљег смањења буке, простор између преграда испуњен је акустичним материјалима. Овај приступ примењен је у јединственој комбинацији са много других карактеристика и метода, као што су: звучно изолован погон независтан од ваздуха типа *Stirling* и коморе са дизел-мотором; еластична црева и компензатори; ограничен максимални проток течности и ваздуха у цевима; минимални пречник савијања цеви и специјални дизајн трупа и осталих делова подморнице.

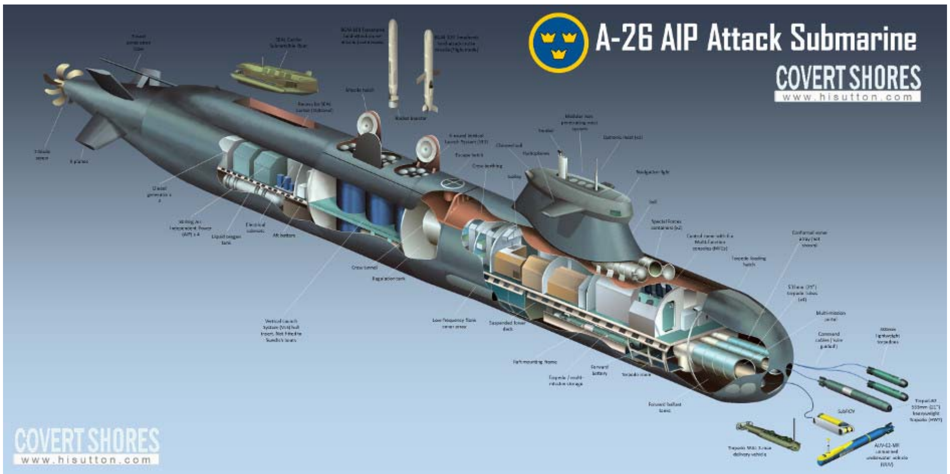

Подморница класе А-26

У једну од подморница нове генерације спада и А-26 са линијама трупа које су пројектоване тако да умање ударне силе експлозија, што се види на торњу или „једру” који има неуобичајен испупчен профил. Сама конструкција погона независног од ваздуха омогућава много тиши рад у односу на претходне подморнице, омогућавајући нове патролне мисије.

Компанија Saab наводи да је подморница А-26 у великој мери отпорна на ударне таласе од експлозија мина и дубинских бомби. Подморница са свом посадом је уживо тестирана на експлозије дубинских бомби на само неколико метара дубине ради провере отпорности трупа, али и самих електронских уређаја.

Стелт (невидљива) технологија компаније Saab спада у најтише технологије које су икада примењене на подморницама класе *Gotland*. Иначе, једну шведску подморницу класе *Gotland* на лизинг је узела и америчка морнарица ради провере откривања својих нуклеарних подморница, јер је таква класична подморница, захваљујући својој стелт конструкцији и технологији, успела да у поморским маневрима „потопи" једну француску и једну америчку нуклеарну подморницу (*USS Houston*), а дошла је и на положај одакле је могла да лансира торпеда и елиминише и амерички нуклеарни носач авиона *USS Ronald Reagan*.

Ако је подморница претходне класе *Gotland* могла да оствари овакве резултате, шта ће тек моћи нова класа *Blekinge*?

Драган М. Вучковић (*Dragan* M. Vučković),
e-mail: draganvuckovic64@gmail.com,
ORCID iD: http://orcid.org/0000-0003-1620-5601

Firefly: Израелска „лутајућа" муниција (или дрон камиказа)[4]

Изгледа као црни штап и лебди у ваздуху, али се забија у непријатеља брзином од 70 км на час.

Firefly (свитац) јесте најновије оружје које набавља израелско министарство одбране од компаније Rafael Advanced Defense Systems. Беспилотна летелица намењена је наоружању пешадије. Посебно је пројектована за употребу војницима који се боре у градском окружењу, пружајући им могућност да путем лебдеће беспилотне летелице круже око зграда, прецизно откривајући и елиминишући терористе или непријатељеве снаге.

Firefly спада у класу „лутајуће" муниције, неку врсту самоубилачких беспилотних летелица и припада великој породици ракета типа *Spike* које користе чак тридесет три земље. Сједињене Државе су такође купиле ракете *Spike* за своје јуришне хеликоптере *AH-64 Apache*. Ракете *Spike* познате су као убице тенкова, али *Firefly* спада у ред много мањег оружја које има масу од само 3 кг и представља део опреме пешадије. У новије време пешадија све чешће користи мање беспилотне летелице ради надзора и напада, али је њихова употреба још у повоју. Израел који је још 1980. године почео да употребљава беспилотне летелице сада тражи могућност интегрисања „лутајућег" оружја за копнене снаге.

Летелицу *Firefly* развиле су компанија Rafael и израелско министарство одбране, а пројектована је за решавање проблема које је Израел уочио у недавним конфликтима. Ради се о ситуацијама када се

[4] The National Interest, May 10, 2020

војне снаге боре у урбаним подручјима или против милитаната који су укопани или сакривени, као што су снајперисти, оператери ручних бацача или импровизованих експлозивних средстава. У тим ситуацијама врло је корисно имати на располагању „лутајућу” муницију која спроводи надзор и напад.

Беспилотна летелица Firefly

Беспилотном летелицом *Firefly* управља се путем таблета, а налази се спакована у тубу. Ради се о робустној конструкцији, а летелица се враћа кориснику само једним кликом на таблету. Има и могућност отказивања мисије, а поседује сензоре захваљујући којима избегава телефонске каблове, дрвеће или друге препреке на које може да налети.

Компанија Rafael наводи да је идеја пројектовања овог оружја потекла још у рату 1967. године. За време битке за Јерусалим израелски војници су морали да нападну јорданске позиције на стратешком узвишењу названом „брдо муниције”. Израелци су претрпели велике губитке, а један од преживелих постао је инжењер у компанији Rafael и пласирао идеју о лебдећем „лутајућем” оружју.

То је пројектил који се налази склопљен у малом канистеру. Може летети на даљинама до 500 метара, има батерију која се брзо мења, а могуће је демонтирати и експлозивно пуњење када се летелица користи само за надзор. Пројектанти предвиђају употребу летелице на нивоу чете или вода. Очекује се да ће бити произведена велика количина за израелске снаге. Израелска војска и полиција већ користи велики број разних врста беспилотних летелица, а очекује се да ће прво ватрено крштење имати против група као што су Хезболах или Хамас у следећих пар година, мада се не искључује ни употреба у Сирији.

Овакве врсте летелица, поред надзора и дејства против укопаног непријатеља, могу бити употребљене и за нападе на скупље мете, као што је потврђено у Либији, где су турске беспилотне летелице напале и уништиле неколико руских противракетних система *Панцир*. Наводи се да су системе *Панцир*, поред наоружаних беспилотних летелица *Барјактар*, нападале и мање самоубилачке беспилотне летелице.

Драган М. Вучковић (*Dragan* M. Vučković),
e-mail: draganvuckovic64@gmail.com,
ORCID iD: http://orcid.org/0000-0003-1620-5601

Прототип минобацача *MZ-204 Highlander* је спреман[5]

Руски самоходни минобацач *MZ-204 Highlander,* развијен на шасији вишенаменског оклопног возила *Tigr-M,* успешно је завршио све релевантне тестове.

MZ-204 Highlander у положају за отварање ватре

MZ-204 Highlander је самоходни минобацач са артиљеријским системом 120 мм монтираним на задњем делу возила са електричним увођењем параметара елевације и азимута. Његова основна предност у односу на сличне системе јесте што се посада налази у самом возилу за време отварања ватре.

[5] May 2020 www.armyrecognition.com

MZ-204 Highlander у положају за пуњење

Операција припреме и испаљивања мина из минобацача спроводи се без напуштања возила. Пре испаљивања мина цев минобацача се спушта хоризонтално. Преко посебног прозора за пуњење које се затвара оклопљеним поклопцем, пунилац поставља мину у цев минобацача. Након тога цев минобацача се аутоматски пење у позицију за отварање ватре. Оперативна ситуација и подаци у вези с циљевима приказују се на мултифункционалним ЛЦД дисплејима у боји.

MZ-204 Highlander ради потпуно аутоматизовано и може добијати податке о циљевима од беспилотних летелица.

Систем може користити и подешавајућу муницију као што су врло прецизне мине *Gran* 120 мм.

Драган М. Вучковић (*Dragan* M. Vučković),
e-mail: draganvuckovic64@gmail.com,
ORCID iD: http://orcid.org/0000-0003-1620-5601

Операција „Пустињски штит” и БПЛ *Baryaktar TB2*[6]

Сиријско ратно ваздухопловство је, 27. фебруара 2020. године, извршило прецизан ваздушни удар на двоспратну зграду у сиријском граду Balioun, у коју су се склониле турске снаге од удара сиријске артиљерије, а које су подржавале протурске побуњенике. У ваздушном удару страдало је 34 турска војника, а 30 их је рањено.

Турски војни конвој који је ушао у Сирију преко границе Kafr Lusin и кретао се према југу провинције Идлиб

Напад је покренуо серију догађаја који су кулминирали прекидом ватре 5. марта. Међутим, у спорном периоду од седам дана турске снаге су употребиле огроман број беспилотних летелица, што по турским званичницима представља „војну иновацију која је демонстрирала турски технолошки напредак на бојном пољу”.

Овај борбени период приморао је сиријске снаге на брзу адаптацију. Сиријски друштвени медији наводили су да је употребљен велики број турских беспилотних летелица (БПЛ) *Baryaktar TB2* и да је сиријска војска морала брзо да научи да не концентрише своје снаге на терену, да сакрива возила и да користи противваздушне снаге.

Турско министарство одбране је тврдило да је у операцији „Пустињски штит”, у којој је употребљен велики број БПЛ, закључно са 1. мартом избачено из строја 2200 сиријских војника, 103 тенка, системи ПВО и 72 хаубице. Операција је зауставила налет сиријских трупа.

[6] Jane’s Defence International May 2020

Није могуће потврдити турске тврдње, али је један руски репортер, у својим извештајима из региона 4. марта, написао да је између 25. и 28. фебруара сиријска војска претрпела значајне губитке, укључујући 23 тенка, 16 борбених возила пешадије и 9 вишецевних лансера ракета.

У том периоду турске БПЛ су летеле по групама од по 6 летелица на већим висинама ради извиђања и напада на циљеве са наводећим ракетама – једна летелица би уочила циљ, док би друга лансирала ракету са даљине од неколико километара.

Изгледа да је највећи број употребљених БПЛ припадао типу *Baryaktar TB2,* турског произвођача Baykar. Компанија наводи да летелица достиже висину од 8230 м и има аутономију лета до 24 часа. Комплетан систем *Baryaktar TB2* састоји се од саме БПЛ, земаљске контролне станице и копненог информационог терминала са додатним визуелним терминалом и генератором.

Координација две БПЛ Baryaktar TB2. Једна лети близу циља, омогућавајући ласерско вођење и врши координацију ракета које лансира друга БПЛ.

Беспилотна летелица има домет до 150 км, а претпоставља се да је лансирана са аеродрома Hatay, у Турској. Летелица лети крстарећом брзином од 129 км на час, покреће је мотор од 100 КС, док резервоар за гориво прима 300 литара горива. *Baryaktar TB2* има носивост до 150 кг и може носити до четири навођена пројектила (као што су *MAM-L* и *MAM-C* компаније *Roketsan*), као и електрооптички систем са термалном и дневном камером. Слика са летелице преноси се у реалном времену, а може се пренети и на друге уређаје са оперативним системом *Windows*.

MAM-L је микропројектил, масе до 22 кг, домета до 8 км који се може продужити до 14 км са инерцијалним и сателитским навигационим системом. Поседује близински упаљач са полуактивним ласерским трагачем. Овакав начин рада захтева ласерско озрачивање са друге БПЛ или неке друге платфореме. Потребно је да циљ буде констатно видљив. Ракета може бити опремљена тандем- експлозивном бојевом главом, противтенковском кумулативном бојевом главом или термобаричком бојевом главом, што објашњава разноврсност погођених циљеве од тенкова до пешадије.

MAM-C је још мањи пројектил, масе до 6,5 кг, домета до 8 км, и користи исти начин ласреског навођења. Ракета може бити опремљена вишенаменском бојевом главом са парчадним, запаљивим и пробојним дејством.

Током сукоба у Украјини обе стране су употребљавале БПЛ на сличан начин – лансирале су убојна средства на непријатељеве позиције.

Међутим, претпоставља се да је примарни циљ турских БПЛ у Идлибу био координација са турском артиљеријом. На снимцима се види испаљивање ракета са вишецевног лансера ракета *TRG 300* у правцу Идлиба.

Овај ВЛР има максимални домет до 120 км и користи инерцијални и сателитски систем за вођење ракета. Бојева глава има масу од 105 кг и ефикасан радијус дејства до 70 м. Уз самоходне хаубице *Firtina* 155 mm овај систем је најчешће коришћен у дејствима турске војске током поменутих седам дана.

Беспилотне летелице морале су да обезбеде координате циљева за турски *TRG 300* путем ласерског означивача. Исти метод морао је бити коришћен и за употребу самоходних хаубица, али се не зна да ли је Турска имала приступ ласерски вођеним артиљеријским гранатама које би наводиле БПЛ. Овај метод се разликује од метода које је Русија користила са својим БПЛ у Украјини. Претпоставља се да је начин циљања руских БПЛ мање прецизан и да захтева директно прелетање циљева и слање координата својој артиљерији или употребу референтних тачака.

Војни извори наводе да су турске снаге употребиле сложен начин електронског ратовања у операцији у Идлибу. Изгледа да су Турци употребили и своју другу сателитски вођену БПЛ *Anka-S*, ради пресретања електронских комуникација. Непознато је о којим таласним дужинама се радило, али сама летелица има неколико антена које се користе за геолоцирање радио-комуникација.

Турци су у Идлибу употребили и копнени систем за електронско ратовање *Koral* који потискује непријатељеву ПВО одбрану тако што прибавља информације и омогућава брзу размену информација на сложеном бојишту. Систем се састоји од возила за електронску подршку и електронски напад. Може се употребити за ометање непријатељевих радара ПВО, а утврђује и њихову тачну локацију.

Беспилотна летелица *Anka-S* и копнени систем *Koral* вероватно су употребљени као део комбинованих снага којима је био задатак да ограниче могућност сиријских снага за координацију одбране против БПЛ и артиљеријских система. Претпоставља се да су турски системи електронског ратовања имали за циљ откривање потенцијалних циљева и отежавање непријатељевог одговора.

Једна БПЛ Baryaktar TB2 користи ласерско озрачивање. Овим методом добијају се тачне координате циља.

Специфичност турског сценарија је и употреба летелице за рано упозоравање и контролу *E-7T Peace Eagle,* која има за циљ координацију ваздушне одбране. У овом случају авион је коришћен за обезбеђивање информација БПЛ преко копнених терминала и турске командне и контролне мреже. Употреба ове летелице додатно је обезбедила употребу БПЛ у борби.

И поред овакве комбиноване операције претпоставља се да су Турци изгубили чак 20 БПЛ.

Слична операција спроведена је и у Либији, где турске снаге подржавају снаге Владе националног јединства у борби против снага генерала Хафтара, где је страдало неколико руских система *Панцир*.

Драган М. Вучковић (*Dragan* M. Vučković),
e-mail: draganvuckovic64@gmail.com,
ORCID iD: http://orcid.org/0000-0003-1620-5601

ПОЗИВ И УПУТСТВО АУТОРИМА

ПРИГЛАШЕНИЕ И ИНСТРУКЦИЯ ДЛЯ АВТОРОВ РАБОТ

CALL FOR PAPERS AND INSTRUCTIONS FOR AUTHORS

ПОЗИВ И УПУТСТВО АУТОРИМА О НАЧИНУ ПРИПРЕМЕ ЧЛАНКА

Упутство ауторима о начину припреме чланка за објављивање у *Војнотехничком гласнику* урађено је на основу Акта о уређивању научних часописа, Министарства за науку и технолошки развој Републике Србије, евиденциони број 110-00-17/2009-01, од 09. 07. 2009. године. Примена овог Акта првенствено служи унапређењу квалитета домаћих часописа и њиховог потпунијег укључивања у међународни систем размене научних информација. Засновано је на међународним стандардима ISO 4, ISO 8, ISO 18, ISO 215, ISO 214, ISO 18, ISO 690, ISO 690-2, ISO 999 и ISO 5122, односно одговарајућим домаћим стандардима.

Војнотехнички гласник / Vojnotehnički glasnik / Military Technical Courier (втг.мо.упр.срб, www.vtg.mod.gov.rs, ISSN 0042-8469 – штампано издање, e-ISSN 2217-4753 – online, UDC 623+355/359, DOI: 10.5937/VojnotehnickiGlasnik; https://doi.org/10.5937/VojnotehnickiGlasnik), јесте мултидисциплинарни научни часопис Министарства одбране и Војске Србије. Часопис објављује научне и стручне чланке из области основних истраживања (математике, рачунарских наука и механике) и технолошког развоја (електронике, телекомуникација, информационих технологија, машинства, материјала и хемијских технологија), као и техничке информације о савременим системима наоружања и савременим војним технологијама. Часопис прати јединствену интервидовску техничку подршку Војске на принципу логистичке системске подршке, области основних, примењених и развојних истраживања, као и производњу и употребу средстава наоружања и војне опреме. Часопис објављује и остала теоријска и практична достигнућа која доприносе усавршавању свих припадника српске, регионалне и међународне академске заједнице, а посебно припадника војски и министарстава одбране.

Уређивачка политика Војнотехничког гласника заснива се на препорукама Одбора за етичност у издаваштву (COPE Core Practices), као и на најбољим прихваћеним праксама у научном издаваштву. Војнотехнички гласник је члан COPE (Committee on Publication Ethics) од 2. маја 2018. године.

Министарство просвете, науке и технолошког развоја Републике Србије, сагласно одлуци из члана 27. став 1. тачка 4), а по прибављеном мишљењу из члана 25. став 1. тачка 5) Закона о научноистраживачкој делатности („Службени гласник РС”, бр. 110/05, 50/06-испр. и 18/10), утврдило је категоризацију Војнотехничког гласника, за 2019. годину:

за област технолошки развој:

– на листи часописа за електронику, телекомуникације и информационе технологије:

категорија водећи научни часопис националног значаја **(М51)**,

– на листи часописа за материјале и хемијске технологије:

категорија научни часопис националног значаја **(М52)**,

– на листи часописа за машинство:

категорија научни часопис националног значаја **(М52)**,

за област основна истраживања:

– на листи часописа за математику, рачунарске науке и механику:

категорија научни часопис **(М53)**.

Усвојене листе домаћих часописа за 2019. годину могу се видети на сајту Војнотехничког гласника, страница *Категоризација часописа* (Министарство просвете, науке и технолошког развоја Републике Србије још увек није објавило званичну категоризацију научних часописа за 2020. годину).

Детаљније информације могу се пронаћи и на сајту Министарства просвете, науке и технолошког развоја Републике Србије.

Подаци о категоризацији могу се пратити и на сајту КОБСОН-а (Конзорцијум библиотека Србије за обједињену набавку).

Категоризација часописа извршена је према Правилнику о поступку и начину вредновања и квантитативном исказивању научноистраживачких резултата истраживача, који је прописао Национални савет за научни и технолошки развој (Службени гласник РС, број 38/2008).

У складу са овим правилником и табелом о врсти и квантификацији индивидуалних научноистраживачких резултата (у саставу Правилника), објављени рад у Војнотехничком гласнику вреднује се са 2 бода (категорија М51), 1,5 бод (категорија М52) и 1 бод (категорија М53).

Часопис се прати у контексту Српског цитатног индекса – СЦИндекс (база података домаћих научних часописа) и Руског индекса научног цитирања (РИНЦ). Подвргнут је сталном вредновању (мониторингу) у зависности од утицајности (импакта) у самим базама и, посредно, у међународним (Clarivate Analytics) цитатним индексима. Детаљи о индексирању могу се видети на сајту Војнотехничког гласника, страница *Индексирање часописа*.

Војнотехнички гласник омогућава и примењује Creative Commons (CC BY) одредбе о ауторским правима. Детаљи о ауторским правима могу се видети на сајту часописа, страница *Ауторска права и политика самоархивирања*.

Радови се предају путем онлајн система за електронско уређивање АСИСТЕНТ, који је развио Центар за евалуацију у образовању и науци (ЦЕОН).

Приступ и регистрација за сервис врше се на сајту www.vtg.mod.gov.rs, преко странице *АСИСТЕНТ* или *СЦИНДЕКС*, односно директно на линку aseestant.ceon.rs/index.php/vtg.

Детаљно упутство о регистрацији и пријави за сервис налази се на сајту www.vtg.mod.gov.rs, страница *Упутство за АСИСТЕНТ*.

Потребно је да се сви аутори који подносе рукопис за објављивање у Војнотехничком гласнику региструју у регистар ORCID (Open Researcher and Contributor ID), према упутству на страници сајта *Регистрација за добијање ORCID идентификационе шифре*.

Војнотехнички гласник објављује чланке на српском, руском и енглеском језику (arial, српска ћирилица или српска латиница, величина слова 11 pt, проред Single).

Поступак припреме, писања и уређивања чланка треба да буде у сагласности са *Изјавом о етичком поступању* (http://www.vtg.mod.gov.rs/izjava-o-etickom-postupanju.html).

Чланак треба да садржи сажетак са кључним речима, увод, разраду, закључак, литературу и апстракт са кључним речима на енглеском и руском језику (без нумерације наслова и поднаслова). Обим чланка треба да буде око једног ауторског табака (16 страница формата А4 са проредом Single), а највише 24 странице.

Чланак треба да буде написан на обрасцу за писање чланка, који се у електронској форми може преузети са сајта на страници *Образац за писање чланка*.

Наслов

Наслов треба да одражава тему чланка. У интересу је часописа и аутора да се користе речи прикладне за индексирање и претраживање. Ако таквих речи нема у наслову, пожељно је да се придода и поднаслов. Наслов треба да буде преведен и на енглески и руски језик.

Ови наслови исписују се испред сажетка на одговарајућем језику.

Текући наслов

Текући наслов се исписује са стране сваке странице чланка ради лакше идентификације, посебно копија чланака у електронском облику. Садржи презиме и иницијал имена аутора (ако аутора има више, преостали се означавају са „et al." или „и др."), наслове рада и часописа и колацију (година, волумен, свеска, почетна и завршна страница). Наслови часописа и чланка могу се дати у скраћеном облику.

Име аутора

Наводи се пуно име и презиме (свих) аутора. Веома је пожељно да се наведу и средња слова аутора. Имена и презимена домаћих аутора увек се исписују у оригиналном облику (са српским дијакритичким знаковима), независно од језика на којем је написан рад.

Назив установе аутора (афилијација)

Наводи се пун (званични) назив и седиште установе у којој је аутор запослен, а евентуално и назив установе у којој је аутор обавио истраживање. У сложеним организацијама наводи се укупна хијерархија (нпр. Универзитет одбране у Београду, Војна академија, Катедра природно-математичких наука). Бар једна организација у хијерархији мора бити правно лице. Ако аутора има више, а неки потичу из исте установе, мора се, посебним ознакама или на други начин, назначити из које од наведених установа потиче сваки од наведених аутора. Афилијација се исписује непосредно након имена аутора. Функција и звање аутора се не наводе.

Контакт подаци

Адреса или е-адреса свих аутора даје се поред имена и презимена аутора.

Категорија (тип) чланка

Категоризација чланака обавеза је уредништва и од посебне је важности. Категорију чланка могу предлагати рецензенти и чланови уредништва, односно уредници рубрика, али одговорност за категоризацију сноси искључиво главни уредник.

Чланци у *Војнотехничком гласнику* класификују се на научне и стручне чланке.

Научни чланак је:

– оригиналан научни рад (рад у којем се износе претходно необјављени резултати сопствених истраживања научним методом);

– прегледни рад (рад који садржи оригиналан, детаљан и критички приказ истраживачког проблема или подручја у којем је аутор остварио одређени допринос, видљив на основу аутоцитата);

– кратко или претходно саопштење (оригинални научни рад пуног формата, али мањег обима или прелиминарног карактера);

– научна критика, односно полемика (расправа на одређену научну тему, заснована искључиво на научној аргументацији) и осврти.

Изузетно, у неким областима, научни рад у часопису може имати облик монографске студије, као и критичког издања научне грађе (историјско-архивске, лексикографске, библиографске, прегледа података и сл.), дотад непознате или недовољно приступачне за научна истраживања.

Радови класификовани као научни морају имати бар две позитивне рецензије.

Ако се у часопису објављују и прилози ваннаучног карактера, научни чланци треба да буду груписани и јасно издвојени у првом делу свеске.

Стручни чланак је:

– стручни рад (прилог у којем се нуде искуства корисна за унапређење професионалне праксе, али која нису нужно заснована на научном методу);

– информативни прилог (уводник, коментар и сл.);

– приказ (књиге, рачунарског програма, случаја, научног догађаја, и сл.).

Језик рада

Језик рада може бити српски, руски или енглески.

Текст мора бити језички и стилски дотеран, систематизован, без скраћеница (осим стандардних). Све физичке величине морају бити изражене у Међународном систему мерних јединица – SI. Редослед образаца (формула) означава се редним бројевима, са десне стране у округлим заградама.

Сажетак

Сажетак јесте кратак информативан приказ садржаја чланка који читаоцу омогућава да брзо и тачно оцени његову релевантност. У интересу је уредништава и аутора да сажетак садржи термине који се често користе за индексирање и претрагу чланака. Саставни делови сажетка су увод/циљ истраживања, методи, резултати и закључак. Сажетак треба да има од 100 до 250 речи и треба да се налази између заглавља (наслов, имена аутора и др.) и кључних речи, након којих следи текст чланка.

Кључне речи

Кључне речи су термини или фразе које адекватно представљају садржај чланка за потребе индексирања и претраживања. Треба их додељивати ослањајући се на неки међународни извор (попис, речник или тезаурус) који је најшире прихваћен или унутар дате научне области. За нпр. науку уопште, то је листа кључних речи Web of Science. Број кључних речи не може бити већи од 10, а у интересу је уредништва и аутора да учесталост њихове употребе буде што већа. Кључне речи дају се на језику на којем је написан чланак (сажетак) и на енглеском језику. У чланку се пишу непосредно након сажетка.

Систем АСИСТЕНТ у ту сврху користи специјалну алатку KWASS: аутоматско екстраховање кључних речи из дисциплинарних тезауруса/речника по избору и рутине за њихов одабир, тј. прихватање односно одбацивање од стране аутора и/или уредника.

Датум прихватања чланка

Датум када је уредништво примило чланак, датум када је уредништво коначно прихватило чланак за објављивање, као и датуми када су у међувремену достављене евентуалне исправке рукописа наводе се хронолошким редоследом, на сталном месту, по правилу на крају чланка.

Захвалница

Назив и број пројекта, односно назив програма у оквиру којег је чланак настао, као и назив институције која је финансирала пројекат или програм, наводи се у посебној напомени на сталном месту, по правилу при дну прве стране чланка.

Претходне верзије рада

Ако је чланак у претходној верзији био изложен на скупу у виду усменог саопштења (под истим или сличним насловом), податак о томе треба да буде наведен у посебној напомени, по правилу при дну прве стране чланка. Рад који је већ објављен у неком часопису не може се објавити у Војнотехничком гласнику (прештампати), ни под сличним насловом и измењеном облику.

Табеларни и графички прикази

Пожељно је да наслови свих приказа, а по могућству и текстуални садржај, буду дати двојезично, на језику рада и на енглеском језику.

Табеле се пишу на исти начин као и текст, а означавају се редним бројевима са горње стране. Фотографије и цртежи треба да буду јасни, прегледни и погодни за репродукцију. Цртеже треба радити у програму word или corel. Фотографије и цртеже треба поставити на жељено место у тексту.

За слике и графиконе не сме се користити снимак са екрана рачунара програма за прикупљање података. У самом тексту чланка препоручује се употреба слика и графикона непосредно из програма за анализу података (као што су Excel, Matlab, Origin, SigmaPlot и други).

Навођење (цитирање) у тексту

Начин позивања на изворе у оквиру чланка мора бити једнообразан.

Војнотехнички гласник за референцирање (цитирање и навођење литературе) примењује Харвардски систем референци, односно Харвардски приручник за стил (Harvard Referencing System, Harvard Style Manual). У самом тексту, у обичним заградама, на месту на којем се врши позивање, односно цитирање литературе набројане на крају чланка, обавезно у обичној загради написати презиме цитираног аутора, годину издања публикације из које цитирате и, евентуално, број страница. Нпр. (Petrović, 2012, pp.10–12).

Детаљно упутство о начину цитирања, са примерима, дато је на страници сајта *Упутство за Харвардски приручник за стил*. Потребно је да се позивање на литературу у тексту уради у складу са поменутим упутством.

Систем АСИСТЕНТ у сврху контроле навођења (цитирања) у тексту користи специјалну алатку CiteMatcher: откривање изостављених цитата у тексту рада и у попису референци.

Напомене (фусноте)

Напомене се дају при дну стране на којој се налази текст на који се односе. Могу садржати мање важне детаље, допунска објашњења, назнаке о коришћеним изворима (на пример, научној грађи, приручницима), али не могу бити замена за цитирану литературу.

Листа референци (литература)

Цитирана литература обухвата, по правилу, библиографске изворе (чланке, монографије и сл.) и даје се искључиво у засебном одељку чланка, у виду листе референци. Референце се не преводе на језик рада и набрајају се у посебном одељку на крају чланка.

Војнотехнички гласник, као начин исписа литературе, примењује Харвардски систем референци, односно Харвардски приручник за стил (Harvard Referencing System, Harvard Style Manual).

Литература се обавезно пише на латиничном писму и набраја по абецедном редоследу, наводећи најпре презимена аутора, без нумерације.

Детаљно упутство о начину пописа референци, са примерима, дато је на страници сајта *Упутство за Харвардски приручник за стил*. Потребно је да се попис литературе на крају чланка уради у складу са поменутим упутством.

Нестандардно, непотпуно или недоследно навођење литературе у системима вредновања часописа сматра се довољним разлогом за оспоравање научног статуса часописа.

Систем АСИСТЕНТ у сврху контроле правилног исписа листе референци користи специјалну алатку RefFormatter: контрола обликовања референци у складу са Харвардским приручником за стил.

Пропратно писмо (само за ауторе из Републике Србије и по посебном захтеву уредника)

Поред чланка доставља се пропратно писмо у којем треба истаћи о којој врсти чланка се ради, који су графички прилози (фотографије и цртежи) оригинални, а који позајмљени.

У пропратном писму наводе се и подаци аутора: име, средње слово, презиме, чин, звање, е-маил, адреса послодавца (ВП), кућна адреса, телефон на радном месту и кућни (мобилни) телефон, рачун и назив банке, СО места становања, број личне карте и ЈМБ грађана.

Сви радови подлежу стручној рецензији.

Списак рецензената Војнотехничког гласника може се видети на страници сајта *Списак рецензената*. Процес рецензирања објашњен је на страници сајта *Рецензентски поступак*.

Адреса редакције:
Војнотехнички гласник
Вељка Лукића Курјака 33
11042 Београд
e-mail: vojnotehnicki.glasnik@mod.gov.rs.

Главни и одговорни уредник
мр *Небојша* Гаћеша, дипл. инж.
nebojsa.gacesa@mod.gov.rs,
https://orcid.org/0000-0003-3217-6513,
тел: војни 40-260 (011/3603-260),
066/8700-123

ПРИГЛАШЕНИЕ И ИНСТРУКЦИЯ ДЛЯ АВТОРОВ О ПОРЯДКЕ ПОДГОТОВКИ СТАТЬИ

Инструкция для авторов о порядке подготовки статьи к опубликованию в журнале «Военно-технический вестник» разработана в соответствии с Актом о редактировании научных журналов Министерства науки и технологического развития Республики Сербия, № 110-00-17/2009-01 от 09.07.2009 г. Применение этого Акта способствует повышению качества отечественных журналов и их более полному вовлечению в международную систему обмена научной информацией. Инструкция соответствует международным стандартам ISO 4, ISO 8, ISO 18, ISO 215, ISO 214, ISO 18, ISO 690, ISO 690-2, ISO 999, ISO 5122 и соответствующим стандартам Республики Сербия.

Военно-технический вестник (**Vojnotehnički glasnik / Military Technical Courier**), втг.мо.упр.срб, www.vtg.mod.gov.rs/index-ru.html, ISSN 0042-8469 – печатное издание, e-ISSN 2217-4753 – online, UDK 623+355/359, DOI: 10.5937/VojnotehnickiGlasnik; https://doi.org/10.5937/VojnotehnickiGlasnik, является мультидисциплинарным научным журналом Министерства обороны и Вооруженных сил Республики Сербия.. В журнале публикуются научные и профессиональные статьи, исследующие такие области как: математика, компьютерные науки и механика, а также области технологического развития: электроника, телекоммуникации, информационные технологии, машиностроение, материалы и химические технологии, в журнале также публикуется: техническая информация о современных системах вооружения и современных военных технологиях. Журнал следит за единой межвидовой технической поддержкой вооруженных сил, основанной на принципах системной логистики, за прикладными и инновационными научными исследованиями, в том числе, в области производства вооружения и военной техники. В журнале публикуются и прочие теоретические и практические достижения, которые способствуют повышению квалификации представителей сербского, регионального и международного академического сообщества, особенно военнослужащих Министерства Обороны и Вооружённых сил.

Редакционная политика журнала «Военно-технический вестник» основана на рекомендациях Комитета по этике научных публикаций (COPE Core Practices), а также на лучшей практике в научно-издательской деятельности. «Военно-технический вестник» является членом COPE со 2 мая 2018 года.

Министерство образования, науки и технологического развития Республики Сербия, согласно решению принятому в соотвествии со ст. 27 абзац 1, пункт 4 и на основании толкования ст. 25 абзац 1 пункт 5 Закона о научно-исследовательской деятельности («Службени гласник РС», № 110/05, утвердило категоризацию «Военно-технического вестника» за 2019 год:

Категории в области технологического развития:

– Область электроники, телекоммуникаций и информационных технологий:

ведущий научный журнал национального значения **(M51)**,

– Область материалов и химической технологии:

научный журнал национального значения **(M52)**,

– Область механики:

научный журнал национального значения **(M52)**.

Категории в области основных исследований:

– Область математика, компьютерные науки, технические науки:

научный журнал **(M53)**.

С информацией относительно категоризации за 2019 год можно ознакомиться на странице сайта «Военно-технического вестника» *Категоризация Вестника* (Министерством просвещения, науки и технологического развития Республики Сербия пока не произведено официального ранжирования научных журналов за 2020 год).

Более подробную информацию можно найти на сайте Министерства образования, науки и технологического развития Республики Сербия.

С информацией о категоризации можно ознакомиться и на сайте КОБСОН (Консорциум библиотек Республики Сербия по вопросам объединения закупок).

Категоризация Вестника проведена согласно Положению о порядке и способе категоризации научно-исследовательских результатов, утверждённого Национальным комитетом по науке и технологиям (Службени гласник РС, № 38/2008).

В соответствии с вышеуказанным Положением и таблицей с показателями классификации и категоризации индивидуальных научно-исследовательских результатов, являющейся неотъемлемой частью Положения, научная статья, опубликованная в «Военно-техническом вестнике», оценивается следующим способом: 2 балла (категория М51), 1,5 балла (категория М52) и 1,5 балл (категория М53).

Журнал соответствует стандартам Сербского индекса научного цитирования (СЦИндекс/SCIndeks) – наукометрической базы данных научных журналов Республики Сербия, а также Российского индекса научного цитирования (РИНЦ). Журнал постоянно подвергается мониторингу и оценивается количественными наукометрическими показателями, отражающими его научную ценность, в т.ч. опосредованно в международных индексах цитирования (Clarivate Analytics).

С информацией об индексировании можно ознакомиться на странице сайта журнала *Индексирование Вестника*.

«Военно-технический вестник» обеспечивает читателям возможность открытого доступа, в соответствии с положениями об авторских правах, утверждёнными Creative Commons (CC BY). С инструкцией об авторских правах можно ознакомиться на странице *Авторские права и политика самоархивирования*, перейдя по ссылке http://www.vtg.mod.gov.rs/index-ru.html.

Рукописи статей направляются в редакцию журнала с использованием online системы ASSISTANT, запущенной Центром поддержи развития образования и науки (ЦПРОН).

Регистрация в системе и оформление прав доступа выполняется по адресу http://www.vtg.mod.gov.rs/index-ru.html, через страницу *ASSISTANT* или *СЦИНДЕКС* (aseestant.ceon.rs/index.php/vtg).

С инструкцией по регистрации и правам доступа можно ознакомиться по адресу http://www.vtg.mod.gov.rs/index-ru.html, на странице *Инструкция по ASSISTANT*.

Все авторы, предоставляющие свои рукописи для публикации в редакцию журнала «Военно-технический вестник» должны пройти предварительную регистрацию в реестре ORCID (Open Researcher and Contributor ID). Эта процедура осуществляется в соответствии с инструкцией, размещенной на странице сайта *Регистрация в реестре ORCID для присвоения идентификационного кода*.

«Военно-технический вестник» публикует статьи на сербском, русском или английском языках (Arial, шрифт 11 pt, пробел Single).

Процесс подготовки, написания и редактирования статьи должен осуществляться в соответствии с принципами *Этического кодекса* (http://www.vtg.mod.gov.rs/etichyeskiy-kodyeks.html).

Статья должна содержать резюме с ключевыми словами, введение, основную часть, выводы, список использованной литературы и резюме с ключевыми словами на английском языке (без нумерации заголовков и подзаголовков). Объём статьи не должен превышать один авторский лист (16 страниц формата А4 с пробелом Single).

Статья должна быть набрана на компьютере с использованием специально подготовленного редакцией макета, который можно скачать на странице сайта *Правила и образец составления статьи*.

Заголовок

Заголовок должен отражать тему статьи. В интересах журнала и автора необходимо использовать слова и словосочетания, удобные для индексации и поиска. Если такие слова не содержатся в заголовке, то желательно их добавить в подзаголовок. Заголовок должен быть переведён на английский язык. Название заголовка (подзаголовка) пишется перед резюме на соответствующем языке.

Текущий заголовок

Текущий заголовок пишется в титуле каждой страницы статьи с целью упрощения процесса идентификации, в первую очередь копий статьей в электронном виде. Заголовок содержит в себе фамилию и инициал имени автора (в случае если авторов несколько, остальные обозначаются с «et al.» или «и др.»), название работы и журнала (год, том, выпуск, начальная и заключительная страница). Заголовок статьи и название журнала могут быть приведены в сокращенном виде.

ФИО автора

Приводятся полная фамилия и полное имя (всех) авторов. Желательно, чтобы были указаны инициалы отчеств авторов. Фамилия и имя авторов из Республики Сербия всегда пишутся в оригинальном виде (с сербскими диакритическими знаками), независимо от языка, на котором написана работа.

Наименование учреждения автора (аффилиация)

Приводится полное (официальное) наименование и местонахождение учреждения, в котором работает автор, а также наименование учреждения, в котором автор провёл исследование. В случае организаций со сложной структурой приводится их иерархическая соподчинённость (напр. Военная академия, кафедра военных электронных систем, г. Белград). По крайней мере, одна из организаций в иерархии должна иметь статус юридического лица. В случае если указано несколько авторов, и если некоторые из них работают в одном учреждении, нужно отдельными обозначениями или каким-либо другим способом указать в каком из приведённых учреждений работает каждый из авторов. Аффилиация пишется непосредственно после ФИО автора. Должность и специальность по диплому не указываются.

Контактные данные

Электронный адрес автора указываются рядом с его именем на первой страницы статьи.

Категория (тип) статьи

Категоризация статьей является обязанностью редакции и имеет особое значение. Категорию статьи могут предлагать рецензенты и члены редакции, т.е. редакторы рубрик, но ответственность за категоризацию несет исключительно главный редактор. Статьи в журнале распределяются по следующим категориям:

Научные статьи:

– оригинальная научная статья (работа, в которой приводятся ранее неопубликованные результаты собственных исследований, полученных научным методом);

– обзорная статья (работа, содержащая оригинальный, детальный и критический обзор исследуемой проблемы или области, в который автор внёс определённый вклад, видимый на основе автоцитат);

– краткое сообщение (оригинальная научная работа полного формата, но меньшего объёма или имеющая предварительный характер);

– научная критическая статья (дискуссия-полемика на определённую научную тему, основанная исключительно на научной аргументации) и научный комментарий.

Однако, в некоторых областях знаний научная работа в журнале может иметь форму монографического исследования, а также критического обсуждения научного материала (историко-архивного, лексикографического, библиографического, обзора данных и т.п.) – до сих пор неизвестного или недостаточно доступного для научных исследований. Работы, классифицированные в качестве научных, должны иметь, по меньшей мере, две положительные рецензии.

В случае если в журнале объявляются и приложения, не имеющие научный характер, научные статьи должны быть сгруппированы и четко выделены в первой части номера.

Профессиональные статьи:

– профессиональная работа (приложения, в которых предлагаются опыты, полезные для совершенствования профессиональной практики, но которые не должны в обязательном порядке быть обоснованы на научном методе);

– информативное приложение (передовая статья, комментарий и т.п.);

– обзор (книги, компьютерной программы, случая, научного события и т.п.).

Язык работы

Работа может быть написана на сербском, русском или английском языке.

Текст должен быть в лингвистическом и стилистическом смысле упорядочен, систематизирован, без сокращений (за исключением стандартных). Все физические величины должны соответствовать Международной системе единиц измерения – СИ. Очередность формул обозначается порядковыми номерами, проставляемыми с правой стороны в круглых скобках.

Резюме

Резюме является кратким информативным обзором содержания статьи, обеспечивающим читателю быстроту и точность оценки её релевантности. В интересах редакции и авторов, чтобы резюме содержало термины, часто используемые для индексирования и поиска статьей. Составными частями резюме являются введение/цель исследования, методы, результаты и выводы. В резюме должно быть от 100 до 250 слов, и оно должно находится между титулами (заголовок, ФИО авторов и др.) и ключевыми словами, за которыми следует текст статьи.

Ключевые слова

Ключевыми словами являются термины или фразы, адекватно представляющие содержание статьи, необходимые для индексирования и поиска. Ключевые слова необходимо выбирать, опираясь при этом на какой-либо международный источник (регистр, словарь, тезаурус), наиболее используемый внутри данной научной области. Число ключевых слов не может превышать 10. В интересах редакции и авторов, чтобы частота их встречи в статье была как можно большей. Ключевые слова даются на языке, на котором написана статья (резюме), и на английском языке. В статье они пишутся непосредственно после резюме.

Программа ASSISTANT предоставляет возможность использования сервиса KWASS, автоматически фиксирующего ключевые слова из источников/словарей по выбору автора/редактора.

Дата получения статьи

Дата, когда редакция получила статью; дата, когда редакция окончательно приняла статью к публикации; а также дата, когда были предоставлены необходимые исправления рукописи, приводятся в хронологическом порядке, как правило, в конце статьи.

Выражение благодарности

Наименование и номер проекта, т.е. название программы благодаря которой статья возникла, совместно с наименованием учреждения, которое финансировало проект или программу, приводятся в отдельном примечании, как правило, внизу первой страницы статьи.

Предыдущие версии работы

В случае если статья в предыдущей версии была изложена устно (под одинаковым или похожим названием, например, в виде доклада на научной конференции), сведения об этом должны быть указаны в отдельном примечании, как правило, внизу первой страницы статьи. Работа, которая уже была опубликована в каком-либо из журналов, не может быть напечатана в «Военно-техническом вестнике» ни под похожим названием, ни в изменённом виде.

Нумерация и название таблиц и графиков

Желательно, чтобы нумерация и название таблиц и графиков были исполнены на двух языках (на языке оригинала и на английском). Таблицы подписываются таким же способом как и текст и обозначаются порядковым номером с верхней стороны. Фотографии и рисунки должны быть понятны, наглядны и удобны для репродукции. Рисунки необходимо делать в программах Word или Corel. Фотографии и рисунки надо поставить на желаемое место в тексте. Для создания изображений и графиков использование функции снимка с экрана (скриншота) не допускается. В самом тексте статьи рекомендуется применение изображений и графиков, обработанных такими компьютерными программами, как: Excel, Matlab, Origin, SigmaPlot и др.

Ссылки (цитирование) в тексте

Оформление ссылок на источники в рамках статьи должно быть однообразным. «Военно-технический вестник» для оформления ссылок, цитат и списка использованной литературы применяет Гарвардскую систему (Harvard Referencing

System, Harvard Style Manual). В тексте в скобках приводится фамилия цитируемого автора (или фамилия первого автора, если авторов несколько), год издания и по необходимости номер страницы. Например: (Petrović, 2010, pp.10-20). Рекомендации о способе цитирования размещены на странице сайта *Инструкция по использованию Гарвардского стиля*. При оформлении ссылок, цитат и списка использованной литературы необходимо придерживаться установленных норм. Программа ASSISTANT предоставляет при цитировании возможность использования сервиса CiteMatcher, фиксирующего пропущенные цитаты в работе и в списке литературы.

Примечания (сноски)

Примечания (сноски) к тексту указываются внизу страницы, к которой они относятся. Примечания могут содержать менее важные детали, дополнительные объяснения, указания об использованных источниках (напр. научном материале, справочниках), но не могут быть заменой процедуры цитирования литературы.

Литература (референции)

Цитированной литературой охватываются, как правило, такие библиографические источники как статьи, монографии и т.п. Вся используемая литература в виде референций размещается в отдельном разделе статьи.

Названия литературных источников не переводятся на язык работы.

«Военно-технический вестник» для оформления списка использованной литературы применяет Гарвардскую систему (Harvard Style Manual). В списке литературы источники указываются в алфавитном порядке фамилий авторов или редакторов. Рекомендации о способе цитирования размещены на странице сайта *Инструкция по использованию Гарвардского стиля*. При оформлении списка использованной литературы необходимо придерживаться установленных норм.

При оформлении списка литературы программа ASSISTANT предоставляет возможность использования сервиса RefFormatter, осуществляющего контроль оформления списка литературы в соответствии со стандартами Гарвардского стиля.

Нестандартное, неполное и непоследовательное приведение литературы в системах оценки журнала считается достаточной причиной для оспаривания научного статуса журнала.

Все рукописи статей подлежат профессиональному рецензированию.

Список рецензентов журнала «Военно-технический вестник» размещён на странице сайта *Список рецензентов*. Процесс рецензирования описан в разделе *Правила рецензирования*.

Почтовый адрес редакции:
«Војнотехнички гласник»
ул. Велька Лукича Куряка 33
11042 Белград, Республика Сербия
e-mail: vojnotehnicki.glasnik@mod.gov.rs.

Главный и ответственный редактор
Кандидат технических наук *Небойша* Гачеша
nebojsa.gacesa@mod.gov.rs
https://orcid.org/0000-0003-3217-6513
тел: +381 11 3603 260, +381 66 8700 123

CALL FOR PAPERS AND ARTICLE FORMATTING INSTRUCTIONS

The instructions to authors about the article preparation for publication in the *Military Technical Courier* are based on the Act on scientific journal editing of the Ministry of Science and Technological Development of the Republic of Serbia, No 110-00-17/2009-01 of 9th July 2009. This Act aims at improving the quality of national journals and raising the level of their compliance with the international system of scientific information exchange. It is based on international standards ISO 4, ISO 8, ISO 18, ISO 215, ISO 214, ISO 18, ISO 690, ISO 690-2, ISO 999 and ISO 5122 and their national equivalents.

The Military Technical Courier / Vojnotehnički glasnik (www.vtg.mod.gov.rs/index-e.html, втг.мо.упр.срб, ISSN 0042-8469 – print issue, e-ISSN 2217-4753 – online, UDC 623+355/359, DOI: 10.5937/VojnotehnickiGlasnik; https://doi.org/10.5937/VojnotehnickiGlasnik) is a multidisciplinary scientific journal of the Ministry of Defence and the Serbian Armed Forces. The journal publishes scientific and professional papers covering fundamental research (mathematics, computer science and mechanics) and technological development (electronics, telecommunications, information technologies, mechanical engineering, material science and chemical technologies) as well as technical data on modern weapon systems and military technologies. The journal covers inter-service technical support to the Army on the principle of logistic system support; fundamental, applied and development research; production and use of weapons and military equipment. Also, the journal publishes other theoretical and practical achievements leading to professional development of all members of Serbian, regional and international academic communities as well as members of the military and ministries of defence in particular.

The editorial policy of the Military Technical Courier is based on the COPE Core Practices and the journal articles are consistent with accepted best practices in their subject areas. As of 2 May 2018, the Military Technical Courier is a member of COPE (Committee on Publication Ethics).

Pursuant to the decision given in Article 27, paragraph 1, point 4, and in accordance with the acquired opinion given in Article 25, paragraph 1, point 5 of the Act on Scientific and Research Activities (Official Gazette of the Republic of Serbia, No 110/05, 50/06-cor and 18/10), the Ministry of Education, Science and Technological Development of the Republic of Serbia classified the Military Technical Courier for the year 2019

in the field technological development:
– on the list of periodicals for electronics, telecommunications and IT,
category: leading scientific periodical of national interest **(M51)**,
– on the list of periodicals for materials and chemical technology,
category: scientific periodical of national interest **(M52)**,
– on the list of periodicals for mechanical engineering,
category: scientific periodical of national interest **(M52)**,
in the field fundamental research:
– on the list of periodicals for mathematics, computer sciences and mechanics,
category: scientific periodical **(M53)**.

The approved lists of national periodicals for the year 2019 can be viewed on the website of the Military Technical Courier, page *Journal categorization* (The Ministry of Education, Science and Technological Development of the Republic of Serbia has not yet published the official evaluation of scientific journals for 2020).

More detailed information can be found on the website of the Ministry of Education, Science and Technological Development of the Republic of Serbia.

The information on the categorization can be also found on the website of KOBSON (Consortium of Libraries of Serbia for Unified Acquisition).

The periodical is categorized in compliance with the Regulations on the procedure and method of evaluation and quantitative formulation of scientific and research results of researchers, stipulated by the National Council for Scientific and Technological Development (*Official Gazette of RS*, No 38/2008). More detailed information can be found on the website of the Ministry of Education, Science and Technological Development.

In accordance with the Regulations and the table about types and quantification of individual scientific and research results (as a part of the Regulations), a paper published in the *Military Technical Courier* scores 2 (two) points (category M51), 1,5 (one and a half) point (category M52) and 1 (one) point (category M53).

The journal is in the Serbian Citation Index – SCIndex (data base of national scientific journals), in the Russian Index of Science Citation/Российский индекс научного цитирования (RINC/РИНЦ) and is constantly monitored depending on the impact within the bases themselves and indirectly in the international (e.g. Clarivate Analytics) citation indexes. More detailed information can be viewed on the website of the Military Technical Courier, page *Journal indexing*.

Military Technical Courier enables open access and applies the Creative Commons Attribution (CC BY) licence provisions on copyright. The copyright details can be found on the *Copyright notice and Self-archiving policy* page of the journal's website.

Manuscripts are submitted online, through the electronic editing system ASSISTANT, developed by the Center for Evaluation in Education and Science – CEON.

The access and the registration are through the Military Technical Courier site http://www.vtg.mod.gov.rs/index-e.html, on the page *ASSISTANT* or the page *SCINDEKS* or directly through the link (aseestant.ceon.rs/index.php/vtg).

The detailed instructions about the registration for the service are on the website http://www.vtg.mod.gov.rs/index-e.html, on the page *Instructions for ASSISTANT*.

All authors submitting a manuscript for publishing in the Military Technical Courier should register for an ORCID ID following the instructions on the web page *Registration for an ORCID identifier*.

The Military Technical Courier publishes articles in Serbian, Russian or English, using Arial and a font size of 11pt with Single Spacing.

The procedures of article preparation, writing and editing should be in accordance with the *Publication ethics statement* (http://www.vtg.mod.gov.rs/publication-ethics-statement.html).

The article should contain the abstract with keywords, introduction, body, conclusion and references (without heading and subheading enumeration). The article length should not exceed 24 pages of A4 paper format.

The article should be formatted following the instructions in the Article Form which can be downloaded from website page *Article form*.

Title

The title should be informative. It is in both Journal's and author's best interest to use terms suitable for indexing and word search. If there are no such terms in the title, the author is strongly advised to add a subtitle. The title should be given in English as well.

The titles precede the abstract and the summary in an appropriate language.

Letterhead title

The letterhead title is given at a top of each page for easier identification of article copies in an electronic form in particular. It contains the author's surname and first name initial (for multiple authors add "et al"), article title, journal title and collation (year, volume, issue, first and last page). The journal and article titles can be given in a shortened form.

Author's name

Full name(s) of author(s) should be used. It is advisable to give the middle initial. Names are given in their original form (with diacritic signs if in Serbian).

Author's affiliation

The full official name and seat of the author's affiliation is given, possibly with the name of the institution where the research was carried out. For organizations with complex structures, give the whole hierarchy (for example, University of Defence in Belgrade, Military Academy, Department for Military Electronic Systems). At least one organization in the hierarchy must be a legal entity. When some of multiple authors have the same affiliation, it must be clearly stated, by special signs or in other way, which department exactly they are affiliated with. The affiliation follows the author's name. The function and title are not given.

Contact details

The postal addresses or the e-mail addresses of the authors are given in the first page.

Type of articles

Classification of articles is a duty of the editorial staff and is of special importance. Referees and the members of the editorial staff, or section editors, can propose a category, but the editor-in-chief has the sole responsibility for their classification.

Journal articles are classified as follows:
Scientific articles:

– Original scientific papers (giving the previously unpublished results of the author's own research based on scientific methods);

– Review papers (giving an original, detailed and critical view of a research problem or an area to which the author has made a contribution demonstrated by self-citation);

– Short communications or Preliminary communications (original scientific full papers but shorter or of a preliminary character);

– Scientific commentaries or discussions (discussions on a particular scientific topic, based exclusively on scientific argumentation) and opinion pieces.

Exceptionally, in particular areas, a scientific paper in the Journal can be in a form of a monograph or a critical edition of scientific data (historical, archival, lexicographic, bibliographic, data survey, etc.) which were unknown or hardly accessible for scientific research.

Papers classified as scientific must have at least two positive reviews.

If the journal contains non-scientific contributions as well, the section with scientific papers should be clearly denoted in the first part of the Journal.

Professional articles:

– Professional papers (contributions offering experience useful for improvement of professional practice but not necessarily based on scientific methods);

– Informative contributions (editorial, commentary, etc.);

– Reviews (of a book, software, case study, scientific event, etc.)

Language

The article can be in Serbian, Russian or English.

The grammar and style of the article should be of good quality. The systematized text should be without abbreviations (except standard ones). All measurements must be in SI units. The sequence of formulae is denoted in Arabic numerals in parentheses on the right-hand side.

Abstract and summary

An abstract is a concise informative presentation of the article content for fast and accurate evaluation of its relevance. It contains the terms often used for indexing and article search. A 100- to 250-word abstract has the following parts: introduction/purpose of the research, methods, results and conclusion.

Keywords

Keywords are terms or phrases showing adequately the article content for indexing and search purposes. They should be allocated heaving in mind widely accepted international sources (index, dictionary or thesaurus), such as the Web of Science keyword list for science in general. The higher their usage frequency is, the better. Up to 10 keywords immediately follow the abstract and the summary, in respective languages.

For this purpose, the ASSISTANT system uses a special tool KWASS for the automatic extraction of key words from disciplinary thesauruses/dictionaries by choice and the routine for their selection, i.e. acceptance or rejection by author and/or editor.

Article acceptance date

The date of the reception of the article, the dates of submitted corrections in the manuscript (optional) and the date when the Editorial Board accepted the article for publication are all given in a chronological order at the end of the article.

Acknowledgements

The name and the number of the project or programme within which the article was realised is given in a separate note at the bottom of the first page together with the name of the institution which financially supported the project or programme.

Article preliminary version

If an article preliminary version has appeared previously at a meeting in a form of an oral presentation (under the same or similar title), this should be stated in a separate note at the bottom of the first page. An article published previously cannot be published in the *Military Technical Courier* even under a similar title or in a changed form.

Tables and illustrations

All the captions should be in the original language as well as in English, together with the texts in illustrations if possible. Tables are typed in the same style as the text and are denoted by Arabic numerals at the top. Photographs and drawings, placed appropriately in the text, should be clear, precise and suitable for reproduction. Drawings should be created in Word or Corel.

For figures and graphs, proper data plot is recommended i.e. using a data analysis program such as Excel, Matlab, Origin, SigmaPlot, etc. It is not recommended to use a screen capture of a data acquisition program as a figure or a graph.

Citation in the text

Citation in the text must be uniform. The Military Technical Courier applies the Harvard Referencing System given in the Harvard Style Manual. When citing sources within your paper, i.e. for in-text references of the works listed at the end of the paper, place the year of publication of the work in parentheses and optionally the number of the page(s) after the author's name, e.g. (Petrovic, 2012, pp.10-12). A detailed guide on citing, with examples, can be found on Military Technical Courier website on the page *Instructions for Harvard Style Manual*. In-text citations should follow its guidelines.

For checking in-text citations, the ASSISTANT system uses a special tool CiteMatcher to find out quotes left out within papers and in reference lists.

Footnotes

Footnotes are given at the bottom of the page with the text they refer to. They can contain less relevant details, additional explanations or used sources (e.g. scientific material, manuals). They cannot replace the cited literature.

Reference list (Literature)

The cited literature encompasses bibliographic sources such as articles and monographs and is given in a separate section in a form of a reference list.

References are not translated to the language of the article.

In compiling the reference list and bibliography, the Military Technical Courier applies the Harvard System – Harvard Style Manual. All bibliography items should be listed alphabetically by author's name, without numeration. A detailed guide for listing references, with examples, can be found on Military Technical Courier website on the page *Instructions for Harvard Style Manual*. Reference lists at the end of papers should follow its guidelines.

In journal evaluation systems, non-standard, insufficient or inconsequent citation is considered to be a sufficient cause for denying the scientific status to a journal.

All articles are peer reviewed.

The list of referees of the Military Technical Courier can be viewed at website page *List of referees*. The article review process is described on the *Peer Review Process* page of the website.

Address of the Editorial Office:
Vojnotehnički glasnik / Military Technical Courier
Veljka Lukića Kurjaka 33
11042 Belgrade, Republic of Serbia
e-mail: vojnotehnicki.glasnik@mod.gov.rs.

Editor in chief
Nebojša Gaćeša MSc
nebojsa.gacesa@mod.gov.rs
https://orcid.org/0000-0003-3217-6513
tel.: +381 11 3603 260, +381 66 8700 123

Ликовно-графички уредник
мр *Небојша* Кујунџић,
e-mail: nebojsa.kujundzic@mod.gov.rs

Техничко уређење
мр *Небојша* Гаћеша, e-mail: nebojsa.gacesa@mod.gov.rs,
https://orcid.org/0000-0003-3217-6513

Лектор
Добрила Милетић, професор,
e-mail: miletic.dobrila@gmail.com

Превод на енглески
Јасна Вишњић, професор,
e-mail: jasnavisnjic@yahoo.com, https://orcid.org/0000-0003-1728-4743

Превод на руски
др Карина Авагјан,
e-mail: karinka2576@mail.ru

Превод на немачки
Гордана Богдановић
e-mail: gordana.bogdanovic@yahoo.com

Превод на француски
Драган Вучковић,
e-mail: draganvuckovic64@gmail.com, https://orcid.org/0000-0003-1620-5601

ЦИП – Каталогизација у публикацији:
Народна библиотека Србије, Београд

623+355 / 359
355 / 359

ВОЈНОТЕХНИЧКИ гласник : научни часопис
Министарства одбране Републике Србије =
Military Technical Courier : scientific
periodical of the Ministry of Defence of the
Republic of Serbia / одговорни уредник
Небојша Гаћеша. - Год. 1, бр. 1 (1953) -
- Београд (Браће Југовића 19) : Министарство
одбране Републике Србије, 1953- (Београд :
Војна штампарија). - 24 cm

Доступно и на: http://www.vtg.mod.gov.rs
Тромесечно. - Друго издање на другом медијуму:
Vojnotehnički glasnik (Online) = ISSN 2217-4753
ISSN 0042-8469 = Војнотехнички гласник
COBISS.SR-ID 4423938

Цена: 600,00 динара,
Тираж: 100 примерака

На основу мишљења Министарства за науку, технологију и развој Републике Србије, број 413-00-1201/2001-01 од 12. 9. 2001. године,
часопис „Војнотехнички гласник“ је публикација од посебног интереса за науку.

УДК: Народна библиотека Србије, Београд

Художественный редактор
Магистр дизайна, *Небойша* Куюнджич,
e-mail: nebojsa.kujundzic@mod.gov.rs

Технический редактор
Кандидат технических наук *Небойша* Гачеша, e-mail: nebojsa.gacesa@mod.gov.rs,
https://orcid.org/0000-0003-3217-6513

Корректор
Добрила Милетич,
e-mail: miletic.dobrila@gmail.com

Перевод на английский язык
Ясна Вишнич,
e-mail: jasnavisnjic@yahoo.com, https://orcid.org/0000-0003-1728-4743

Перевод на русский язык
Д.филол.н. *Карина* Кареновна Авагян,
e-mail: karinka2576@mail.ru

Перевод на немецкий язык
Гордана Богданович,
e-mail: gordana.bogdanovic@yahoo.com

Перевод на французский язык
Драган Вучкович,
e-mail: draganvuckovic64@gmail.com, https://orcid.org/0000-0003-1620-5601

CIP – Каталогизация в публикации: Национальная библиотека Сербии, г. Белград

623+355 / 359
355 / 359

ВОЕННО-ТЕХНИЧЕСКИЙ вестник: научный журнал
Министерства обороны Республики Сербия=
Military Technical Courier : scientific
periodical of the Ministry of Defence of the
Republic of Serbia / главный редактор
Небойша Гачеша. – Первый выпуск (1953) –
г. Белград (ул. Браче Юговича, д. 19): Министерство
обороны Республики Сербия, 1953- (Белград:
Военная типография). - 24 см
Размещено на сайте:
http://www.vtg.mod.gov.rs
Ежеквартально - Издание в электронном виде:
Военно-технический вестник (Online) = ISSN2217-4753
ISSN 0042-8469 = Военно-технический вестник
COBISS.SR-ID 4423938

Цена: 600,00 динаров
Тираж: 100 экземпляров

На основании решения Министерства науки и технологий Республики Сербия,
№ 413-00-1201/2001-01 от 12. 9. 2001 года, журнал «Военно-технический вестник»
объявлен изданием, имеющим особое значение для науки.

УДК: Национальная библиотека Сербии, г. Белград

Graphic design editor
Nebojša Kujundžić MA,
e-mail: nebojsa.kujundzic@mod.gov.rs

Copy editing
Nebojša Gaćeša MSc, e-mail: nebojsa.gacesa@mod.gov.rs,
https://orcid.org/0000-0003-3217-6513

Proofreader
Dobrila Miletić BA,
e-mail: miletic.dobrila@gmail.com

English translation and polishing
Jasna Višnjić BA,
e-mail: jasnavisnjic@yahoo.com, https://orcid.org/0000-0003-1728-4743

Russian translation and polishing
Karina Avagyan PhD,
e-mail: karinka2576@mail.ru

German translation and polishing
Gordana Bogdanović,
e-mail: gordana.bogdanovic@yahoo.com

French translation and polishing
Dragan Vučković,
e-mail: draganvuckovic64@gmail.com, https://orcid.org/0000-0003-1620-5601

CIP – Catalogisation in the publication: National Library of Serbia, Belgrade

623+355 / 359
355 / 359

ВОЈНОТЕХНИЧКИ гласник : научни часопис Министарства одбране Републике Србије = Military Technical Courier : scientific periodical of the Ministry of Defence of the Republic of Serbia / одговорни уредник Небојша Гаћеша. - Год. 1, бр. 1 (1953) - - Београд (Браће Југовића 19) : Министарство одбране Републике Србије, 1953-(Београд : Војна штампарија). - 24 cm

Доступно и на:
http://www.vtg.mod.gov.rs
Тромесечно. - Друго издање на другом медијуму:
Vojnotehnički glasnik (Online) = ISSN 2217-4753
ISSN 0042-8469 = Војнотехнички гласник
COBISS.SR-ID 4423938

Price: 600.00 RSD
Printed in 100 copies

According to the Opinion of the Ministry of Science and Technological Development No 413-00-1201/2001-01 of 12th September 2001, the *Military Technical Courier* is a publication of special interest for science.

UDC: National Library of Serbia, Belgrade

ВТГ
ОД 1953.
ГОДИНА

ВТБ
С 1953.
ЛЕТ

MTC
SINCE 1953
YEARS